



UNIVERSITY OF TRENTO - Italy

International PhD Program in Biomolecular Sciences

Centre for Integrative Biology

XXVIII Cycle

Mechanisms of brain wiring by axonal miRNAs: miR-181 and miR-182

Tutor and Advisor

Dr. Marie-Laure Baudet

CIBIO - University of Trento

Ph.D. Thesis of

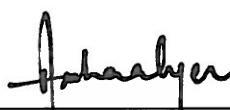
Archana Iyer

CIBIO - University of Trento

Academic Year 2015-2016

Declaration of authorship

'I, **Archana Iyer**, confirm that this is my own work and the use of all material from other sources have been properly and fully acknowledged'.

A handwritten signature in black ink, appearing to read 'Archana Iyer', is written above a horizontal line.

Signature of PhD candidate

(Archana Iyer)

This thesis is dedicated to my beloved mother

Acknowledgements

I would like to express my sincere gratitude to my supervisor Dr. Marie-Laure Baudet for her relentless support and guidance that helped me grow as a scientist. Marie-Laure has been an incredible mentor and I am thankful for her insightful comments and encouragement to answer very cool biological questions and teaching me challenging techniques. She has helped immensely in channeling my ideas, supported me when I faltered and provided many opportunities that have enabled me to reach this stage and for which I am eternally grateful.

Big hugs and thanks to all my lab members– Stephanie, Michela, Simone, Eloina, Antoneta, Lorenzo and Emma for their love and family like support. Stephanie thanks for the wonderful cakes, positive encouragement during laser capture sessions, for proof-reading my thesis and for all the bioinformatic analysis. Michi thanks for your love that will be ‘engrained’ in my head, your adorable company during cultures, laser capture sessions and our lovely vinbrule evenings. Elo, many thanks to you for your cheerful presence, lots of support in addition to all the fantastic help with the qPCR. Simo, thanks for your crazy ideas, brotherly love (and annoyance) and tons of help for my work. Anto, thanks for your enthusiasm and lovely spirit. I would also like to thank past lab members – Fabio (thanks for your company and teaching/struggling with me on the LCM), Sara (thanks to your smile and hugs that encouraged me a lot), Sindhu (thanks for being there for me and for all the upliftment in times of need), Silvia and Marco thanks for your help and all the fun we had. Many thanks to Emma, Katia and Lorenzo, for being so helpful, kind and wonderful and who made my lab work and the ordering processes extremely easy.

I would like to express my sincere thanks to all our collaborators- especially Prof Christine Holt, Dr. Anäis Bellon, Dr. Cei Abreu Goodger and his lab. I am thankful to Dr. Vladimir Benes and the Genecore Facility for the library preparation and sequencing.

I would like to thank the then Tutor of mine, Prof Paolo Macchi for his scientific enthusiasm. I also would like to thank my PhD co-ordinator, Prof Anna Cereseto for

running a very excellent PhD program. I am thankful to my PhD committee and external referees for their time and valuable feedback.

I am very grateful to the Animal house facility guys especially Sergio, Ilaria and Marta for managing the facility in a fantastic manner and providing animals. Ilaria, many thanks for extending your assistance always. I thank the Advanced Imaging Facility incharge- Giorgina and Sara for their time and support with the microscopes. Many thanks to the HTS facility people – Valentina, Michael and Pamela for assisting me with the bioanalyzer runs. Also am thankful to Dr. Gabriela Viero and her post doc Marta for the bioanalyzer runs at the FBK.

Immense thanks to Betty for organizing all the PhD events and helping making the bureaucratic processes very easy. Extended thanks to Giorgia Moser and Patrizia Paoli for help with the administrative procedures.

I thank all my dear batchmates–Annachiara, Dario, Steve, Natthakan, Toan, Cristiana and Vasundhara for making my PhD a very memorable time and for all the merriment. Also specially thankful to Debasmita (thanks for your love and fantastic company, for late nights in CIBIO, our never-ending blabbering, enjoyable experience with food and more food), Annachiara(thanks for your love, strong support, our endless talks and our CIBIO dinners), Dario(for being such an amazing companion at all times), Ruben and Kavitha (for your loving presence that included crazy and lovely moments that giving me tons of memories and support), Jacopino (for the immense fun and laughter) Steve (for your wonderful company, your car rides and for sharing joyful and troublesome times), Francesca and Tiziana for their wonderful uplifting spirit and love. Without any of you I would not have been able to get past difficult times.

My sincere thanks also goes to Prof Simona Casarosa and Dr. Andrea Messina for their initiative to establish the frog facility. I am thankful to Dr. Albrecht Haase for introducing me to the two-photon microscope and the fun imaging session. Tons of thanks to CIBIO management guys- Anna Helander, Paolo Struffi, Marco Adami and

Luca Andreetti for their invaluable help and immense support in managing lab life in CIBIO. My thanks to the Povo2 reception office team who aided in many aspects.

I would like to thank all the people in CIBIO for assisting me in many ways and for the enjoyable company.

And finally I would like to enormously thank my beloved family who are miles away and yet have always made me feel supported by their excellent virtual presence. I thank my dearest parents for their endless love and constant reassurance that made me believe in myself. Thanks to my dear brother who in countless ways has always cheered me up. My sincere thanks go to my parents-in-law for their love and encouragement. And last but not least, am very thankful to my loving husband for his strong support, trust, patience and confidence in me that enabled me to reach this stage.

Table of Contents

LIST OF FIGURES.....	10
LIST OF TABLES.....	13
LIST OF ABBREVIATIONS.....	14
ABSTRACT	17
CHAPTER 1: INTRODUCTION	18
1.1 AXON GUIDANCE	18
1.1.1 <i>Structure of a Growth Cone.....</i>	19
1.2 MECHANISMS OF AXON GUIDANCE	20
1.1.2 <i>Extra cellular matrix adhesion</i>	21
1.1.3 <i>Cell surface adhesion molecules.....</i>	22
1.1.4 <i>Canonical guidance cues.....</i>	23
1.1.4.1 Netrins.....	23
1.1.4.2 Semaphorins.....	27
1.1.4.3 Slits.....	29
1.1.4.4 Ephrins	31
1.1.4.5 Morphogens and growth factors	33
1.3 XENOPUS RETINO-TECTAL SYSTEM	34
1.3.1 <i>Formation of optic vesicle.....</i>	34
1.3.2 <i>Birth of retinal cells.....</i>	35
1.3.3 <i>Axonogenesis.....</i>	36
1.3.4 <i>Extension towards Optic Nerve Head.....</i>	38
1.3.5 <i>Optic chiasm.....</i>	39
1.3.6 <i>Optic Tract.....</i>	40
1.3.7 <i>Target termination and branching.....</i>	43
1.4 AXONS: SPECIALIZED SUB COMPARTMENTS OF NEURONS	50
1.4.1 <i>Need for local protein synthesis</i>	50
1.4.2 <i>Localization of protein synthesis machinery</i>	51
1.4.3 <i>Evidence of local protein synthesis in axons.....</i>	52
1.5 BIOGENESIS OF MIRNAS	59
1.5.1 <i>miRNA processing.....</i>	59

1.5.2	<i>miRNA induced silencing complex</i>	61
1.5.3	<i>Mechanisms of gene silencing</i>	62
	Target degradation	63
	miRNA-mediated translational repression	64
1.5.4	<i>Non-canonical miRNA biogenesis</i>	65
1.6	MIRNAS IN AXON GUIDANCE	66
1.6.1	<i>Long Range guidance</i>	66
1.6.2	<i>Fasciculation</i>	69
1.6.3	<i>Axon targeting</i>	70
1.6.4	<i>Axonal branching</i>	71
1.6.5	<i>miRNA profiling within axons</i>	72
1.6.6	<i>miRNA RISC machinery is present in GCs</i>	79
1.6.7	<i>Local roles of miRNA in outgrowth</i>	81
1.6.8	<i>Role for RNA binding proteins</i>	83
	RATIONALE	88
	HYPOTHESIS	90
	MOLECULAR HYPOTHESIS	91
	AIMS.....	93
	CHAPTER 2 : MIR-182 REGULATES SLIT2 MEDIATED AXON GUIDANCE	95
2.1	ABSTRACT:	95
2.2	MATERIALS AND METHODS	96
2.2.1	<i>Embryos</i>	96
2.2.2	<i>Morpholinos (MOs)</i>	96
2.2.3	<i>Electroporation</i>	97
2.2.4	<i>Retinal explant culture</i>	97
2.2.5	<i>Laser capture microdissection in vitro</i>	97
2.2.6	<i>Purity of axonal preparation</i>	98
2.2.7	<i>Laser capture microdissection in vivo</i>	98
2.2.8	<i>in situ Hybridization</i>	99
2.2.9	<i>ISH probes</i>	100
2.2.10	<i>Pathway analysis</i>	100
2.2.11	<i>Statistical analysis</i>	101
2.3	RESULTS	102
2.3.1	<i>miR-182 is expressed in photoreceptor layer in Xenopus retinal sections</i>	102

2.3.2	<i>Laser capture microdissection enables detection of miR-182 in RGC cell bodies and axons in vivo</i>	103
2.3.3	<i>miR-182 regulates axon targeting in optic tectum in vivo</i>	104
2.3.4	<i>miR-182 sensor can be used ascertain miR-182 activity and compartmentalized action</i>	108
2.3.5	<i>Slit2 silences miR-182 activity in RGC axons</i>	110
2.3.6	<i>Slit2 mediated decreased in miR-182 activity occurs via receptors Robo2 and 3</i>	111
2.3.7	<i>Slit2 stimulation does not lead to miR-182 degradation</i>	113
2.4	DISCUSSION	117
CHAPTER 3 MIR-181A/B IN XENOPUS LAEVIS AXONAL PATHFINDING		121
3.1	ABSTRACT	121
3.2	MATERIALS AND METHODS	122
3.2.1	<i>Embryos</i>	122
3.2.2	<i>Morpholinos (MOs)</i>	122
3.2.3	<i>Mimics</i>	124
3.2.4	<i>Electroporation</i>	125
3.2.5	<i>Optic pathway visualization</i>	126
3.2.6	<i>Quantification of aberrantly projecting axons</i>	126
3.2.7	<i>Blastomere microinjection</i>	127
3.2.8	<i>In situ hybridization</i>	127
3.2.9	<i>Retinal explant culture</i>	128
3.2.10	<i>Laser capture microdissection in vivo</i>	128
3.2.11	<i>Collapse assay</i>	129
3.2.12	<i>Immunohistochemistry</i>	129
3.2.13	<i>Statistical analysis</i>	130
3.2.14	<i>Microfluidic chamber</i>	130
3.2.15	<i>Imaging</i>	131
3.2.16	<i>Library preparation and sequencing</i>	131
3.3	RESULTS	133
3.3.1	<i>miR-181a/b are expressed by RGCs</i>	133
3.3.2	<i>miRNA processing and silencing machinery are present in axons and GCs</i>	134
3.3.3	<i>MOs successfully knockdown miR-181a/b</i>	137
3.3.4	<i>miR-181a/b loss of function causes misprojection of axons within tectum</i>	142
3.3.5	<i>miR-181a/b regulate GC responsiveness to specific chemorepellent cues – netrin1 and Sema3A</i>	145

3.3.6	<i>miR-181a/b loss-of-function mediated by MOs is specific to miR-181a/b.....</i>	150
3.3.7	<i>Impaired responsiveness of morphant GC to Sema 3A is specific to miR-181a and b.....</i>	153
3.3.8	<i>What are the molecular mechanisms employed by miR-181a/b to induce accurate RGC axon targeting?</i>	156
3.3.1.1.1	Sample collection with LCM:.....	157
3.3.1.1.2	Optimisation of library preparation and sequencing:	162
3.3.1.1.3	Identification of candidate miR-181a/b targets.....	164
3.4	DISCUSSION	169
3.5	FUTURE PERSPECTIVES.....	175
3.5.1	<i>Translatome profiling</i>	175
3.5.2	<i>Assessing local regulation of miR-181a/b.....</i>	176
	GENERAL DISCUSSION.....	179
	CONCLUSIONS AND FUTURE PERSPECTIVES	181
	APPENDIX.....	182
	REFERENCES	185

List of Figures

Figure 1-1: Cue mediated axon guidance.	18
Figure 1-2: Structure of the GC and schematic of GC components	19
Figure 1-3: Axonal GC is guided with the help ECMs that harbor cell adhesion and guidance molecules. .	21
Figure 1-4: Netrin1 is a crucial midline axon guidance cue in vertebrates, worms and flies	27
Figure 1-5: Different classes Semaphorins and their receptors.	29
Figure 1-6: Repulsion mediated roles of Slit in axon guidance.	31
Figure 1-7: Bi-directional signaling in ephrins and Ephs	32
Figure 1-8: Context dependent cellular response by Eph-ephrin interaction with different effectors.	32
Figure 1-9: Formation of the optic vesicle.	35
Figure 1-10: Retinal cells and their time of birth.....	36
Figure 1-11: RGC axonogenesis.....	37
Figure 1-12: Netrin1 and Laminin in combination help RGC axons to exit the eye.	39
Figure 1-13: Schematic depicting RGC axons at the chiasm.	40
Figure 1-14: Schematic showing RGC axons in the optic tract.....	43
Figure 1-15: Schematic of RGCs axons within the tectum.....	45
Figure 1-16: A somaless RGC axon of <i>Xenopus laevis</i> approaching the target, tectum.	50
Figure 1-17: Specific mRNAs are transported and translated in response to various guidance cues	58
Figure 1-18: pri-miRNA structure	59
Figure 1-19 : Pri-miRNA recognition by microprocessor complex	60
Figure 1-20: Reconstruction of human Dicer structure obtained from Cryo-electron microscope.....	61
Figure 1-21: Structure of human AGO2.	62
Figure 2-1: Schematic showing pathway width analysis.	101
Figure 2-2: Schematic of experimental paradigm showing stage 40 embryo sectioned for ISH	102
Figure 2-3: miR-182 ISH in stage 40 retinal sections.	102
Figure 2-4: Taqman RT-qPCR for miR-182 and snRNA-U6 in RGC and axons	104
Figure 2-5: Open brain preparation to analyse visual pathway defects.	105
Figure 2-6: Pathway analysis in co-MO and miR-182-MO.....	106
Figure 2-7: Quantification of pathway width.	107
Figure 2-8: Axon length measurement	107
Figure 2-9: Sensor construct design.	109
Figure 2-10: Detection of dGFP and mCherry.	109
Figure 2-11: Experimental paradigm to assess miR-182 activity upon Slit2 signalling	110
Figure 2-12: Quantification of miR-182 activity.....	111
Figure 2-13: Measurement of miR-182 activity.	112

Figure 2-14: Laser capture in vitro	115
Figure 2-15: In vitro axon purity test.....	116
Figure 2-16: Quantification of miR-182 by $\Delta\Delta$ CT method in LCM	116
Figure 3-1: MO directed against pre-miR-181a-1	123
Figure 3-2: MO directed against pre-miR-181a-2	123
Figure 3-3: Schematic of stage 40 embryo sectioned for ISH	133
Figure 3-4: Expression of miR-181a/b at stage 40.	134
Figure 3-5: Eye explant in culture	135
Figure 3-6: Amino acid sequences alignment between Ago2 mouse and <i>Xenopus laevis</i>	136
Figure 3-7: Expression of miRNA processing and silencing machinery	137
Figure 3-8: MO design for blocking pre-miR-181a-1 and a-2	139
Figure 3-9: MO against mature miR-181b	139
Figure 3-10: Microinjection mediated loss-of-function using MO to target the entire CNS.....	140
Figure 3-11: Electroporation offers spatial and temporal control towards MO injection.	141
Figure 3-12: Schematic of electroporation mediated loss-of-function.	141
Figure 3-13: ISH on electroporated embryos	142
Figure 3-14: Schematic showing open book preparation to visualize the optic pathway following loss-of- function.	143
Figure 3-15: miR-181-MO in vivo phenotype.....	143
Figure 3-16: Quantification of phenotype in miR-181-MO	144
Figure 3-17: Sema3A, Netrin1 and Slit2 expression in <i>Xenopus</i> brain at stage 40	145
Figure 3-18: Paradigm for Collapse assay	146
Figure 3-19 ISH showing knock down of miR-181a and b following microinjection of the MO.	147
Figure 3-20: miR-181 knock down in cut axons	147
Figure 3-21: PS dependent collapse response	148
Figure 3-22: Quantification of collapsed GCs in co-MO or miR-181-MO	149
Figure 3-23: Experimental set up for ISH following mimic electroporation.....	151
Figure 3-24: ISH for mimic validation.	152
Figure 3-25: Mimic expression in electroporated morphant eyes.....	153
Figure 3-26: Schematic for in vitro rescue experiment	153
Figure 3-27: Rescue of Sema3A responsiveness in morphants by miR-181a/b mimics.	154
Figure 3-28: miR-181a/b mimics rescue aberrant misprojection of morphant axons in vivo.....	155
Figure 3-29: Quantification of in vivo rescue.....	156
Figure 3-30: RGCs and axons labeled in vivo	158
Figure 3-31: Comparison of fast frozen vs fixed tissue	159
Figure 3-32: Diffuse EGFP signal in fast frozen tissue compared to fixed tissue.	159

Figure 3-33: Effect of sucrose length on RNA quality and Yield	160
Figure 3-34: Parameters of laser settings used to optimize cutting.	161
Figure 3-35: Comparison of different RNA extraction kits.	162
Figure 3-36: Model for miR-181 regulation of Gsk3 β and Crmp2	172
Figure 3-37: Microtubule loop in a paused GC.	173
Figure 3-38: Tools to assess local regulation of miRNA in axons	177

List of tables

Table 1.1.4.1: Expression of Netrin and its receptor in different organisms.	25
Table 1.1.4.2: Expression of different Slit and Robos in different species.....	30
Table 1.3.7.1: Table showing various cues involved in <i>Xenopus laevis</i> RGC axon guidance	46
Table 1.4.3.1: Cues regulating axonal mRNA translation.	54
Table 1.6.5.1: List of miRNAs enriched or depleted in axons, or present in GCs.....	73
Table 1.6.6.1: Reports of miRNA processing machinery in neurons.	80
Table 1.6.8.1: Summary of different miRNA roles in axon guidance	85
Table 1.6.8.2: Role of miRNAs in axons that promote outgrowth or elongation.	87
Table 2.3.1: Influence of fixative on the RNA quality and yield:	114
Table 3.3.5.1: The recombinant cues used for collapse	148
Table 3.3.8.1: Summary of Library preparation and reads obtained	164
Table 3.3.8.2: Transcriptome data from WT RGC, Axon ,co-MO and miR-181-MO	165
Table 3.3.8.3 Candidate mRNAs identified by their high Target Express scores	166
Table 3.3.8.4 Filtering candidates based on fold change	167
Table 3.5.2.1: List of products and catalogue numbers	182

List of abbreviations

µg	Microgram
AGO	Argonaute
ANOVA	Analysis of Variance
BDNF	Brain Derived Neurotrophic Factor
BMP	Bone Morphogenetic Protein
CAM	Cell Adhesion Molecule
cAMP	Cyclic Adenosine Mono Phosphate
CNS	Central Nervous System
Co-MO	Control Morpholino
Crmp2	Collapsin Response Mediator Protein 2
CSPG	Chondroitin Sulfate Proteoglycan
DCC	Deleted in Colorectal Cancer
dGFP	Destabilized Green Fluorescent Protein
Dpysl2	Dihydropyrimidinase-related protein 2
DRG	Dorsal Root Ganglion
DSCAM	Down Syndrome Cell Adhesion Molecule
ECM	Extra Cellular Matrix
EGFP	Enhanced Green Fluorescent Protein
FITC	Fluorescein IsoThioCyanate
FMRP	Fragile X Mental Retardation Protein
GC	Growth Cone
Gsk3β	Glycogen Synthase Kinase 3 Beta
HSPG	Heparan Sulfate Proteoglycan
ISH	In Situ Hybridization
L-15	Leibovitz L-15 Medium
LCM	Laser Capture Microdissection
LNA	Locked Nucleic Acid

mCherry	Monomeric Cherry
miR-181-MO	Mix of Morpholinos: pre-miR-181a-1,a-2 and miR-181 b
miRNA	Micro Ribo Nucleic Acid
MMP	Matrix Metallo Protease
MO	Morpholino
mRNA	Messenger Ribo Nucleic Acid
NGF	Nerve Growth Factor
NRP	Neuropilin
PEN	Polyethylene Naphthalate
PFA	Paraformaldehyde
pg	Picogram
PLXN	Plexin
POL	Polyester
Pre-miR	Precursor microRNA
Pri-miRNA	Primary micro RNA
qPCR	Quantitative Polymerase Chain Reaction
RGC	Retinal Ganglion Cell
RhoA	Ras Homolog A
RIN	RNA Integrity Number
RNA	Ribo Nucleic Acid
Robo	Roundabout
ROCK	Rho-associated kinase
RT	Reverse Transcriptase
SEM	Standard Error of the Mean
Sema3A	Semaphorin 3A
Shh	Sonic Hedgehog
snRNA-U6	Small Nuclear Ribo Nucleic Acid – U6 spliceosomal RNA
St	Stage

Syndig1	Synapse Differentiation-Inducing Gene 1
Tubb3	Tubulin 3
UNC5	Uncoordinated 5
UTR	Untranslated Region

Abstract

The highly complex nervous system is built upon an intricate network of neurons. In order to make a functional network, the establishment of precise connections is crucial. Neuronal networks are established early during development when neurons send out axons that navigate through complex environments to connect to their target. Chemotropic attractant or repellent cues, cell adhesion molecules, morphogens and a wide range of factors secreted or expressed by guidepost cells enable axon guidance. The leading tip of the axon, the GC is important to sense the environment and integrate extracellular signals to navigate precisely. The axonal GC has a large repertoire of mRNAs that are dynamic in nature. Local regulation of transcripts in navigating axons is suspected to ensure precise pathfinding. However, mechanisms involving regulation of expression of these transcripts within GCs are largely unknown.

This thesis investigates whether microRNAs, one of the quintessential posttranscriptional regulators, can regulate axon guidance by fine-tuning mRNA expression within subcellular compartments. To explore microRNA roles in axon guidance, *Xenopus laevis* visual system was used as a model. Profiling axons of retinal ganglion cells revealed the presence of miRNAs within axons. The most abundant axonal miRNAs, the miR-181 family and miR-182, exhibit distinct roles in regulating axon guidance *in vivo*. Loss of function analyses suggests that both miRNA families are required for accurate axonal targeting but involve different mechanisms. Thus, specific axonal microRNAs locally regulate mRNAs contributing to error-free pathfinding.

CHAPTER 1: Introduction

1.1 AXON GUIDANCE

During development, neurons send out a thread like process called axon that connects to distant target neurons or tissues. While reaching out to the target, axons are guided in a stepwise manner. Guidepost cells present along the way secrete or express chemotropic cues that guide axons to their targets. Axons thus avoid erroneous paths and navigate precisely. Once the right target is found, the axons branch out to eventually form synaptic terminals in the appropriate target area.

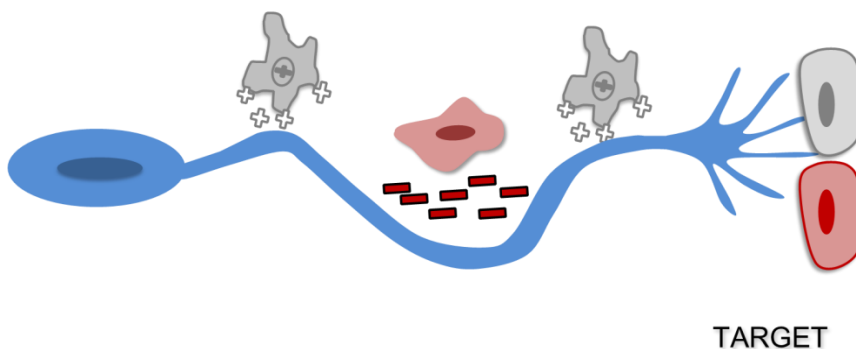


Figure 1-1: Cue mediated axon guidance.

Axons are tipped with highly motile structures called ‘growth cones’ that are equipped to sense and respond to the cues present in the environment (Figure 1-1). Growth cone (GC) membranes have receptors that can bind to the secreted chemo-attractive or repellent ligands enabling GC steering.

1.1.1 STRUCTURE OF A GROWTH CONE

GCs are comprised of two distinct regions: i) The central core which is composed of microtubules (known as the C domain) and ii) The peripheral region (the P domain) composed of actin rich filopodia and lamellipodia (Figure 1-2) (Vitriol & Zheng 2012).

Filopodia are slender cytoplasmic extensions composed of long actin filaments arranged in bundles while Lamellipodia are present between filopodia and are composed of short branched actin filaments. Both are dynamic and enable GCs to remodel their cytoskeleton upon encountering various cues facilitating GC steering (Dent et al. 2011).

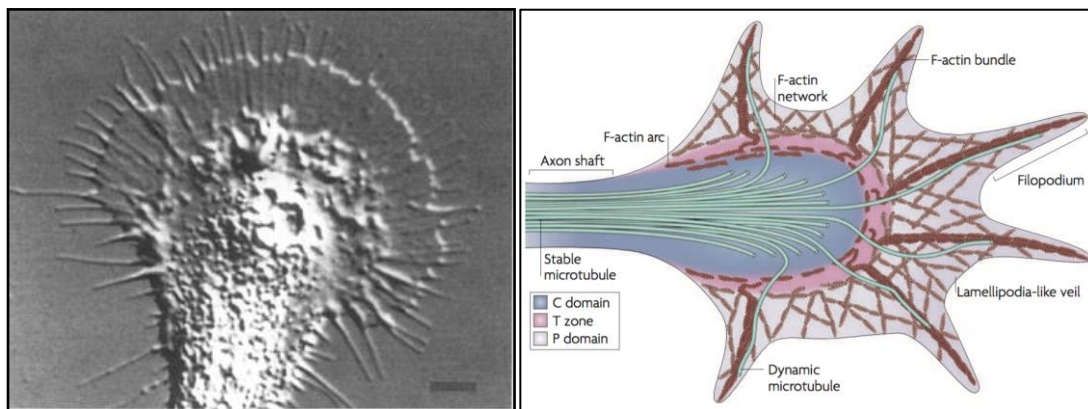


Figure 1-2: Structure of the GC and schematic of GC components
Courtesy- Principles of neural science, Kandel, 4th edition. GC components schematic adapted from Lowery, Van Vactor, 2009 (Lowery & Van Vactor 2009)

Filopodia can extend by means of addition of actin monomers into polymeric filaments. Studies in *Aplysia* and chick ganglion cells have given insight into understanding how the filopodia stimulates the GC to advance, turn or retract when it encounters specific cues mediated by the actin polymerization or depolymerization (Heidemann 1996; Suter & Forscher 2000; Lowery & Van Vactor 2009).

The central domain is not as dynamic as the peripheral region. It is a dense array of microtubules that extends from the axonal shaft and supports GC movement. The microtubule array within the C region facilitates transport of organelles and is also rich in mitochondria and membranous organelles (Vitriol & Zheng 2012; Hur et al. 2012). Between the P and the C region, lies the T zone (transition zone) which is composed of

actomyosin contractile structures (Figure 1-2). These structures play crucial roles in regulation of actin and microtubules in the GC.

As the axon progresses, the GC assumes different shapes and speeds depending on its position within the tract (Harris et al. 1987). These variations in shapes and speeds highlight GC dynamics and are suggestive of the molecular complexity of the pathway they grown on. In addition, GCs from the same axonal pathway differ with respect to age (Kim et al. 1991; Nordlander 1987). The shape also depend on whether the axons are pioneers or followers (Lopresti et al. 1973). Pioneer axons set up the first connection between a neuron and its target and they rely on guidepost cells to pathfind (Bentley & Caudy 1983). Follower axons, on the other hand, use the route previously set up by the pioneers as a scaffold in addition to being guided by cues (Pittman et al. 2008). Variations in morphology have also been attributed to differences in neuronal types (Nordlander 1987).

1.2 MECHANISMS OF AXON GUIDANCE

The observations that axonal outgrowth in embryos occur in a highly reproducible pattern and that axons have preferences of specific substrates *in vivo* implies that axons are actively guided by information in the surrounding environment (Raper & Mason 2010). The availability of biochemical, genetic and molecular techniques in the last 20 years facilitated the identification of molecules that promote and guide axons. These studies identified four major families of guidance cues: Netrins, Slits, Semaphorins and Ephrins (Alex L Kolodkin & Tessier-Lavigne 2011a). Additional molecules known to be involved in other developmental processes were later discovered to also have functions in neuronal wiring. These include cell adhesion molecules, morphogens and growth factors (Alex L Kolodkin & Tessier-Lavigne 2011a). Axon guidance processes may be viewed as a sequence of structured events that can permit the axon to grow, turn, retract or halt. Guidance cues can be chemotropic attractant or repellent in nature with long or short range of action (Tessier-Lavigne & Goodman 1996). There are several protein-protein

interactions facilitating guidance. The following section is a brief description of these guidance cues.

1.1.2 EXTRA CELLULAR MATRIX ADHESION

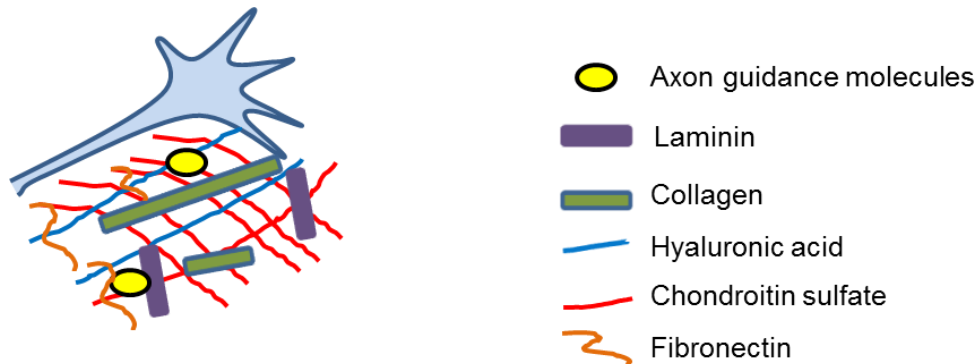


Figure 1-3: Axonal GC is guided with the help ECMs that harbor cell adhesion and guidance molecules.

The extra cellular matrix is a complex meshwork of various molecules. It consists mainly of chondroitin sulfate (CSPGs) and heparin sulfate proteoglycans, hyaluronic acid and a range of glycoproteins that are expressed in cellular interstices (Figure 1-3). The extra cellular matrix (ECM) also harbors many axon guidance molecules and serves as a substrate to which growing axons can adhere (Maeda 2015). ECM molecules such as the CSPGs are expressed by cells lining the axonal tract. For instance in the visual optic tract: CSPGs are expressed in pial surface, the neuroepithelium and in the neuropil (Walz et al. 2002) Laminin, another component of the ECM, is present within the vitreal surface to enable axons to exit the eye and enter into the optic nerve head (Höpker et al. 1999).

Heparan sulfate proteoglycans (HSPGs) are another type of ECM molecule that are expressed on cell surfaces (Irie et al. 2002). HSPGs contain a core protein and a highly sulfated glycosaminoglycan sugar chains that can bind to various growth factors, proteases and receptors (Irie et al. 2002). HSPGs have a large structural diversity owing to different post translational modifications that include the addition of sulphate groups to the sugar chains (Lindahl et al. 1998). Depending on the position of the sulfation on the sugar chain, HSPGs are named accordingly. These sulfations are carried out by sulfotransferases that transfer sulfate groups to specific sugar chain at specific Carbon

positions. HS2 sulfotransferase (HS2st), for example, transfers sulfate to C2 of the sugar chain (Lindahl et al. 1998; Irie et al. 2002). This distinct structure of HSPG with its discrete sulfation regions was found to be important for axonal pathfinding. In the mouse visual pathway, HS sulfation specifically on sugar residues at C2 or C6 directs RGC axons towards the optic chiasm (Pratt et al. 2006). Mice mutant for sulfotransferases HS2st or HS6st display a disorganized axonal bundle at the optic chiasm. Expression of these sulfotransferases coincides with Slit expression that prevents axons from invading inappropriate regions. Mice with mutant sulfotransferases have RGC axons that are less responsive to Slit2 and thereby lead to navigational errors. Thus different sulfations of HS side chains are important direct axons through the optic chiasm (Pratt et al. 2006).

1.1.3 CELL SURFACE ADHESION MOLECULES

Prior to the discovery of canonical guidance molecules, cell adhesion was thought of as a possible mechanism for axonal guidance. Indeed, cell adhesion molecules not only mediate axonal adhesion based roles but can also function as signaling molecules (Alex L Kolodkin & Tessier-Lavigne 2011b). Cell adhesion molecules (CAMs) belong to two large families that are involved in axonal pathfinding: 1) Immunoglobulin (Ig) and 2) Cadherin superfamilies. CAMs can function as ligands or receptors (Tessier-Lavigne & Goodman 1996). Some CAMs are expressed on neuronal membranes and can mediate homophilic interactions that permit axonal fasciculation. Ig CAM- FasciclinII, for example, is a glycoprotein expressed on a restricted subset of axons in grasshopper CNS neurons and drosophila motoneurons. Fasciclin II was found to be important for GCs of a specific neuronal subset to recognize, fasciculate and extend in a bundle. Thus, shown to be important for selective fasciculation (Lin & Goodman 1994; Harrelson & Goodman 1988). Some CAMs belonging to the Ig superfamily can function as heterophilic ligands or receptors involved in signaling functions. For example, DCC and Robo families are a part of the Ig superfamily that mediate guidance by signaling through Netrin and Slit ligands respectively. The role of CAMs belonging to the cadherin superfamily such as N-Cadherin were found to be important guidance molecules for chick optic axons. N-cadherin mediates cell to cell adhesion and is used as a guide molecule for migration of

optic axons on cell surfaces expressing N-cadherin. Chick optic axons only recognize N-cadherin and not E-cadherin for migration thus demonstrating specificity in the guidance mechanism (Matsunaga et al. 1988). Similarly, different other types of CAMs are known to promote axon outgrowth, guidance, target recognition and synapse formation. These are Receptor protein tyrosine kinases that include Ephrin receptors and Fibroblast Growth Factor receptors and Trk family of neurotrophin receptors (Tessier-Lavigne, Marc 1996).

1.1.4 CANONICAL GUIDANCE CUES

The relative distances that axons navigate are large. Error free connection to their targets is achieved by stepwise navigation (Tessier-Lavigne & Goodman 1996). Axonal trajectories are made up of short segments that terminate at a guidepost cell presenting guidance information. In addition, the first axons that reach their target, act as scaffolds for following axons. Advances in cell culture, biochemical studies and genetics uncovered canonical axon guidance cue families: Netrins, Slits, Semaphorins and Ephrins (Tessier-Lavigne & Goodman 1996).

The following section reviews some of these classically well-known guidance cues.

1.1.4.1 *Netrins*

Netrin is derived from the Sanskrit word called ‘Netr’ which means ‘the one who guides’ (Cirulli & Yebra 2007). Netrins are secreted proteins of ~600 amino acids that are related to the laminin family of guidance molecules (Tessier-Lavigne, Marc 1996). Both ligand and receptors for Netrin are highly conserved (Colamarino & Tessier-Lavigne 1995). Netrins mediate both chemotactic attractive or repulsive responses depending on the axonal type (Colamarino & Tessier-Lavigne 1995), the substrate (Höpker et al. 1999) and the receptor to which they bind (Keleman & Dickson 2001). Netrin1 may act as an attractant or repellent depending on the expression of Deleted in colorectal cancer (DCC), Down Syndrome Cell Adhesion Molecule (DSCAM) and Uncoordinated 5 (UNC5) on the responsive cell. Expression of DCC and UNC5 mediate repulsion while DCC and DSCAM mediate attractive response of Netrin1 (Lai Wing Sun et al. 2011).

These ligands are molecularly highly conserved and are known to be very important for midline crossing of axons (Table 1.1.4.1). Importantly, Netrin1 is not known to play a role in *Xenopus laevis* RGC axon crossing at the midline (optic chiasm). However it is present at the optic nerve head and is important for *Xenopus* RGC axons to exit the eye (Höpker et al. 1999) (Figure 1-4) (Reviewed in detail in section 1.3.4) and also important for RGC axons in tectal branching and synapse formation (Manitt et al. 2009).

Table 1.1.4.1: Expression of Netrin and its receptor in different organisms.

Guidance Cue	Cell type	Organism	Ligand type	Receptor	Cell type	(+/-)	Function	Reference
Netrin	Ventral floor plate of the developing spinal cord	Nematode	UNC-6	UNC-40	Ventral cord motorneurons and neuroblasts migrating longitudinally along epidermis	+	UNC-40 -important for ventral migration of cells by steering towards UNC-6	(Chan et al. 1996; Serafini et al. 1994)
				UNC-5	Pioneer neurons and Motorneurons	-	UNC-5- orients growing axons in a dorsal direction. Required for dorso ventral migrations of pioneer axons and migrating cells along the body wall of C elegans	(Ishii et al. 1992)
	Midline cells in the CNS	Drosophila	Netrin A and B	Frazzled	Commissural and longitudinal axons	+	Commissural and motor axons expressing Frazzled are attracted by Netrin at the midline	(Kolodziej et al. 1996; Harris et al. 1996; Mitchell et al. 1996)
				UNC-5	Subset of motor axons(Segmental nerve) that exit CNS without crossing midline	-	UNC-5 is expressed on a subset of motor axons that enable exiting CNS without crossing midline	(Keleman & Dickson 2001)

	Chick spinal cord floor plate	Vertebrates	Netrin-1 and 2	DCC and Neogenin	Spinal commissural axons	+	Expressed on spinal commissural axons and important for outgrowth of commissural axons towards netrin-1 in vitro	Keino-Masu et al.,1996, Kennedy et al.,1994,Serafini et al.,1994
				UNC-5	Xenopus spinal axons	-	Expression of Unc5 converts attraction of netrin1 to repulsion in Xenopus spinal neurons	Hong et al.,1999
	E11-E14 Mouse optic fissure and optic disc		Netrin1	DCC	Retinal Ganglion cell body and axons	+	Guides RGC axons to the optic disc	Deiner et al.,1997

(+/-) – (Attraction/ Repulsion)

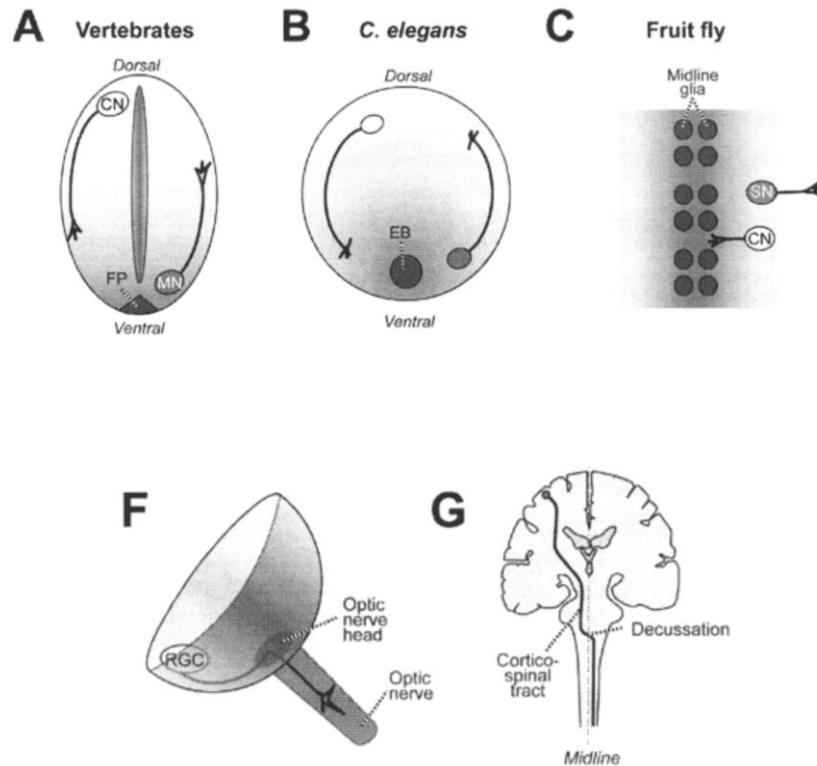


Figure 1-4: *Netrin1* is a crucial midline axon guidance cue in vertebrates, worms and flies
 Adapted from (Bagnard 2007). Abbreviations: Fp: Floor plate, MN: Motor Neuron, CN: Commissural
 neuron, EB: Epidermoblast, SN: Segmental nerve, RGC: Retinal Ganglion Cell.

1.1.4.2 Semaphorins

Semaphorins are a large family of cell surface and secreted molecules of approximately 500 amino acids (Alex L Kolodkin & Tessier-Lavigne 2011a). Semaphorins signal through the Plexin receptor families (Figure 1-5). Nine plexins have been identified in vertebrates (PLXN A1-A4, PLXN B1-B3, PLXN C1 and PLXND1) and two in invertebrates (Plexin A and B known as Plex A and Plex B). Plex A is a receptor for class 1 semaphorins (Sema1a and 1b) (Winberg et al. 1998) while Plex B is a receptor for Sema2a semaphorins (Ayoob et al. 2006) and in *Drosophila* both are known to control CNS and motor axon pathfinding (Winberg et al. 1998; Ayoob et al. 2006). In vertebrates, Sema3, Sema5 and Sema6 signal through PLXNA while Sema4 signals through PLXN B (Pasterkamp 2012). Sema3 also requires binding to Neuropilin which is a co-receptor. Neuropilin I are receptors for class III Semaphorins (Winberg et al. 1998). Neuropilin

(formerly known as A5 protein) was first shown in *Xenopus* optic tectum where the optic fibers terminate (Takagi et al. 1991; Takagi et al. 1987). Neuropilin-SemaIII/D has been shown to be important for axonal GC collapse in mouse Dorsal Root Ganglion neurons. Neuropilin deficient mice display abnormal trajectory and projection of spinal and cranial nerve fibers. In addition, GC collapse mediated by SemaIII/D is abolished in these homozygous neuropilin mutant embryos (Kitsukawa et al. 1997). A similar effect has also been observed in rat DRG using antibodies that block Neuropilin function and thereby prevent GC collapse (He & Tessier-Lavigne 1997). Neuropilin II on the other hand does not bind to SemaIII but binds to Sema A, Sema E and Sema IV (Takahashi et al. 1998; Chen et al. 1997). Thus specificity of Semaphorin signaling can also be attributed to the type of Neuropilin receptors expressed on the responsive cells. Interestingly, in *Xenopus* retinal ganglion cells (RGCs) Sema3A responsiveness is regulated by miR-124 through NRP1 expression. Knockdown of miR-124 results in delayed expression of NRP1 and insensitivity of axonal GCs to Sema3A (Baudet et al. 2012). This further results in axonal targeting errors *in vivo* (Baudet et al. 2012). Thus, highlighting the significance of receptor expression in the right time that can contribute to precise axonal pathfinding.

The binding of semaphorins activates downstream signaling molecules such as protein kinases, GTPases and cytoskeleton related proteins (Pasterkamp 2012). Although mainly thought to act as chemorepellents, Semaphorins can also mediate attraction. For instance, in rat cortical dendrites, Sema3A is a chemoattractant and mediates this response through soluble guanylate cyclase that directs dendrite outgrowth (Polleux et al. 2000).

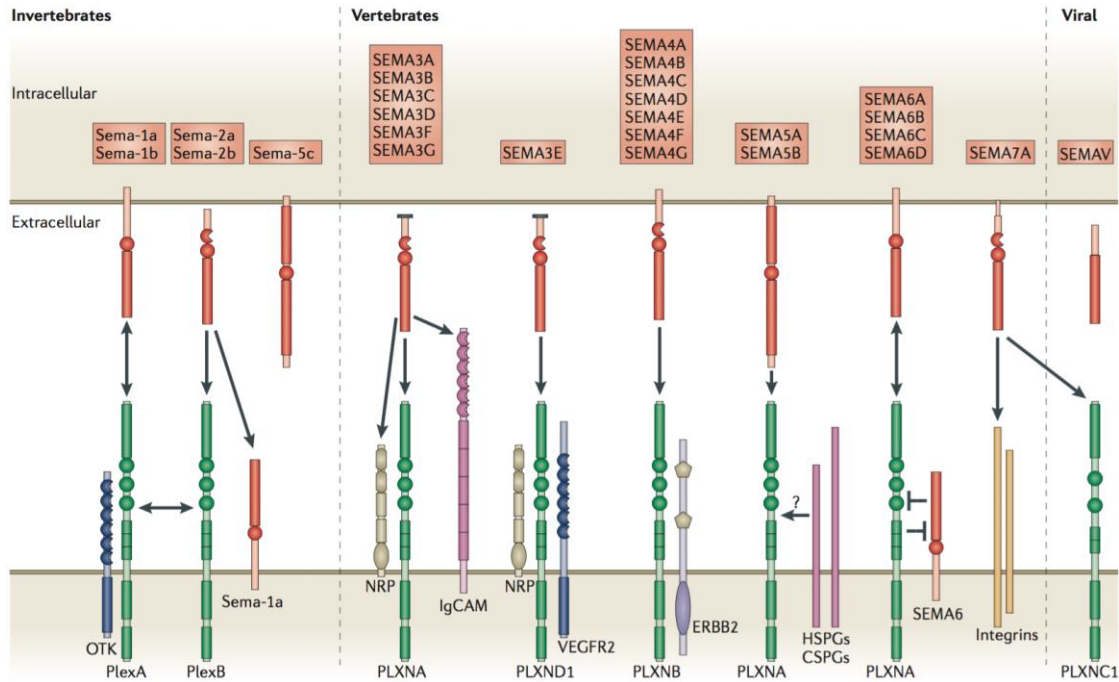


Figure 1-5: Different classes Semaphorins and their receptors.

Based on structure and phylogeny, semaphorins have been divided into eight classes and their distribution being: Sema1, 2 and 5 are present in invertebrates, Sema3-7 in vertebrates and SemaV found in certain DNA viruses. Adapted from (Pasterkamp 2012).

1.1.4.3 Slits

Slit proteins are a class of secreted glycoproteins that are chemorepellent in nature and signal through receptors of the Roundabout (Robo) family (Hutson et al. 2003). The Slit gene was first identified in drosophila following which several homologs were discovered in nematodes and vertebrates (Chédotal 2007). Slit is a repulsive cue that plays an important role in midline crossing in drosophila and *C.elegans* (Kidd et al. 1999; Rothberg et al. 1988; Hao et al. 2001). Midline is an important choice point as axons have to choose whether to cross over or stay ipsilateral. Slits prevent crossing of Robo-expressing axons while enabling crossing of non-Robo expressing axons only once (Hutson et al. 2003). This function is similar in the midline crossing axons in mammalian spinal cord where expression of Robo3 enables crossing of commissural axons at the midline (Sabatier et al. 2004). In vertebrates however, Slit prevents midline crossing

specifically in the mammalian forebrain and maintains the dorsoventral position of axonal projections (Bagri et al. 2002). In addition, within the visual system Slits prevent premature crossing of axons at the chiasm (Plump et al. 2002) (Figure 1-6). Each slit protein contains 4 Leucine-rich regions (LRR). The LRR regions of the Slit2 protein themselves are sufficient to bind to the Robo receptor, the downstream signaling of which confers the repulsive nature to these proteins (Chen et al. 2001). Slits mediate axon guidance in both vertebrates and invertebrates through largely repulsion-based mechanism.

Table 1.1.4.2: Expression of different Slit and Robos in different species.

Abbreviations: D-V: Dorso Ventral, A-P: Anterio-posterior, OB: Olfactory bulb, SVZ: Sub ventricular zone

Species	Slit	Receptor	Cell type	Function	Reference
C.elegans	SLT-1	SAX3	AVM sensory neurons	Acts in midline guidance along D-V and A-P axis	(Hao et al. 2001)
Drosophila	dSlit	Robo	Commissural axons	Expressed by midline glia and important as short range repellent for midline crossing and long range repellent for mesoderm migration from midline	(Kidd et al. 1999; Rothberg et al. 1988)
Vertebrates	Slit1,2,3	Robo1,2,3	Commissural axons, motor neurons, RGC layer	In mammalian forebrain, prevents midline crossing axonal growth into ventral regions, enables commissural axon crossing at the midline in spinal cord, prevent premature crossing at optic chiasm, control RGC pathfinding and targeting	(Brose et al. 1999; Itoh et al. 1998; Bagri et al. 2002; Sabatier et al. 2004; Chen et al. 2001; Plump et al. 2002; Ringstedt et al. 2000)

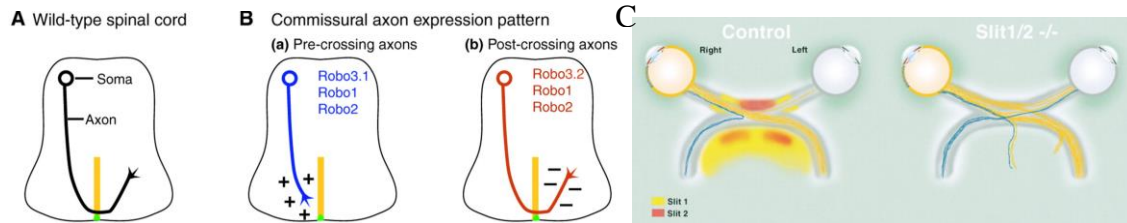


Figure 1-6: Repulsion mediated roles of Slit in axon guidance.

Fig (A): WT spinal commissural axon crossing. B) a) Pre crossing axons that express Robo receptors 1,2 and 3.1 are attracted by the midline. b) After crossing commissural axons are repelled by the midline (C) Displays requirement of Slit1 and 2 at the optic chiasm for RGC axons to project ipsilaterally. Slit1 and 2 double knockout mice exhibit misprojection in ipsilaterally projecting axons. Adapted from Ypsilanti et al.,2010 and Plump et al.,2002.

1.1.4.4 Ephrins

Ephrins are ligands that are tethered to the cell surface. Ephrins bind to Eph receptors that are the largest sub family of receptor tyrosine kinases (Klein 2004; Tessier-Lavigne, Marc 1996).

Ephrins are categorized into two subfamilies: Five classes of Ephrin-A and three classes of Ephrin-B (Alex L Kolodkin & Tessier-Lavigne 2011a). Ephrin-As are tethered to the cell surface via glycosylphosphatidylinositol (GPI) linkages and Ephrin-Bs are transmembrane proteins (Alex L Kolodkin & Tessier-Lavigne 2011a). The Ephrins mainly function as short range guidance cues (Alex L. Kolodkin & Tessier-Lavigne 2011). Upon binding to Eph receptor ephrins can initiate bidirectional signaling - reverse signaling in ephrin expressing cell and forward signaling in Eph receptor expressing cell (Egea & Klein 2007) (Figure 1-7).

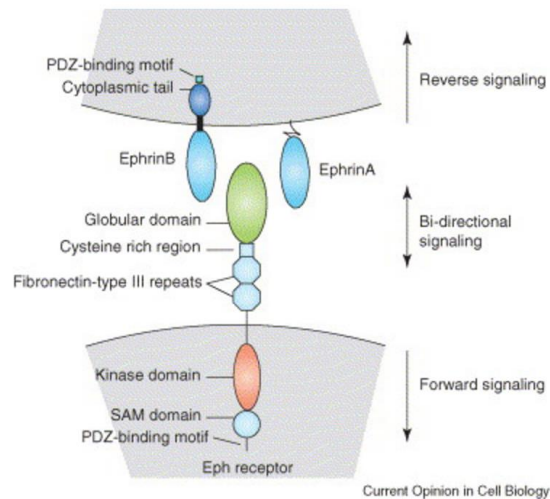


Figure 1-7: Bi-directional signaling in ephrins and Ephs
Adapted from (Klein 2004).

These cues can be attractant or repulsive depending on the downstream signaling cascade initiated (McLaughlin et al. 2003).

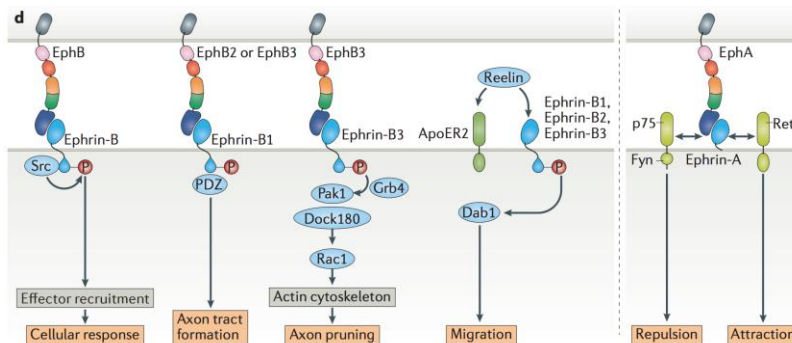


Figure 1-8: Context dependent cellular response by Eph-ephrin interaction with different effectors.
Adapted from Kania and Klein 2016 (Kania & Klein 2016)

Depending on the downstream effector molecules activated, Eph-ephrin interactions can mediate different biological functions (Figure 1-8). Ephrins have been implicated in axon guidance (Drescher et al. 1997), fasciculation of axons (axonal bundling) (Winslow et al. 1995) and topographic map formation (Yates et al. 2001; Nakamoto et al. 1996).

1.1.4.5 Morphogens and growth factors

Apart from classical guidance molecules several other factors are known to be important for axon guidance. These are growth factors – the Transforming growth factor β (TGF β) /Bone Morphogenetic Protein (BMP) family in addition to morphogens of the Sonic Hedgehog and Wnt signaling family (Alex L Kolodkin & Tessier-Lavigne 2011b).

BMPs are members of TGF- β superfamily. BMPs as axon guidance molecules have been studied in rat dorsal spinal cord. Commissural axons that are born in the dorsal spinal cord project towards the ventral midline and extend away from dorsal midline. The roof plate of spinal cord secretes BMP7 that acts as a chemorepellent for commissural axons thus preventing them from projecting towards dorsal midline (Augsburger et al. 1999; Yamauchi et al. 2008).

Morphogens belonging to Wnt and Sonic Hedgehog (Shh) family are commonly involved in cell fate determination and tissue patterning but they also have roles in axon guidance suggesting diversity in function. Shh has been shown to act as a chemorepellent in chick retinal ganglion cells at the chiasm. Over-expression of Shh on retinal explants leads to suppression of neurite outgrowth. Further ectopic expression of Shh leads to misprojection of RGC axons on the ipsilateral side (Trousse et al. 2001). Thus suggesting a role for Shh in axonal outgrowth and precise navigation at the chick optic chiasm. As opposed to its inhibitory role in RGC axons, Shh is required for chemo attractant activity of the rat spinal cord floor plate. This mechanism contributes to the projection of commissural axons towards the floor plate (Charron et al. 2003). Roles of Shh in *Xenopus* RGC pathfinding have been described in section 1.3.6.

Wnts are a family of ligands primarily involved in cell differentiation, proliferation, cell polarity and tissue morphogenesis (Yam & Charron 2013). However, several axon-guidance related roles have also been described. Wnt3, present within the chick optic tectum in a medial high to lateral low gradient is important for retinotectal mapping. Axons from the dorsal or ventral retina show different concentration dependent responses to Wnt3 and thereby form termination zones in the appropriate tectal area (Schmitt et al.

2006). In rodent spinal cord, Wnt4 is important for commissural axon extension within the spinal cord upon crossing the midline (Lyuksyutova et al. 2003). Similarly, Wnt5a alongwith its receptor, Ryk has important role within the mouse corpus callosum, a forebrain region where subsets of cortical axons project to contralateral side. Ryk knock out leads to an aberrant phenotype in post crossing axons. It leads to the formation of contralateral axon bundles, misrouting of axons back to the midline and also leads to defasciculation. Wnt5a expressed around the corpus callosum acts as a chemorepellent through Ryk to promote axon escape from the midline(Keeble 2006).

Thus, morphogens also play crucial roles by acting as chemorepellent or attractant in various contexts to promote precise axonal navigation.

In the following section, the model I used for exploring molecular mechanisms of axon guidance -the retino-tectal system, in *Xenopus laevis* is described.

1.3 XENOPUS RETINO-TECTAL SYSTEM

The *Xenopus* retino-tectal system is comprised of axons from the retinal ganglion cells located within the eye projecting towards the contralateral optic tectum in an orderly fashion and thus creating a topographic representation of the visual field. Some of the major steps involved in formation of this visual projection are described in the following section -

1.3.1 FORMATION OF OPTIC VESICLE

The optic vesicle is a result of lateral protrusion of the neural tube(Hollyfield 1973). Beginning at stage 17, the neural tube evaginates laterally to form the optic vesicle, which is composed of cells that will eventually differentiate into the retina(Hollyfield 1973). At stage 19, [the lens is formed and it fills the cavity of the eye vesicle(Hollyfield 1973).By stage 22, a distinct eye vesicle is formed which is connected to the neural tube by the optic stalk (Figure 1-9). By a process of invagination, the eye vesicle folds on itself to form a double walled eye cup (Figure 1-9) (Holt 1980) .The posterior portion of

the optic vesicle differentiates later on to form the pigment epithelium (Hollyfield 1973; Holt 1980).

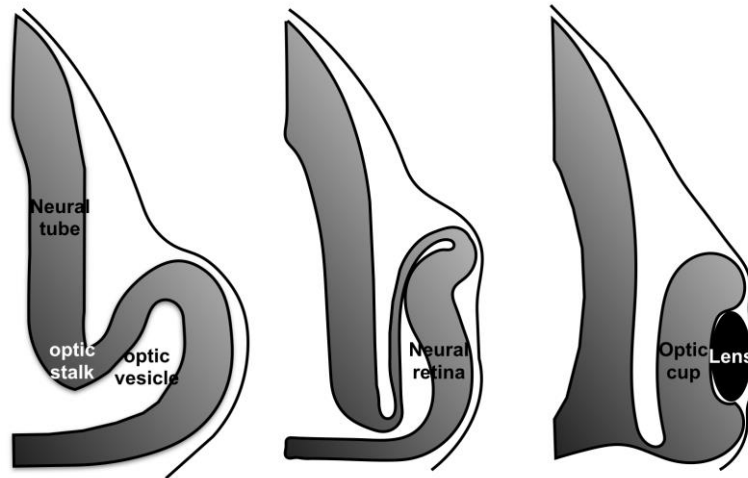


Figure 1-9: Formation of the optic vesicle.
Adapted from (Holt 1980).

1.3.2 BIRTH OF RETINAL CELLS

Post stage (st) 22, the cells of the retinal neuroepithelium undergo division to give rise to a collection of cells without being committed to a specific cell fate. Tritiated thymidine incorporation experiments and *in vitro* eye culture (Holt et al. 1988) demonstrate that by st 24-25 most of the dividing cells exit the cell cycle and become postmitotic and by st 37/38 most of the cells residing in different retinal layers are already born (Holt et al. 1988) It was also observed that there is only a subtle gradient in the way the cells are added to each layer (Holt et al. 1988)

Between st 25 and st 35/36 cells are born in all layers however, ganglion cells exit cell cycle first. RGCs are born at st 25 (shown as 1 in Figure 1-10), followed by photoreceptor cells at st 35. The inner layer is born next which is composed of Muller glia, bipolar cells and amacrine cells. The outer nuclear layer is composed of horizontal cells (Figure 1-10, 4) that are born after the amacrine cells (Figure 1-10, 3) The inner nuclear layer are the last to become post mitotic at stage 37/38 (Figure 1-10, number 5).

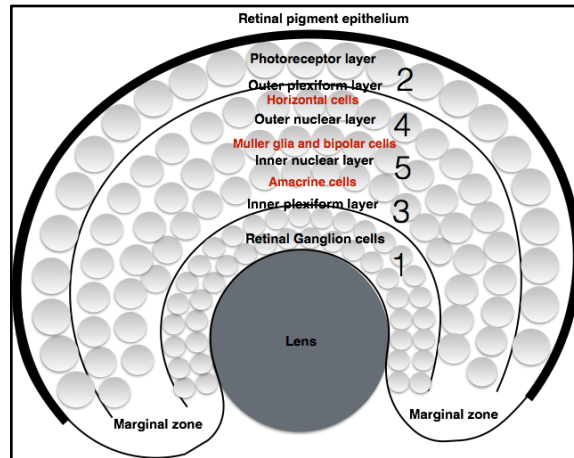


Figure 1-10: Retinal cells and their time of birth. Numbers depict order in which they are born. Illustration based on (Holt et al. 1988).

1.3.3 AXONOGENESIS

Retinal ganglion cells that are born at stage 25, remain indistinguishable from other cell types in the retina until they begin projecting axons (Holt 1989). Axons are initiated at stage 28 and are seen as darkly stained polarized protrusions close to the vitreal surface (Figure 1-11). Newly initiated axons are thick protrusions (4 μ m) compared to elongating axons (1-1.5 μ m) (Holt 1989). Different extra and intracellular factors have been shown to be important for axonogenesis. An example being integrins, that are cell surface receptors made of heterodimers α and β subunits. Integrins are expressed within RGC axons and mediate signaling upon interaction with ECM components specifically Laminin1 thus act as a link between plasma membrane and ECM (Dingwell KS et al. 2000). Laminin1 is expressed at the vitreal surface and promotes axon outgrowth via signaling through integrin receptors (Höpker et al. 1999). This is also observed in the zebrafish eye where laminin that is present at the basal surface of the retina mediates RGC axonogenesis (Randlett et al. 2011). Lilienbaum et al examined that *Xenopus* RGCs expressing chimeric chicken/*Xenopus* β 1-integrin receptor subunits exhibited a significant decrease in RGC axon outgrowth but did not impair GC steering. This showed that integrins are important for intra retinal growth of ganglion cell axons (Lilienbaum et al. 1995). Similarly, the role of cadherin in axon initiation was observed through the expression of a

dominant negative N-cadherin mutant in *Xenopus* retinal cells (Riehl et al. 1996). N-cadherin is a homophilic cell-cell adhesion molecule that is expressed widely in the CNS, including the eye primordia. Within the eye, it is expressed throughout the retinal layers and within RGC axons thus providing a substrate for axon growth (Simonneau et al. 1992; Riehl et al. 1996). Dominant negative N-cadherin disrupts the homophilic interaction, which is important for the outgrowth of RGC axons and dendrites. Misexpression of both β 1-integrins and N-cadherins severely impairs RGC axon outgrowth more than other retinal cells suggesting that their function is more specific in RGC axons these.

Some protocadherins have also been implicated in axon initiation in *Xenopus* RGCs. NF-protocadherin(NFPC) is expressed in the developing retina and is present abundantly in RGC axons. NFPC and its co-factor TAF-1 (Template activating factor) also present within RGC axons are important for axon outgrowth. TAF-1 is thought to play a role in downstream signaling from NFPC. Expression of dominant-negative NFPC or TAF1 exhibited severe impairment in RGC axon outgrowth (Piper et al. 2008). They also have a role in mediating axon extension (reviewed in the section 1.3.6 below) Similarly, for axonal outgrowth and extension, Fibroblast Growth Factors (FGFs), play important roles. RGC axonal GCs express FGF receptors and stimulation of these axons with basic FGF ligands in culture, increase neurite outgrowth suggesting a role for FGF in axon extension through the optic tract (McFarlane et al. 1995).

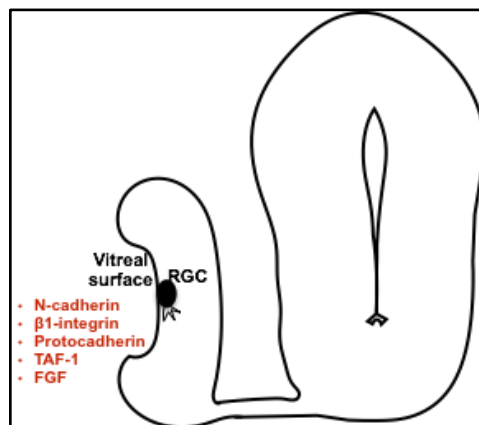


Figure 1-11: RGC axonogenesis.

Schematic of RGC sending out axon close to the vitreal surface. In red, are molecules important for this process.

1.3.4 EXTENSION TOWARDS OPTIC NERVE HEAD

In 1984, [³H]Proline was used to label growing retinal fibers and observations were made on the route taken by RGC axons to reach the tectum (Holt 1984): Dorsal retinal axons were the first to project towards the tectum. At stage 30/31 they reach the optic stalk, which connects the axons to the diencephalon. At stage 32, dorsal RGC axons reach the midline (the optic chiasm) and they then grow dorsocaudally along the rostral and lateral surface of the diencephalon. By stage 37/38, approximately 19 hours after leaving the eye, the dorsal RGC fibers reach the tectum. The RGC axons from the ventral retina lag 6 hours behind with respect to dorsal retinal axons and reach the tectum at stage 40 (Holt 1984). Grant et al. in 1980 also observed a similar time course of RGC projection using the silver staining technique (Grant et al. 1980). The following sections describe molecules that facilitate this journey to the tectum.

Post initiation of axons, through stages 28 and 29/30 (Holt 1984), axons grow ventrally along the vitreal surface and orient towards the optic nerve head (ONH). Upon leaving the retinal ganglion layer, axons extend towards the ONH. Netrin1 a soluble chemoattractant and laminin have a combinatorial role in enabling axons to exit the ONH (Höpker et al. 1999). Laminin is present at the retinal surface and not in the ONH (Figure 1-12), whilst Netrin and its receptor DCC are present in the cells of the ONH and optic nerve (Höpker et al. 1999). RGC axons show repulsive responsiveness towards netrin1 in presence of laminin. When axons move from the vitreal surface expressing laminin towards the ONH, the combination of laminin and netrin engages repulsive turning of axons towards the ONH. Netrin1 repulsion is turned into attraction in absence of laminin in the ONH. Axonal attraction towards netrin1 is facilitated by absence of laminin in the ONH thus permitting axons to move out into the optic tract (Höpker et al. 1999) (See Figure 1-12). Intracellular cAMP levels are known to be important for mediating attractive or repulsive turning responses of axons to cues. Reducing cAMP levels within GCs can convert attractant response to repellent in *Xenopus* spinal axons (Ming et al. 1997; Song et al. 1997). cAMP levels in *Xenopus* RGC axons decrease in the presence of laminin, thus converting Netrin1 attraction into repulsion, similar to spinal axons. In the absence of laminin in the ONH, Netrin1 induces a rise of cAMP thus mediating attractant

response and permitting axons to exit the ONH (Höpker et al. 1999). Interestingly, the cAMP level mediated Netrin1 repulsion also occurs when axons navigate through the optic tract (Shewan et al. 2002). This is described within section 1.3.5.

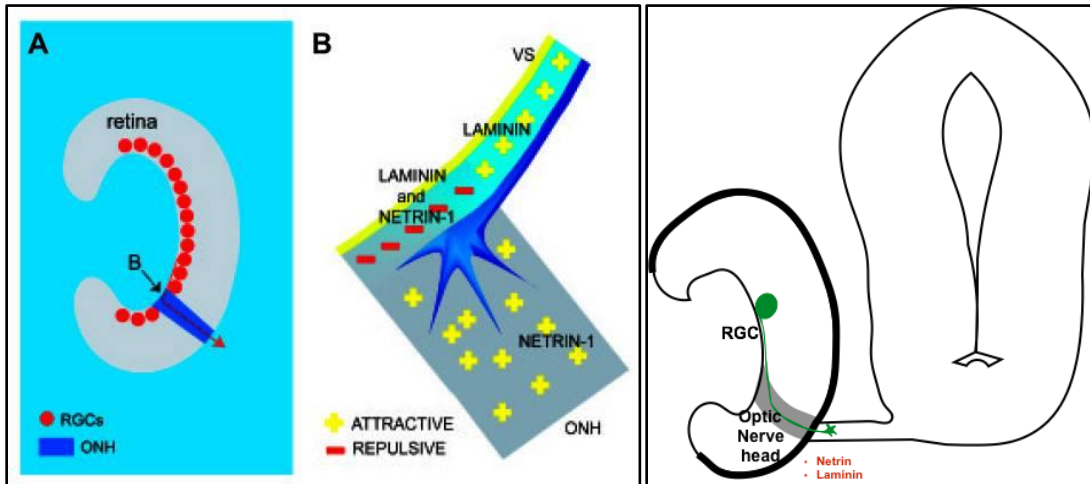


Figure 1-12: Netrin1 and Laminin in combination help RGC axons to exit the eye. Adapted from Mann et al.,2004 (Mann et al. 2004). A) Schematic showing retina with RGCs and the optic nerve head (ONH) in blue. B) Schematic depicting Netrin1 presence within the ONH and Laminin in the Vitreal surface. C) RGCs axons exit optic nerve head with the help of Netrin1 and laminin.

1.3.5 OPTIC CHIASM

RGC axons from the dorsal retina are the first to arrive at the optic chiasm at stage 32 (Holt 1984). The optic chiasm is a point where axons from both eyes decussate. Pre metamorphosis (stage 54), all RGC axons cross over to the contralateral side. Post metamorphosis, in order to establish binocular vision, a subset of axons project ipsilaterally upon reaching the optic chiasm. Nakagawa et al showed that Ephrin B is expressed at the chiasm at this metamorphic stage and not prior so as to enable axons to project ipsilaterally only post metamorphosis (Nakagawa et al. 2000). Different factors facilitate the growth of axons through the chiasm. Matrix Metalloproteases (MMPs) were found to be one of them, as loss of MMPs leads to stalling of axons at the chiasm (Hehr et al. 2005) MMPs are thought to act on the ECM to facilitate axonal forward movement. Hehr et al postulate that MMPs could cleave ECM in order to ease progression of axons forward. It is however unclear whether MMPs act within RGC GCs or in the substrate

through which they project (Hehr et al. 2005). Post chiasm, axons project towards the mid optic tract. In this region, they encounter the optic nerve from the contralateral eye, which is permissive to axon outgrowth. RGC axons bypass the contralateral eye and project dorsally towards the tectum. Rho Associated Kinase (ROCK) is thought to be important for this process. ROCK is expressed in a subset of *Xenopus* retinal cells and the appropriate expression levels of ROCK are thought to prevent axons from re-entering the contralateral eye (Cechmanek et al. 2015). Increased expression of ROCK in a subset of axons can cause misprojection into the contralateral eye. However, not all RGC axons are perturbed by ROCK over expression and project normally suggesting there are unknown mechanisms at play that facilitate extension of RGC axons post chiasm to the tectum.

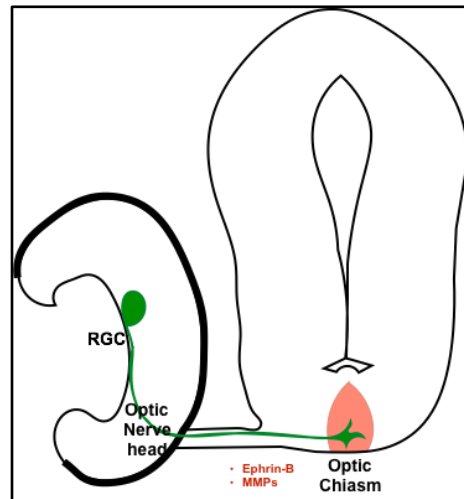


Figure 1-13: Schematic depicting RGC axons at the chiasm.

Cues Ephrin B in metamorphosing frogs enable ipsilateral projections and Matrix Metalloproteases help axons cross the chiasm by degrading the ECM to ease forward movement (Nakagawa et al. 2000; Hehr et al. 2005).

Axonal GCs are highly dynamic in terms of morphology as the axons progress through the pathway. At specific choice points such as the optic nerve head and chiasm, GCs increase in complexity (Holt 1989) suggesting there is a profound degree of molecular information available for the GCs to make directional choices.

1.3.6 OPTIC TRACT

Past the chiasm, retinal axons form the optic tract as they move within the diencephalon towards their target in the midbrain, the tectum. Axons extend towards the tectum following a direct course however some sharp bends occur in certain regions within the pathway. Within the optic tract, at the mid-diencephalic turn, axons make a 45° turn caudally as they progress towards the target (Holt & Harris 1998). The mid-diencephalic turn can be attributed to expression of repulsive cues: Slit1 and Sema3A that are expressed at the turn to promote axons towards the tectum (Atkinson-Leadbetter et al. 2010).

Some of the cues known to be involved in optic tract guidance include Chondroitin Sulfate (CS) proteoglycans, Sonic hedgehog, Netrin1, NF-Protocadherin, Slits and Semaphorins. Their functions are described in the following section. In the developing *Xenopus laevis* visual pathway, Chondroitin Sulfate (CS) proteoglycans are expressed throughout the optic tract and within the *Xenopus* retina. RGC axons extend through a CS rich environment in the tract. CSs are thought to be involved in guiding axons through the diencephalon to their target through cell adhesion mechanisms in addition to binding to guidance cues like Netrin1. Exogenous application of CS causes wide dispersion of axons from their normal trajectory and also decrease their rate of extension (Walz et al. 2002). This could be due to the fact that CSs have been reported to bind to cell adhesion molecules and growth factors and indirectly influence axon guidance (Walz et al. 2002; Yamaguchi et al. 1990; Grumet et al. 1993). Sonic hedgehog is another interesting morphogen that has roles in retinal axon guidance along the optic tract (Gordon et al. 2010) Shh is a repellent cue that is expressed at the ventral optic tract. RGC axons are found to extend through a ‘tunnel’ of Shh expressing tissue. This expression pattern is also similar in chick visual pathway (Trousse et al. 2001). Using cyclopamine to disrupt Shh signaling, several retinal guidance abnormalities were observed post chiasm. These abnormal phenotypes included an increase in RGC projection width along the optic tract, defasciculation of RGC axons, misprojection of axons into the neuroepithelium and tectal targeting errors (Gordon et al. 2010). Shh therefore is very crucial for RGC axon navigation through the optic tract (Gordon et al. 2010). In addition to Shh and CS,

Netrin1 is thought to be important in restricting axons within the optic tract. Axons from older stages (post stage 24) namely stage 32- 37/38, which roughly corresponds to the period in which axons project through the chiasm to tectum, show repulsive responses to Netrin1 (Shewan et al. 2002). This is in contrast to axons exiting the eye (Höpker et al. 1999). This switch in responsiveness from attraction at younger stages to repulsion is a cell-intrinsic age-related phenomenon as opposed to environmental influence. Interestingly, it is correlated with lower cAMP activity. As mentioned in the earlier section, lower cAMP levels are associated with repulsive behavior towards Netrin1 (Ming et al. 1997). In addition, the expression of receptors DCC and A2bR (Adenosine receptor type 2b) implicated in transducing Netrin1 signaling are known to influence cAMP levels. DCC and A2bR decline with age thus contributing to a repulsive response (Shewan et al. 2002). Unc5, is a known Netrin1 receptor that mediates repulsion in various other species. However, in *Xenopus*, RGCs are not known to express Unc-5 (Hong et al. 1999).

Axon extension is furthermore assisted by cell adhesion molecules specifically, NF-Protocadherin. NFPC mediates homophilic interaction within the optic tract that also expresses NFPC, to extend axons from the mid-diencephalon towards the tectum. Interestingly, Sema3A is also involved in promoting NFPC interaction and thereby guiding axons. Loss-of-function of NFPC leads to stalling of axons within the tract specifically at the caudal turn, the point in the pathway where axons make a 45° turn. Sema3A, expressed at this turn stimulates translation of NFPC within RGC axons to promote the cell adhesion between the extending axons and the substrate (Leung et al. 2013).

The mid diencephalon is also receptive to Slit receptors Robo2 and 3 expressed within RGC axons. Slit1 present in the mid-diencephalon mediates signaling through Robo2 and 3 to enable axon extension (Hocking et al. 2010).

Interestingly, both Slit1 and Sema3A expression in the mid-diencephalon are maintained by the expression of FGFs (Atkinson-Leadbetter et al. 2010). Inhibition of the FGF receptor leads to a reduction in Sema3A and Slit1 levels resulting in RGC axons being

arrested at the mid-diencephalon. FGFs, thus, play a role in maintaining guidance cue expression by regulating their transcription (Atkinson-Leadbeater et al. 2010).

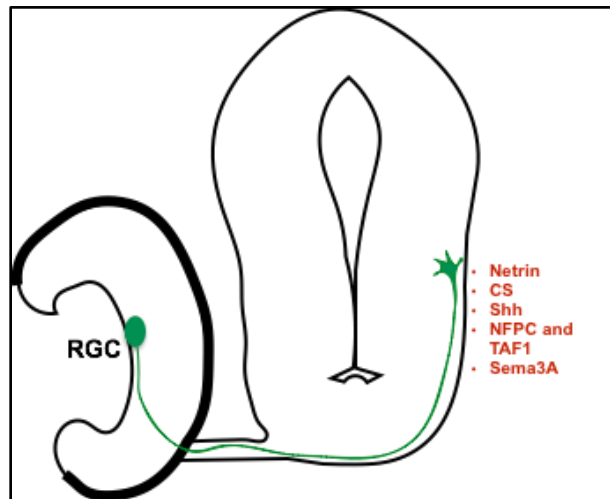


Figure 1-14: Schematic showing RGC axons in the optic tract

Target recognition: As axons approach the tectum, their speed decreases (Harris et al. 1987). Average axonal speed is reported to be about 52 $\mu\text{m}/\text{h}$ and as the GCs approach the tectum it decreases to 16 $\mu\text{m}/\text{h}$ and is followed by terminal branching (Harris et al. 1987). As noted earlier, the morphology of the axonal GCs changes as they approach the tectum. Characterized by large GCs with many lamellipodia, the GCs assume an overall more complex shape than when they are moving forward within the optic tract (Harris et al. 1987). This is due to the fact that the optic tract has several cues (as mentioned in the above section) and the complex morphology of GCs is correlated with actively sensing of cues and forward movement within the tract. While once, the GCs approach the tectum, several chemorepellent cues stall the movement and thereby lowering GC speed and change in shape.

1.3.7 TARGET TERMINATION AND BRANCHING

The arrival of the axons at their target triggers formation of a complex set of arbors forming the terminal branches on the axon shaft. These terminal branches are often formed behind the GC (Harris et al. 1987). Initiation of the terminal branch results in change in the morphology of the leading GC as it reduces in size and becomes one of the

branches (Harris et al. 1987). The drastic change in morphology and speed of these GCs is due to the diverse molecular terrain. Several factors that are present along the optic tract and enable axons to propel forward are no longer expressed at the anterior border of the tectum thus changing axon shapes and slowing down their movement. FGF and FGF2-binding heparin sulfate (HS) are examples to this point. Exogenous FGF or HS cause retinal axons to veer off their target (McFarlane et al. 1995) and axons abruptly bypass the tectum and project ventrally or dorsally around it. The optic tract is surrounded by regions expressing different FGF receptors (Atkinson-Leadbetter et al. 2010) in addition to retinal GCs themselves (McFarlane et al. 1995).

The importance of heparan sulfate proteoglycans have been mentioned in an earlier section(1.1.2). HSPGs are also involved in precise targeting of RGC axons in the *Xenopus* optic pathway. Exogenous addition of HS causes severe targeting errors and leads to axons to entirely bypassing the tectum (Walz et al. 2002), a phenotype similar to inhibiting sulfation of HS (Irie et al. 2002). In addition, sulfotransferases, HS2st and HS6st are expressed broadly within the tectum and along the border of the dorsal optic tract respectively. This suggests that a specific HS sequence and its sulfation is important for retinal axon targeting (Irie et al. 2002).

Cues present within or around the tectum also enable axons to stall and form branches. Interestingly, Netrin-1 has roles in retinotectal development wherein signaling mediated through its receptor DCC helps axons to differentiate into pre-synaptic sites and initiate branches at the tectum (Manitt et al. 2009).

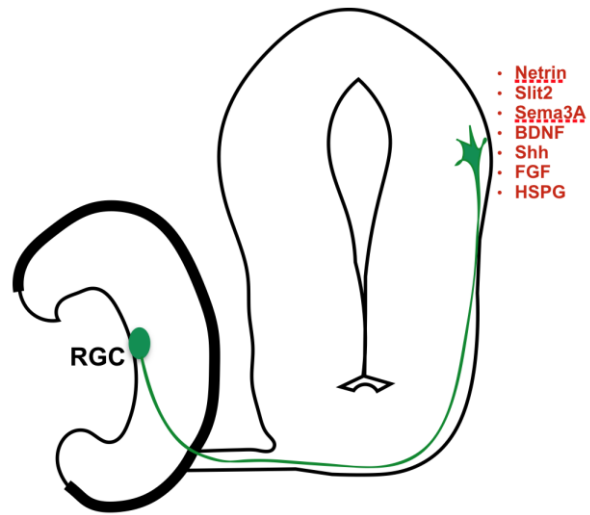


Figure 1-15: Schematic of RGCs axons within the tectum.
 Abbreviations: FGF: Fibroblast Growth Factor, BDNF: Brain Derived Neurotrophic Factor, Shh: Sonic Hedgehog, HS: Heparan Sulfate Proteoglycans

Table 1.3.7.1: Table showing various cues involved in *Xenopus laevis* RGC axon guidance

Cue	Receptor	Region of expression	Stage of detection	Role	Reference
Netrin1	Dcc	Neural plate, optic vesicle, Midbrain-hindbrain boundary	St 12- St 19	Induces DCC mediated attractive turning and GC complexity <i>invitro</i>	(De La Torre et al. 1997)
		Ventral eye primordium in the presumptive Optic Nerve head and optic stalk, Ventral midline	St 27, 28		
	A2bR	Dorsal and ventral diencephalon, Posterior tectum	St 39	Exit into optic nerve ; Responsiveness of GCs switch from attraction to repulsion	(Shewan et al. 2002; Höpker et al. 1999)
	Dcc	Tectal neurons	St 44-45	Axonal branching and synaptogenesis	(Manitt et al. 2009)
	Dcc, Unc-5	Optic tectum, Ventral high-dorsal low along ventricle wall	St 45	Pre- and post - synaptic arbor morphology (RGC and tectal neurons)	(Nagel et al. 2015)
				St 40	Axonal branch initiation, induce back branching

Cue	Receptor	Region of expression	Stage of detection	Role	Reference
Sema3A	Plexin1/2/3, Neuropilin1	Midbrain optic tract, Ventral border of the optic tectum and caudal midbrain (posterior tectum)	St33/34- St 41	Nrp1 mediates Sema3A response in GCs from st 35/36. Sema3A elicits branching post 1 hr	(Campbell et al. 2001)
			St 40	Induces NFPC expression within RGC axons and enables axonal growth from mid-optic tract to tectum	(Leung et al. 2013)
Slit2	Robo2	Inner plexiform layer of the eye, Dorsal midline, anterior and posterior margin of tectum.	St 40	Activates translation regulators and MAP kinases in RGC GCs.	(Piper et al. 2006)
		Ciliary margin and retinal pigment epithelium; Amacrine cells at St 45	St 28; St 45		(Chen et al. 2000)

Cue	Receptor	Region of expression	Stage of detection	Role	Reference
Slit1	Robo1 and 2	Floor plate of neural tube, RGC layer - weak expression	St 30-35	Slit2 promotes dendrite branching and complexity in vitro. Robo 2 and 3 important for RGC axon extension and guidance	(Hocking et al. 2010)
Slit2	Robo1 and 2	Floor plate and roof plate, proliferative ciliary margin zone ; INL	St 35-36; St 37/38		
	Robo1,2,3	Robo1 not expressed in retina; Robo2 expressed widely in Ganglion cell layer; Robo3 light staining in GCL in St 33/34 but not St 37/38	St 33/34- St 40		
Slit1/Slit2	Robo1 and 2	Ventral diencephalon. Expression in the retina is widespread, including the RGC layer	St 33/34- 37/38		(Atkinson- Leadbeater et al. 2010)
ephrinB1	EphB1	IPL, OPL and INL in the eye. Also present in Optic nerve head. Dorsal optic tectum in area devoid of visual input	St 28-40	Important for ipsilateral projections	(Mann et al. 2002; Nakagawa et al. 2000)
ephrinB2	EphB2	RGC and IPL (more dorsal and less ventral), dorsal midline of the tectum	St 28-40		(Mann et al. 2002)

Cue	Receptor	Region of expression	Stage of detection	Role	Reference
ephrinB3 and B4	Eph B3 and B4	Present in all retinal layers. Ephrin B3 is expressed more in dorsal retina while ephrin B4 is expressed more in ventral retina. ephrinB3 is present high in tectum without D-V gradient	St 28-40		(Mann et al. 2002)
Chondroitin sulfate proteoglycans		Optic tract	St 37/38	Important for RGC axon guidance along the optic tract	(Walz et al. 2002)
Laminin	Integrin	Vitreous surface of the optic disk	St 37/38	Enables RGC axon to exit from the eye	(Höpker et al. 1999)
Sonic Hedgehog	Patched 1 and Smoothed	Ventrally adjacent to the optic tract and optic chiasm.	St 32- 38	Important for RGC axon guidance within optic tract and for targeting in tectum	(Gordon et al. 2010)
NF-Protocadherin (NFPC)	NFPC (homophilic interaction)	Caudal turn, Mid-dorsal optic tract, neuroepithelium and RGC axons	St 40	Important for axon growth and turning along mid optic tract. NF-PC is regulated by Sema3A-NP1	(Leung et al. 2013)

1.4 AXONS: SPECIALIZED SUB COMPARTMENTS OF NEURONS

Experiments in chick sensory ganglia *in vitro* (Hughes 1953; Shaw & Bray 1977) and *Xenopus laevis* retinal ganglia *in vivo* (Harris et al. 1987) demonstrate that a growing axon separated from its cell body does not regress and die. The isolated axons instead continue to grow and extend for up to 3 hours and reach their target *in vivo* precisely without any errors. They are also capable of forming branches in the tectum (Harris et al. 1987). This suggests that the ability of the axon and its GC to sense its environment and respond to various cues is present locally and its pathfinding behavior is largely autonomous without the involvement of the soma.

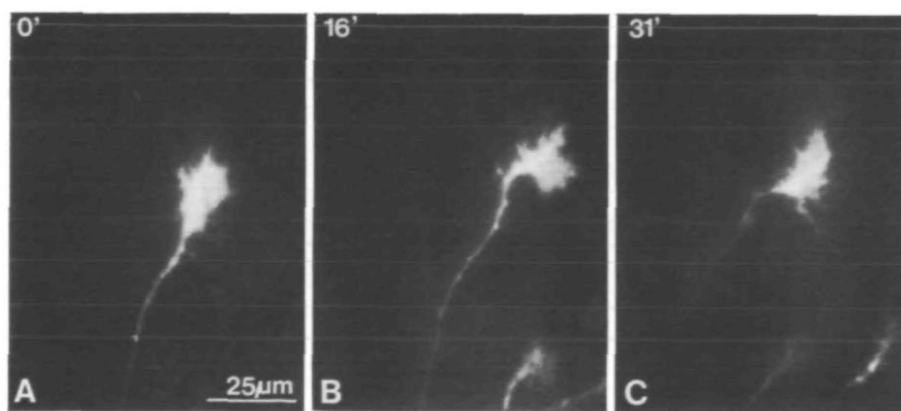


Figure 1-16: A somaless RGC axon of *Xenopus laevis* approaching the target, tectum. As the GC approaches the target(A), it abruptly turns and its morphology becomes more complex (B, C). Adapted from Harris et al., 1987 (Harris et al. 1987)

1.4.1 NEED FOR LOCAL PROTEIN SYNTHESIS

In order for axons to be autonomous from their cell bodies they require the machinery to respond to a cue-filled environment and modify their cytoskeletal apparatus to steer towards or away from such cues. Indeed the GC of axons contains all the machinery needed for local protein synthesis (Campbell & Holt 2001). Interestingly, growing axons contain a large repertoire of mRNAs, which is dynamic in nature and changes over the course of development (Zivraj et al. 2010)– The advantages of local protein synthesis are manifold: 1) mRNAs that need to be expressed at specific time points can be stored locally at the GC and kept translationally silent until needed. Upon cue exposure, specific mRNAs can be translated when required (Yao et al. 2006; Leung et al. 2006) 2) Proteins

that are required for the growing tip of the axon can be synthesized only at the GC instead of having ectopic expression, and possibly spurious activity where not needed, in other parts of the cell included during protein transport (Jung et al. 2012) 3) By using the 3'UTR of mRNAs as zipcodes, different populations of mRNAs can be transported to different parts of the cell without changing the protein structure or function they encode (Jung et al. 2012). 4) Within the GC itself, asymmetrical protein synthesis may be important for directional steering (Leung et al. 2006).

Early studies in 1967 and 1968 demonstrated that axons without soma could carry out protein synthesis in both vertebrate and invertebrates. These studies employed radioactive labeling of amino acids in addition to protein synthesis inhibitors (Giuditta et al. 1968; Koenig 1967) and demonstrated that protein synthesis occurs in axons. However, it is still unclear how specific mRNAs are translated locally in the axons.

1.4.2 LOCALIZATION OF PROTEIN SYNTHESIS MACHINERY

Using more sensitive biochemical approaches evidence for the presence of ribosomal RNA, mRNAs and actively translating polysomes was discovered in giant squid axoplasm (Giuditta et al. 1986; Giuditta et al. 1980; Giuditta et al. 1991). Electron microscopy revealed the presence of polyribosomes at the base of dendritic spines in the dentate gyrus of the rat hippocampus. The selective localization of polyribosomes gave rise to ideas that local protein synthesis of cytoskeletal elements could be undertaken for modulating spine activity, size or shape (Oswald Steward, Levy 1982). As opposed to dendrites, evidence for presence of ribosomes in axons was restricted to only the axonal initial segment but not throughout the axonal length in the mature nervous system (Palay et al. 1968; Steward & Ribak 1986). The axonal initial segment is a post-synaptic site for inhibitory synapses. The inability to detect ribosomes in mature axonal GCs combined with the prevalent notion that ribosomes could be only detected on post-synaptic sites suggested that pre synaptic sites or GCs may not possess protein synthesizing machinery. In embryonic axons, Tennyson observed in 1970, clusters of ribosomes in the entire length of embryonic rabbit dorsal root ganglion axons alongwith endoplasmic reticulum,

mitochondria and neurofilaments using electron microscopy. Further, electron microscopy identified the presence of ribosomes in mammalian embryonic cortical axons (Bassell et al. 1998). This study also showed that cue-regulated isoform specific beta-actin mRNAs are transported to axons (Bassell et al. 1998).

1.4.3 EVIDENCE OF LOCAL PROTEIN SYNTHESIS IN AXONS

Campbell and Holt first demonstrated a functional need for local protein synthesis in axons in *Xenopus* retinal ganglion cell axons in 2001. This study showed that axons separated from their soma employ protein synthesis in order to have a turning response to chemotropic gradient of Netrin1 and Sema3A. When translation is inhibited, the response of GCs towards these cues is abolished. It was thus shown that guidance cues elicit local protein synthesis, as seen by a marked increase in translation initiation factors. There have been other means of demonstrating local protein synthesis in axons. For example, using compartmentalized chambers known as the Campenot chamber (originally developed in 1977) it was possible to show that local protein synthesis takes place in axons (Eng et al. 1999) Furthermore, several axonally localized mRNAs encoding for various guidance cue receptors were shown to be translated in growing axons in order to enable axons response to cues by stimulating local protein synthesis (Brittis et al. 2002).

Very interestingly, Leung et al (Leung et al. 2006) and Yao et al (Yao et al. 2006) revealed that when *Xenopus laevis* retinal and spinal neuronal GCs are stimulated with a gradient of Netrin-1 or BDNF, β -actin mRNA is rapidly transported to the side of the gradient and translated locally within axons in an asymmetric manner. If protein synthesis is blocked the attractive turning response of the GC towards the cue is abolished. It was also shown that β -actin mRNA is transported with the help of an RNA binding protein, ZBP-1 that binds to the 3'UTR of the mRNA and prevents its translation until cue stimulation (Yao et al. 2006). The translation of this mRNA is very specific to the cue exposed as this response is not observed upon stimulation of other cues like Sema3A or Slit2

Interestingly, cue dependent protein synthesis is strongly related to the concentration of the extracellular cue. Very high concentrations of the cue do not elicit protein synthesis within GCs suggesting a physiological role for this phenomenon (Nedelec et al. 2012).

Apart from embryonic period, axonal mRNA localization in response to neurotrophins or guidance cues has been seen also in adult sensory axons. Willis et al showed that NGF, BDNF and NT-3 regulate mRNA levels in adult rat DRG axons and use distinct signaling cascades to localize individual mRNAs. In addition expression levels of different mRNAs are regulated by different cues like Sema3A and are distinct from that of the neurotrophins (Willis et al. 2007). Proteomic analysis shows that the treatment of BDNF or NGF selectively increases translation of cytoskeletal mRNAs (Willis 2005) (Table 1.4.3.1).

Table 1.4.3.1: Cues regulating axonal mRNA translation.

Reference	Model Organism	As seen by	mRNA translated	Cue involved in translation	RNA Binding protein	Function
Koenig et al.,1965(1)	Cat hypoglossal and cervical synpathetic nerve	Acetyl choline esterase assay with inhibitors for AChE and PS	-	-		
Edstrom 1966	Goldfish Mauthner neuron					
Koenig et al.,1967	Rabbit intracranial spinal accessory nerve root	[3H] Leucine incorporation	-	-		
Giuditta et al.,1968	Squid	Incorporation of radioactive C14 labeled amino acids and inhibited by PSI				
Davis et al.,1992	Snail	[3H] Leucine labeled amino acid incorporation and inhibition by PSI				
Campbell et al 2001	Xenopus RGC	Cut axons and use of PSI	eIF4E and eIF-4EBP1	Sema3A, Netrin1		GC collapse

Lee et al.,2003	Sympathetic neurons	Cut axons with incorporation of radioactive ³⁵ S and use of PSI	b-actin,Actin depolymerizing factor, Neurofilament	NGF		
Wu et al.,2005	Rat DRG	Cut axons	Rho A	Sema3A	-	GC collapse
Willis et al.,2005	Adult rat DRG	Porous Membrane	β-actin, vimentin,peripherin	NGF, BDNF		Axon regeneration
Hengst et al.,2006	Rat DRG	Campanot chambers	Rho A	Sema3A		GC collapse
Leung et al.,2006	Xenopus RGC	Cut axons	β-actin	netrin-1	ZBP-1	GC turning
Yao et al.,2006	Xenopus spinal neurons	Focal laser induced photolysis	β-actin	BDNF	ZBP-1	GC turning
Piper et al.,2006	Xenopus RGC	Cut axons and use of PSI	cofilin	Slit2	-	GC collapse
Cox et al.,2008	Mouse and rat DRG	Boyden chamber	CREB	NGF		Neuronal survival
Yan et al.,2009	C.elegans	Cut axons	CEBP-1		Dlk1	Axon regeneration

Hengst et al.,2009	Rat DRG	Microfluidic Chambers	Par3	NGF, netrin-1		Axonal outgrowth
Aschrafi et al.,2010	Rat SCG	Campenot chambers	CoxIV	NGF		Axon elongation
Andreassi et al., 2010	Rat sympathetic neurons	Compartmentalized chambers	Impa1	NGF		Axonal maintenance
Nie et al.,2010	Mice RGC	Boyden chamber	-	Ephrin A		Axon guidance
Aschrafi et al.,2012	Rat SCG	Campenot chambers	CoxIV and ATP5G1	NGF		Axonal outgrowth
Yoon et al.,2012	Xenopus RGC	Cut axons	lamin B2			Axonal maintenance
Gracias et al.,2014	Rat DRG	Microfluidic Chambers	TC10, Par3	NGF		GC Membrane expansion and outgrowth
Wang et al.,2015	Mouse DRG	Microfluidic Chambers	Map1b, Calm1	NGF	FMRP	Axon elongation
Gervasi et al.,2016	Rat SCG	Campenot chambers	Tyrosine hydroxylase			Neurotransmitter synthesis

Jain et al.,2016	mouse hippocampus	Starve and stimulation paradigm	DSCAM	Netrin1	FMRP, CPEB	Axon growth and guidance
------------------	-------------------	---------------------------------	-------	---------	------------	--------------------------

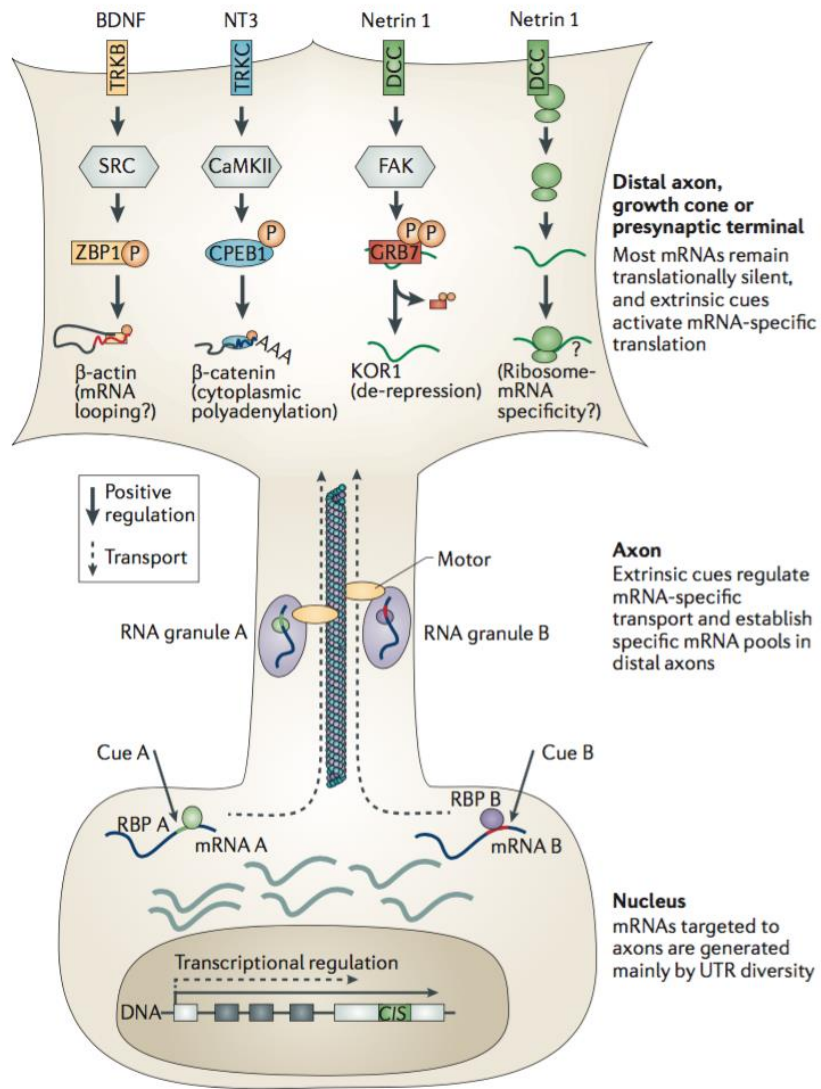


Figure 1-17: Specific mRNAs are transported and translated in response to various guidance cues

Adapted from (Jung et al. 2012)

1.5 BIOGENESIS OF miRNAS

miRNAs are conserved small non coding RNAs about 21-23 nt that are post transcriptional regulators of gene expression (Jonas & Izaurralde 2015). They are vital regulators shown to be important in the regulation of every cellular process investigated so far (Filipowicz et al. 2008).

1.5.1 MIRNA PROCESSING

Expression of miRNA genes begins when RNA Pol II initiates transcription to give rise to long (over 1 kb) primary transcripts known as pri-miRNA. The pri-miRNA contains hairpin structures in which the miRNA sequences are embedded (Lee et al. 2004). The pri-miRNA (Figure 1-18) contains single stranded RNA segments flanking a stem and loop structure (Ha & Kim 2014). The stem is about 33-35 bp followed by a single stranded terminal loop (Ha & Kim 2014).

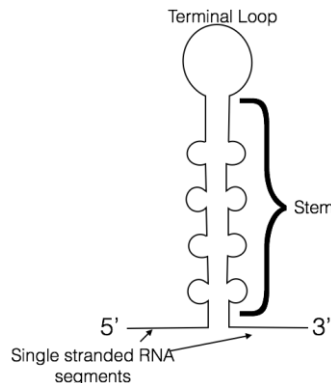


Figure 1-18: pri-miRNA structure

The pri-miRNA undergoes a maturation process to become a substrate for RNase III, Drosha in the nucleus. Drosha is an endonuclease that acts specifically on double stranded RNA substrates (Gregory et al. 2004). Drosha along with an important cofactor Di George Syndrome Critical Region (DGCR8), which is a ds RNA binding protein (Gregory et al. 2004), initiates site specific cleavage releasing the hairpin of ~65 bp called pre-miRNA. (Lee et al. 2003). Drosha along with DGCR8 form the microprocessor complex. The cleavage on the pri-miRNA is defined and occurs 11 bp

upstream the basal junction and 22bp from the apical junction (Han et al. 2006). Further, in order to mediate efficient processing specific features of the pri-miRNA sequence help in the recognition by RNA binding proteins. These are sequence elements namely a basal CNNC, UG and a terminal GUG motif that contribute to efficient processing. (Auyeung et al. 2013).

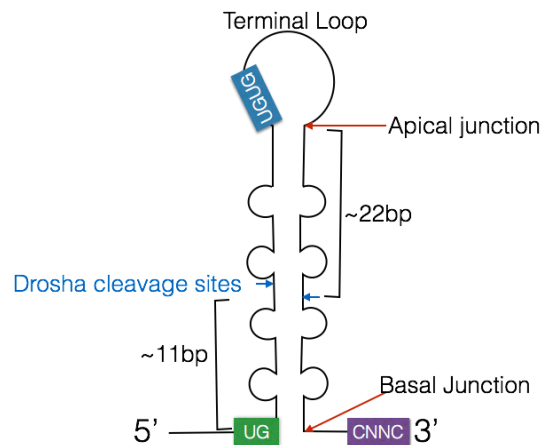


Figure 1-19 : Pri-miRNA recognition by microprocessor complex

This pre-miRNA is then exported to the cytoplasm by Exportin5(Exp5). Exportin 5 forms a complex with pre-miRNA and RAN-GTP (GTP binding nuclear protein) Upon translocation from the nucleus into the cytoplasm, GTP hydrolysis results in disassembly and release of the pre-miRNA (Lund et al. 2004; Bohnsack et al. 2004; Yi et al. 2003). In the cytoplasm, the pre-miRNA then serves as a substrate for another RNase III namely Dicer that cleaves the terminal loop of the pre-miRNA to generate a double stranded miRNA (Grishok et al. 2001; Bernstein et al. 2001; Ketting et al. 2001). The C-terminal of Dicer contains the RNase III domains that dimerise to form the catalytic core and the N-terminal serves as a pre-miRNA recognition domain (Tsutsumi et al. 2011). See (Figure 1-20) The PAZ domain (Piwi-Ago-Zwille) binds to the terminal region of the pre-miRNA. The distance between the PAZ domain and RNase III domain serves as a molecular ruler to cleave pre-miRNAs at a fixed distance (Macrae et al. 2006; Park et al. 2011; Tian et al. 2014). Dicer binds to pre-miRNA with a preference for a two-nucleotide 3' overhang that is produced by Drossha (Macrae et al. 2006).The Dicer cleavage site

exists at a fixed distance of 21-25 nucleotides from the 3' end (the 3' counting rule)(Zhang et al. 2004). On the 5' end, Dicer binds and cleaves the pre-miRNA 22 nucleotides away from the 5' end (the 5' counting rule)(Park et al. 2011)

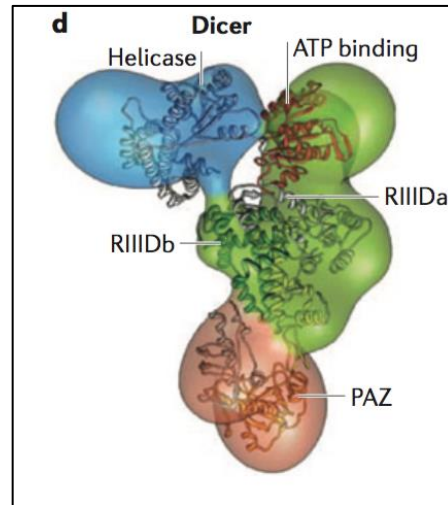


Figure 1-20: Reconstruction of human Dicer structure obtained from Cryo-electron microscope. Abbreviations: RIIIDa, b:RNase III domains a and b, PAZ: Piwi-Ago-Zwille domain, MID:Middle domain. Figure from (Ha & Kim 2014)

1.5.2 miRNA INDUCED SILENCING COMPLEX

The double stranded RNA resulting from Dicer cleavage is then loaded onto specific Argonaute (AGO) proteins to form an effector complex called RNA induced silencing complex (RISC) (Hammond et al. 2001). The AGO proteins are composed two lobes: N terminal lobe with N terminal domain and a PAZ domain, C terminal lobe with middle(MID) domain and PIWI (P-element induced wimpy testis) domain (Ha & Kim 2014). Post miRNA duplex loading onto AGO, the passenger strand of the double stranded miRNA is cleaved leading to the formation of a mature RISC composed of one of the four Ago proteins (Ago1-4) and guide strand of the miRNA. The guide strand is determined based on the thermodynamic stability of the two ends of the miRNA duplex with the unstable terminus at the 5' side becoming the guide strand (Khvorova et al. 2003; Schwarz et al. 2003). The miRISC complex mediates post-transcriptional silencing of the target mRNAs that can have partial or full complementarity to the miRNA. Perfect complementary mRNAs are cleaved by AGOs that are catalytically active (Ameres & Zamore 2013). However, in animals, usually the mRNA targets are partially

complementary and therefore cleavage does not occur. In humans, only AGO2 is catalytically active while AGO1, AGO3 and AGO4 are not (Ipsaro & Joshua-Tor 2015). Ago proteins are crucial for miRNA mediated gene silencing as loss of Ago leads to impairment in miRNA silencing in mammals and flies (Schmitter et al. 2006; Behm-Ansmant et al. 2006).

AGO family proteins can be co-purified with their accessory protein, GW-182 and are required for gene silencing (Jonas & Izaurralde 2015).

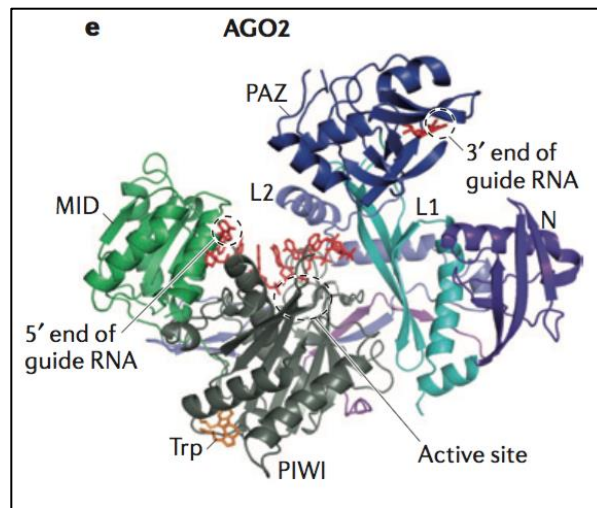


Figure 1-21: Structure of human AGO2.

Abbreviations : PAZ: Piwi-Ago-Zwille domain, MID:Middle domain, Figure from (Ha & Kim 2014)

The GW182 protein family contains an amino-terminal AGO binding domain and a carboxy-terminal silencing domain. These domains have multiple tryptophan (W) motifs flanked by glycine residues in the form of GW, WG or GWG repeats. The W motifs serve to bind to AGO proteins. The GW182s can interact with the cellular deadenylase complex to mediate miRNA degradation (Jonas & Izaurralde 2015).

1.5.3 MECHANISMS OF GENE SILENCING

Gene silencing is a result of a combination of mechanisms – Translational repression, deadenylation, decapping and 5' to 3' mRNA degradation (Fabian & Sonenberg 2012).

Target degradation

miRNAs mediate gene silencing through translation repression followed by mRNA degradation (Huntzinger & Izaurralde 2011; Ipsaro & Joshua-Tor 2015; Fabian & Sonenberg 2012)

Global analysis of change in protein production upon miRNA induction or repression as observed in cultured mammalian cells demonstrate that degradation of miRNA targets is a widespread phenomenon (Guo et al. 2010; Selbach et al. 2008; Eichhorn et al. 2014; Baek et al. 2008; Hendrickson et al. 2009). These studies employed strategies that include pSILAC, SILAC, polysome and ribosome profiling that give a global snapshot of the effect of miRNA on the proteome. Eichhorn et al showed that translational repression occurs when a miRNA is first introduced but by the time repression begins, miRNA mediated mRNA destabilization is the dominant effect (Eichhorn et al. 2014) miRNA mediated mRNA degradation accounts for 66-90% of the miRNA mediated repression in mammalian cells (Eichhorn et al. 2014).

mRNA degradation is carried out by the cellular 5' to 3' mRNA decay pathway (Behm-Ansmant et al. 2006; Giraldez et al. 2006). Studies indicate that the mammalian poly(A) tail is composed of 50-100 adenosines (Subtelny et al. 2014). mRNA is first deadenylated with the help of PAN2 and PAN3 that carry out the first phase of deadenylation followed by CCR4-NOT complex mediated deadenylation (Wahle & Winkler 2013). PAN2-PAN3 have partially redundant roles in deadenylation. It is not clear when CCR4-NOT follows deadenylation however, in the absence of PAN2-PAN3, CCR4-NOT can mediate deadenylation (Wahle & Winkler 2013). mRNAs are then decapped by decapping protein, DCP2 (Jonas & Izaurralde 2013). Deadenylated and decapped mRNAs are then targeted by the cellular exoribonuclease, XRN1, which mediates cleavage in the 5' to 3' direction and thus degrades the mRNA (Jonas & Izaurralde 2015). Decapping factors interact with XRN1 to mediate efficient mRNA degradation and to prevent accumulation of mRNA decay intermediates (Jonas & Izaurralde 2013; Braun et al. 2012). Decapping factors, argonaute proteins, GW182 proteins along with XRN1 localize into mRNA processing bodies known as P bodies. These cytoplasmic foci contain proteins involved

in both translational repression and mRNA decapping and decay processes (Jonas & Izaurralde 2013; Fabian & Sonenberg 2012).

Apart from mediating degradation, GW 182 and Ago2 play important roles in miRNA mediated repression (Filipowicz et al. 2008). Blocking GW182 in *Drosophila* S2 cells or blocking its interaction with Ago2 results in failure in miRNA mediated silencing of mRNAs both *in vitro* and *in vivo* (Behm-Ansmant et al. 2006; Eulalio et al. 2008; Yao et al. 2011; Till et al. 2007; Fabian et al. 2009; Takimoto et al. 2009) Interestingly, the CCR4-NOT complex can not only mediate degradation of mRNA but can also in some cellular contexts effect translational repression without causing mRNA deadenylation and decay (Chekulaeva et al. 2011; Zekri et al. 2013; Bawankar et al. 2013; Cooke et al. 2010).

miRNA-mediated translational repression

Although mRNA degradation seems to be the predominant mechanism of action, miRNAs also trigger translational repression. Through use of artificial mRNA reporters lacking poly A tails which thus resist deadenylation, it was shown that miRISCs have the ability to repress translation without mRNA degradation. (Wu et al. 2006; Braun et al. 2011; Chekulaeva et al. 2011; Fukaya & Tomari 2011; Fukaya & Tomari 2012; Ricci et al. 2013; Eulalio et al. 2008; Zekri et al. 2013; Mishima et al. 2012; Iwasaki et al. 2009; Pillai et al. 2005; Humphreys et al. 2005). One of the first studies highlighting miRNA role in repressing translational initiation revealed that miRNAs repress translation of m7G-capped mRNAs but not mRNAs containing a nonfunctional cap or an IRES(Internal ribosome entry site) (Pillai et al. 2005; Humphreys et al. 2005).

Another example of mRNA translation repression observed in human hepatoma cells delineated reversibility of miRNA repression. Liver specific miR-122 represses CAT1 mRNA, which localizes to P-bodies. Following stress conditions, CAT1 mRNA is released from P-bodies and recruited to polysomes. This indicates that miRNA mediated repression can be reversed in specific conditions (Bhattacharyya et al. 2006).

The question of whether miRNA mediated translational repression occurs before deadenylation decay was addressed by use of ribosome profiling in zebrafish embryos

and drosophila. Ribosome profiling experiments in zebrafish and drosophila have shown that translation repression of the mRNA precedes mRNA deadenylation *in vivo* (Bazzini et al. 2012; Djuranovic et al. 2012).

It is therefore still unknown what determines if an mRNA will follow degradation or translational repression.

1.5.4 NON-CANONICAL miRNA BIOGENESIS

Apart from the canonical biogenesis pathway, microRNAs can also be generated via alternative mechanisms (Yang & Lai 2011; Xie & Steitz 2014). These alternative mechanisms generate miRNAs that bypass processing by micro-processor or are produced in a Dicer independent manner (Babiarz et al. 2008). One of the first indications of non-canonical pathway was from Drosha-independent mirtron production (Berezikov et al. 2007). A pre-miRNA is generated through mRNA splicing from mirtron loci without Drosha processing. Post splicing, the resulting lariat is debranched, trimmed and modified into a stem-loop structure that resembles a pre-miRNA (Flynt et al. 2010). Other unconventional miRNAs can originate from non-coding RNAs such as tRNAs (Babiarz et al. 2008), small nucleolar RNAs (snoRNAs) (Ender et al. 2008) or small nuclear RNA-like viral RNAs (Cazalla et al. 2011). An example of Dicer independent mechanism for miRNA production is the miR-451 biogenesis (Cifuentes et al. 2010; Yang et al. 2010; Cheloufi et al. 2010). miR-451 is an erythropoietic miRNA that requires the catalytic activity of Ago2. The pri-miR-451 is processed by Drosha to generate a short hairpin that is directly loaded onto Ago2.

The pre-miRNAs produced from canonical pathway possess a two-nucleotide 3' overhang and these belong to group I pre-miRNAs. Group II pre-miRNAs on the other hand have a short one nucleotide long 3' overhang (Heo et al. 2012). Group II pre-miRNAs are mostly members of let-7 family. The extension of 1 nucleotide in these pre-miRNAs is mediated through Terminal uridylyl transferases that carry out monouridylation to be processed by Dicer efficiently (Heo et al. 2012).

The presence of alternative pathways reflects evolutionary flexibility in miRNA biogenesis.

1.6 miRNAs IN AXON GUIDANCE

The nervous system is the site of an intricate ‘miRNome’, as numerous miRNAs are enriched or specifically expressed there at specific time and place (Krichevsky et al. 2003; Johnston & Hobert 2003; S. Chang et al. 2004; Hsieh 2012; Zou et al. 2013). Recent large-scale studies have revealed that individual miRNAs fine-tune the expression of hundreds of transcripts (Baek et al. 2008; Selbach et al. 2008; Guo et al. 2010). The regulatory potential of miRNAs in developing organisms, and particularly in the nervous system, thus appears infinite. The roles of miRNAs in promoting the complexity and accuracy required for circuit formation, and axon guidance in particular, have however just started to emerge.

Summarised here is an extract of the review I co-wrote during my PhD thesis (Iyer et al., 2014), where I highlight the roles of miRNAs in key steps of axon pathfinding, namely long-range guidance, fasciculation and targeting in addition to recent findings. In annexure – the review is attached.

1.6.1 LONG RANGE GUIDANCE

Pinter & Hindges 2010 were the first to report that miRNAs, as a class of molecules, are important for long-range axon navigation using mice retinal ganglion cells (RGCs) as a model. RGCs are the only projection neurons of the retina and convey visual information to higher brain centers. In wild type monocular species, almost all RGC axons decussate at the optic chiasm, a midline structure. Whereas in binocular species, such as mice, some axons do not cross at the chiasm, but remain ipsilateral. The midline is thus an important choice point. The authors observed that, in absence of most miRNAs, many contralateral-projecting RGC axons failed to cross at the chiasm, and instead, aberrantly navigated ipsilaterally or overshot the midline. The molecular mechanisms leading to this phenotype is unknown to date. To abolish miRNA function, Pinter and Hindges used mutant mice where Dicer, a key enzyme responsible for the maturation of most miRNAs (Bernstein et al. 2001; Grishok et al. 2001; Ketting et al. 2001; Knight & Bass 2001), was conditionally ablated in Rx-expressing cells including RGCs and cells forming the optic

chiasm. Depletion of miRNAs in these mutants could, therefore, either lead to impaired cue expression by guidepost cells at the midline, or to altered sensitivity of RGC GCs to midline cues following misexpression of their cognate receptors or associated signaling molecules. Several ligand-receptor pairs are known to mediate midline crossing in mice: ephrin-B2/EphB1 (Nakagawa et al. 2000; Williams et al. 2003), Slit 1/2/Robo1/2, (Plump et al. 2002; Plachez et al. 2008) VEGF164/Neuropilin-1 (Erskine et al. 2011), Sema 6D/Nr-CAM, and Plexin A1 (Kuwayama et al. 2012). Their direct or indirect regulation by miRNAs is however unknown to date except for Neuropilin-1 (Baudet et al. 2012; Cui et al. 2012; Zhang et al. 2012) and Robo 1 and 2 (Alajez et al. 2011; Fish et al. 2011; Yang et al. 2012). Of interest, miR-218 was documented to target Slit receptors Robo 1 and 2 in non-neural cells such as cancer cells (Alajez et al. 2011; Fish et al. 2011; Yang et al. 2012) suggesting it might also play a role in neurons including axons where it is also expressed (Sasaki et al. 2013). Overall, this study is the first *in vivo* evidence to show that miRNAs may impact projecting neurons, guidepost cells, or both.

miR-9 was also recently documented to regulate the long-range guidance of thalamocortical (TCAs) and corticofugal axons (CFAs) tracts (Shibata et al. 2011). Both tracts cross the telencephalon and navigate through the internal capsule, a telencephalic structure, before reaching their final destination (Molnár et al. 2012). Migration of guidepost cells called “corridor cells” to the internal capsule is a crucial event in TCA and CFA pathfinding. These cells create a permissive corridor within the medial ganglionic eminence (MGE), a telencephalic region, normally non-permissive to the growth of TCAs, and thus enable these axons to cross the telencephalon prior to reaching their final destination (López-Bendito et al. 2006). To address the roles of miR-9 specifically in telencephalic development, Shibata, and colleagues generated miR-9-2/3 double mutant mice lacking two of the three miR-9 pre-cursors, namely miR-9-2, and miR-9-3 (Shibata et al. 2011). In miR-9-2/3 double mutants, CFAs and TCAs were severely misrouted. CFAs poorly innervated the internal capsule. Similarly, TCAs failed to reach this region, and instead aberrantly projected into the hypothalamus, an area that they normally avoid. The deregulated molecular mechanisms leading to this phenotype

are unclear, and likely to be complex. Evidence suggests that the TCA and CFA aberrant projections might be attributed to impaired patterning of corridor cells, although the possibility that miR-9 acts cell-autonomously in these projecting tracts cannot be excluded. Indeed, the topographical distribution of corridor cells within the telencephalon was affected; corridor neurons were expanded or dispersed in mutant animals. In addition, corridor cell markers *islet-1* and *Meis2* (predicted targets of miR-9) expression appeared to be qualitatively up regulated in miR-9-2/3 double mutant mice. The mechanistic implication of this dysregulation on the pathfinding defects observed is, however, unclear. Thus, these data suggest that miR-9 may ensure the proper development of corridor cells and in turn the accurate projection of TCA and CFA to this intermediate target. Together, this study points to the interesting possibility that long-range axon guidance defects might indirectly arise from miRNA-induced impaired patterning of guidepost cells.

Finally, *lin-4* was recently reported to also regulate long-range guidance of the axonal projection of anterior ventral microtubule (AVM) neurons in *C. elegans* larvae (Zou et al. 2012). In wild type animals, AVM axons project to the nerve ring, a neuropil considered as the *C. elegans*' brain. Before projecting anteriorly toward their target, AVM neurons are guided by two chemotropic cues that, together, orient the axons ventrally toward the midline. SLT-1 (Slit) repels AVM axons, preventing them from projecting dorsally, and UNC-6 (Netrin) attracts AVM axons ventrally (C. Chang et al. 2004). The authors examined whether *lin-4*, a miRNA expressed in AVM during axon pathfinding, is important for UNC-6-mediated axon guidance. *lin-4* was found to inhibit UNC-6 signaling during AVM axon guidance (Zou et al. 2012). Importantly, *lin-4* acted cell-autonomously, at least in part, and specifically in post-migrating neurons. LIN-14, a transcription factor and well-described target of *lin-4*, is also expressed in AVM neurons. LIN-14 was found to mediate *lin-4* action on AVM guidance and to potentiate UNC-6 mediated attraction of AVM axons by acting on UNC-40 (DCC) receptors. Surprisingly, *lin-14* did not alter *unc-40* promoter activity. Instead, it enhanced UNC-40 protein expression via an unknown mechanism, shifting its distribution from the confined

perinuclear region to the whole cell. Intriguingly, *lin-4* and *lin-14* are broadly expressed in *C. elegans*, and both are found in several UNC-40 guided neurons. This suggests that a *lin-4/lin-14* based conserved regulatory pathway might modulate UNC-6-mediated axon attraction of other tracts. In addition, miR-125, a *lin-4* ortholog, is also present in neurons of vertebrates (Sempere et al. 2004; Smirnova et al. 2005), indicating that this ancient microRNA may have conserved its guidance function. Overall, this study revealed that *lin-4* regulates cue-mediated attraction by modulating the signaling pathway of a receptor to guidance cue. Importantly, it also provided evidence that miRNAs can act cell-autonomously to modulate axon guidance to the midline. In summary, a few studies have revealed that miRNAs regulate long-range axon navigation, acting cell autonomously on projecting neurons, and possibly on guidepost cells.

1.6.2 FASCICULATION

Pioneers axons begin their pathfinding journey in an environment devoid of axons and are the first to establish connection with the target. Follower axons arise at a later time point in development and can progress along the pathway through axon-axon contact, thereby using topographical information provided by pioneers (Pittman et al. 2008). The process by which those co-extending axons form tight bundles is called fasciculation and is thought to be mediated by various classes of molecules including neural cell adhesion molecules (NCAM) but also guidance cues (Huber et al. 2005; Luxey et al. 2013). As reviewed below, some evidence suggests that miRNAs could play a role in the formation of these fasciculated bundles.

Giraldez et al. (2005) (Giraldez et al. 2005) reported that Maternal Zygotic (MZ) Dicer zebrafish mutants, devoid of maternal and embryonic sources of Dicer, exhibit several defasciculated axon tracts. Specifically, fasciculation of the post-optic commissure and hind-brain axonal scaffold, formed by longitudinal and commissural tracts, were severely disrupted in the absence of most miRNAs. Although defasciculation can lead to aberrant axonal trajectory (Huber et al. 2005), projections were correctly established at least for longitudinal hindbrain axons. In addition, early patterning and fate specification

was preserved in these animals. This suggests that these defects may be linked to altered molecular programs specifically in these projecting neurons, although impaired cue expression within the axonal environment cannot be formally ruled-out. Interestingly, exogenous miR-430 family members partly rescued this phenotype. This suggests that members of this family, or other uncharacterized miRNAs, may alter the expression or signaling of molecules mediating bundling of these tracts. Such molecules may include Sema3D and its cognate receptor Neuropilin-1A, which is known to promote fasciculation of hindbrain longitudinal axons in zebrafish (Wolman et al. 2004; Kwok et al. 2012). A defasciculation phenotype of RGC axons was also observed in Rx-conditional Dicer knockout mice (Pinter & Hindges 2010). In these animals, RGC axons failed to form a tight bundle within the retina. In addition at the midline, axons that aberrantly projected ipsilaterally were defasciculated, while axons overshooting the chiasm formed a secondary defasciculated tract. Interestingly, Sema 3D, Plexin A-1, Nr-CAM, Slit1, and 2 are implicated in the fasciculation of RGC axons (Ringstedt et al. 2000; Plump et al. 2002; Kuwajima et al. 2012) suggesting that their signaling might be derailed in Dicer mutants. Overall, miRNAs appear to regulate fasciculation, although the molecular mechanisms and the nature of the miRNAs involved are still largely elusive.

1.6.3 AXON TARGETING

After their long journey, axons reach their final destinations. Targeting of axons to their exact partner is absolutely essential, as it ensures proper circuit formation. This process is highly complex and requires several classes of molecules that promote defasciculation and specific entry within the target region, restricts any further elongation but also prevent axons from exiting the target-area. Cue-mediated restriction of the target-area is a highly regulated process in which miRNAs have been recently shown to play a role (Baudet et al. 2012).

Using *Xenopus laevis*, Baudet et al. (2012) (Baudet et al. 2012) uncovered a miRNA based signaling pathway that regulates axon targeting of RGCs to the optic tectum. Knockdown of miR-124 neither altered the birth of RGCs nor the general progression of

their differentiation. However, it appeared to affect post-mitotic RGCs axon projection. While long-range guidance was unaffected, a subset of axons failed to appropriately stall within the optic tectum. Instead, they invaded *Sema3A* expressing territories in the ventral border, normally repellent to these axons at this stage. The effect of miR-124 is likely to be cell-autonomous, as straying axons were observed both when miR-124 was knocked down in cells of the central nervous system (which include RGCs and tectal cells), and also when knocked down at a later developmental stage in retinal cells. In addition, GC responsiveness to *Sema3A* was impaired in miR-124 morphants. The authors also elucidated the molecular pathway mediating miR-124-regulated *Sema3A* repulsion. miR-124 indirectly promoted the expression of Neuropilin-1, a *Sema3A* receptor, at the GC, since its depletion decreased Neuropilin-1 levels within GCs *in vitro* and axons *in vivo*. miR124 regulated Neuropilin-1 via the silencing of its conserved target coREST, a cofactor of the global neuronal repressor REST (RE1-silencing transcription factor). Indeed, knockdown of coREST rescued Neuropilin-1 levels at the GC, and also GC responsiveness to *Sema3A*, in miR-124 morphants *in vitro*. Overall, this study uncovered a complex mechanism whereby miR-124 ensures RGC axonal response to *Sema3A*, at the right time and place, by dynamically inhibiting coREST repression of Neuropilin-1 within maturing RGCs. It also revealed for the first time that a miRNA regulates axon guidance (targeting) *in vivo*.

1.6.4 AXONAL BRANCHING

Once axons reach their target, GCs stop to navigate and change morphology to form branches called as branching. Do miRNAs play a role in axonal branching? To answer this, Marler et al. (2014) (Marler et al. 2014) explored the role of miR-132 on axonal branching by gain and loss of function studies. Interestingly, miR-132 is expressed in the RGC layer in mouse retina during the period of axonal targeting and branching. Neurotrophins play crucial roles in axonal branching. Therefore the authors investigated whether BDNF, a crucial neurotrophin mediates its role via miR-132 in axonal branching. Exposure of BDNF upregulated miR-132 expression in the retina and on axonal cultures as observed by qPCR. miR-132 gain-of –function studies showed that RGC axons have

increased branching, while loss –of –function of miR-132 results in decrease in branching *in vitro*. *In vivo*, miR-132 loss-of-function caused a delay in formation of axonal termination zones in mouse superior colliculus. Mechanistically, miR-132 keeps its target p250 GAP repressed during the period of axonal branching, as expression of p250GAP leads to suppression of branching and formation of termination zones. Prior to branching, p250GAP is expressed in high amounts and prevents premature axonal branching. Once axons enter the target rich in BDNF, miR-132 is upregulated which subsequently downregulates its target p250GAP and thus permits appropriate formation of axonal branches and termination zones.

1.6.5 miRNA PROFILING WITHIN AXONS

Recent studies have profiled miRNAs directly within developing distal axons (also comprising GCs) using different technical approaches and biological systems (Natera-Naranjo et al., 2010; Sasaki et al., 2013; Hancock et al., 2014). These have revealed that a complex miRNome exists in distal axons and that several miRNAs are enriched (or depleted) in this compartment (Table 1.6.5.1).

Table 1.6.5.1: List of miRNAs enriched or depleted in axons, or present in GCs

¹ miRNA detected (“present”) in axons and GCs

² miRNAs enriched in axons and detected in GCs by fluorescent *in situ* hybridization

³ neuron cultured for 3-10 days *in vitro*

⁴ neurons cultured for 4 days *in vitro*

Abbreviations: E, embryonic day; DRG, Dorsal Root Ganglion; SCG, Superior Cervical Ganglion; st, stage; P, postnatal day.

miRNAs	Age	Species	Neuron type	Enriched/Depleted in axons ¹	Method used	Reference
let-7c	P3 ³	Rat	SCG	Enriched	Microarray & qRT-PCR	Natera Naranjo et al.,2010
let-7-e	E13.5 ⁴	Mouse	DRG	Enriched	qRT-PCR	Hancock et al.,2014
let-7-i	E13.5 ⁴	Mouse	DRG	Depleted	qRT-PCR	Hancock et al.,2014
miR-9	E16 ⁴	Mouse	Cortical	Depleted	Multiplex qRT-PCR	Sasaki et al.,2013
miR-9 ¹	E17 ⁴	Mouse	Cortical	Present	qRT-PCR	Dajas-Bailador et al.,2012
miR-15b	P3 ³	Rat	SCG	Enriched	Microarray & qRT-PCR	Natera Naranjo et al.,2010
miR-16 ²	P3 ³	Rat	SCG	Enriched	Microarray & qRT-PCR	Natera Naranjo et al.,2010
miR-16	E13.5 ⁴	Mouse	DRG	Depleted	qRT-PCR	Hancock et al.,2014
miR-17	E13.5 ⁴	Mouse	DRG	Enriched	qRT-PCR	Hancock et al.,2014

miR-18a	E18	Rat	Cortical	Enriched	RT-PCR	Zhang et al., 2013
miR-19a	E18	Rat	Cortical	Enriched	RT-PCR	Zhang et al., 2013
miR-19b	E13.5 ⁴	Mouse	DRG	Enriched	qRT-PCR	Hancock et al.,2014
miR-23a	P3 ³	Rat	SCG	Enriched	Microarray & qRT-PCR	Natera Naranjo et al.,2010
miR-23b	P3 ³	Rat	SCG	Enriched	Microarray & qRT-PCR	Natera Naranjo et al.,2010
miR-24	P3 ³	Rat	SCG	Enriched	Microarray & qRT-PCR	Natera Naranjo et al.,2010
miR-24	E13.5 ⁴	Mouse	DRG	Enriched	qRT-PCR	Hancock et al.,2014
miR-26a	P3 ³	Rat	SCG	Enriched	Microarray & qRT-PCR	Natera Naranjo et al.,2010
miR-29a	E13.5 ⁴	Mouse	DRG	Enriched	qRT-PCR	Hancock et al.,2014
miR-30b	E13.5 ⁴	Mouse	DRG	Enriched	qRT-PCR	Hancock et al.,2014
miR-30c	E13.5 ⁴	Mouse	DRG	Enriched	qRT-PCR	Hancock et al.,2014
miR-34b-3p	E13.5 ⁴	Mouse	DRG	Depleted	qRT-PCR	Hancock et al.,2014
miR-92	E18	Rat	Cortical	Enriched	RT-PCR	Zhang et al., 2013
miR-103	P3 ³	Rat	SCG	Enriched	Microarray & qRT-PCR	Natera Naranjo et al.,2010
miR-106a	E13.5 ⁴	Mouse	DRG	Enriched	qRT-PCR	Hancock et al.,2014

miR-124	P3 ³	Rat	SCG	Depleted	Microarray & qRT-PCR	Natera Naranjo et al.,2010
miR-125a-5p	E13.5 ⁴	Mouse	DRG	Enriched	qRT-PCR	Hancock et al.,2014
miR- 125b	P3 ³	Rat	SCG	Enriched	Microarray & qRT-PCR	Natera Naranjo et al.,2010
miR-127	P3 ³	Rat	SCG	Enriched	Microarray & qRT-PCR	Natera Naranjo et al.,2010
miR-132 ²	E13.5 ⁴	Mouse	DRG	Enriched	qRT-PCR	Hancock et al.,2014
miR-134 ¹	St22	Xenopus	Spinal	Present	qRT-PCR, FISH	Han et al.,2011
miR-135a	E16 ⁴	Mouse	Cortical	Depleted	Multiplex qRT-PCR	Sasaki et al.,2013
miR-137	E16 ⁴	Mouse	Cortical	Depleted	Multiplex qRT-PCR	Sasaki et al.,2013
miR-138	E13.5 ⁴	Mouse	DRG	Enriched	qRT-PCR	Hancock et al.,2014
miR-181a-1 ²	E16 ⁴	Mouse	Cortical	Enriched	Multiplex qRT-PCR	Sasaki et al.,2013
miR-182	E13.5 ⁴	Mouse	DRG	Enriched	qRT-PCR	Hancock et al.,2014
miR-185	P3 ³	Rat	SCG	Enriched	Microarray & qRT-PCR	Natera Naranjo et al.,2010
miR-191	E13.5 ⁴	Mouse	DRG	Enriched	qRT-PCR	Hancock et al.,2014
miR-195	E16 ⁴	Mouse	Cortical	Depleted	Multiplex qRT-PCR	Sasaki et al.,2013
miR-196c	E13.5 ⁴	Mouse	DRG	Depleted	qRT-PCR	Hancock et al.,2014

miR-204	P3 ³	Rat	SCG	Enriched	Microarray & qRT-PCR	Natera Naranjo et al.,2010
miR-206	P3 ³	Rat	SCG	Depleted	Microarray & qRT-PCR	Natera Naranjo et al.,2010
miR-218	E16 ⁴	Mouse	Cortical	Depleted	Multiplex qRT-PCR	Sasaki et al.,2013
miR-221 ²	P3 ³	Rat	SCG	Enriched	Microarray & qRT-PCR	Natera Naranjo et al.,2010
miR-296	E16 ⁴	Mouse	Cortical	Depleted	Multiplex qRT-PCR	Sasaki et al.,2013
miR-297	P3 ³	Rat	SCG	Depleted	Microarray & qRT-PCR	Natera Naranjo et al.,2010
miR-320	P3 ³	Rat	SCG	Enriched	Microarray & qRT-PCR	Natera Naranjo et al.,2010
miR-328	E16 ⁴	Mouse	Cortical	Depleted	Multiplex qRT-PCR	Sasaki et al.,2013
miR-328	E13.5 ⁴	Mouse	DRG	Enriched	qRT-PCR	Hancock et al.,2014
miR-329	P3 ³	Rat	SCG	Enriched	Microarray & qRT-PCR	Natera Naranjo et al.,2010
miR-342-3p	E13.5 ⁴	Mouse	DRG	Enriched	qRT-PCR	Hancock et al.,2014
miR-361	E16 ⁴	Mouse	Cortical	Enriched	Multiplex qRT-PCR	Sasaki et al.,2013
miR-379	E16 ⁴	Mouse	Cortical	Depleted	Multiplex qRT-PCR	Sasaki et al.,2013
miR- 382	P3 ³	Rat	SCG	Enriched	Microarray & qRT-PCR	Natera Naranjo et al.,2010
miR-384-5p	E13.5 ⁴	Mouse	DRG	Enriched	qRT-PCR	Hancock et al.,2014

miR-423	E16 ⁴	Mouse	Cortical	Depleted	Multiplex qRT-PCR	Sasaki et al.,2013
miR-434-3p	E16 ⁴	Mouse	Cortical	Depleted	Multiplex qRT-PCR	Sasaki et al.,2013
miR-434-3p	E13.5 ⁴	Mouse	DRG	Enriched	qRT-PCR	Hancock et al.,2014
miR-484	E13.5 ⁴	Mouse	DRG	Enriched	qRT-PCR	Hancock et al.,2014
miR-495	E13.5 ⁴	Mouse	DRG	Enriched	qRT-PCR	Hancock et al.,2014
miR-532 ²	E16 ⁴	Mouse	Cortical	Enriched	Multiplex qRT-PCR	Sasaki et al.,2013
miR-541	P3 ³	Rat	SCG	Enriched	Microarray & qRT-PCR	Natera Naranjo et al.,2010
miR-680	E13.5 ⁴	Mouse	DRG	Enriched	qRT-PCR	Hancock et al.,2014
miR-685	E16 ⁴	Mouse	Cortical	Enriched	Multiplex qRT-PCR	Sasaki et al.,2013
miR-709	E16 ⁴	Mouse	Cortical	Enriched	Multiplex qRT-PCR	Sasaki et al.,2013
miR-720	E16 ⁴	Mouse	Cortical	Enriched	Multiplex qRT-PCR	Sasaki et al.,2013

As suggested by Hancock et al.,2014 (Hancock et al. 2014), this would be consistent with the differential expression of axonal mRNA repertoires at different developmental stages or in different species (Zivraj et al. 2010; Gumy et al. 2011). High throughput profiling of miRNAs has yet to be documented. However, in these studies, several miRNAs were also detected in GCs by fluorescent in situ hybridization: miR-16 and miR-221 in SCG neurons (Natera-Naranjo et al. 2010), miR-532 and miR-181a-1* in E16 cortical neurons and in dissociated hippocampal neurons (Sasaki et al. 2013) and miR-132 in E13.5 DRG explants culture (Hancock et al. 2014). Importantly the list and number of enriched axonal miRNAs, in all three studies, is strikingly different. Several reasons might explain these results. First, miRNAs might be differentially distributed in axons depending on the species (rat vs. mouse), cell type (SCG, cortical, and DRG neurons) and developmental stage (P3, E16, E13.5). Second, these differences may be due to different axonal culture (compartmentalized chamber vs. neuronal ball) and profiling methodologies (microarray/qRT-PCR vs. multiplex qRT-PCR). Third, they may be due to limited coverage of the known mature miRNAs to date (miRbase release 19), and the different cut-off values used for analyses. In addition in the first two studies, the majority of miRNAs appear to be distributed in both cell body and axonal compartments, suggesting that most miRNAs might not have a preferred site of action (Natera-Naranjo et al. 2010; Sasaki et al. 2013). Intriguingly, the presence of miRNAs in axons and GCs, and to some extent differentially expressed miRNAs derived from the same polycistron (Natera-Naranjo et al. 2010; Kaplan et al. 2013; Zhang et al. 2013), suggest that a mechanism of transport similar to that speculated for dendrites exists (Kosik 2006). Mature miRNAs could thus be translocated along axons to GCs either as individual molecules, as precursors, or within ribonucleoparticle bound to their targets and components of the silencing machinery. For instance, pre-miR-134 was recently documented to localize to dendrites through DEAH-box helicase DHX36-mediated transport (Bicker et al. 2013). Overall, these findings point to the possibility that miRNAs might be transported to and function within GCs to modulate steering.

1.6.6 miRNA RISC MACHINERY IS PRESENT IN GCS

Several studies have demonstrated the silencing machinery RISC (RNA-induced silencing complex) is present and functional in GC, further supporting a potential role of miRNA in GCs. Argonautes (ago) are the catalytic components of RISC. Four Ago proteins are reported in vertebrates (mammals), each binding a similar repertoire of miRNA and mRNA targets (Meister 2013). While ago2 was reported to induce mRNA target cleavage with perfect complementarity with a given miRNA, the roles of ago1, 3, and 4 are still elusive. Another RISC component, GW182 protein family (TNRC6 in mammals), coordinates all downstream steps in gene silencing (Pfaff et al. 2013). Key molecules for small RNA-mediated silencing such as ago2 (Zhang et al. 2013; Hancock et al. 2014), ago 3 and 4 (Hengst et al. 2006), eIF2c (Eukaryotic Initiation Factor 2C) (Aschrafi et al. 2008) and GW182 (Dajas-Bailador et al. 2012a) were detected in the embryonic and perinatal distal axons, and/or GCs of various cell types (Table 1.6.6.1).

Table 1.6.6.1: Reports of miRNA processing machinery in neurons.

¹ neurons cultured for 3-7 days in vitro; ² neurons cultured for 3 days in vitro. Abbreviations: DIV: Days in vitro; DRG: Dorsal Root Ganglion; SCG: Superior Cervical Ganglion

RISC component	Species	Neuron type	Age	Reference
Dicer	Rat	DRG	E15 ¹	Hengst et al.,2006
	Rat	Cortical	E18	Zhang et al.,2013
	Rat	SCG	P3 ²	Aschrafi et al.,2008
	Mouse	DRG	E13.5 ²	Hancock et al.,2014
ago2	Rat	Cortical	E18	Zhang et al.,2013
	Mouse	DRG	E13.5 ²	Hancock et al.,2014
ago3	Rat	DRG	E15 ²	Hengst et al.,2006
ago4	Rat	DRG	E15 ²	Hengst et al.,2006
GW-182	Mouse	Cortical	E17 ²	Dajas-Bailador et al.,2012

In addition, one study also revealed that RISC is functional in distal axons (Hengst et al. 2006). Exogenous siRNA directed against RhoA, a small GTPase protein led to the decrease in RhoA transcript and RhoA immunoreactivity in distal axons. Importantly, FITC-labeled siRNA was not detected in proximal axons, and no RhoA mRNA knockdown was detected in the somatodendritic compartment. Taken together, these data revealed that exogenous siRNA-induced silencing exists in distal axons (Hengst et al. 2006). It would be interesting to explore whether RISC can also mediate endogenous miRNA action in this compartment, and most specifically in GCs. Intriguingly, the RISC component Dicer is also detected in distal axons, including GCs (Hengst et al. 2006; Zhang et al. 2013; Hancock et al. 2014). This suggests that, as in dendrites (Bicker et al. 2013), pre-miRNAs could be transported and processed into mature miRNAs, in this compartment. Axonal transfection of pre-miR-338 and pre-miR-16 indeed result in a substantial increase in their concomitant mature form in axons, suggesting that miRNA

processing does occur in distal axons (Aschrafi et al. 2008; Kar et al. 2013). Several key components are thus present in GCs and/or distal axons, and RNA interference occurs in this compartment, suggesting that miRNAs are likely to be functional there. The documented presence of RISC components Armitage, MOV10 and Dicer (Lugli et al. 2005; Ashraf et al. 2006; Banerjee et al. 2009) in pre- and post-synaptic compartments underscore that miRNAs may have broader subcellular sites of action in polarized cells like neurons.

1.6.7 LOCAL ROLES OF miRNA IN OUTGROWTH

The presence of RISC within GCs suggests that miRNAs could act locally within this compartment and shape the local transcriptome during axon guidance. In particular, miRNAs could regulate local translation, known to play a role in GC steering in response to some cues (Jung et al. 2011). Although this has yet to be clearly demonstrated, recent studies suggest that it might be the case.

miRNAs are known to regulate outgrowth in development and following injury (Wu & Murashov 2013; Chiu et al. 2014). miRNA-mediated silencing of mRNA was recently reported to occur locally within axons to modulate outgrowth. Axonal miRNAs were initially documented to inhibit the translation of cytoskeletal regulatory molecules locally (Dajas-Bailador et al. 2012a; Hancock et al. 2014). Using mice cortical neurons, Dajas-Bailador et al. (2012) (Dajas-Bailador et al. 2012a) first revealed that a miRNA, miR-9, modulates the translational repression of exogenous Map1b (microtubule-associated protein 1b) 3'UTR, which has a key role in the regulation of dynamic microtubules. Short BDNF stimulation modulated miR-9 expression, while inhibition of miR-9 affected axonal growth only when applied locally in axons, suggesting that BDNF affects this developmental process via local, miRNA-mediated translational control of a cytoskeletal regulator. Further support for such local mechanisms came in a recent study from Flanagan's group (Hancock et al. 2014). Hancock and colleagues reported that axon-enriched miR-132 promotes embryonic DRG axon outgrowth by targeting endogenous p120RasGAP (Rasa1), a protein involved in cytoskeletal regulation (Hancock et al. 2014). Interestingly, miR-132-induced increase in axonal Rasa1 protein level was

dependent on local protein synthesis, as it was abolished in the presence of translation inhibitor applied to severed axons (Hancock et al. 2014). This demonstrated that miR-132 acts indeed within this cell compartment to regulate target translation, removing the possibility of cross talk with the cell body. Of note, Rasa 1 was previously reported to mediate responsiveness to chemotropic cues but here, miR-132 activity did not change upon stimulation by a few guidance molecules suggesting that these findings may not be strictly transposed to the guidance field (Hancock et al. 2014). In addition, axonal miRNAs were also recently documented to promote outgrowth by silencing axonal transcripts other than cytoskeletal regulators. Using 3d rat SCG neurons, Kar and colleagues reported that axon abundant miR-16 reduces the levels of the eukaryotic translation initiation factors eIF2B2 and eIF4G2 mRNAs, specifically within axons without affecting the levels of these transcripts in the soma (Kar et al. 2013). Interestingly, axonal miR-16 reduced outgrowth, and siRNA-mediated decrease in eIF2B2 and eIF4G2 levels in axons lead to inhibition of local protein synthesis and reduced axon extension. Together, this suggests that miR-16 might regulate elongation by modulating the axonal protein synthetic system. Finally using rat E18 cortical neurons, (Zhang et al. 2013) documented that axonal miR-19a, a member of the miR-17-92 cluster, regulates axon outgrowth via PTEN (phosphatase and tensin homolog), a negative regulator of the PI3K/mTOR signaling pathway. Importantly, axonal miR-19a regulates PTEN protein levels specifically within axons and not at the cell soma suggesting compartmentalized action for this miRNA. Local regulation of mRNA by miRNA has thus been reported in axons in a biological context of elongation.

The possibility that miRNA-mediated regulation of GC turning via local regulation of mRNA is further supported by a recent study. Several years ago, miR-134 was shown to locally modulate the size of dendritic spines of rat hippocampal cells (Schratt et al. 2006). This miRNA keeps Limk1, a kinase regulating actin polymerization, in a dormant untranslated state, and releases its repression in response to extracellular BDNF stimulation. Limk1 is thus translated, resulting in spine size increase (Schratt et al. 2006). Zheng's group recently investigated whether this mechanism is conserved in GCs of *X. laevis* spinal neurons, where they detected this miRNA (Han et al. 2011). Similar to

dendritic spines, miR-134 was found to be important for BDNF-induced GC attraction. In addition, miR-134 appeared to regulate protein synthesis in response to this cue, as loss- and gain-of-function of miR-134 in the whole embryo blocked protein synthesis dependent turning response of GCs. The effect of this miRNAs on spinal neuron cell bodies cannot be formally excluded, since miR-134 was knocked down or overexpressed in whole embryos, and not exclusively in axons. Limk1, also detected in spinal GCs, was confirmed as a *bona fide* target of miR-134 in *Xenopus* by *in vivo* luciferase assay. This suggests that Limk1 may mediate miR-134 regulation of BDNF-induced GC attraction. All-in-all, this study provided the first evidence, that GC turning can be modulated by miRNAs. It also indicated that conserved miRNA-based local control may exist in neuronal compartments, enabling the acute regulation of cytoskeletal dynamics in response to external stimuli.

miRNAs may have conserved important developmental roles, including axon guidance, throughout evolution. Indeed, miRNAs appear to regulate pathfinding in several species, ranging from *Drosophila* and *C. elegans* to mice and guidance miRNAs affect the same pathway in different species (e.g., the visual pathway of lower vertebrate Baudet et al., 2012 (Baudet et al. 2012) vs. higher vertebrates Pinter and Hindges, 2010 (Pinter & Hindges 2010)). Moreover, a specific miRNA, miR-9, regulates guidance of different tracts (Shibata et al. 2011). Interestingly, two of the four miRNAs involved in guidance, miR-124, lin-4/miR-125, are highly conserved, and considered as ancient miRNAs with neural-like function (Christodoulou et al. 2010). Expectedly, these miRNAs appear to have multifactorial neural action, and besides regulating guidance, also modulate earlier developmental events such as neurogenesis, cell fate determination, lineage progression, and later events such as synaptogenesis (Gao 2010).

1.6.8 ROLE FOR RNA BINDING PROTEINS

Recent evidence has revealed that miRNA function could be modulated by different means. For instance, RNA-binding proteins (RNA-BP) were shown to either act in concert with miRNAs to promote silencing or, on the contrary, to compete for binding sites (Krol et al. 2010). For instance miR-125a and Fragile X mental retardation protein

(FMRP) were revealed to act cooperatively at the 3'UTR of PSD-95 mRNA to inhibit translation of this transcript within synapses (Muddashetty et al. 2011). miRNAs can also actively regulate RNA-BP in neurons (Fiore et al. 2009). RNA-BPs play important roles in developing projection neurons, ensuring mRNA transport and translational repression (Hörnberg & Holt 2013). It is therefore conceivable that these two classes of molecules act in a coordinated manner to modulate transcript levels during axon guidance. In addition, other classes of non-coding RNAs, such as endogenous circular miRNA (Hansen et al. 2013; Memczak et al. 2013) and long-non-coding RNAs, have emerged as important regulators of miRNA action, acting as decoy or sponges that sequester, and thus buffer miRNAs in the cell (Salmena et al. 2011). Such endogenous competing RNAs (ceRNAs) might also include transcripts of protein-coding genes, whose miRNA-mediated silencing does not affect their function (Seitz 2009; Salmena et al. 2011). In projection neurons, these ceRNAs could modulate miRNA access to their target transcript, providing an additional layer of regulation, and enabling fine-tuning of their translation. However, their existence and function in cells during axon guidance is yet to be demonstrated.

Table 1.6.8.1: Summary of different miRNA roles in axon guidance

Role of miRNA	Reference	miRNA	Model Organism	Cell type	Function in	Role	Target mRNA
Long range guidance	Pinter and Hindges et al.,2010	Dicer cKO	Mouse	Retinal ganglion cells	RGCs	Pathfinding. miRNAs important for axonal crossing at the chiasm	Not analysed
	Zou et al.,2012	lin-4	C elegans	Anterior Ventral Microtubule Neurons	AVM neurons	lin-4 suppresses production of transcription factor LIN-14 to inhibit attraction to UNC-6	LIN-14
	Shibata et al.,2011	miR-9	Mouse	Thalamocortical and corticofugal axons	Telencephalic development	miR-9 important for development of guidepost cells to enable precise projection of TCA and CFA axons to intermediate target - internal capsule	Islet1 and Meis-2

Fasciculation	Giraldez et al.,2005	Maternal-zygotic Dicer mutant and miR-430	Zebrafish	Post optic commissure and hindbrain	Morphogenesis and axonal fasciculation	miRNAs important for fasciculation of post optic commissure and hindbrain axonal scaffold	Not analysed
	Pinter and Hindges et al.,2010	Dicer cKO	Mouse	Retinal ganglion cells	RGCs	miRNAs regulate formation of a tight bundle of RGC axons within the eye	Not analysed
Axon Targeting	Baudet et al.,2012	miR-124	Xenopus laevis eyes	Retinal ganglion cells	RGCs	Regulates RGC GC Responsiveness to Sema3A	CoREST
Axon Branching	Marler et al., 2014	miR-132	Mouse	Retina	Axons	BDNF upregulates miR-132 and contributes to branching + Involved in maturation of RGC termination zone	p250GAP
Chemotropic response to cues	Han et al.,2011	miR-134	Xenopus	Spinal neurons	GCs	Appropriate Responsiveness to BDNF	Limk1

Table 1.6.8.2: Role of miRNAs in axons that promote outgrowth or elongation.

Local roles within axons	Wang et al., 2015(Wang et al. 2015)	miR-181d	Mouse	DRG E 13.5	Axons	Axon enriched miR-181d regulates axon elongation by targeting Map1b and Calm1 . NGF triggers transcript release from FMRP. FMRP and miR-181 d mediate NGF induced axon elongation	Map1b, Calm1
	Dajas Bailador et al., 2012(Dajas-Bailador et al. 2012a)	miR-9	Mouse	Cortical	Axons	miR-9 regulates Axon extension and branching and responds locally to BDNF levels	Map1b
	Hancock et al.,2014(Hancock et al. 2014)	miR-132	Mouse	DRG	Axons	miR-132 regulates extension of axons. Acts as a developmental timer	Rasa1

Rationale

Axon guidance is a highly intricate process of brain wiring in which GCs traverse through molecularly distinct terrains in order to reach their target. In the developing brain, axonal tracts are established with extreme precision. Errors in the pathfinding process can lead to the formation of inappropriate connections that result in abnormal function. Therefore, it is crucial for axons to sense and respond to extracellular cues in the right manner. Understanding molecular mechanisms underlying axonal pathfinding can give important clues into brain function. Molecules involved in axon guidance are conserved to a large extent across various organisms therefore making it vital to get a mechanistic understanding and draw parallels amongst various species.

Cue-mediated signaling leads to complex remodeling of the cytoskeleton in GCs, which in turn regulates its directional steering and interactions with other axons, cells, and the environment (Dent et al. 2011). Remarkably, the GC is a subcellular compartment that can function with a great deal of independence from the cell body, since severed GCs can navigate on their own along the pathway for a few hours (Harris et al. 1987) and possess all the machinery necessary to respond to cues (Vitriol & Zheng 2012). GCs and axons are packed with complex and dynamically changing mRNA repertoires (Taylor et al. 2009; Zivraj et al. 2010). Bursts of mRNA translation are also known to mediate GC turning in response to several cues (Jung & Holt 2011). Interestingly, mRNA regulation has emerged as an important mechanism to promote crisp GC steering (Jung et al. 2011). **However, the molecular mechanisms that regulate selective localization and transient translation of transcripts at the GC are largely unknown.**

Several lines of evidence suggest that miRNAs may be involved in this regulation. miRNAs are key cellular regulators which ensure that proteins are expressed at precise levels, at the right time and place (Bartel 2009; Ebert & Sharp 2012), a process essential for the accuracy of GC steering. Furthermore, miRNAs have been found to modulate several guidance cues and receptors outside the nervous system. miRNAs have been implicated in regulating pathological processes such as cancer and tumor progression by regulating guidance molecules (Iyer et al. 2014). For instance, miR-218 regulates Robo1

and 2 in cancer cells (Yang et al. 2012). miRNAs also modulate guidance cues and their receptors in endothelial cells. For instance: miR-181b regulates neuropilin1 in endothelial cells (Cui et al. 2012). In addition, a few but key studies have revealed the importance of miRNAs in axon guidance in several species: miR-124 and miR-134 in *Xenopus laevis* (Baudet et al. 2012; Han et al. 2011) and lin-4 in *C.elegans* (Zou et al. 2012). These studies have shown that miRNAs play an important role in the cell soma. miRNAs have been detected within axonal GCs in different classes of neurons from various species (Natera-Naranjo et al. 2010; Sasaki et al. 2013; Hancock et al. 2014). In addition, miRNA processing and silencing machinery have been reported to be present in this compartment (Hengst et al. 2006; Hancock et al. 2014; Zhang et al. 2013). The possibility that miRNA regulate transcripts in axons and GCs to promote axon extension has been documented (Dajas-Bailador et al. 2012b; Wang et al. 2015; Aschrafi et al. 2008).

Hypothesis

I hypothesize that miRNAs regulate expression of mRNAs within the axonal GC to enable highly precise GC steering.

General Hypothesis:

The dominant mechanism employed by miRNAs to modulate the transcriptome within subcellular compartments is unknown for any cell type. miRNAs control gene expression in a post-transcriptional manner by regulating mRNA translation or mRNA stability (Filipowicz et al. 2008). Which of these mechanisms are at play and how timing influences one mechanism over another is still unclear (Bazzini et al. 2012).

Some studies show that miRNAs induce translational repression without mRNA decay (Pillai et al. 2005; Mathonnet et al. 2007; Olsen & Ambros 1999) while others point that mRNA is the more dominant effect (Eichhorn et al. 2014; Guo et al. 2010; Baek et al. 2008). More recent studies in zygotic zebrafish during development *in vivo* (Bazzini et al. 2012), in mammalian cells including transformed human cell lines, primary cultures of B cells, neutrophils and macrophages from mice (Eichhorn et al. 2014) and drosophila S2 primary cells (Djuranovic et al. 2012) have shown that translation is repressed before target mRNAs are deadenylated and degraded. Thus, miRNAs appear to interfere with the initiation step of translation (Bazzini et al. 2012; Djuranovic et al. 2012).

Based on these recent findings, two possible mechanisms of mRNA regulation in GCs may occur during steering. On the one hand, miRNAs could silence translation, keeping the transcript dormant until a cue is encountered, and a newly synthesized protein is required. From a large pool of transcripts present within the GC, only selective transcripts are translated in response to guidance cues (Jung et al. 2012). miRNAs could be crucial in enabling translation at the right time and place by keeping transcripts silent until cue exposure. There is evidence to this effect outside the context of guidance wherein miR-181d represses Map1b and Calm1 transcripts within axons and releases repression upon cue stimulation (Wang et al. 2015). This has also been observed within dendrites whereby miR-134 silences Limk1 mRNA silent until BDNF stimulation releases its repression (Schratt et al. 2006). Thus, the translation repression of miRNAs within compartments could be advantageous as the mRNAs need not be repeatedly

transported during the phase of guidance and can be stored locally in a silent form. And when needed the mRNA can be rapidly de-repressed to make many copies of a protein that in turn promotes GC steering.

On the other hand, cue-induced activation of miRNAs could lead to mRNA decay, when transcripts are no longer needed in a subsequent stage of development within the axonal compartment or to arrest the production of newly synthesized proteins.

This could also be the case because predominantly miRNA mediates silencing gene expression by accelerated target mRNA degradation (Jonas & Izaurralde 2015). Since axon guidance is a multistep process, miRNAs within the GC could be mediating mRNA degradation of transcripts no longer needed for a subsequent guidance step. This could be advantageous for the axonal compartment to be equipped with rapidly changing mRNAs whilst facing distinct molecular terrains. Cue-induced miRNA-mediated mRNA degradation has been observed in mouse RGC wherein BDNF stimulation leads to upregulation of miR-132 that downregulates its target p250GAP (Marler et al. 2014) so as to enable precise branching and development of termination zones. Kar et al reported that axon abundant miR-16 reduces the mRNA level of the eukaryotic translation initiation factors eIF2B2 and eIF4G2, specifically within axons (Kar et al. 2013). Axonal miR-19a regulates PTEN protein levels specifically within axons and not at the cell soma suggesting compartmentalized action for this miRNA (Zhang et al. 2013).

MOLECULAR HYPOTHESIS

I envision the following functions for miRNAs at the GC:

- 1) miRNAs primarily regulate mRNA translation in axons: miRNAs could be important to select specific transcripts for translation upon exposure to specific cues.
- 2) miRNAs primarily regulate mRNA stability in axons
 - 2.1. miRNA induces the degradation of transcripts that are no longer needed: silencing could arrest cue-induced translation of mRNA, thereby terminating GC response to a given chemotropic cue.
 - 2.2. miRNAs may enable the developmentally timed expression of transcripts, thus ensuring that specific pool of mRNAs, but not others, are present within the GCs at a given developmental step of brain wiring, and available for

translation.

I also envision that both mechanisms are not mutually exclusive and could coexist, affecting different transcripts and / or different developmental stages.

In my thesis I have investigated whether miRNAs could be key players in inducing GC steering *in vivo* and in culture by modulating transcripts locally. To address this, I have used the *Xenopus laevis* visual system as a model system.

To explore which miRNAs could be important for *Xenopus* retinal pathfinding, an unbiased high-throughput miRNA-seq analysis was carried out within a collaborative framework to profile miRNAs specifically within RGC axons in culture from stage 37/38 embryos. This approach provided ranking of a cohort of axonal miRNAs and in-depth sequence information on all the possible miRNAs present within axons. 148 miRNAs were detected in axons (Annexel Fig 1). Two different classes of miRNAs together composed of 50% of the total miRNAs detected and were the most abundant in RGC axons: miR-182 and miR-181a and b.

I focused on these most abundant miRNAs and investigated their role in axon guidance and their mechanisms of action.

For miR-181a and b

Specifically, I:

- 1) Performed loss-of-function targeting specifically retinal cells, including retinal ganglion cells to explore if these miRNAs are involved in mediating cell autonomous, RGC axon guidance *in vivo*.
- 2) Analyzed whether miRNAs regulate chemotropic cue-induced GC responsiveness.
- 3) Determined whether any phenotype obtained following miRNA-mediated loss-of-function was specific.
- 4) Attempted to understand miRNA-mediated mechanism and mode of action by analyzing differential gene expression in RGC and axon compartments by RNA-seq.
- 5) Developed tools to investigate whether miRNA act locally within axons.

For miR-182, I*:

- 1) Performed loss-of-function targeting specifically retinal cells, including retinal ganglion cells to explore if miR-182 is involved in mediating RGC axon guidance in a cell autonomous manner *in vivo*.
- 2) Used sensor constructs to test for miR-182 activity and carried out cell autonomous delivery of the same.

- 3) Tested if the sensor is suitable for measuring miR-182 activity in GCs by validating the presence of the sensor plasmids specifically within axons.
 - 4) Determined if miR-182 levels change upon Slit2 stimulation on WT axons.
- *- Done in collaboration with other authors on the manuscript.

2.1 ABSTRACT

Using an unbiased high throughput screening approach, we found that miR-182 was the most abundantly expressed miRNA in RGC axons. Here, we have investigated whether miR-182 contributes to selecting specific transcripts for local protein translation. This work was performed as a joint effort between the Baudet laboratory at CIBIO and Christine Holt Laboratory at the University of Cambridge. We discovered that miR-182 locally targets cofilin1 mRNA and blocks its translation. miR-182 silencing activity is released by Slit2 stimulus which releases miR-182 repression and thereby promotes cofilin1 translation.

To explore miR-182 roles in axon guidance, loss-of-function approach mediated approach was used. Both broad CNS based knock down and retinal cell specific knockdown approaches showed that miR-182 is required for restricting targeting area of axons within the tectum. Since, straying axons within the tectum seemed to be localized to Slit2 expressing territories, Slit2 loss-of-function was carried out to answer if Slit2 limits axons within a specific area. And indeed it was found that Slit2 morphants phenocopied the miR-182 loss-of-function phenotype suggesting that Slit2 is a target restricting cue. Further, turning assay showed that axonal sensitivity to Slit2 was abolished in miR-182 morphants. Using target prediction, cofilin1 mRNA, a regulator of actin cytoskeleton, was found to be a highly conserved miR-182 binding site. Cofilin1 (cfl-1) mRNA was ascertained as miR-182 target through luciferase reporter assay. Furthermore, local translation of cfl-1 mRNA within GCs required the presence of miR-182 as observed by quantitative immunofluorescence and kaede protein based reporter assay. Interestingly, activity of miR-182 within RGC GCs was found to be modulated upon Slit2 signalling via Robo2/3 receptors. And finally, mechanism of miR-182 was also uncovered wherein, Slit2 stimulation lifts off cfl-1 repression without leading to miR-182 degradation. Thus, this data shows local roles of miR-182 within axons enabling their precise targeting by selecting cofilin1 for translation upon specific cue exposure.

In this chapter, I will delineate the role of miR182 especially highlighting evidences the mechanisms through which miR182 influences axonal targeting in the *Xenopus laevis* visual pathway. I will specifically elaborate my contributions to this project.

My contributions towards this project are as follows:

1. I performed an *in vivo* loss-of function of miR-182 to analyse pathfinding defects
2. Towards understanding miR-182 activity with and without Slit2, I carried out electroporations and culture of miR-182 sensor plasmids.
3. The presence of these sensor plasmids within axons were tested by using laser capture microdissection mediated RNA extraction *in vitro*
4. To test the influence of Slit2 on miR-182 activity, I carried out RNA extraction from laser captured samples upon exposure to Slit2.

The results of this project are published in Jan 2017 in the journal-Cell Reports (in Annexure).

2.2 MATERIALS AND METHODS

2.2.1 EMBRYOS

X. laevis embryos were obtained by *in vitro* fertilization. *Xenopus* adult frogs were induced with hormone and eggs were obtained and fertilised *invitro* (Cornel & Holt 1992), raised in 0.1X Marc's Modified Ringer's solution (MMR 10X: 1M NaCl; 20mM KCl; 10mM MgSO₄; 20mM CaCl₂; 50mM HEPES, pH 7.5) at 14°C and staged according to Nieuwkoop and Faber,1994 (Nieuwkoop P. 1994). All animal experiments were approved by the University of Trento Ethical Review Committee.

2.2.2 MORPHOLINOS (MOS)

Antisense (MOs) tagged with 3'Fluorescein were designed and supplied by Genetools. The MO was designed to target mature *X.laevis* miR-182. The sequence for miR-182 was obtained from miRbase for *X.tropicalis*. The miR182 mature sequence is identical between the two *Xenopus* species as verified by the sequencing data obtained on *X.laevis* from Baudet et al., 2012 (Baudet et al. 2012).

Sequence of Xla miR-182: 5' TTTGGCAATGGTAGAACTCACA 3'

The miR-182 and control MOs were used at 250 μ M.

The sequences of MOs used were:

Xtr-miR-182 –MO: 5' TGTGAGTTCTACCATTGCCAAA 3'

Custom control-MO: 5' GTGTAACACGTCTATACGCCCA 3'

2.2.3 ELECTROPORATION

For electroporation, stage 26 embryos were used. Embryos were dechorionated and washed once in 0.1X MMR. Few embryos at a time were rinsed once briefly in 1X MBS (Modified Barth's Saline) and anesthetized in 1X MBS + MS222 (0.2%). The embryos were then placed in a T shaped sylgard chamber and the MOs with reporter (pCS2-EGFP or pCS2-CAAX-Cherry: 0.5 μ g/ul) were injected and electroporated in one eye with conditions similar to those previously described (Falk et al. 2007). I noticed that FITC labelled-MO bleached easily preventing their localization through imaging and this is why I opted for the use of mCherry reporter construct alongside FITC-MO. The reporter was used to evaluate the success of electroporation and also since it is membrane bound it was possible to trace the axons along the pathway.

2.2.4 RETINAL EXPLANT CULTURE

Whole retinas from stage 37/38 embryos were dissected and cultured at 20°C for 24 h in 60% L15 minimal medium containing antibiotics (PSF 100X stock) on 12mm glass coverslips. Prior to culture, glass coverslips were coated with poly-l-lysine (10 μ g ml⁻¹) overnight at 20°C, washed with water and coated with Laminin (10 μ g ml⁻¹) for 1 hr at room temperature. Embryos were anesthetized in 60% L15 containing MS222 and retinas were dissected and culture was done as mentioned in Baudet et al. 2012

2.2.5 LASER CAPTURE MICRODISSECTION *IN VITRO*

Xenopus embryos at stage 35/36 were cultured on RNase free POL (Polyester) membranes with 60% L15 medium for 24 hrs in 1ml of L15 medium. The following day, cultures were stained with FM-1-43FX dye for 20 mins in order to visualise axonal processes and to visualise fibroblasts and cell bodies. Following staining, cultures were fixed in 1% PFA for 5 mins and subjected to ethanol dehydration (25%, 50%, 75%, 90%

and 100%) for 30s - 1 min each. Axons and eye explants were captured in separate tubes using the Leica microdissector LMD6500. RNA was extracted using the Ambion RNAqueous micro kit or the Norgen RNA extraction micro kit. The quality of the RNA was determined using the Agilent bioanalyzer 2100 with the Agilent Pico Chip.

2.2.6 PURITY OF AXONAL PREPARATION

Axons obtained from *in vitro* laser capture were subjected to a purity test. To ensure that the isolated axons were free of cell bodies and other contaminants, axonal RNA was subjected to RT-PCR for the presence of β -Actin and the absences of Map2. Total RNA isolated from axons was reverse transcribed using random hexamers followed by PCR using primers for Map2, β -actin and Histone H4 with 35-40 cycles.

β -actin Forward primer: 5'- CGTAAGGACCTCTATGCCAA- 3'

β -actin Reverse primer: 5'- TGCATTGATGACCATACAGTG- 3'

Map2 Forward primer: 5'- CACGTACTCCTGGAACACCC – 3'

Map2 Reverse primer: 5' - TGGAACCACAACGAGACTGA- 3'

Histone H4 Forward primer 5'- GGCAAAGGAGGAAAAGGACT-3'

Histone H4 Reverse primer 5'-GAGAGCGTACACCACATCCA- 3'

2.2.7 LASER CAPTURE MICRODISSECTION *IN VIVO*

Laser capture microdissection was performed on retinal ganglion cells and axons *in vivo* as follows: Embryos were electroporated with control sensor plasmids containing dGFP and mCherry reporter at 0.5 μ g/ μ l at stage 26.

Well electroporated embryos were sorted and were fixed at stage 40 in 4% PFA (prepared as mentioned above but using RNase free 10X PBS and RNase free water and a fresh vial of PFA was used each time). Fixation was carried out for 15 mins followed by 1X PBS rinse thrice. Embryos were kept covered at all times. Following fixation, embryos were treated with 30% Sucrose made in 1X RNase free PBS placed on ice for 1 hr. Only 5 embryos were processed per tube and timings for fixation and sucrose treatment were strictly followed. Following sucrose treatment, embryos were embedded in blocks containing OCT on dry ice and stored in the -80°C until use. On the day of laser capture, embryos were sectioned with cryostat at 14 μ m thickness and taken on

PEN membrane slide. (One slide was processed each time). The processing of slides was done as follows - 95% ethanol - 30s, 75%, 50% (twice), 75%, 95%, 100%(twice) - each 30 seconds followed by one quick wash with Xylene (in the hood), then 5 mins of fresh Xylene (second mailer also done in the hood), Air dried in the hood for 5 mins and then placed in a RNase free falcon containing dessicant. The sections were immediately laser captured using Leica LMD6500 microdissector. The settings used were: Magnification: 63X, Power: 32-34, Aperture: 1, Speed: 16-18, Specimen Balance: 0, Offset: 200. RGC and Axon samples were collected simultaneously on different caps containing lysis buffer with Beta-mercaptoethanol. Following capture, RNA was extracted using Norgen Single cell RNA extraction kit and RNA was eluted in RNase free water. Quality of RNA was estimated using Agilent Bioanalyser 2100 with Agilent Pico Chip.

2.2.8 *IN SITU* HYBRIDIZATION

The protocol was adapted from Obernosterer et al.,2007 (Obernosterer et al. 2007). Embryos were fixed at stage 40 in 4% PFA (made in 1X RNase free PBS) for 2 hrs and treated with 30% Sucrose prepared in 1X RNase free PBS for 1 hour on ice. Embryos were embedded in OCT and stored at -80°C until use. Sections containing eye and brain were taken on the cryostat at 14µm on SuperFrost slides. Following sectioning and drying (for maximum 3 hrs) they were fixed briefly with 4% PFA for 10 mins and rinsed thrice with DEPC treated water. Acetylation was carried out for 10 mins (Acetylation solution : For 500ml: 442ml of DEPC water, 925µl of 31.5% HCl, 6ml Triethanolamine, mixed to dissolve and finally just before use, 1.125 ml of Acetic Anhydride was added and stirred to dissolve). *Acetylation removes positive charges from amino groups of proteins, thus reducing background binding of the negatively charged probe to the tissue sections and to the slide.*

Following acetylation, Proteinase K treatment was done (at final concentration of 5µg/ml) for precisely 5 mins and then rinsed thrice with DEPC water. *Protease treatment serves to increase target accessibility by partly digesting the protein that surrounds the target nucleic acid.* The slides were then blotted and pre-hybridization solution [containing the following components at final concentrations: 50% deionised formamide, 5X SSC, 5X Denhardtts solution, 200g/ml yeast RNA, 500µg/ml denatured

salmon sperm DNA (*decreases the chance of non-specific binding*) and 0.4g Blocking reagent] was added (170µl) and parafilm strip was placed over the solution and kept for 4 hrs at room temperature. After which, the pre-hybridization was blotted and fresh hybridization solution containing denatured probe (Control or miR-181a and miR-181b at 1nM concentration) was added and the slides were kept in a hybridization oven at 55°C for 16 hrs. The following day, the sections are treated with a series of stringency washes using 5X and 0.2X SSC at 55°C, followed by block with 10% sheep serum at room temperature for 1 hr and subsequently anti-digoxigenin antibody (1:2000) was prepared in 10% sheep serum and treated overnight at 4°C. On day 3, the slides were rinsed in buffer B1(1M Tris pH:7.5, 5M NaCl) thrice followed by Buffer B3 (0.5M Tris pH 9.5, 0.5M NaCl) for 10 mins. The detection of the miRNA was revealed by a color reaction using substrates NBT and BCIP prepared in buffer B3 (For 50 ml solution, NBT: 170µl, BCIP:175µl, Levamisol: 120µl,10% Tween : 250µl)

2.2.9 ISH PROBES

DIG labelled LNA oligonucleotides complementary to *X.tropicalis* (xtr)-miR-182 (5'-ACTCACCGACAGCGTTGAATGTT-3') and scrambled probes (5'-TTCACAATGCGTTATCGGATGT-3') were obtained from Exiqon. *X.tropicalis* directed probes were used as the sequence is identical to that of *X.laevis* as mentioned above. 1nM of the probes were used as final concentration.

2.2.10 PATHWAY ANALYSIS

Open brain preparations (as described in methods in chapter 3) of control or miR-182 morphant embryos were imaged using Zeiss Observer Z1 using z stack projections to view the entire contralateral pathway. The width of the pathway was measured along the contralateral part of the brain at specific locations following Walz et al., 2002 (Walz et al. 2002). A grid composed of 10 concentric circles was superimposed onto the image of the visual pathway taken at 10X magnification such that the centre of the grid coincided with the optic chiasm and the grid size was adjusted such that the 10th concentric circle coincided with the posterior boundary of the tectum as observed in brightfield. The pathway width was determined by the intersection of the intermediate concentric circles

on the grid with that of the pathway (and labelled as C1, C2 and so on) and was normalised to the brain size. The brain size was calculated by distance between intersection point of the grid at the posterior boundary of the tectum to the centre of the chiasm (Figure 2-1).

For measurements, GNU Image Manipulation Program (version 2.8.6) was used.

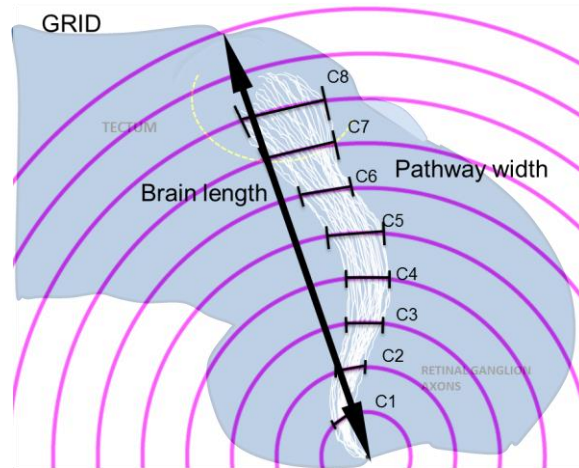


Figure 2-1: Schematic showing pathway width analysis.

2.2.11 STATISTICAL ANALYSIS

All experiments were carried out at least 3 times unless stated otherwise. D'Agostino & Pearson Omnibus Normality tests were carried out for all the datasets.

2.3 RESULTS

Here I present results that I obtained. In **italics** are parts of experiments carried out by other authors on the manuscript.

2.3.1 miR-182 IS EXPRESSED IN PHOTORECEPTOR LAYER IN XENOPUS RETINAL SECTIONS

High throughput profiling of miRNAs in axons revealed that miR-182 was the most abundantly present miRNA in this compartment (Annex1, fig. 1).

Presence of miR-182 in retinal axons suggests that they may also be present within the soma. Using ISH on coronal sections of *Xenopus laevis* embryos for miR182 I confirmed that this is indeed the case (Figure 2-2)

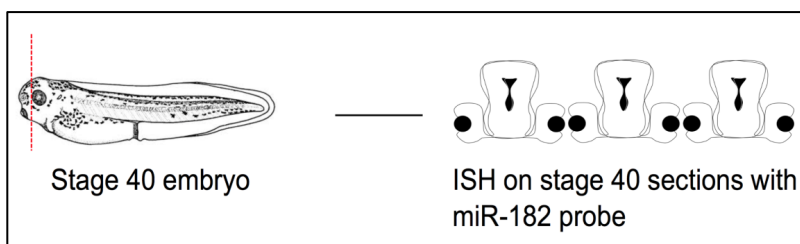


Figure 2-2: Schematic of experimental paradigm showing stage 40 embryo sectioned for ISH

Through ISH, I observed that miR-182 was localized in the photoreceptor layer alone but not in RGCs nor in any other retinal cells (Figure 2-3).

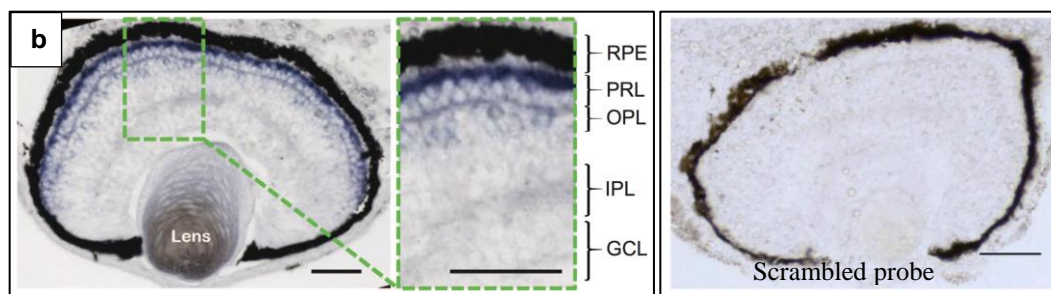


Figure 2-3: miR-182 ISH in stage 40 retinal sections.

Abbreviations: RPE: retinal pigment epithelium; PRL: Photoreceptor layer; GCL: Ganglion Cell Layer.
Scale bar: 50 μ m.

Although surprising in light of our sequencing result, it is consistent with the literature (Baudet et al. 2012; Hancock et al. 2014). We thus reasoned that miR-182 is likely to be transiently present in RGCs and trafficked in axons rapidly or that pre-miR-

182 is instead trafficked to the GCs where it is processed. We explored below the first possibility.

2.3.2 LASER CAPTURE MICRODISSECTION ENABLES DETECTION OF MIR-182 IN RGC CELL BODIES AND AXONS *IN VIVO*

Next, we addressed whether miR-182 may be present in RGC soma below ISH detection levels. We thus employed Taqman RT-PCR, a more sensitive technique to detect miRNA than ISH since it includes an amplification step. In order to ascertain the presence of miR-182 in RGCs *in vivo* by Taqman RT-qPCR assay, I collected RGCs using LCM. Firstly, in order to label the RGCs, I electroporated pCS2-EGFP plasmid (0.5µg/µl) at stage 26 and fixed the embryos at stage 40 and processed them for LCM (as described in Materials and Methods section Chapter 3, section 3.2)

I was able to selectively capture EGFP labeled RGC cell bodies from the retina and to obtain RNA specifically from this compartment. In parallel, I extracted RNA from whole eyes.

qPCR analysis using Taqman PCR revealed the presence of miR-182 in RGC soma, at levels that were 8 fold lower than that found in whole eyes. Since whole eye is composed of other cells apart from RGCs that may contain low levels of miR-182, there is a good likelihood that miR-182 depletion in RGC is underestimated.

miR-182 is thus present within RGCs in low levels as detected by Taqman qPCR (Figure 2-4, c)

Similarly, I used LCM to extract axons (axons were taken from sections specifically, from the optic tract and tectum) and by means of qPCR we also confirmed presence of miR-182 within axons (Figure 2-4, d).

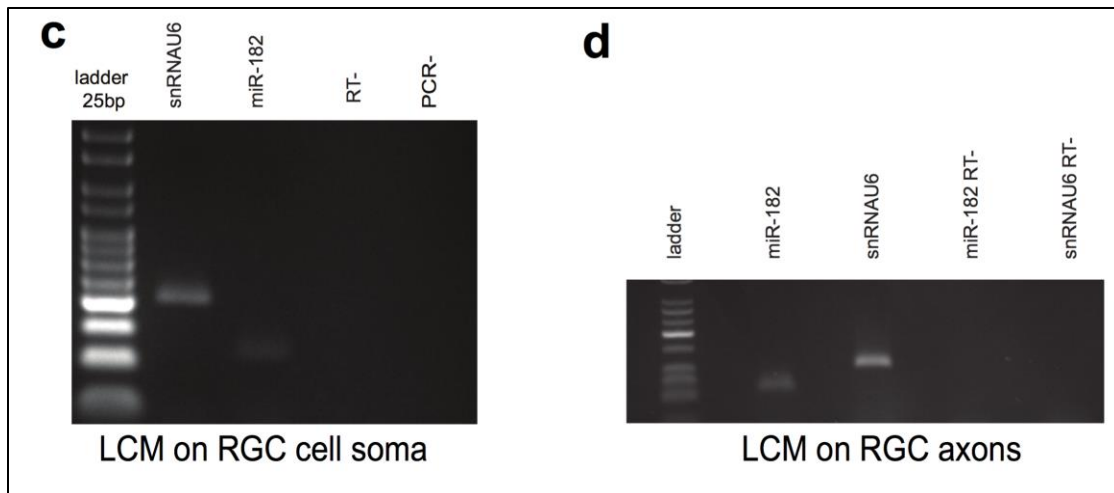


Figure 2-4: Taqman RT-qPCR for miR-182 and snRNA-U6 in RGC and axons
Abbreviations: PCR-: no cDNA control. RT-: No reverse transcriptase control

2.3.3 miR-182 REGULATES AXON TARGETING IN OPTIC TECTUM *IN VIVO*

miR-182 is found to be the most abundant miRNA, representing about 25% of the miRNAs expressed within axons (Annexe 1, Table S1). The combined evidence that this miRNA is lowly present within cell bodies but abundantly within axons suggests an exclusive axonal role. Thus, we wanted to explore the role of miR-182 during axon guidance in the *Xenopus laevis* developing visual system using a loss of function approach. I used electroporation as a tool to deliver miR-182 MOs at stage 26 to specifically target only retinal cells. This enables me to assess cell autonomous roles of miR-182 within retinal cells. This is in contrast to microinjection that enables a broad knock down that can commence from very early stages when CNS cells are specified. Along with the MOs, I used pCS2-CAAX Cherry to assess the efficiency of electroporation and to visualize the pathway to check for pathfinding defects. This is because I noticed that FITC labelled-MOs bleached easily preventing the identification of the visual pathway through imaging. At stage 40, I analysed the brains using open brain preparations.

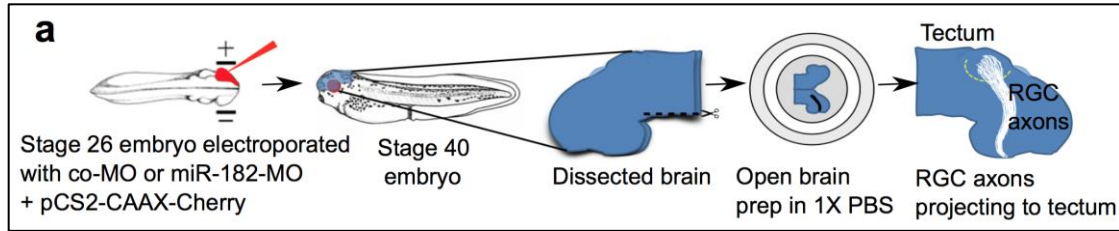


Figure 2-5: Open brain preparation to analyse visual pathway defects.

These are preparations where the brain is severed in its ventral side, then both hemispheres flatten down but still connected at their dorsal extremity. With these, it is possible to visualize labelled axons that project from the optic chiasm along the contralateral brain hemisphere to the tectum and thus to analyse the possible presence of aberrantly projecting axons. However, this preparation is not amenable to observation of the optic pathway from the eye to the optic chiasm and one has to resort to sectioning for these additional analyses.

I quantified the width of the pathway at specific location (see Section 2.2.10, p. 100 for full methodological description).

miR-182 morphant embryos displayed a significant increase of +16.5% (S.E.M \pm 3.51) of the retino-tectal pathway width (Figure 2-6 b and c) compared to control MO electroporated embryos at the anterior border of the tectum where RGC axons enter the tectum (Two ANOVA following Bonferroni post test, $p < 0.01$) (Figure 2-7 d).

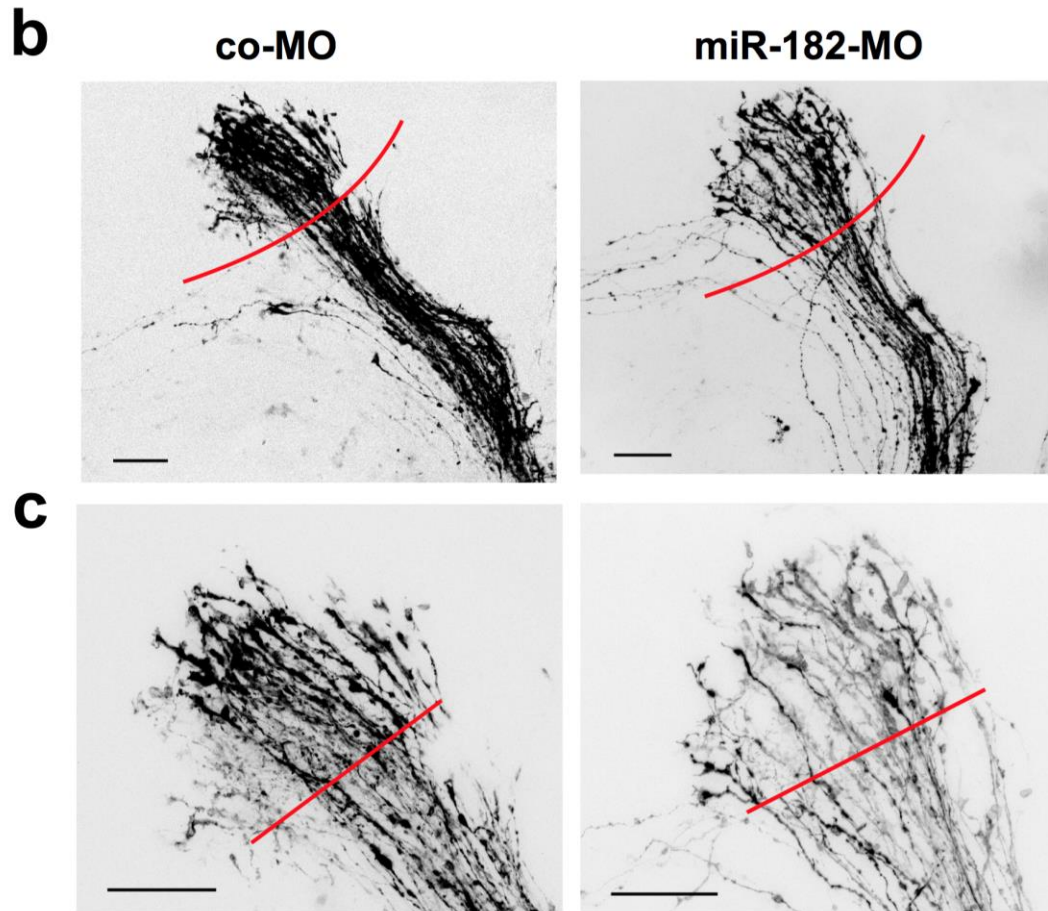


Figure 2-6: Pathway analysis in co-MO and miR-182-MO
(b) co-MO or miR-182-MO axons expressing pCS2-CAAX Cherry. Red curved line shows anterior tectal boundary. (c) Higher magnification highlighting RGC axons within tectum. Red line shows width of the pathway.

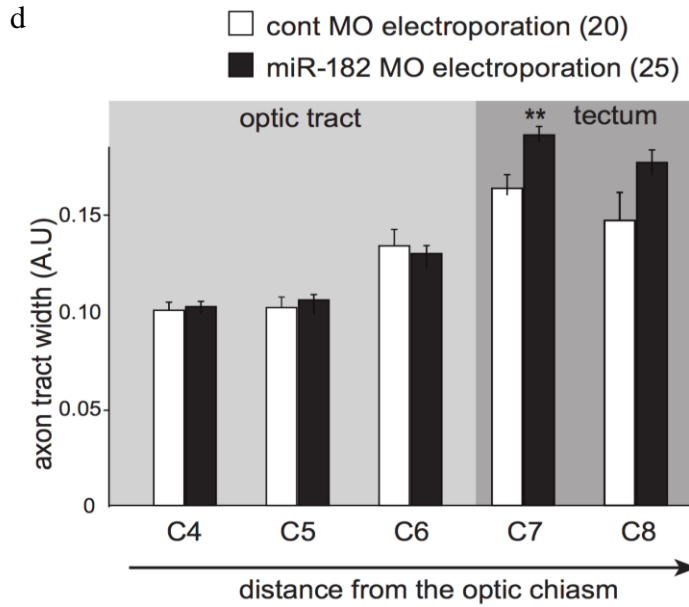


Figure 2-7: Quantification of pathway width. Number of brains analysed displayed within brackets. Two way ANOVA followed by Bonferroni post-test, $**p < 0.01$

Since different embryos vary in sizes the ratios of pathway width were normalized to the brain size.

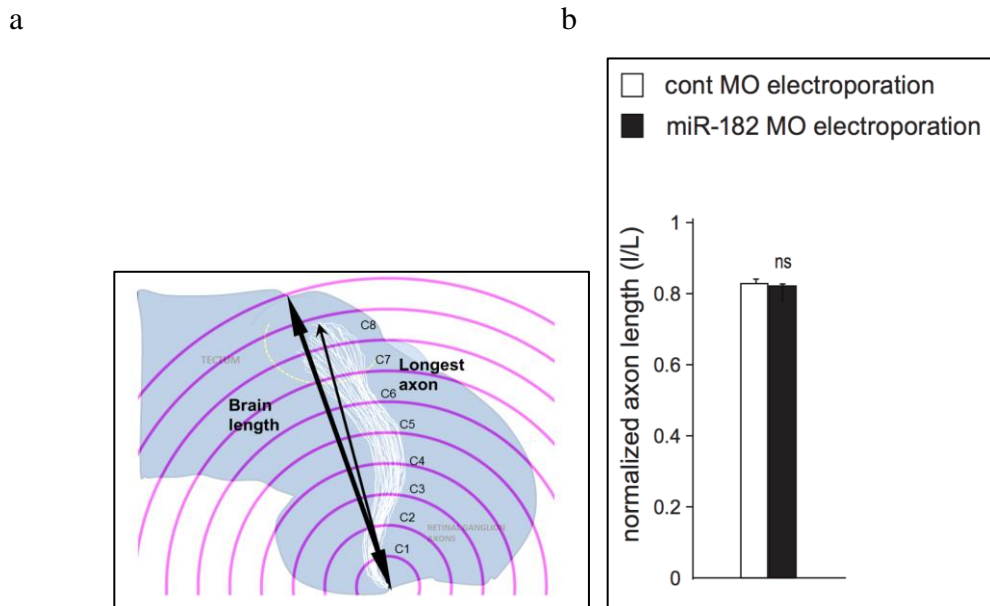


Figure 2-8: Axon length measurement (a): Schematic representation displaying method of pathway width analysis and measurement of axonal length. (b): Quantification of axon length normalised to brain size showing no difference between co-MO and miR-182-MO. Abbreviations: ns: Not significant

Given that the size of the tectal neuropil is very small at this age, approximately 150 μ m, 40 μ m expansion of the projection in the target represents a significant change in retinotectal connectivity.

The fact that miR-182 MO electroporated axons project over a broader targeting regions could mean that these axons fail to respond to chemorepellent cues present surrounding the tectum and that there could be defasciculation within the axonal bundle. *We next conducted a series of in vitro and in vivo experiments that revealed that axonally localized miR-182 regulates responsiveness specifically to Slit2. Indeed, in the absence of miR-182, RGC axons fail to respond to Slit2 in culture, and morphant axons aberrantly project nearer to slit2 expressing territories within the tectum in vivo. Slit-2 loss-of-function phenocopies miR-182 loss-of-function. We next identified cofilin-1 as a key miR-182 target using the target prediction algorithm Targetexpress (Ovando-Vazquez et al., 2016) (annexe 1, figure 5A), luciferase assay using cell lines (annexe 1, figure 5 B-D), and immunofluorescence on GCs in culture (annexe 1, figure 5 E,F). Taken together, these data suggested that miR-182 blocks cofilin1 translation in unstimulated GCs.*

2.3.4 miR-182 SENSOR CAN BE USED ASCERTAIN miR-182 ACTIVITY AND COMPARTMENTALIZED ACTION

We next asked whether miR-182-mediated silencing activity could be in turn released by Slit2 locally within GCs. To address this, our laboratory developed a reporter sensor construct of miR-182 activity. This miR-182-Sensor expresses destabilized GFP (dGFP) under the regulation of a 3'UTR containing three sequences complementary to miR-182, and mCherry as an internal control. Any increase in miR-182 activity should lead to the decrease of dGFP while leaving mCherry expression levels unaltered. In control-Sensor, the three sequences complementary to miR-182 are replaced by scrambled sequences. It should thus be inert to change in miR-182 activity.

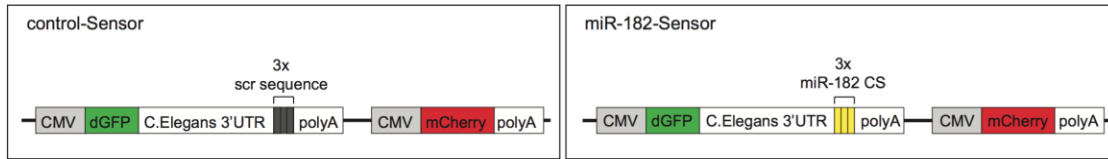


Figure 2-9: Sensor construct design.

miR-182 sensor can detect miR-182 local activity in axons, only if GFP and mCherry are present within this compartment. Therefore, I first assessed whether GFP and mCherry mRNA expressed by the sensor are located within RGC axons in culture. We used Control and not miR-182 sensor because we wanted to assess the presence of the reporters without the influence of miR-182 binding and know if the sensors are suitable to assess miR-182 activity in axons. I carried out electroporation of the sensor in embryos and I captured *in vivo* RGC axons from the optic tract and the neuropil within the tectum, that were labeled with dGFP and mCherry. I subsequently carried out RNA extraction. Care was taken to avoid detecting Sensor plasmid. To avoid the detection of the Sensor plasmid, RNA was DNase treated and the reverse transcription was carried out using oligo-dT primers. *By PCR, we detected the presence of amplicons of the expected size of 377bp using dGFP and mCherry specific 322bp* (Figure 2-10)

This result suggests that the two transcripts dGFP and mCherry are present within axons and therefore the sensor construct is suitable to assess miR-182 activity within axons.

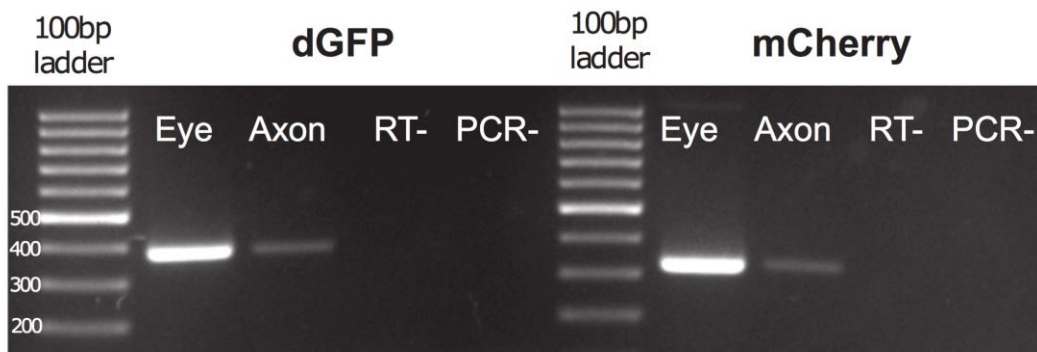


Figure 2-10: Detection of dGFP and mCherry.

Illustrative picture of gel following RT-PCR of d2GFP and mCherry from axons electroporated with sensor.

2.3.5 SLIT2 SILENCES miR-182 ACTIVITY IN RGC AXONS

We next investigated whether Slit2 stimulation alters miR-182 activity specifically within GCs. The finding that miR-182 is an important part of Slit2 signaling points to the idea that Slit2 could be modulating miR-182 activity within the GCs.

We measured change in miR-182 activity by quantifying d2GFP/ mCherry ratio of the sensor. If Slit2 abolishes miR-182 activity, miR-182 would no longer silence d2GFP mRNA and d2GFP would thus be translated into a fluorescent protein. mCherry expression is expected to be unchanged. This will be reflected in the increase in the ratio for d2GFP / mCherry fluorescence. This was explored by means of using control and miR-182 sensor plasmids.

My contribution towards this was electroporation of the miR-182 and control sensor plasmids in embryos and culturing them at stage 37. *Following which Slit2 stimulation was carried out and image analysis was performed (Figure 2-11). We found that Slit2 stimulation (for 10minutes) leads to an increase in d2GFP/ mCherry ratios within cultured GCs suggesting that miR-182 activity is decreased (annexe 1, Fig 7B.).*

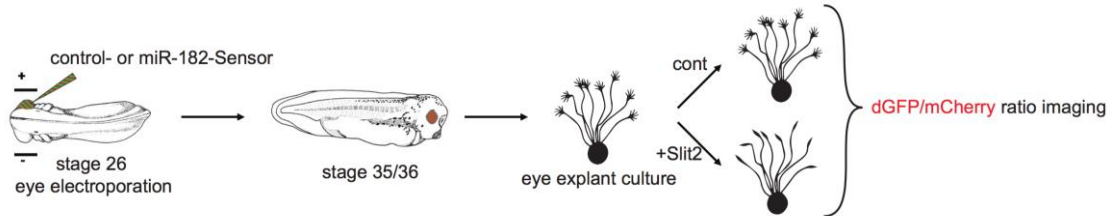


Figure 2-11: Experimental paradigm to assess miR-182 activity upon Slit2 signalling

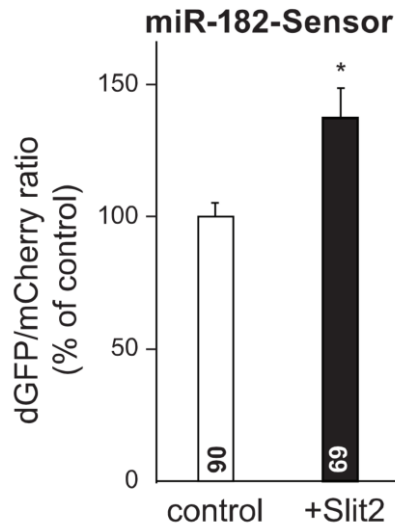


Figure 2-12: Quantification of miR-182 activity. miR-182 activity assessed by dGFP/mCherry ratio with and without Slit2 exposure on miR-182 sensor.

2.3.6 SLIT2 MEDIATED DECREASED IN miR-182 ACTIVITY OCCURS VIA RECEPTORS ROBO2 AND 3

Slit2 mediates signaling through its receptors Robo1, 2 and 3 (Hocking et al. 2010; Jen et al. 2004; Sabatier et al. 2004). Therefore, we asked whether Robo receptors are involved in Slit2 mediated regulation of miR-182 activity. Robo2 and 3 but not Robo1 are expressed in *Xenopus* RGCs. We used dominant negative (dn) constructs for Robo2 and 3 receptors to block Slit2 signaling. Dominant negative constructs are expression vectors coding for receptors, Robo 2 and 3 that lack a cytoplasmic tail (Hocking et al. 2010). Thus, they are useful, as Slit2 binding to these receptors cannot mediate downstream signalling thereby blocking Slit2 signaling. These dnRobo proteins interfere with endogenous receptors for Slit2 (Stein & Tessier-Lavigne 2001; Whitford et al. 2002). If Slit2 signaling is indeed responsible for miR-182 regulation, blocking Slit2 receptors Robo 2 and 3 should lead to increase in miR-182 activity reflected by decrease in d2GFP/ mCherry ratio. To assess this, I electroporated the sensor plasmids (control and miR-182 sensor) along with dnRobo2 and 3 at stage 26. At stage 37/38, I cultured eye explants for slit2-mediated collapse (10 mins of Slit2 exposure) and subsequent image analysis (Figure 2-13).

Quantification analysis of d2GFP/ mCherry ratio directly within GCs revealed that electroporation of dnRobo2 and 3 to RGCs lead to a 33.69% (S.E.M±12.26%) decrease in d2GFP/ mCherry ratio in Slit2 stimulated culture compared to control. This indicates that miR-182 activity is increased in the presence of dnRobo2 and 3. It further suggests that Robo2 and 3 mediate Slit2-induced loss of miR-182 activity in GCs. For technical reasons, specifically with respect to handling several conditions of the explant coverslips (to be used within the time frame of appropriate Slit2 exposure) proved to be difficult. Therefore no Slit2 control was not used. Since in neurons Robo2/3 are largely known to mediate Slit2 dependent downstream responses it seemed unlikely that dominant receptors could be functioning independent of Slit2. However, dnRobo2/3 mediating decrease of the dGFP/mCherry in a Slit2 independent manner cannot be formally ruled out.

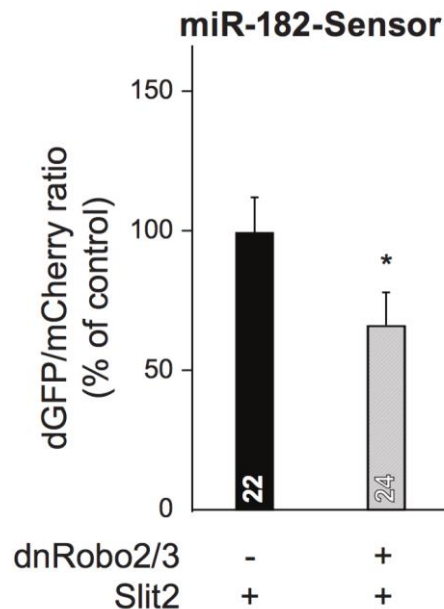
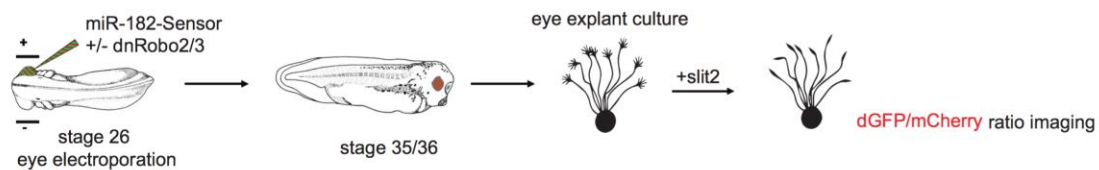


Figure 2-13: Measurement of miR-182 activity.

(a) Schematic of experimental paradigm showing measurement of miR-182 activity following Slit2 inhibition with dominant negative Robo2/3 receptor constructs. (b): Quantification of dGFP/ mCherry

*ratio in miR-182 sensor electroporated axons. Numbers within bars represent number of GCs analysed. Statistics: *p =0.0348, Mann Whitney (Two tailed test). Abbreviations: dn: dominant negative*

2.3.7 SLIT2 STIMULATION DOES NOT LEAD TO miR-182 DEGRADATION

Slit2 stimulation leads to decrease in miR-182 activity as observed by sensor experiments. How does Slit2 modulate miR-182 expression? miR-182 could merely be displaced off its target transcripts but remaining unaffected itself reflecting decrease in its activity but not expression levels. Alternatively, miR-182 could be degraded. Therefore, to examine this, we investigated miR-182 levels from axons treated with Slit2 using qPCR.

We decided to adopt an approach that would enable to collect pure cultured axons following slit2 stimulation I thus optimized a protocol to capture pure cultured axons by LCM. This approach is particularly challenging due to the high number of explants required with excellent outgrowth to obtain enough material, whilst, at the same time, reducing the level of contaminating detached retinal and mesenchymal cells.

During the optimization process I optimized a variety of protocol parameters, such as the type of membrane used, the type of fixative, including fixative concentration and length of fixation.

Membranes: Leica provides membranes made of different materials. I chose POL membranes for explant cultures as these provided more consistent axonal outgrowth in comparison to other membrane types as it supported axonal outgrowth most consistently than other membrane types that I tried. The other membranes did not support axonal outgrowth or were not suited to culture with liquid. In addition, cultures were seeded on POL slides that are made of thin membrane therefore making it very challenging to seed explants without disrupting the membrane.

Fixation: 1% PFA for 5 mins was chosen as opposed to the routinely used 4% (See table- I used the parameter highlighted in yellow). As excessive or residual fixatives may lead to increased crosslinking between RNA and proteins, thereby decreasing RNA yield, explants were only fixed lightly to obtain good quality RNA. Additionally, in contrast to thicker tissue sections or whole embryos already exposed axons are amenable to fixation with 1%PFA. In addition, presence of excessive PFA can be inhibitory for PCR reactions. In addition, 1% PFA is amenable for culture that already have axons

exposed, as opposed to thicker tissue section or whole embryos where higher concentration of fixative is needed to ensure complete cross-linking.

Table 2.3.1: Influence of fixative on the RNA quality and yield:

Concentration of Paraformaldehyde (PFA)	Length (in mins)	RIN (RNA Integrity Number)	Yield (in pg/ μ l)
2%	10	2.4	65
1%	10	3.1	184
No fixation	-	Explants detached	Explants detached
1%	5	6.3	425

Laser settings also had to be optimized for this procedure to enable efficient cutting of axons. I carried out *in vitro* laser capture microdissection of axons treated with Slit2. Wild type eye explants (70 eyes per slide) were cultured on RNase free POL membranes and were treated with Slit2 or PBS for 10 mins. Following Slit2 exposure, explants were fixed and dehydrated and subject to laser capture.

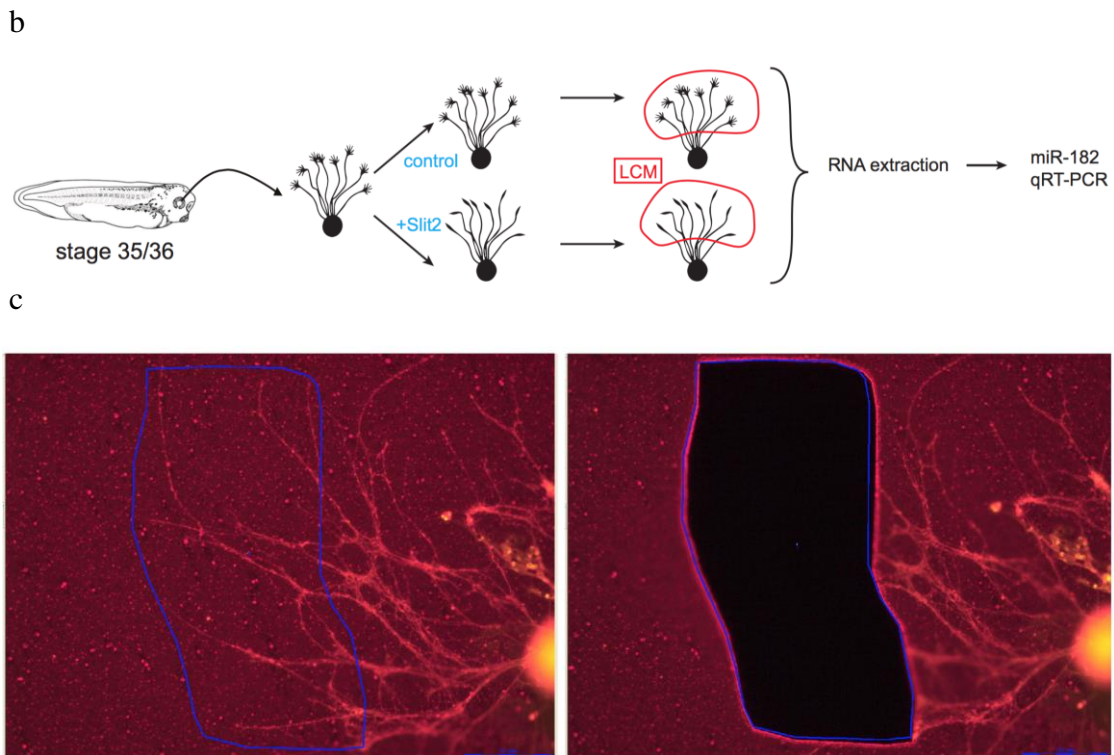


Figure 2-14: Laser capture in vitro

(b): Schematic of the experimental set up showing analysis of miR-182 expression from axons isolated following Slit2 treatment. (c): Illustrative images of explants and axons before and after laser capture microdissection (LCM)

Specifically, axons from explants were captured in order to avoid cell body contamination and RNA was extracted (Figure 2-14, b). Axons were first assessed for their purity by RT PCR for β -actin, histone 4 and Map2. Axonal RNA devoid of cell body contaminants or other non-neuronal cells should test positive for β -actin, known to be present in axons (Leung et al. 2006), while negative for histone and map2. Indeed, I found that axons were pure and free from other contaminants thus enabling assessment of miR182 exclusively within the axonal compartment (Figure 2-15).

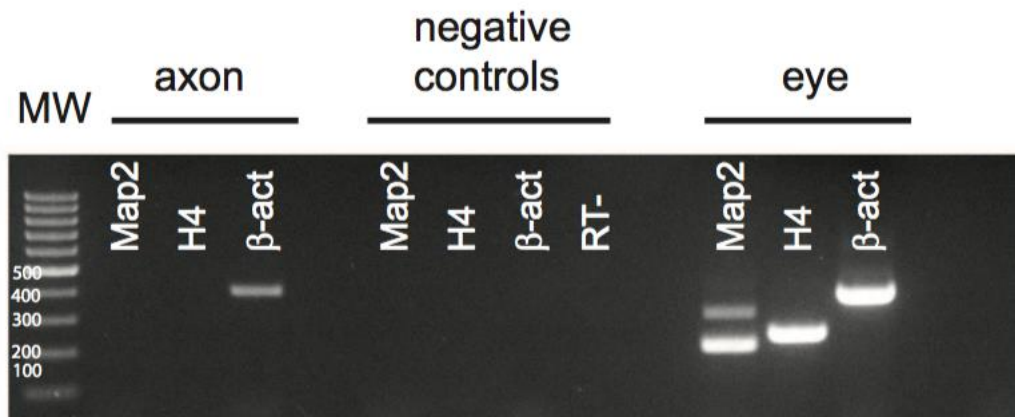


Figure 2-15: *In vitro* axon purity test. Gel following RT-PCR reaction for assessing purity of axons isolated via LCM. Abbreviations: RT no template negative control, H4: Histone H4

Following purity check, miR-182 levels were quantified using Taqman qPCR. qPCR analysis revealed that miR-182 levels were unchanged in slit2 compared to vehicle treated culture ($-4 \pm 10.9\%$) (Mann Whitney test, non-significant). miR-182 levels were normalized to U6 expression.

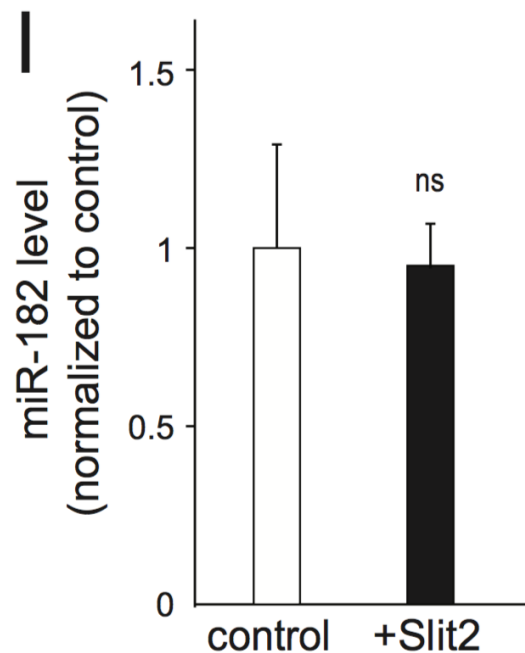


Figure 2-16: Quantification of miR-182 by $\Delta\Delta CT$ method in LCM

This suggests that miR-182 is inactivated by Slit2 in axonal GCs without leading to its degradation. This implies that miR-182 inactivation by Slit2 may be reversible.

2.4 DISCUSSION

Growing axons have recently been discovered to contain a large number of miRNAs(Sasaki et al. 2013; Natera-Naranjo et al. 2010). Axons are ideal sites for miRNA action given that they comprise a large population of dynamically changing mRNAs(Zivraj et al. 2010). During axon guidance, a range of extracellular signals determines the expression of specific mRNAs within the rapidly advancing GC. Of the several transcripts expressed only a subset are translated at any given time locally therefore begging the question: How are transcripts not ready for translation kept silent within GCs? miRNAs and RNA binding proteins are emerging candidates that regulate translation of mRNAs.

However, very little is known in the context of axon guidance about how miRNAs mediate cue specific mRNA translation and importantly how these miRNAs are regulated themselves.

Here, we demonstrate the role of an axonal miRNA, miR-182, in regulating precise axonal targeting of RGC axons. miR-182 was found to be the highly abundant miRNA with an average read counts per million (cpm) of 17.49 representing 25% of the abundant miRNAs detected within axons. Interestingly we found that this miRNA is largely depleted within RGC cell bodies (8-fold difference with respect to whole eye) suggesting an exclusive axonal role for this miRNA. Other reported axonally enriched miRNAs with a defined functional role are miRNAs involved in axon extension. These are miR-132 and miR-181c in mouse DRG neurons(Hancock et al. 2014; Wang et al. 2015). Very few miRNAs to date have been shown to have roles in axonal targeting. miR-124 has been important for this function(Baudet et al. 2012) but it is not known to be an axonal abundant miRNA.

Our data show that miR-182 is required for defining the region of innervation for retinal axons within the tectum. It is important to note that miR-182 loss-of-function does not cause long range guidance defects. Morphant RGC axons project normally until they reach the tectum however, the pathway width significantly increases and RGC axons cover a larger expanse within the tectum. This could have implications on precise formation of post synaptic targets. Studies in mouse superior colliculus that looked at processes post axonal targeting and along the lines of formation of RGC axonal

termination zones within their target have found a miRNA to be important in this process. miR-132 is important for axonal branching and loss-of-function of miR-132 affects RGC axon termination zone(TZ)in mouse superior colliculus(SC)(Marler et al. 2014). TZs are regions within the SC around which axons branch. Immature TZs are larger in size characterized with scattered axonal branches while Mature TZs are more focused at the appropriate topographic location with intense arborization pattern. miR-132 loss-of-function leads to broader termination zones where axonal branches are sparse but more wide spread suggestive of an immature TZ. Thus, miR-132 plays a role in development of TZ zone in mouse SC while maintaining topographic targeting. Thus, different miRNAs could be carrying out distinct specialized roles.

miR-124 is another miRNA which is required for regulation of axonal targeting Loss of miR-124 leads to ventral projection of axons from the tectum which results due to altered Sema3A responsiveness. Interestingly, both miR-124 and miR-182 very selectively affect GC responsiveness to specific cues.

How do miRNAs mediate their action? There are several mechanisms of miRNA mediated post transcriptional gene repression(Filipowicz et al. 2008). miRNA mediated repression leading to target degradation is found to be the most prevalent mechanism in mammalian cells(Selbach et al. 2008; Baek et al. 2008; Hendrickson et al. 2009; Guo et al. 2010; Subtelny et al. 2014; Eichhorn et al. 2014). miRNAs can also repress mRNAs at the translation level where miRISC binding can result in inhibition of initiation(Pillai et al. 2005) or elongation(Petersen et al. 2006) of mRNA translation. It is now known that miRNA mediated translation block leads to mRNA decay(Bazzini et al. 2012; Djuranovic et al. 2012). However, miRNA mediated translational repression is observed to occur in some contexts. In support of our model whereby Slit2 relieves repression of miR-182 from cofilin1 mRNA there are other examples in the field that demonstrate similar mechanisms. miR-134 in rat hippocampal neurons within dendrites mediates repression of Limk1 until BDNF stimulation that leads to de-repression of Limk1 to modulate spine size(Schratt et al. 2006). Similarly, miR-181d along with FMRP is known to repress mRNAs Map1b and Calm1 in mouse DRG axons(Wang et al. 2015). Upon NGF exposure, this repression is relieved. This suggests that perhaps miRNAs can be used to keep transcripts from expression until the right cue exposure. The contrary

has also been observed in mouse RGCs where BDNF stimulation leads to increase in miR-132 levels that lead to downregulation of its target, p250-GAP(Marler et al. 2014). This suggests that miRNAs could be working in either direction to regulate mRNA expression.

What happens to the miRNA itself upon cue exposure? In our case, Slit2 exposure does not lead to miR-182 degradation. This is also the case for miR-134 in dendrites(Schratt et al. 2006) and miR181d in axons(Wang et al. 2015). Relief of miRNA repression does not seem to be associated with miRNA degradation at least in these cases. While we haven't explored this facet, but it is possible that relief of repression by miR-182 could be mediated by RNA binding proteins. This was observed in mouse hippocampal dendrites where FMRP dephosphorylation upon mGlu-R (metabotropic glutamate receptor) signaling leads to release of Ago2 bound miR-125a from its transcript PSD-95(Muddashetty et al. 2011). miR-125a is localized to dendrites and regulates spine density and branching by targeting PSD-95. Both FMRP is important for miR-125a inhibition and similarly miR-125a binding to its target is important for FMRP mediated repression. Upon activation through mGlu-R, miR-125a bound to Ago2 dissociate from FMRP. This is further thought to result in miRNA decay(Muddashetty et al. 2011). This is however not observed in another model where NGF triggers release of FMRP and miR-181d from its transcripts without miR-181d –Ago2 being dissociated from FMRP (Wang et al. 2015). FMRP loss-of-function results in failure of miR-181d delivery to axons but not its levels. Therefore, it is possible that miRNAs not cleared from the compartment could be readily available and reused for another round of repression. Thus, in our context miR-182 activity but not levels being affected upon Slit2 stimulation could be a sign for a reversible mechanism of repression. Therefore, either by preventing axonal delivery (as in case of miR-181d) by FMRP(Wang et al. 2015) or by reducing miRNA activity (as in case of miR-182) the miRNAs could themselves be regulated without leading to their degradation thus providing energy-effective solutions within axonal compartments. Firstly, more miRNAs are not needed to be transported from the cell body and existing ones can be recycled to be used on various transcripts. Secondly, the response time can be reduced greatly by having miRNAs mediate a

reversible target de-repression. This could benefit navigating GCs that are constantly exposed to cues in a rapid manner.

Thus the role of RNA binding proteins in miRNA mediated repression could serve as an interesting aspect to be further investigated in our context.

In conclusion, miR-182 regulates axonal pathway width in the target by repressing cfl-1 mRNA. Upon Slit2 stimulation, miR-182 is released from cfl-1 without subsequent mRNA degradation. Thus, this study highlights the role of miR-182 in axonal targeting *in vivo* and acts as a switch to permit translation of cfl1 thus enabling GC turning.

3.1 ABSTRACT

This chapter describes the role of miR-181a and b in *Xenopus laevis* visual circuit formation. Our axonal miRNA profile analysis has revealed that mature miR-181a/b are highly abundant in axons representing, together, about 25% of the total miRNAs detected in axons. To understand the significance of this finding, I explored the role of this family specifically with a loss-of-function approach. By blocking the function of miR-181a and miR-181b in developing embryos using MOs, I was able to uncover that this family has an important role in axon guidance *in vivo*. Indeed, a significant proportion of RGC axons fail to target the tectum precisely and form aberrant projections. In addition, miR-181a/b morphant axons in culture show decreased responsiveness to specific tectal cues, Sema3A And Netrin1, while their response to Slit2, also expressed by the tectum, is unaltered. This suggests that miR-181a/b modulate the responsiveness to specific cues. We further observed that rescuing miR-181a/b levels with exogenous miRNA mimics restored the responsiveness to Sema3A within GCs, confirming that the phenotype observed can indeed be attributed to miR-181a and b. Thus, miR-181a/b play important roles in axonal targeting by modulating Sema3A and Netrin1 responsiveness in axons. Insight into mRNAs regulated by miR-181a/b can reveal the mechanism of action through which miR-181a and b oversee precise navigation within axons. I have thus next started to characterize targets that are regulated by these miRNAs in RGCs. For this, we developed an approach that combined the selective collection of RGC compartments, soma and axons, *in vivo* by laser capture microdissection (LCM) with high throughput RNA-seq profiling from low sample size. Analysis is currently underway to identify miR-181a/b direct targets and explore whether this miRNA family differentially act on neuron compartments. As a parallel approach, we have also identified which mRNAs, collected from RGC axons and soma by LCM, are predicted to be targeted by miR-181a/b. Interestingly, targets regulating Sema3A and netrin1 GC responsiveness have one of the highest probability to be *bona fide* miR-181a/b targets. Thus, miR-181a/b have emerged as crucial molecules in regulating axonal targeting and GC responsiveness towards tectal cues.

3.2 MATERIALS AND METHODS

(Catalogue numbers to products can be found on the appendix. Please refer to p. 182)

3.2.1 EMBRYOS

X. laevis embryos were obtained by *in vitro* fertilization. *Xenopus* adult frogs were induced with hormone and eggs were obtained and fertilised *in vitro* (Cornel & Holt 1992), raised in 0.1X Marc's Modified Ringer's solution (MMR 10X: 1M NaCl; 20mM KCl; 10mM MgSO₄; 20mM CaCl₂; 50mM HEPES, pH 7.5) at 14°C and staged according to Nieuwkoop and Faber, 1994 (Nieuwkoop P. 1994). All animal experiments were approved by the University of Trento Ethical Review Committee.

Stage of embryos used:

- For MO mediated knock down
 - By microinjection: 8 cell stage (when dorsal blastomeres are formed that specify the nervous system)
 - By electroporation: Stage 26 (before axons exit the eye (Holt 1989))
- For collapse assay and laser capture microdissection *in vitro*: Stage 37/38 (correspond to *in vivo* stage when pioneer axons begin to reach the target)
- Pathway visualization and *In situ* hybridization on sections and Laser capture microdissection *in vivo*: Stage 40 (most axons have reached the target)

3.2.2 MORPHOLINOS (MOS)

Antisense (MOs) tagged with 3'Fluorescein were designed and supplied by Genetools.

Usage of MOs: MOs were resuspended in sterile water to obtain a concentration of 1mM for each. Accurate stock concentrations were further determined by using Nanodrop by diluting an aliquot with 0.1N HCl. MOs were stored at -20°C or at room temperature in 10ul aliquots.

MO sequences were designed based on the pre-miRNA sequence for *Xenopus tropicalis* obtained from miRBase and from *Xenopus laevis* sequence obtained from next-generation sequencing (Baudet et al., 2012).

- pre-miR-181a-1 in *Xenopus laevis* is located on chromosome 4S and 4L. Between the two locus (4S and 4L) there is a single nucleotide mismatch. This mismatch is at the loop region. Comparison against *Xenopus tropicalis*, we observed that the *Xenopus laevis* pre-miR-181a-1 4S is exactly identical to *Xenopus tropicalis* pre-miR-181a-1. Our MO sequence does not span this mismatch region but is against region spanning part of the loop and part of the 5p sequence. This region directed by the MO is exactly identical amongst *Xenopus laevis* (both chromosome 4S and 4L) and *Xenopus tropicalis*.

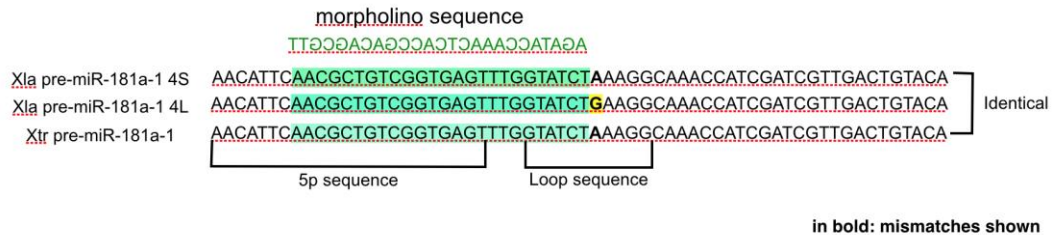


Figure 3-1: MO directed against pre-miR-181a-1

- pre-miR-181a-2 in *Xenopus laevis* is similarly located on chromosome 8L and 8S. Between the two loci there is a single mismatch as shown below within the loop sequence. In comparison with *Xenopus tropicalis*, there is a difference of a single nucleotide also contained within the loop sequence. The MO targets part of the 5p and part of the loop sequence and does not span the mismatches. Thus the region targeted by the MO like in pre-miR-181a-1 is identical in both species as shown below.

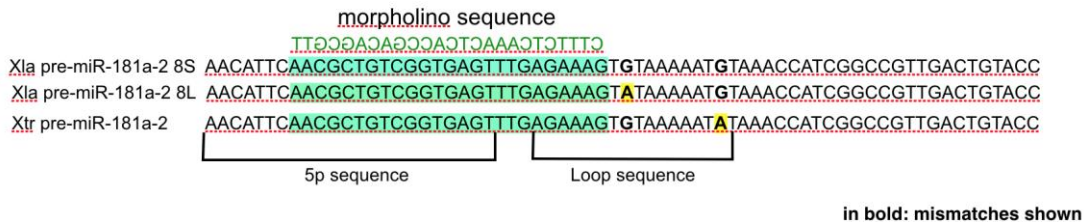


Figure 3-2: MO directed against pre-miR-181a-2

Sequences of MOs used:

Xenopus tropicalis pre-miR-181a-1-MO: 5'AGATACCAAACCTCACCGACAGCGTT 3',

Xenopus tropicalis pre- miR-181a-2-MO: 5' CTTTCTCAAACCTCACCGACAGCGTT 3',

Xenopus tropicalis miR-181b: 5' CCCACCGACAGCAATGAATGTT 3'

Custom control-MO: 5' GTGTAACACGTCTATACGCCCA 3'

Standard control-MO: 5' CCTCTTACCTCAGTTACAATTTATA 3'

Since MOs targeting the pre-miRNA and mature miRNA differ in length, we designed control MOs to match the corresponding 25nt sequence of the pre-miR namely the standard control that was 25 nt long and a custom control sequence corresponding to 22 nucleotides of miR-181b.

Preparation of MOs with reporter

Since MOs stored as frozen aliquots can come out of solution, MOs were thawed from -20°C and heated at 65°C for 5 mins, vortexed briefly and spun down. MOs, control-MO or miR-181a/b-MO were diluted to a concentration of 250µM with RNase free water along with 0.5 µg/µl of pCS2-CAAX-Cherry reporter plasmid.

The concentrations used were: For miR-181 a/b knockdown: 62.5µM Xtr pre-miR-181a-1 MO, 62.5µM Xtr pre-miR-181a-2 MO, 125µM miR-181b MO were prepared in 6µl.

For the control MOs: 125µM custom control MO, 125 µM standard control MO were prepared in 6µl.

3µl of the solution were filled into the capillary and (roughly 8-10nl) were injected within the optic stalk.

3.2.3 MIMICS

Rescue experiments were carried out using double stranded RNA molecules to mimic native microRNA. These were designed to mimic both miR-181a and miR-181b and were received as 20nmol pellets that were resuspended with 1X RNase DNase free PBS to obtain a stock concentration of 100µM.

Sequence of the mimics:

xtr-miR-181a-5p - MIMAT0003625 – 5' AACAUUCAACGCUGUCGGUGAGU -3'

xtr-miR-181b MIMAT0003609 – 5' AACAUUCAUUGCUGUCGGUGGG- 3'

Negative control: cel-miR-67 - MIMAT0000039 –
5'UCACAACCUCCUAGAAAGAGUAGA- 3'

For *in vitro* rescue, these mimics were injected and electroporated (25µM of miR-181a + 25µM miR-181b) along with a reporter plasmid pCS2-CAAX-Cherry (0.5µg/µl) in order to assess the success of electroporation. CAAX is enables membrane tagging and thereby enable to visualise axons. Control or miR-181a/b mimics were electroporated in embryos microinjected with control (1nl containing 76µM custom control, 72.5µM standard control) or miR-181a and b MO (1nl containing 45µM pre-miR-181a-1, 45µM pre-miR-181a-2 and 50.6µM) microinjected embryo.

For *in vivo* rescue, mimics were electroporated (at the above concentration) serially after MO electroporation. MO were electroporated along with pCS2-EGFP while mimics were electroporated along with pCS2-CAAX-Cherry so as to enable visualisation of the pathway.

3.2.4 ELECTROPORATION

For electroporation, stage 26 embryos were used. Embryos were dechorionated and washed once in 0.1X MMR. Few embryos at a time were rinsed once briefly in 1X MBS (Modified Barth's Saline) and anesthetized in 1X MBS + MS222 (0.2%). The embryos were then placed in a T shaped sylgard chamber and the MOs with reporter (pCS2-EGFP or pCS2-CAAX-Cherry: 0.5µg/ul) were injected and electroporated in one eye with conditions similar to those previously described (Falk et al. 2007). I noticed that FITC labelled-MO bleached easily preventing their localization through imaging and this is why I opted for the use of mCherry reporter construct alongside FITC-MO. The reporter was used to evaluate the success of electroporation and also since it is membrane bound it was possible to trace the axons along the pathway.

For laser capture, in order to process tissue with ethanol and still visualise axons post processing, I used pCS2-EGFP as a reporter as opposed to membrane bound CAAX-Cherry since CAAX-Cherry gets bleached upon dehydration with ethanol. Following electroporation, embryos were rinsed once in 0.1X MMR and then transferred to fresh 0.1X MMR and grown at 14°C until stage 40.

Embryos were sorted after 48 hrs to check for expression of the reporter in the eye and were sacrificed 5 days post electroporation.

3.2.5 OPTIC PATHWAY VISUALIZATION

To check for pathfinding defects, embryos that were adequately electroporated (as seen after sorting for pCS2-EGFP or pCS2-CAAX-Cherry expression) were fixed at stage 40 in 4% PFA for 2 hrs at room temperature (2ml of 4% PFA was prepared as follows: 16% PFA: 500 μ l + 10X PBS: 200 μ l + 1.3ml distilled water). Following fixation, embryos were rinsed thrice in 1X PBS. Embryos were kept in eppendorfs covered with foil at all times to avoid bleaching of fluorescent proteins. Embryos were dissected on sylgard with insect pins to remove the eye and brain. The brain was then cut on the ventral midline to open the two hemispheres as an open book. This preparation is described as open brain prep. See (Figure 3-14) A coverslip was prepared as follows: A 24 mm glass circular glass coverslip was taken on which two reinforcement labels of 12mm were stuck on top of each other to create a well/depression. The cut brain was then aspirated with 1X PBS and placed inside the well. The brain was flipped and opened such that the outer (dorsal) part of the hemispheres faced down on the glass. The medial/inner part of the hemispheres were exposed always keeping the prep immersed in 1X PBS followed by mounting with a 12 mm glass coverslip. This temporary preparation was visualized immediately using an inverted fluorescence microscope. The visual pathway was thus observed using Zeiss Observer Z1 and Leica DMI8. The apotome module and / or z-stack projections were taken for observing detailed axonal projections.

3.2.6 QUANTIFICATION OF ABERRANTLY PROJECTING AXONS

Axonal projections that were imaged at 40X were analysed by going through individual stacks of the z projections and counting number of electroporated / fluorescing axons that projected aberrantly (forming loops or bends from the optic projection). The ratio of total number of aberrantly projecting axon to total number of electroporated axons was calculated. The data were not normally distributed as seen by Pearson Omnibus normality test therefore Mann-Whitney test was used to determine the significance of the percentage of aberrantly projecting axons.

3.2.7 BLASTOMERE MICROINJECTION

For microinjection, jelly coat from embryos was removed (dejelling). Dejelling was done at 4-cell stage using dejelling solution (For 25 ml of solution, 0.2M Tris pH 8.8 and 0.2M DTT were used and made up volume with water. Stock conc of Tris pH 8.8 and DTT :1M). Dejelling was carried out for 5 mins with intermittent swirling. Embryos were checked to see if the jelly coat was removed and then washed several times in 0.1X MMR. Embryos were transferred to an injection dish containing 4% Ficoll prepared in 0.1X MMR to enable them to sink and were aligned such that the dorsal blastomeres faced the injection needle. (The 2 smaller and lighter of the 4 cells were considered as the dorsal blastomeres). Prior to injection, the capillary containing MOs was calibrated to get the required drop size to achieve the right 1nl volume. Once embryos reached 8-cell stage, to knock down miR-181-MO: 1nl containing 45µM pre-miR-181a-1, 45µM pre-miR-181a-2 and 50.6µM miR-181b or for control: 1nl containing 76µM custom control, 72.5µM standard control MOs (fluorescein tagged) were injected in both dorsal blastomeres. Following injection, embryos were transferred to 0.1X MMR and kept at 14°C. The following day, medium was changed and dead embryos if any were discarded. At neurula stage (stage 19), embryos were sorted to check for fluorescence. Only embryos containing equal fluorescence in both halves of the central nervous system were considered. Embryos were then raised until stage 37/38 and eyes were dissected and cultured to perform collapse assay or *in situ* hybridization.

3.2.8 IN SITU HYBRIDIZATION

DIG labelled LNA oligonucleotides complementary to *Xenopus tropicalis* (Xtr) - miR-181a (5'DigN/-ACTCACCGACAGCGTTGAATGTT/DigN/-3'), xtr-miR-181b (5'-CCCACCGACAGCAATGAATGTT-3') and scrambled probes (5'-DigN/GTGTAACACGTCTATACGCCCA/DigN/3') were obtained from Exiqon. The sequence of mature miR-181a and miR-181b in *X.tropicalis* are identical to that of *X.laevis* as verified by sequencing results obtained from Baudet et al.,2012.

miR-181a: 5'-AACATTCAACGCTGTCGGTGAGT-3'

miR-181b: 5'-AACATTCATTGCTGTCGGTGGG-3'

Protocol was adapted from Obernosterer et al.,2007 (Obernosterer et al. 2007) as explained in section 2.2.8. Control or miR-181a and miR-181b probes were added at 1nM.

3.2.9 RETINAL EXPLANT CULTURE

Whole retinas from stage 37/38 embryos were dissected and cultured at 20°C for 24 h in 60% L15 minimal medium containing antibiotics (PSF 100X stock) on 12mm glass coverslips. Prior to culture, glass coverslips were coated with poly-l-lysine (10 µg ml⁻¹) overnight at 20°C, washed with water and coated with Laminin (10 µg ml⁻¹) for 1 hr at room temperature. Embryos were anesthetized in 60% L15 containing MS222 and retinas were dissected and culture was done as mentioned in Baudet et al.,2012 (Baudet et al. 2012)

3.2.10 LASER CAPTURE MICRODISSECTION *IN VIVO*

Laser capture microdissection was performed on retinal ganglion cells and axons *in vivo* as follows: Embryos were electroporated with control or miR-181 a/b MOs along with pCS2-EGFP reporter plasmid (0.5µg/µl) as explained above. Well electroporated embryos were sorted and were fixed at stage 40 in 4% PFA (prepared as mentioned above but using RNase free 10X PBS and RNase free water and a fresh vial of PFA was used each time). Fixation was carried out for 15 mins followed by 1X PBS rinse thrice. Embryos were kept covered at all times. Following fixation, embryos were treated with 30% Sucrose made in 1X RNase free PBS placed on ice for 1 hr. Only 5 embryos were processed per tube and timings for fixation and sucrose treatment were strictly followed. Following sucrose treatment, embryos were embedded in blocks containing OCT on dry ice and stored in the -80°C until use. On the day of laser capture, embryos were sectioned with cryostat at 14µm thickness and taken on PEN membrane slide. (One slide was processed each time.)

The processing of slides was done as follows - 95% ethanol - 30s, 75%, 50% (twice), 75%, 95%, 100%(twice) - each 30 seconds followed by one quick wash with Xylene (in the hood), then 5 mins of fresh Xylene (second mailer also done in the hood), Air dried in the hood for 5 mins and then placed in a RNase free falcon containing dessicant. The

sections were immediately laser captured using Leica LMD6500 microdissector. The settings used were: Magnification: 63X, Power: 32-34, Aperture: 1, Speed: 16-18, Specimen Balance: 0, Offset: 200. RGC and Axon samples were collected simultaneously on different caps containing lysis buffer with Beta-mercaptoethanol. Following capture, RNA was extracted using Norgen Single cell RNA extraction kit and RNA was eluted in 5mM Tris (pH:7.6). Quality of RNA was estimated using Agilent Bioanalyser 2100 with Agilent Pico Chip.

3.2.11 COLLAPSE ASSAY

Xenopus eye explants were cultured at stage 37/38 as described above on glass coverslips containing 500 μ l 60% L-15medium. After 24 hrs, retinal explants were bathed in 200ng ml⁻¹ human recombinant Sema3A-FC, 100ng ml⁻¹ Mouse netrin-1 or 250ng ml⁻¹ Slit2 (stored diluted in 0.1% protease-free BSA) or PBS (for control) for 10 minutes followed by fixation in 2% paraformaldehyde (PFA), 7.5% (wt/vol) sucrose for 30 mins. For determining protein synthesis dependent concentration, cycloheximide and rapamycin were used at 50 μ M and 100nM respectively. Post fixations, coverslips were washed and mounted in Immunohistomount. GCs were considered collapsed when they possessed no filopodia, or two or fewer filopodia each shorter than 10 μ m as in Campbell et al.,2001(Campbell et al. 2001). To avoid subjective bias, all collapse analysis was done blind to experimental condition.

3.2.12 IMMUNOHISTOCHEMISTRY

Retinal explants were cultured and fixed as described above. Post fixation explants were permeabilized with 0.1% Triton X-100 for 3 mins followed by washes with PBS. Blocking was carried out with 5% Heat inactivated goat serum (HIGS) for 1hr.

Antibodies used:

- 1) Mouse monoclonal anti-Ago2 (kind gift from Dr. Donal O'carroll, then at EMBL, Monterotondo and used at 1:50 dilution), The Ago2 antibody is a mouse monoclonal raised against the N-terminal region of mouse Ago2 protein.
- 2) Mouse monoclonal anti-acetylated tubulin (mouse IgG2b isotype; Obtained from Sigma and used at 1:1000 dilution).

3) Antibody against Dicer is a Rabbit polyclonal (obtained from Santacruz and used at 1:50 dilution)

Antibodies were incubated overnight at 4°C. The following day, explants were washed thrice in 0.01% TritonX prepared in PBS and incubated with secondary antibody prepared in 5% HIGS for 1 hr in dark at room temperature. 1:1000 dilution of Goat anti mouse or goat anti-rabbit Alexa 488 or 594 (F(ab')₂ fragments) were used. Following secondary antibody incubation, explants were washed and mounted with prolong gold and kept covered at all times. Zeiss inverted axio observer Z1 was used to visualise the signal.

3.2.13 STATISTICAL ANALYSIS

Each experiment was conducted at least three times unless otherwise stated. For all tests, the significance level was $\alpha = 0.05$. Data were analyzed with Prism 6 (GraphPad). Statistical tests used for the corresponding experiment have been mentioned in the figure legends.

3.2.14 MICROFLUIDIC CHAMBER

Note: The chambers used here were prototypes and they differ from conventional chambers by having a rectangular compartment to enable placement of eye explants. Conventional chambers have circular compartments more suited for dissociated cells.

Mattek dishes were treated with poly lysine overnight. Standard Double open microfluidic chamber (DOC150) was sterilised in 100% ethanol and washed several times in sterile distilled water and dried overnight. Following day, the polylysine was washed off from the Mattek dish and dried well. Importantly, both chamber and the coverslip were kept dry in order to allow perfect sealing between the chamber and the coverslip. Sterile DOC150 chamber was placed atop the poly lysine treated dish and pressed such that no air bubbles are trapped. The two compartments were then treated with laminin for 1 hr (prepared in 100% L15) washed once with 60% L15 and replenished with fresh 60% L15 (400µl on eye explant side and 300µl on axonal side).

After culturing (25-30 explants) the chamber plus dish was kept in the incubator at 20°C and observed each day until day3 (without changing medium in between).

3.2.15 IMAGING

The following microscopes were used for imaging and measurements.

- a) For observing explant cultures and counting collapsed GCs, Leica Dmi8 inverted microscope was used. Collapse counting was performed with 20X and 40X phase objectives in combination with 1.5X optovar lens.
- b) For acquisition of open brain preparations, Zeiss Observer Z1 using HXP metal halide lamp in combination with the apotome module was used. To observe all the axons in the bundle, z stack images were taken with Plan-Apochromatic 10x/0.3, EC Plan-Neofluar, 20x/0.5, or EC Plan-Neofluar 40x/0.75 objectives.

Pictures were acquired with AxioCam MR3, 1.4megapixel monochromatic camera. Exposure was variable and maximum intensity projections were done to combine all the z stacks onto one frame.

- a) *In situ* hybridization was observed and imaged on upright widefield Zeiss Imager M2 fluorescence microscope equipped with AxioCam color camera. Images were acquired with EC Plan Neofluar 20X/0.5 and EC Plan Neofluar 10X/0.3 objectives.
- b) Immunohistochemistry: Zeiss observer Z1 inverted microscope was used to take to visualise the fluorescent signal for dicer and tubulin. Images were captured with Plan Apochromat 63X/1.4 oil or Plan Apochromat100X/1.4 oil objectives using HXP metal halide lamp with AxioCam MRm camera with an exposure of 3 seconds. For Ago2, inverted Leica Dmi8 microscope equipped with white Lumencor Solid state white light source and an Andor Zyla 4.2CL10-VSC00962 4.2MP CMOS monochromatic camera was used with a magnification of HC Plan Apochromat CS2 63X/1.4 Oil objective.

3.2.16 LIBRARY PREPARATION AND SEQUENCING

Clontech kit: The sequencing libraries were prepared at EMBL Genomics Core Facility (GeneCore, Heidelberg) using the SMARTer® Stranded Total RNA-Seq kit - Pico Input

Mammalian (Clontech Laboratories, cat. no. 635005) after LiCl clean-up and rRNA removal with the Ribo-Zero rRNA Removal Kit (Human/Mouse/Rat, Illumina, cat. no. MRZH11124). The obtained libraries were subjected to single-end sequencing using the HiSeq4000. After checking the sequencing quality of the raw reads using FastQC, the first 3nt from the 5' end of the read were trimmed according to the manufacturer's recommendations. In addition, the reads were adapter trimmed using Trimmomatic (Bolger et al. 2014).

Nugen kit: The sequencing libraries were prepared at EMBL Genomics Core Facility (GeneCore, Heidelberg) using the Ovation® SoLo RNA-seq System (Nugen) with custom InDA-C primers against Xenopus laevis rRNA sequences using Ing RNA input.

The obtained libraries were subjected to paired-end sequencing using the Illumina NextSeq500 with Mid-75 mode using the Nugen custom R1 sequencing primer. After checking the sequencing quality of the raw reads using FastQC, the first 5nt from the 5' end of the forward read were trimmed according to the manufacturer's recommendations. In addition, the reads were adapter trimmed using Trimmomatic (Bolger et al. 2014). After checking the quality of the trimmed reads with FastQC, the reads were pseudo-aligned against the Xenopus laevis transcriptome (XL_9.1_v1.8.3.2.primaryTranscripts.fa.gz) provided at Xenbase.

3.3 RESULTS

3.3.1 miR-181a/b ARE EXPRESSED BY RGCS

microRNA-seq of RGC axons revealed the presence of miR-181a/b as one of the most abundant family of miRNAs in this compartment. See Annexure 1- Fig (1)

This suggests that miR-181 is first transcribed in RGCs and trafficked out to the axonal compartment. I therefore first validated the presence of miR181a/b in RGC cell body using *in situ* hybridization on retinal tissue section from wildtype embryos.

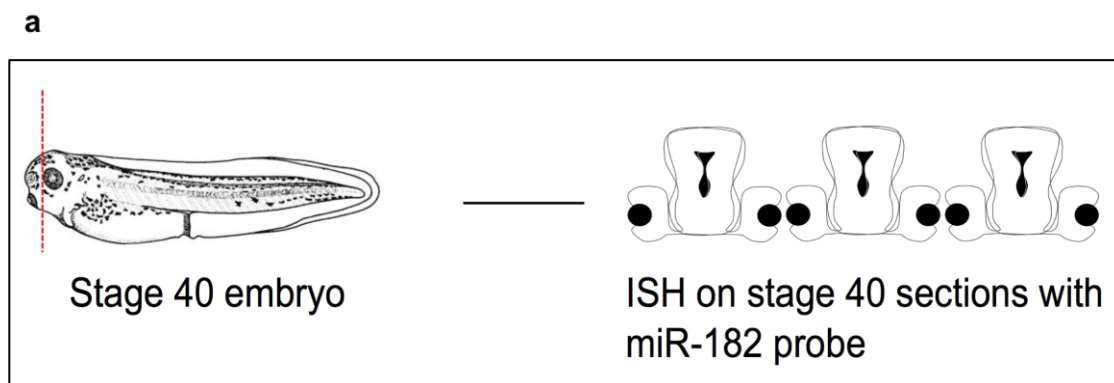


Figure 3-3: Schematic of stage 40 embryo sectioned for ISH

To assess miR-181a and b expression in *Xenopus laevis* visual pathway, I carried out *in situ* hybridization on sections of stage 40 embryos using locked nucleic acid (LNA) probes. LNA probes are a class of high-affinity RNA analogs in which the ribose ring is locked. Thus upon hybridization to complementary sequences the interactions exhibit high thermal stability. Since LNA probes can discriminate between single nucleotide mismatches, LNA probes offer high sequence specificity. The LNA probes although designed against the mature miRNA, are also capable of detecting pre-miRNA.

The LNA probes that I used are digoxigenin tagged oligos at both 5' and 3' ends and offer good detection with high signal to noise ratio. miR-181a and b are expressed within RGCs along with the inner and outer nuclear layers of the retina (Figure 3-4:).

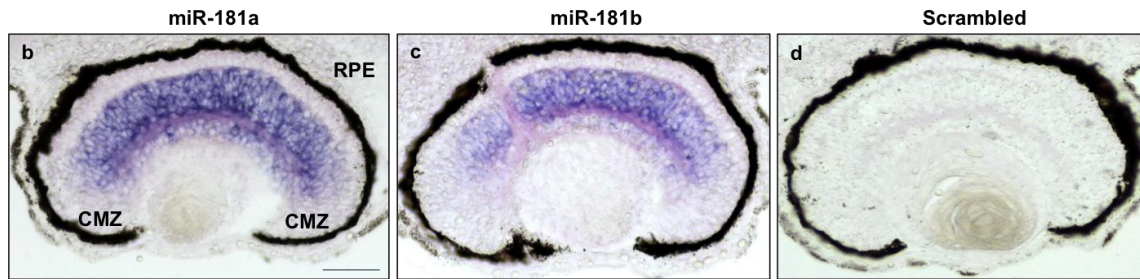


Figure 3-4: Expression of miR-181a/b at stage 40.
(d): Scrambled probe showing no ISH signal.

However, the photoreceptor layer adjoining the retinal pigment epithelium (RPE) do not express miR181a and b suggesting that these cells contain no or low levels of miR-181a and b.

No signal is detected when scrambled probes that do not target any sequence in *Xenopus* are used suggesting that the ISH signal detected is specific for miR-181a and b.

Thus miRNA-seq on axons and *in vivo* ISH on sections show, together, that miR-181a and b are present in both RGC soma and their axons.

3.3.2 miRNA PROCESSING AND SILENCING MACHINERY ARE PRESENT IN AXONS AND GCS

The presence of mature miRNAs within axons is not directly suggestive of their function in this compartment, as it could be a mere effect of diffusion from cell bodies. To test whether mature miRNAs could act within GCs, we tested whether miRISC was detected in this compartment also using eye organoculture.

Eye organoculture enables to grow RGC axons while preserving the retina architecture. Eye explants from stage 37/38 embryos are seeded and left in culture for 24 hrs in culture. The eye explant is intact and not dissociated thereby avoiding losing intercellular interactions. In addition, this explant culture preserves the integrity of the retina structure enabling developmental processes, such as patterning, differentiation, lamination and signaling across the layers to normally progress mimicking *in vivo* conditions. Finally, the optic nerve head is placed directly on the coverslip that is covered with a substrate, laminin, normally found in the visual pathway *in vivo* (Höpker et al. 1999). Axons of RGCs, the only projection neurons of the retina, exit the eye at the optic nerve head. Therefore, only RGC axons elongate from these organocultures. The

success of axon elongation can be clearly observed in phase contrast microscopy (Figure 3-5, a) or following the visualization of the immunoreactivity of α tubulin, a key component of the axon shaft, throughout the length of the axons (Figure 3-5, b). This anti-acetylated tubulin recognizes acetylated forms of α tubulin from various organisms that include human, mouse, pig, bovine, rat, hamster, monkey, chicken and frog (Ledizet & Piperno 1991). Mouse α tubulin shares 97.783% homology with *Xenopus laevis* α tubulin.

One limitation of this culture system is that RGC soma are buried within the explants therefore it is not feasible to observe the expression of proteins following immunostaining within the RGC soma but only within axons and GCs.

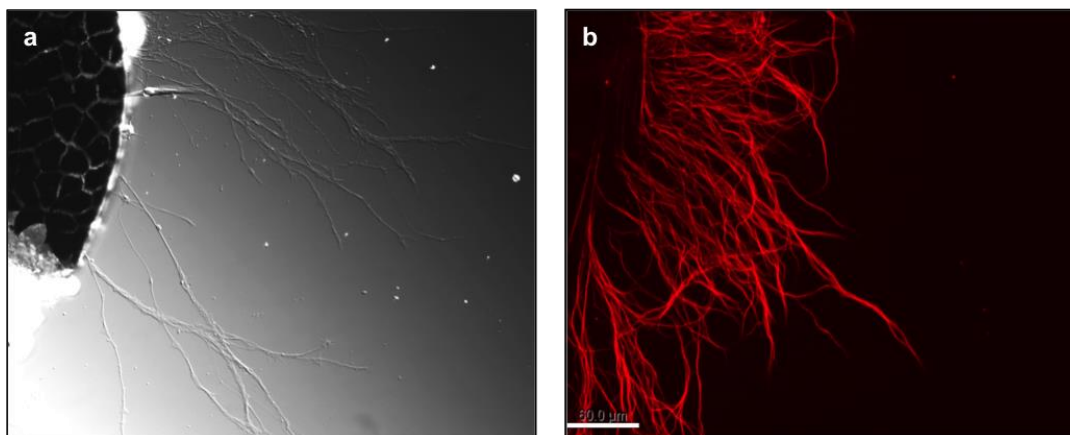


Figure 3-5: Eye explant in culture
(a): st 37+1 day invitro.(b): RGC axons expressing α tubulin.

To address whether mature miRNAs could act within GCs, I assessed whether Argonaute, a crucial component of the RISC complex, is present in axonal compartment using immunostaining for Ago2 on culture.

The peptide sequence used to generate this antibody is PTTSPIPGYAFK and is unique to N-terminal region of Ago2 therefore signal obtained through this antibody binding will not detect Ago3 or Ago4. Ago2 protein in mouse and *Xenopus laevis* share a 96.056% sequence identity (Figure 3-6).

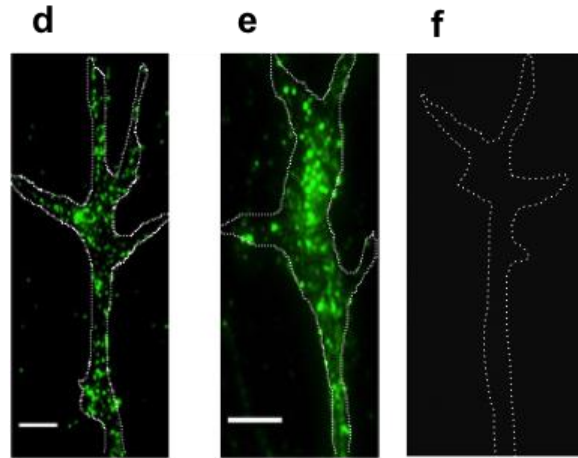


Figure 3-7: Expression of miRNA processing and silencing machinery. Immunostaining for (d)Ago2 and (e) Dicer within axons and GCs of *Xenopus laevis*.

Negative control containing no primary antibody showed no immunoreactive signal suggesting that the signal obtained should be specific (Figure 3-7, f).

Specificity could be further validated by using blocking peptide (the antigen used to raise the primary antibody) along with primary antibody as an additional negative control. However, blocking peptide was not available for this antibody. Alternatively, Ago2 or Dicer knockdown followed by antibody staining could be done to verify antibody specificity. We have attempted to validate Dicer-associated signal in three ways. First, we have indeed attempted to knockdown Dicer with MO but this oligomer design seemed overall inefficient. Second, we performed Western Blotting to ensure that our antibody detected the right Dicer moiety (data from my supervisor, Dr. Marie-Laure). Of note, Ago2 antibody has been validated by western blot in mouse (by Dr. Donal O'Carroll's group whose antibody we use) but not in *Xenopus* but this could be verified in the future. Finally, we have preliminary data in the lab suggesting that Dicer is present in P0 RGC axons of Dicer-HA transgenic mice (unpublished data generated by Eloina Corradi).

3.3.3 MOS SUCCESSFULLY KNOCKDOWN miR-181a/b

I next explored the role of miR-181 family in axon guidance in *Xenopus laevis* visual pathway using a loss-of-function approach. This approach was favoured over gain-of-function, since the physiological role of this miRNA can be analyzed. Having the right

molecular stoichiometry is important for normal cellular function. Exogenously providing miRNAs can increase the ratio of miRNAs to their targets. Therefore this approach might not enable investigation of the intended role within the cell as over expression of the miRNA could lead to non-physiological effects.

To induce the loss-of-function of miRNAs, several methodologies exist: Cre Recombination mediated temporal loss-of-function (mice mostly), temperature sensitive mutants (*C.elegans* and *drosophila*), use of antisense oligonucleotides that include antagomirs and MOs (zebrafish and frogs), miRNA responsive element expressing plasmids called Sponges and tough decoys that contain 2 miRNA binding sites within a structured hairpin.(Sun & Lai 2013).

I used MOs (MOs) that are antisense oligonucleotides that bind to complementary miRNA and inhibit their maturation and activity. I chose MOs because of their stability, lack of innate response and nontoxicity (Jd 2016). Depending on the design, MOs can be effective to inhibit Drosha or Dicer mediated maturation (Kloosterman et al. 2007) (useful to block pri- or pre-miRNA) or assembly onto RISC (block mature miRNA function). Chemically, MO units comprise of a nucleic acid base, a morpholine ring and a non-ionic phosphorodiamidate intersubunit linkage. MOs are not known to degrade the miRNA but instead use an RNase H independent steric blocking mechanism (Genetools). They have been widely used in important studies in zebrafish and frogs to successfully block miRNA function (Coolen et al. 2012).

MOs were created by genetools to block pre-miR-181a-1,pre-miR-181a-2 and mature miR-181b. No appropriate MO was available to block the mature miR-181a. Genetools designed the MOs and found that there exists a moiety with very strong self-complementarity that would have likely resulted in oligo dimerization and minimal antisense activity. For this reason, a MO with a target encompassing the entire mature sequence was not recommended.

Therefore two MOs were considered to block Dicer cleavage site of pre-miR-181a-1 and -2 which both produce mature miR-181a-5p (Figure 3-8). Such overlapping loop oligos are commonly used in the field (Kloosterman et al. 2007).

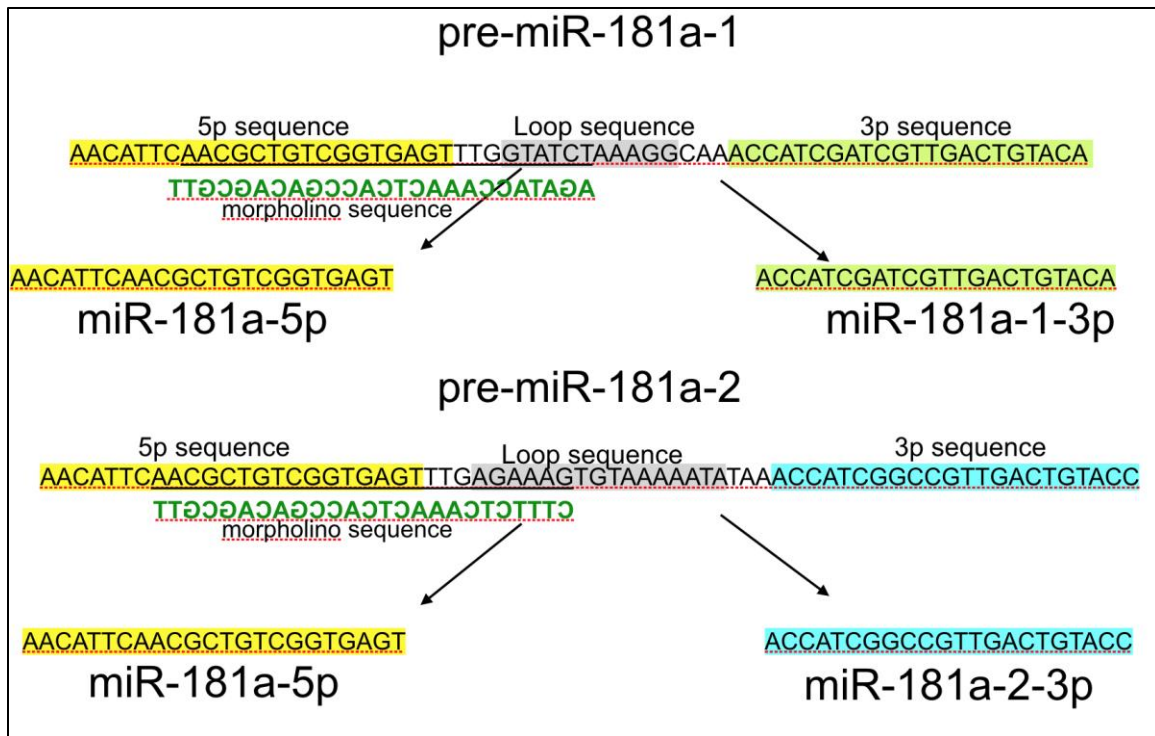


*Figure 3-8: MO design for blocking pre-miR-181a-1 and a-2
The MO (shown in green) blocks the maturation of the miRNA by blocking the Dicer cleavage site and thus preventing formation of miR-181a-5p but also miR-181a-1-3p and a-2-3p.*

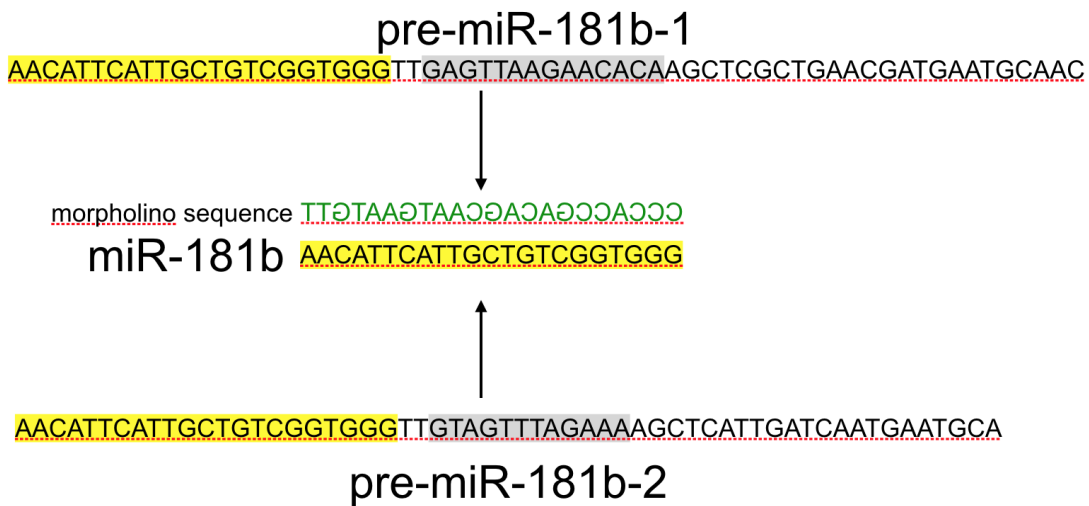


*Figure 3-9: MO against mature miR-181b
MO (shown in green) prevents miRNA activity.*

To induce loss-of-function, two different MO-delivery approaches were undertaken: Microinjection and *in vivo* electroporation and. In microinjection, MOs are delivered in early stage embryos. One can target both dorsal blastomeres at 4 or 8 cell stage (Figure

3-10), which are fated to become cells of the central nervous system (CNS) including retinal cells such as RGCs and target cells of RGC axons in the tectum. Microinjection thus enables a broad knock down that can commence from very early stages when CNS cells are specified.

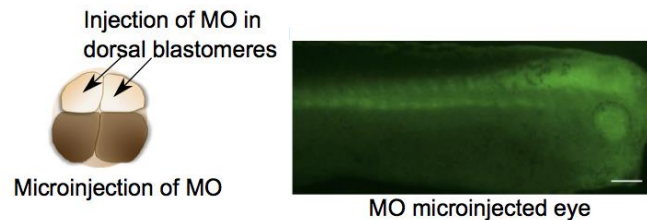


Figure 3-10: Microinjection mediated loss-of-function using MO to target the entire CNS.

One limitation is that cell autonomous roles cannot be studied therefore we used electroporation to overcome this.

Using *in vivo* electroporation, retinal cells, including RGCs, can be specifically targeted within a window of development (stage 22-stage 35/36) (Falk et al. 2007) leaving all remaining cells of the CNS, the tectum in particular, untargeted by the MO. Electroporation thus provides both a temporal and spatial control over delivery. While this technique enables the specific targeting of retinal cells, there are no methodologies available to date that target only the RGCs.

At stage 26, the solution of MOs can be delivered by injection within the optic stalk, and thus eventually diffuses into the eye primordia, between the presumptive neural retina and retinal pigmented epithelium. Upon delivering an electric pulse, transient pores are created within the cell membranes through which MOs can diffuse. The current applied is directional and as a consequence, any negatively charged particles will diffuse towards the cathode during the duration of the square pulse (50ms). This way, charged MO can translocate from the back of the presumptive neural retina to neural retinal cells (Falk et al. 2007). Importantly, morpholine backbone of MOs are not charged but the FITC tagged MOs carry a negative charge, enabling the use of electroporation to deliver MOs.

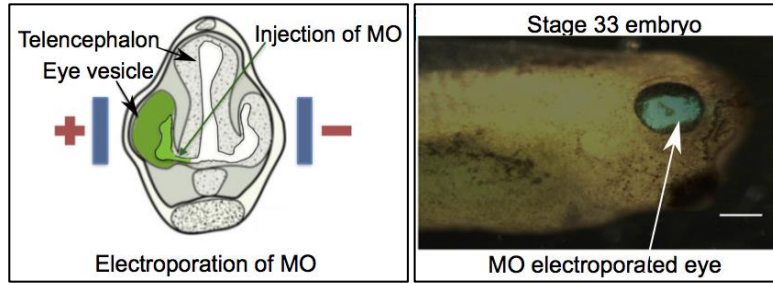


Figure 3-11: Electroporation offers spatial and temporal control towards MO injection.

In our specific experimental paradigms, retinas were targeted at stage 26, just prior to axonogenesis (stage 28) (Holt 1989). Therefore, all targeted RGC soma and their axons should be devoid of functional miRNAs as soon as the axon starts navigating. Any aberrant projection due to MO-mediated loss-of-function can thus be observed throughout the entire length of the visual pathway.

I first validated that the MO-mediated knockdown was complete and persistent throughout period of RGC axon guidance using *in situ* hybridization (ISH) on retina section of stage 40 embryos, when RGC axons have reached the tectum (Figure 3-12).

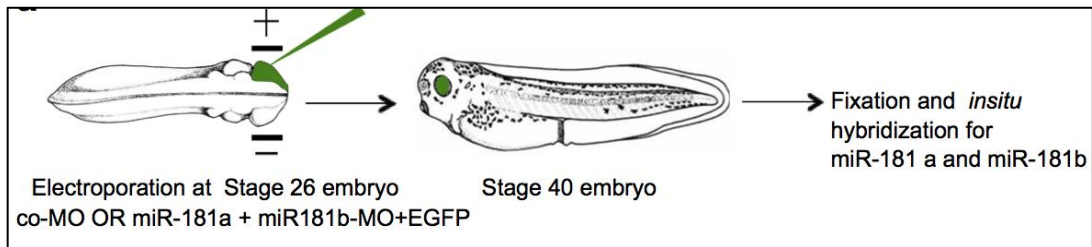
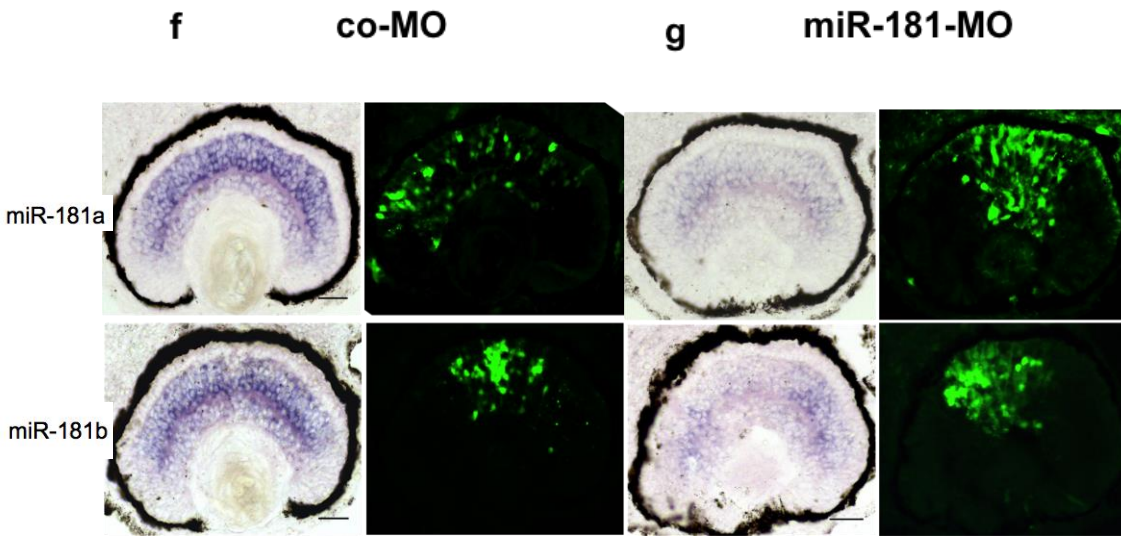


Figure 3-12: Schematic of electroporation mediated loss-of-function.
MOs electroporated alongwith pCS2-EGFP (0.5 μ g/ μ l) to assess success of electroporation.

co-MO electroporated retinas displayed a normal expression pattern of miR-181a and b suggesting that the control MOs do not affect miR-181a/b expression. On the contrary, I detected a reduction in ISH-associated signal for both miR-181a and b upon electroporation (Figure 3-13, f-g) of the three MOs exclusively within electroporated cells.



*Figure 3-13: ISH on electroporated embryos
co-MO (f) and miR-181-MO(g) electroporated embryos. Abbreviations: - co-MO: Control Morpholino;
miR-181-MO: miR-181a and b Morpholino; Scale bar for (b-i): 50µm*

Together, these results suggest that miR-181 MO induce a long-lasting knockdown of miR-181a and b.

3.3.4 miR-181a/b LOSS OF FUNCTION CAUSES MISPROJECTION OF AXONS WITHIN TECTUM

To explore miR-181a/b roles in axonal pathfinding in the visual system, electroporation was used as a tool to induce MO mediated loss-of-function in a spatial and temporal manner. I used MOs against the pre-miR-181a and mature miR-181b as mentioned in the above section alongwith pCS2-CAAX-mCherry, and analysed the pathway at stage 40 when most RGC axons have reached their target, the tectum(Holt 1984). At this stage, I can thus not only examine whether the axons are projecting appropriately to their target region, but I can also analyse whether axons have strayed away from their course en route spanning stage 26-40. I dissected brains to analyse the visual projection on the contralateral hemisphere and used open brain preparations (Figure 3-14). These are preparations where the brain is severed in its ventral side, then both hemispheres flatten down but still connected at their dorsal extremity. With these, it is possible to visualize labelled axons that project from the optic chiasm along the contralateral brain hemisphere to the tectum and thus to analyse the possible presence of aberrantly

projecting axons. However, this preparation is not amenable to observation of the optic pathway from the eye to the optic chiasm and one has to resort to sectioning for these additional analysis.

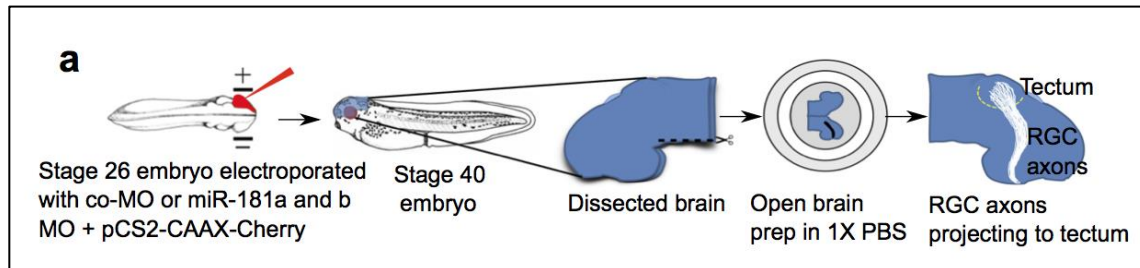


Figure 3-14: Open book preparation to visualize the optic pathway following loss-of-function.

In control embryos electroporated with co-MO, RGC axons appropriately projected along the optic tract and within the tectal region, as expected. In miR-181a/b morphant embryos, on the other hand, a subset of axons was misrouted within the targeting area. These axons failed to stall in the dorso-caudal most part of the tectum and instead, aberrantly turned back towards the optic chiasm, following curve-like trajectories. (Figure 3-15).

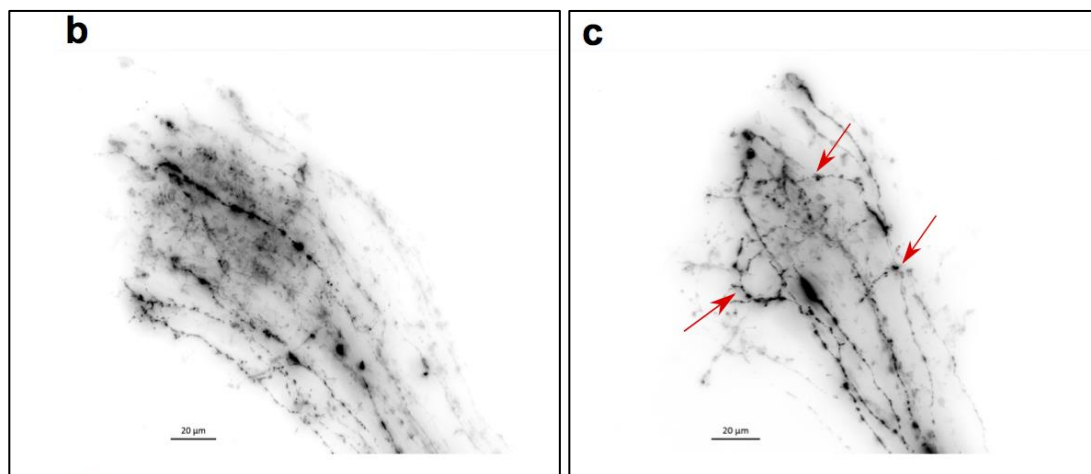


Figure 3-15: miR-181-MO in vivo phenotype.

Representative image of brains where RGC axons are expressing mCherry in (b) co-MO electroporated and (c) in miR-181a and b-MO morphant embryos. A subset of axons formed aberrant projections (arrows)

I quantified this phenotype by first calculating the penetrance that gives a measure of how many brains display the aberrant phenotype. The axons that did not stay confined within the tract and instead formed loop like projections qualified as aberrant

projections. I scanned through z stacks on each image and traced individual axons to observe score aberrant phenotype. Amongst control: 20% (9 out of 45) brains analysed showed aberrant projections. In miR-181a/b morphant, 53.8% (28 out of 52) brains displayed aberrant projections, which corresponds to a statistically significant higher proportion of embryos that display this phenotype (Fisher's exact test, $p=0.0008$). It is common to observe a few axons that stray from their path, even in control brains hence quantification of the extent of the phenotype was essential. I then counted the number of electroporated axons that were aberrantly projecting and normalized to the total number of electroporated axons per brain. The normalized number of looping axons in morphants was 0.2 while that of control embryos was 0.09. Thus, I observed a significant increase in the number of aberrantly projecting axons in morphant embryos compared to control (+222%, SEM: ± 0.029), Mann-Whitney test, $P<0.0001$) (Figure 3-16, e).

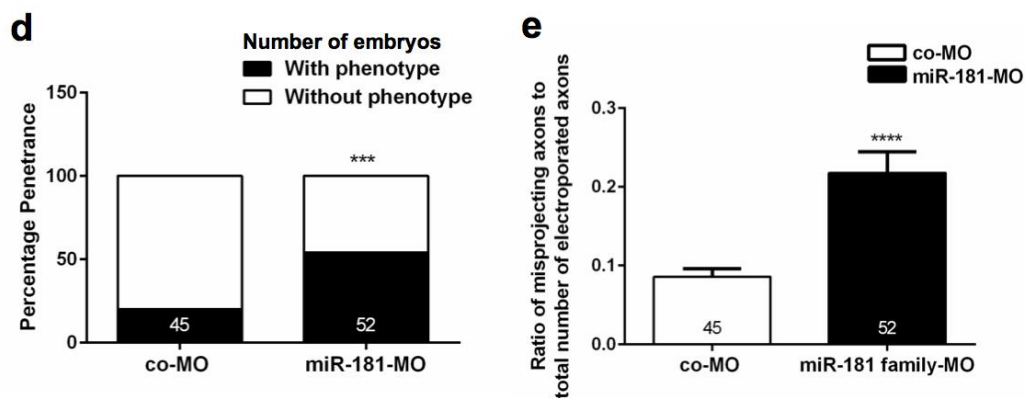


Figure 3-16: Quantification of phenotype in miR-181-MO

*(d) Quantification of penetrance of the aberrant projection phenotype. Numbers in the bars represent number of brains analysed. (Fisher Exact test $***p=0.0008$) (e) Ratio of number of misprojecting axons with respect to total electroporated axons in co-MO and morphant embryos ($****p$ value <0.0001 , Mann Whitney test).*

These data suggest that miR-181 function is important for RGC axon targeting. It further suggests that miR-181a / b is likely to act within RGC, possibly locally within axons. Further, miR-181a/b do not affect long range guidance: miR-181 morphants projected normally until they reach the tectum suggesting miR-181a/b does not affect the axonal outgrowth or projection within the optic tract.

3.3.5 miR-181a/b REGULATE GC RESPONSIVENESS TO SPECIFIC CHEMOREPELLENT CUES – NETRIN1 AND SEMA3A

The visual pathway analysis has shown that long range guidance is unaffected and that morphant axons project normally until they reach the tectum. I therefore explored what is the biological underpinning of this phenotype. I reasoned that axons could have aberrantly projected in miR-181a/b morphants for several reasons.

1) miR-181-a/b is needed by RGC axons to respond to tectal cues and this responsiveness is altered thereby causing misrouting specifically in the tectum. miR-181 does not affect the outgrowth of RGC axons, their ability to cross at the chiasm or to project through the optic tract 2) A subset of the RGC axons could have impaired actin polymerization thus causing aberrant loop like projections. Or 3) Upon reaching tectum, axon-axon adhesion within the main axonal tract is lost thereby causing straying from the projections.

I decided to investigate whether morphant GCs fail to appropriately respond to tectal cues. This was because identifying lack of responsiveness can be tested specifically using purified recombinant cue and any alteration in responsiveness can be quantified. RGC axons encounter a multitude of guidance cues along the tract and also upon reaching the target. Chemorepellent cues that include Sema3A, Netrin1 and Slit2 form a repulsive corridor (Shewan et al. 2002; Hocking et al. 2010; Campbell et al. 2001)

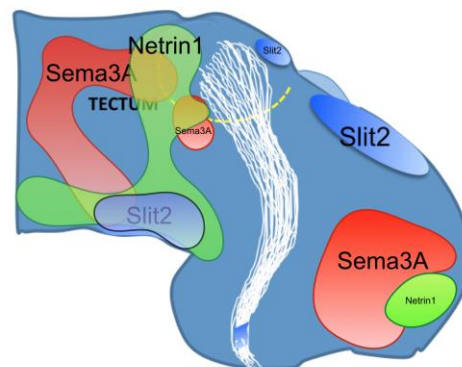


Figure 3-17: Sema3A, Netrin1 and Slit2 expression in *Xenopus* brain at stage 40

These cues are expressed at a time when axons are reaching the tectum thus enabling them to reach the target with accuracy and to form appropriate connections. Their

cognate receptors are expressed by GCs within similar timeframe conferring sensitivity to these cues during axon targeting.

I decided to explore if indeed the responsiveness to these cues is altered upon miR-181 loss-of-function by using *in vitro* assays.

GCs responsiveness can be tested by two assays: Turning (Lohof et al. 1992) and collapse assays (Luo et al. 1993).

Collapse assay is a quantitative assay that enables to score the proportion of GCs that collapse in response to a chemorepellent cue. In addition, all the tectal candidates are chemorepellent. Cultures were grown in 60% L-15 which is a minimum medium containing no exogenous cues or factors. Therefore, the GCs are exposed to solely purified recombinant cues and their response observed is specific to the purified cue presented during the assay.

To test whether morphants show altered responsiveness to tectal cues, I microinjected miR181a/b MOs to target all the RGCs and thus carry out a broad knock down in the entire CNS. In order to achieve this, the three fluorescein tagged MOs were microinjected (at 1nl containing 45 μ M pre-miR-181a-1, 45 μ M pre-miR-181a-2 and 50.6 μ M miR-181b) (fluorescein tagged) at 8-cell stage in both dorsal blastomeres.

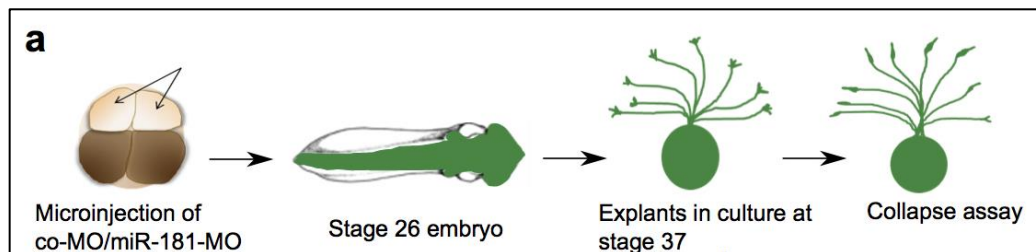


Figure 3-18:Paradigm for Collapse assay

For control, control MO was injected at the same concentration. The efficiency of knock down was tested by ISH. ISH on morphant embryos probed for miR-181a and b show the absence of ISH signal suggesting that the knock down is successful. See Figure 3-19.

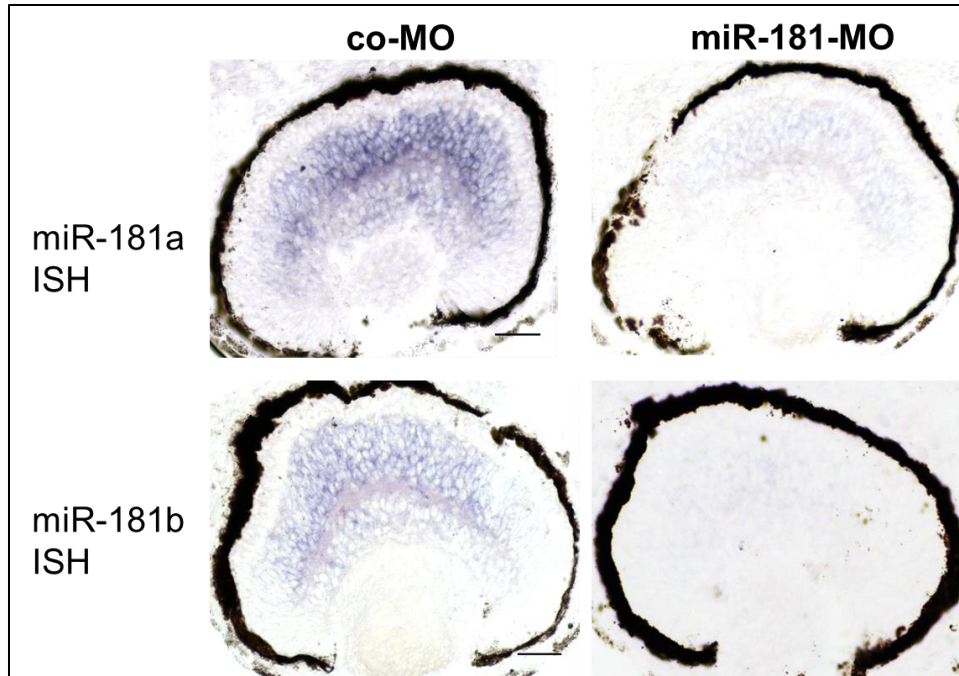


Figure 3-19 ISH showing knock down of miR-181a and b following microinjection of the MO.

The embryos were then sorted for presence of MO exploiting the fact that they are tagged with FITC. At stage 37/38, eye explants from morphant and control embryos were cultured and axons allowed to grow for 24 hrs.

Knock down was also confirmed within axons after removing the explants and leaving axons in culture termed as cut axons. See Figure 3-20. Following RNA extraction from the cut axons, qPCR was performed to check for presence of miR-181. qPCR was performed by Eloina Corradi, PhD student from my lab.

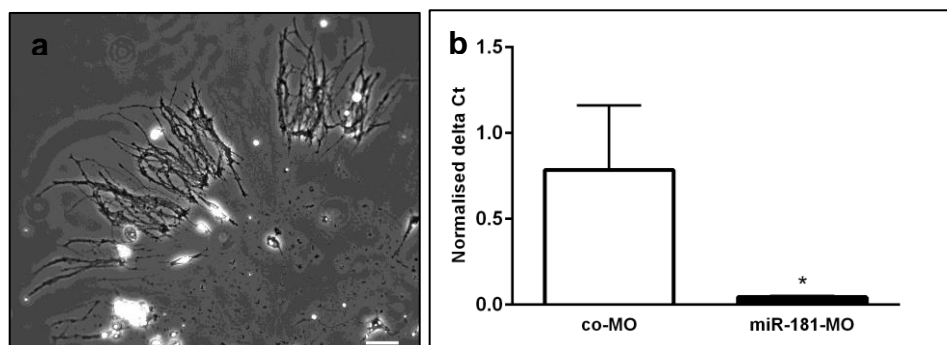


Figure 3-20: miR-181 knock down in cut axons
 (a) Cut axons in culture. (b): miR-181 morphant axons show a significant decrease in miR-181 signal.
 Mann Whitney test (* p value= 0.0286)

Following knockdown validation by ISH and qPCR, responsiveness was tested. Three purified recombinant cues namely Sema3A, netrin1 or Slit2 were used to test responsiveness.

Table 3.3.5.1: The recombinant cues used for collapse

Purified recombinant Cue	Species from which it is obtained	Sequence identity with <i>Xenopus laevis</i>
Sema3A	Homo sapiens	84.367%
Netrin1	Mus musculus	84.934%
Slit2	Mus musculus	86.536%

Firstly, the concentration of the cue that gives a high degree of collapse and that can be blocked by protein synthesis inhibitor was determined for all the 3 cues (Figure 3-21, b-d). PS inhibitor was used in order to determine the concentration at which the cue is dependent on protein synthesis within axons. This concentration is a read out of a physiological response elicited within axons and hence it is important to use this while investigating responsiveness of GCs to cues.

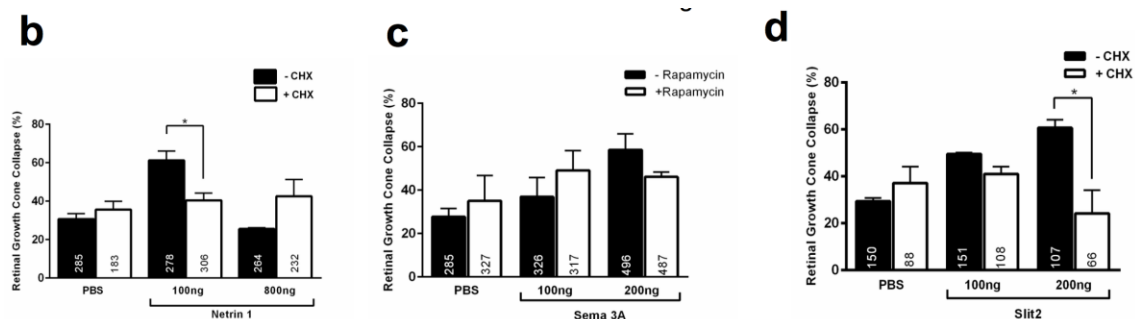


Figure 3-21: PS dependent collapse response

Quantification of GC collapse with or without blocker of protein synthesis (CHX) or mTOR (Rapamycin). Protein synthesis dependent concentrations for Netrin1(b), Sema3A (c) and Slit2 (d) were determined and found to be 100ng for Netrin1 and 200ng for both Sema3A and Slit2. 2-Way ANOVA followed by Holm Sidak multiple comparison post hoc test performed. * p value = 0.0320 for (b), * p = 0.011 for (d)

Having found the respective concentrations, the axons were exposed to sema3A (200ng/ml), netrin1 (100ng/ml) or slit2 (200ng/ml). For control, PBS was used for 10 mins (Figure 3-22, e-g).

Following cue exposure, explants were fixed and the number of collapsed GCs were quantified blind to avoid bias. Quantification of the proportion of collapsed GCs revealed that only 38.99% of morphant axons responded to Sema3A in comparison to an expected collapse response of 57.13% in co-MO. Interestingly, even, netrin-1 exposure induced a lower degree of collapse of 41.42% as opposed to 60.7% in control- MO-injected embryos. A significant decrease in Sema3A (18.14%, $p=0.0424$, S.E.M \pm 7.112%, Two-way ANOVA followed by Sidak multiple comparison post hoc test) and netrin-1 (19.3%, $p=0.037$, S.E.M \pm 6.03%, Two-way ANOVA followed by Holm-Sidak multiple comparison post hoc test) collapse response were thus detected in morphants. (Figure 3-22, e and f). When Slit2 was exposed to morphant GCs, no change in collapse response was observed ($p=0.867$, S.E.M \pm 5.91%, Two-way ANOVA followed by Sidak multiple comparison post hoc test). Both morphant and control GCs showed a collapse of 69.98% (S.E.M \pm 2.39%) and 72.85% (S.E.M \pm 2.98%) respectively (Figure 3-22, g).

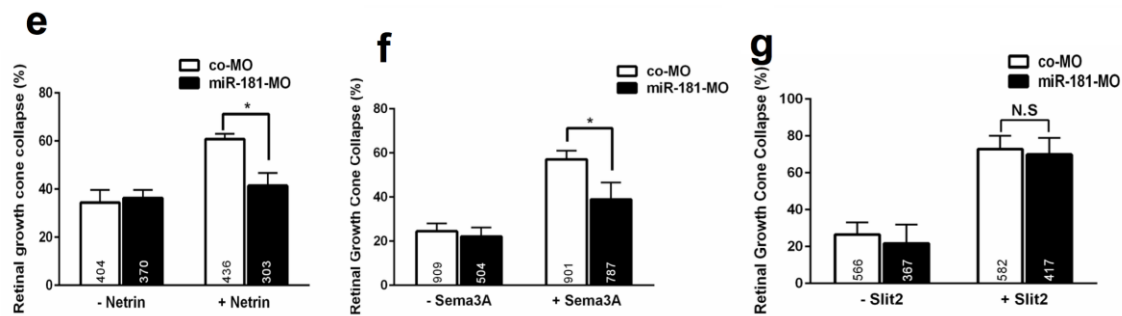


Figure 3-22: Quantification of collapsed GCs in co-MO or miR-181-MO
Bath application with netrin1 (100ng/ml) (e) , Sema3A (200ng/ml) (f) or Slit2 (g). The numbers in the bars indicates total number of GCs counted. Data for Sema3A is obtained from 5 independent experiments ($p=0.0424$); for netrin, $n=4$ (* $p= 0.0372$) and for Slit2 ($p=0.867$), $n = 3$. (2 Way ANOVA followed by Sidak's post hoc multiple comparison test was used to determine the p value). N.S: Not significant. S.E.M represented here Abbreviations: CHX: Cycloheximide; co-MO: Control Morpholino; miR-181-MO: Morpholino against miR-181a and b*

This suggests that miR-181a and b regulate mRNAs involved in sema3A and netrin-1 signaling cascade within RGCs but are not involved in regulating Slit2 signaling. This further indicates that miR-181a and b function is cue-specific.

The *in vivo* phenotype displaying axons misrouting within tectum could be attributed to altered responsiveness to sema3A and netrin-1. Thus morphants, with diminished collapse response might fail to be repelled by these cues therefore instead of terminating in the right zone they project aberrantly.

Growing and navigating axons transport and translate specific mRNAs upon exposure to guidance cues. Most of these mRNAs are a part of cytoskeletal machinery whose translation assists axons to respond to the cues they are faced with. Indeed, Sema3A induces axonal translation of RhoA which is a regulator of actin cytoskeleton (Wu et al. 2005) that enables axonal collapse in mouse DRG neurons Similarly, netrin-1 mediates local protein synthesis of β actin and asymmetric translation of β actin leads to attractive turning towards netrin-1 in *Xenopus* retinal .Thus, miR-181a/b could be targeting either mRNAs and loss-of-function could result in impaired mRNA translation resulting in diminished asymmetry within GCs and decreased collapse response.

Slit2 on the other hand is known to mediate cofilin mRNA translation(Piper et al. 2006) in *Xenopus* retinal GCs. Since morphant axons behave normally towards Slit2 exposure, it is likely that cofilin is not targeted by miR-181a/b.

3.3.6 MIR-181A/B LOSS-OF-FUNCTION MEDIATED BY MOS IS SPECIFIC TO MIR-181A/B.

I next explored if the altered collapse response to Sema3A is indeed specific to miR-181a and b. This was done to test the specificity of the MOs. MOs have been widely used in *Xenopus* and zebrafish communities however there is growing concern with respect to their specificity. For instance, recent literature in zebrafish reveal poor correlation between MO-mediated knock down of phenotypes with mutant phenotypes achieved through CRISPR technology (Kok et al. 2015; Rossi et al. 2015). Although no such comparison has been performed for MO targeting miRNA, I thought that it was important to test MO specificity with appropriate controls since off-targeting of these types of MOs can't be ruled out.

I employed an approach whereby I rescued miR-181 MO-mediated loss-of-function with exogenous miR-181a and b mimics. I used synthetic double stranded oligonucleotides designed to mimic the mature miR-181a and b or control mimics. These mimics are

double stranded oligonucleotides that are processed by the cell's innate miRNA processing machinery to give rise to mature miRNAs. If indeed miR-181a/b are important for Sema3A responsiveness, morphant embryos provided with miR-181a/b mimics would process the oligonucleotides canonically into mature miRNA and employ these to carry out miR-181a/b function. Co-microinjection of both mimics and MO would enable me to target all RGCs as explained above. However, I did not use this approach but rather I electroporated this mimics to morphant and control retina at stage 26 (Figure 3-23).

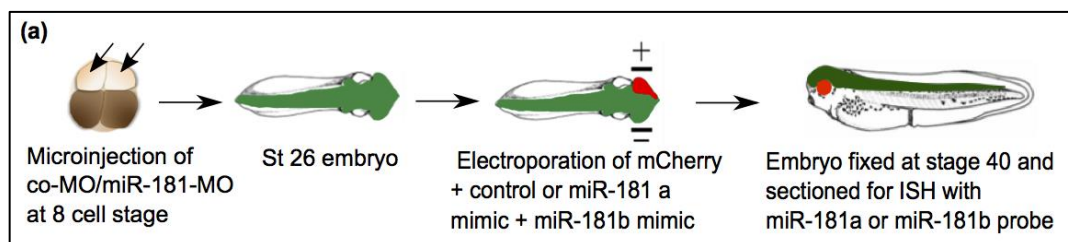


Figure 3-23: Experimental set up for ISH following mimic electroporation.

I favored this approach over co-microinjection for two reasons. First because it enabled me to keep both MO and mimics physically separated. I thereby avoided their putative non-physiological combination in a tube. Second because the presence of mimics at earlier developmental stages where miR181a/b is not normally expressed could also induce a confound.

The appropriate expression of exogenous miR181a/b was verified by ISH on sections (Figure 3-24, a). As expected, co-MO microinjected embryo displayed normal miR-181a/b expression upon control mimic electroporation (Figure 3-24, b and c). miR181a/b associated signal is detected in wild type and in morphant embryos, in areas that are electroporated with miR181a/b mimics but not with control mimics. This suggests that miR-181a/b mimics can rescue miR-181 expression in electroporated areas of the eye in morphants. No signal was visible when scrambled LNA probes were used, suggesting the specificity of the ISH reaction (Figure 3-24, d).

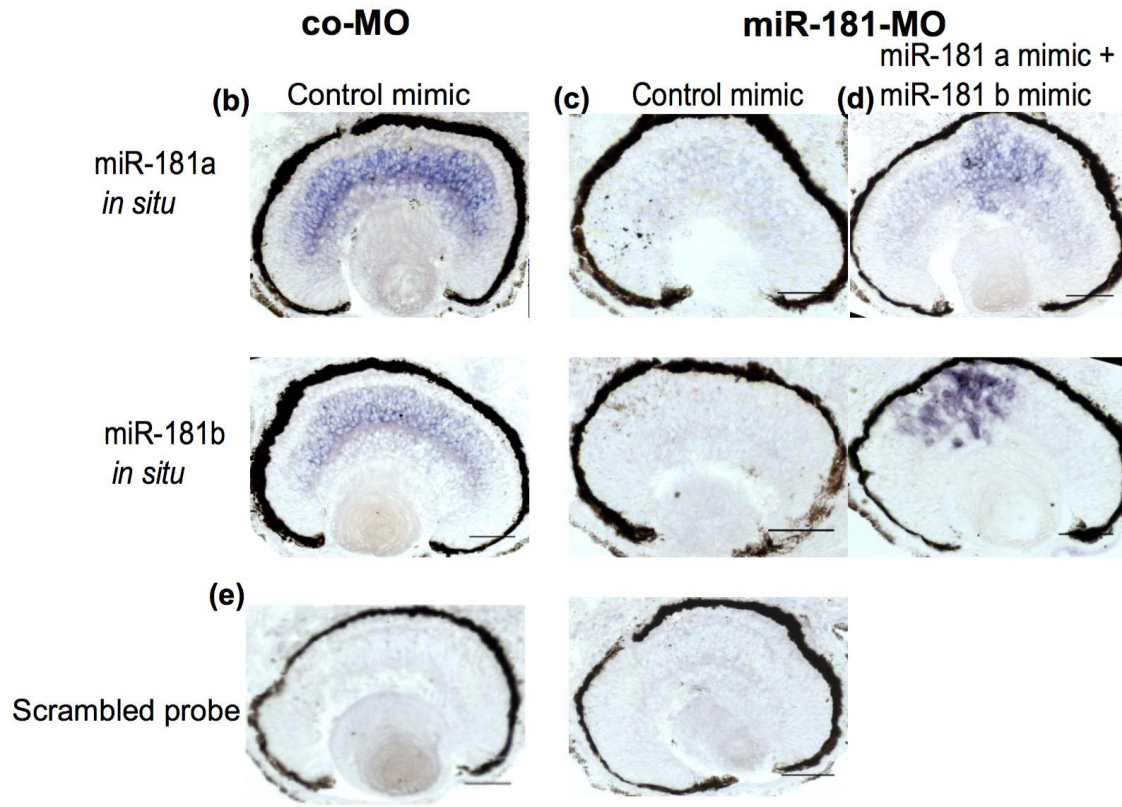
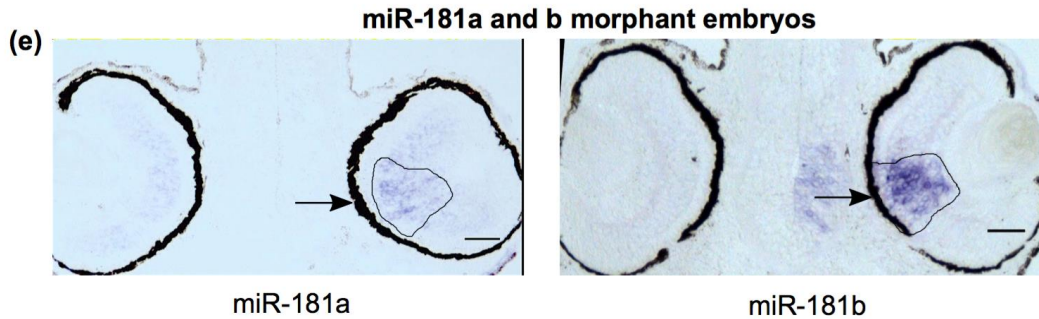


Figure 3-24: ISH for mimic validation.

(b, c) co-MO and miR-181-MO electroporated with Control mimic. (while miR-181a and b mimic electroporated embryos show exogenous expression of miR-181a and b. (c) miR-181a and b are expressed only in miR-181a and b mimic electroporated areas in morphants. (d) Scrambled probes depict specificity of staining. (e) Electroporated areas show expression (arrow) while non electroporated eye has no ISH signal. Scale Bar: 50 μ m.

A lower magnification image is shown below where the spatial and molecular specificity of miR-181 a and b mimics can be fully appreciated (Figure 3-25). An absence of ISH signal is observed in the non-electroporated left eye, whilst a miR181a and b associated ISH signal is clearly visible in the right electroporated eye in the target region in a mutant background.



*Figure 3-25: Mimic expression in electroporated morphant eyes.
Electroporated areas show expression (arrow) while non electroporated eye has no ISH signal.*

3.3.7 IMPAIRED RESPONSIVENESS OF MORPHANT GC TO SEMA 3A IS SPECIFIC TO miR-181a AND b

I next assessed whether the *in vitro* phenotype observed could be attributed to the specific action of miR-181a and b using this mimic-based rescue approach. Using a similar experimental paradigm as that described in Section 3.3.6, I checked if the altered sema3A-responsiveness of morphant axons could be restored. Upon mimic electroporation, I cultured eye explants at stage 37/38, allowed axons to grow for 24hrs and thus reach a corresponding *in vivo* stage 40. I then subjected these culture to Sema3A exposure at 200ng/ml for 10 mins (Figure 3-26).

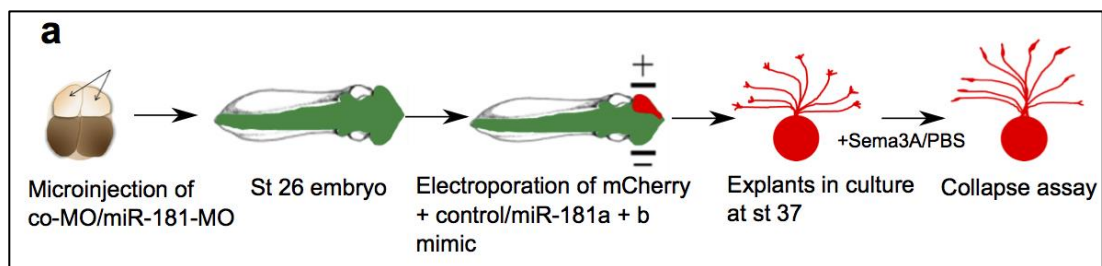


Figure 3-26: Schematic for in vitro rescue experiment

Following fixation, I quantified the percentage of RGC GCs collapsed. As shown in (Figure 3-27) A similar reduction in Sema3A-mediated collapse response to that obtained with miR181-MO was observed when control mimics were electroporated (46.59%, S.E.M±8.34). There was a no significant difference between miR-181 morphants and miR-181 morphant injected with control mimics suggesting that introducing control mimics by themselves do not cause change in morphant

responsiveness. With *Sema3A* exposure, there was a reduction of 30% in collapse response (p value = 0.018), Two-way ANOVA followed by Tukey's multiple comparison post hoc test compared to control GCs that collapsed at 65.96% (S.E.M \pm 3.07).

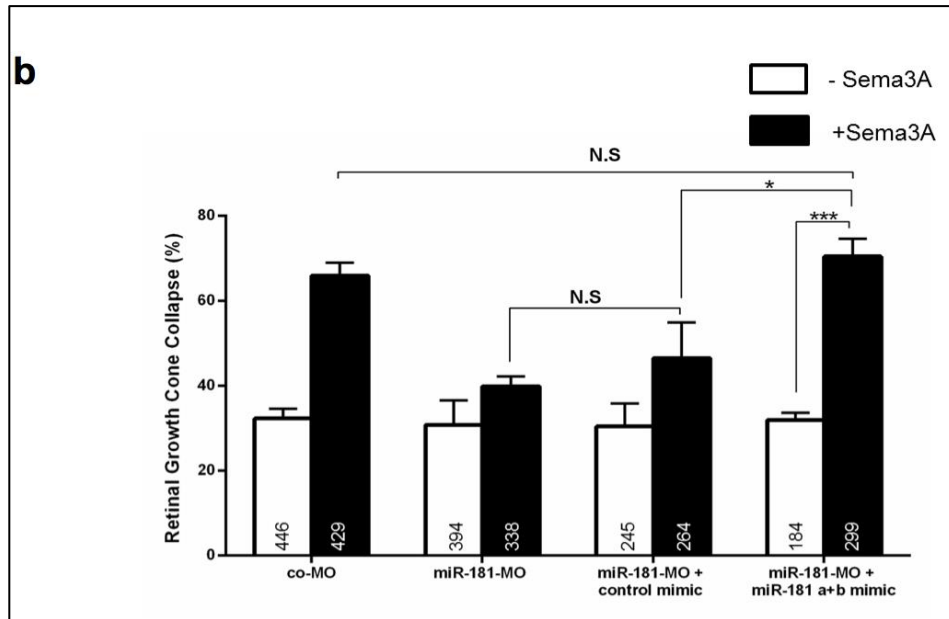


Figure 3-27: Rescue of *Sema3A* responsiveness in morphants by *miR-181a/b* mimics.

In contrast, a full *Sema3A*-induced collapse response was observed following the electroporation of *miR181a* and *b* mimics in mutant background (71%, S.E.M \pm 4.14), that was similar (p value = 0.99), Two-way ANOVA followed by Tukey's multiple comparison post hoc test) to that quantified in control-MO microinjected embryos (65.96% (S.E.M \pm 3.07)). Overall, this suggests that *miR-181a* and *b* mimics rescued the loss-of-function of *miR-181a* and *b*. It further suggests that the loss of *Sema3A* responsiveness detected in morphants can be attributed to the specific action of mature *miR-181a* and *b*.

Further, I validated the rescue on *in vivo* phenotype.

In order to determine if mimics can restore the *in vivo* aberrant projection phenotype in the tectum, I first electroporated *miR-181a/b* MO (at 250 μ M) along with pCS2-EGFP (at 0.5 μ g/ μ l). I then carried out a serial electroporation with mimics – *miR-181a* and *miR-181b* or control (at 50 μ M final concentration) along with pCS2-CAAX Cherry (0.5 μ g/ μ l). At stage 40, embryos were analysed for pathway defects as carried out

earlier in 3.2.6. Here I quantified aberrantly projecting co-electroporated axons (GFP axons corresponding to MO electroporation plus Cherry expressing axons corresponding to mimic electroporation) and the mean of which was normalised to total number of co-electroporated axons.

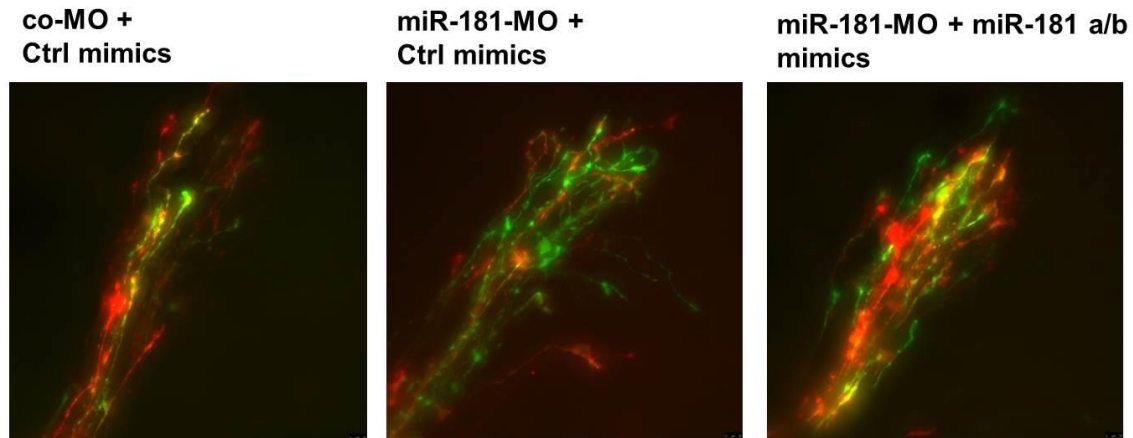


Figure 3-28: miR-181a/b mimics rescue aberrant misprojection of morphant axons in vivo.

I observed that co-MO and control mimic co-electroporated axons projected normally while miR-181 morphant axons co-electroporated with control mimics continued to project aberrantly as noted earlier. This suggests that the control mimics do not alter the morphant phenotype. As expected, the ratio of misprojected axons in morphants (0.16) were significantly higher ($p=0.023$) than co-MO electroporated with control mimics (0.02). When miR-181a and b mimics were co-electroporated within the morphant eye, the ratio of aberrant projections (0.05) is restored close to the control electroporated conditions ($p= 0.06$). Owing to technical difficulties in obtaining many co-electroporated axons, this experiment is currently being reproduced to observe statistical significance.

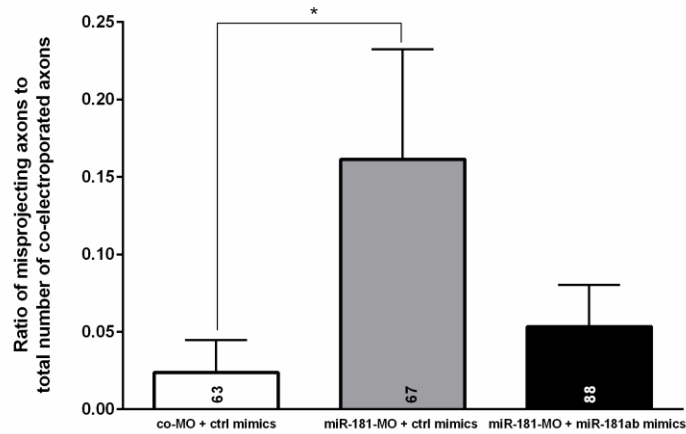


Figure 3-29: Quantification of *in vivo* rescue.

miR-181a/b mimics decrease the aberrant projections in morphant embryo. * $p=0.02$, One way ANOVA with Tukey's multiple comparison test. Numbers on the bars represent total number of co-electroporated axons analysed.

3.3.8 WHAT ARE THE MOLECULAR MECHANISMS EMPLOYED BY *miR-181a/b* TO INDUCE ACCURATE RGC AXON TARGETING?

I next proceeded to dissect out the molecular mechanisms of *miR-181a/b* in axon targeting.

miRNAs control post-transcriptional gene expression by regulating mRNA stability and/or or translation (Filipowicz et al. 2008). The dominant mechanism employed by *miRNAs* to modulate the local transcriptome as a whole is unknown for any cell type. We therefore attempted to assess how *miRNA* preferentially regulate transcripts in compartments using a novel high throughput approach *in vivo*. Our ultimate purpose is to compare the transcriptome to the translome following *miRNA* perturbation. If *miRNA* primarily regulates the transcriptome, then both transcriptome and translome should be similarly modulated upon *miR-181* loss-of-function. If *miRNA* primarily regulates the translome, then the transcriptome should be minimally altered upon *miR-181* knockout.

We first investigated whether *miR-181a/b* could be involved in selective mRNA degradation *in vivo* in RGC subcompartments including axons using RNA seq. We additionally aimed at comparing the transcriptome from RGC soma to axons to further evaluate whether *miR-181* differentially regulate these two distinct subcellular compartments.

For analyzing the transcriptome profile, two major procedures needed optimization:

1) Sample collection and 2) Library preparation. The section below details the optimization performed to be able to successfully and ultimately carry out RNA-seq from compartments *in vivo*.

3.3.1.1.1 Sample collection with LCM:

To perform RNA-seq on compartments, I first needed to optimize the collection of low input material *in vivo*. To do this, I used Laser capture microdissection (LCM) as a tool. With LCM, RGC somas and axons can be specifically isolated *in vivo* following miR-181a/b loss-of-function. This would enable comparison of the transcriptome between co-MO vs miR-181-MO electroporated embryos. Not only is it possible to isolate cells *in vivo* but also one could address the question of whether miR-181a/b acts in specifically within RGCs or axons? As miR-181 is expressed both in cell bodies and in axons, it could be plausible that this miRNA could have differential roles within the two sub compartments.

Pilot LCM: Following MO mediated loss-of-function, embryos were fixed at st 40 with PFA for 15 min, treated with sucrose for 45mins followed by OCT embedding. Following sectioning, tissue was subjected to cresyl violet staining for 15 seconds prior to ethanol dehydration. The entire RGC layer was distinguishable as a distinct layer following cresyl violet staining and the entire layer was captured with LCM (since electroporated EGFP signal was lost following cresyl violet staining). To capture axons, the contralateral visual optic tract (composed of axons) was assumed to be the regions unstained by cresyl violet and terminating in the optic tectum. Laser capture settings used were the following: Magnification: 40X, Power:38-40, Speed: 7-9, Specimen Balance:5, Offset:30 RNA extraction was carried out by Ambion RNaqueous microkit and RNA was eluted in TE buffer at 16µl.

However, with this method there were these drawbacks:

- 1) The RNA quality and yield obtained from axons was very low (RIN: 2, yield: 150pg/µl) while that of RGC was RIN: 6, yield: 200pg/µl.
- 2) All the RGC layer was captured which included cells having MO-mediated knock down (electroporated and non-electroporated). This could lead to dilution in the MO mediated effect.

- 3) Similar to RGCs, all the region composed of axons and surrounding tract region was captured and not specifically electroporated axons.

Since RGCs were of much better quality compared to axons, these samples were used to test library preparation method.

The LCM procedure however needed to be optimized to enable good quality RNA extraction. The following steps were optimized to specifically enable visualization of both RGC and axonal compartments followed by extraction of a good quality RNA. *The optimization procedure was carried out with the help of Stephanie Strohbuecker who carried out RNA extractions and ran the bioanalyzer.*

- 1) Electroporation –Electroporation was chosen over microinjection in order to have targeted delivery of MOs into the retinal cells and thereby explore cell autonomous roles as opposed to a broad knock down. With electroporation of MO with reporter, I could specifically target RGCs (in addition to other retinal cells). Since RGCs are the only projecting neurons, the reporter facilitates labeling of axons projecting from the RGCs and therefore one can capture electroporated cell bodies and labeled axons *in vivo* from the same section. (Figure 3-30)

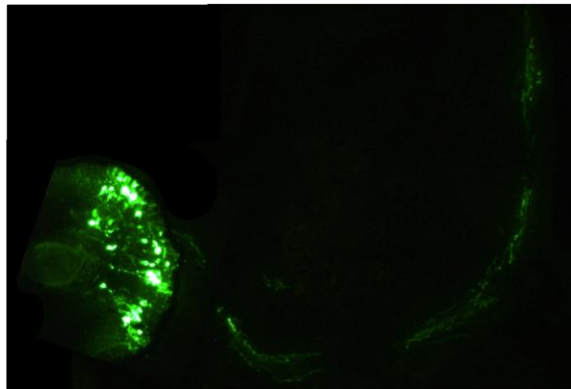


Figure 3-30: RGCs and axons labeled in vivo

- 2) Fixation with paraformaldehyde – As several papers recommend (Espina et al. 2006; Xiang et al. 2004; Su et al. 2004; Liu et al. 2014) using fast frozen tissue sections as opposed to fixed ones in order to obtain a very good quality RNA, I compared the effects of fixation vs no fixation. Electroporated embryos were fixed with 4% PFA or not fixed and embedded. I opted for very brief (15min)

fixation to minimize extensive crosslinking that can inhibit efficient recovery of RNA from the tissue (Khodosevich et al. 2007). In addition, presence of excessive PFA within tissue can be carried over during RNA extraction and can further inhibit library preparation. I therefore rinsed the embryos thoroughly following fixation procedure. With light fixation or no fixation there was no significant difference with respect to RNA quality (RIN: 6.8) (Figure 3-31). RNA yield could not be strictly compared as the amount of tissue collected was not constant. Since embryos are labeled with EGFP, I observed that no fixation led to diffuse EGFP signal within the tissue thereby rendering poor resolution and made it impossible to selectively collect electroporated cells. I therefore concluded that light fixation was required. (Figure 3-32)

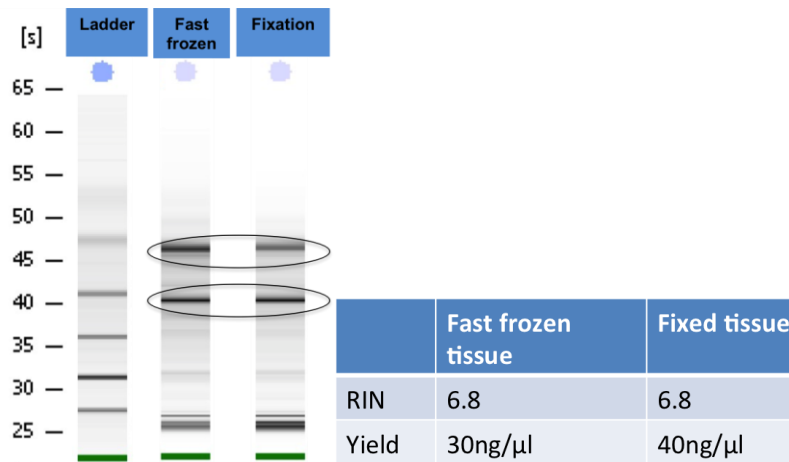


Figure 3-31: Comparison of fast frozen vs fixed tissue

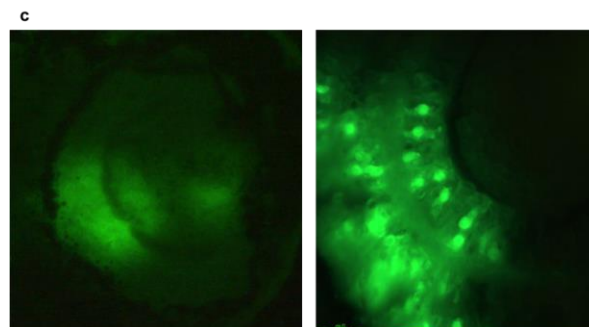


Figure 3-32: Diffuse EGFP signal in fast frozen tissue compared to fixed tissue.

- 3) Sucrose treatment – Sucrose treatment is important for cryoprotection of the tissue to preserve morphology (Portillo et al. 2009). Increased sucrose treatment

post fixation is recommended to decrease water in the tissue and thereby increase RNA yield (Cox et al. 2006) (Ambion Staining Kit). Humidity and hydrated tissue can reactivate endogenous nucleases within the cell thus causing RNA degradation (Bevilacqua et al. 2010; Kube et al. 2007). Therefore, I compared sucrose treatments between 1hr and 2hrs to check for improved RNA quality. I observed no difference in signal, the efficiency of cutting with the laser or RIN with increased sucrose treatment (Figure 3-33). Quality of sucrose also plays a crucial role in processing sections. To that extent, I tested Sucrose from two different suppliers. The sucrose from Acros Organics led to OCT retention therefore prevented efficient cutting. It was found that Sucrose from Fisher seemed to work much better and therefore was used for subsequent experiments.

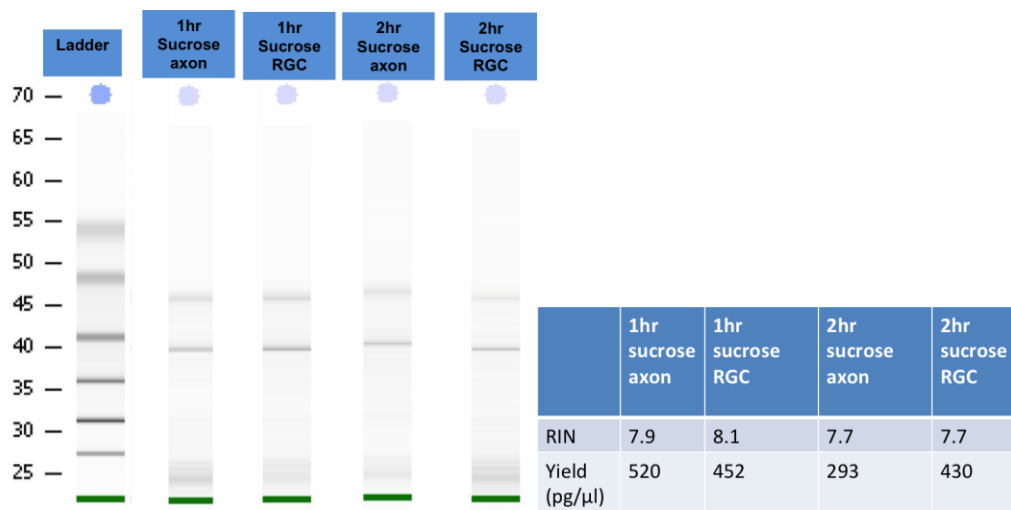


Figure 3-33: Effect of sucrose length on RNA quality and Yield

- 4) Membrane slides, dehydration and laser capture - In order to adhere sections onto slides, I used PEN (Polyethylene naphthalate) vs POL (Polyester) slides. These two types of slides were available as RNase free membranes. PEN membranes are supported by glass slides which offer much better adherence of tissue sections and therefore preserve morphology. POL slides are membranes surrounded by a metallic frame slide and thus the membrane by itself is not stuck to a firm support unlike the PEN glass slides. Therefore, they were not as firm resulting in tissue folding. Post adhesion of sections onto PEN membranes, immediate processing of slides (without storing them in the freezer) led to

significantly improved RIN and preserved EGFP signal. I suspect this was because the tissue was dehydrated without delay thus preventing reactivation of nucleases and preventing signal from bleaching due to freeze thaw cycle.

- 5) Incorporation of Xylene post ethanol dehydration helped in keeping tissue appropriately dehydrated to enable efficient cutting as Xylene causes dehydration of the tissue (Espina et al. 2006). For laser capture, the settings were extensively optimized in order to obtain quick capture without damage to the tissue. By using a faster speed setting, the power of the laser could be reduced and this enabled preserving RNA quality.

Laser settings	Series 1	Series 2	Series 3	Series 4	Series 5	Series 6	Series 6	Series 7
Power	25-28	30	26	26	33	35-38	35-38	31-32
Aperture	1	1	1	1	1	1-3	1	1
Speed	4-10	4	5-7	5	7-10	7-10	7-10	20
Specimen Balance	5	5	15-20	0	5	5	0	0
Offset	200	200	200	200	200	200	200	200
Comments	Did not cut well and tissue burns. Needed repeated cutting	Cutting associated with tissue burn. Not consistent with tissue falling	Did not cut well.	Cut partly well but tissue didn't fall.	Only few areas cut.	Only few areas cut and tissue burnt.	Cut better but tissue burnt.	Cuts and dislodges tissue well without tissue damage

Figure 3-34: Parameters of laser settings used to optimize cutting. Series 7 worked the best.

- 6) RNA extraction – Since the input from laser capture is very low, I tried to compare efficiencies of RNA extraction kits for low yield. Comparisons were done between Norgen microkit, Ambion RNAqueous kit and Norgen single cell RNA extraction kit. These kits were chosen because they were reported to be suitable for extracting RNA from low input laser-captured material. All 3 kits were successful in giving the same RNA quality however the yield differed amongst them. Norgen Microkit gave the least yield while Norgen Single cell kit gave the best yield. Ambion RNAqueous kit gave slightly lesser yield than the Single cell kit (Figure 3-35, f). Further, comparison with Ambion with Norgen single cell kit showed that the single cell kit gave a better yield especially for axons. (Figure 3-35, g)

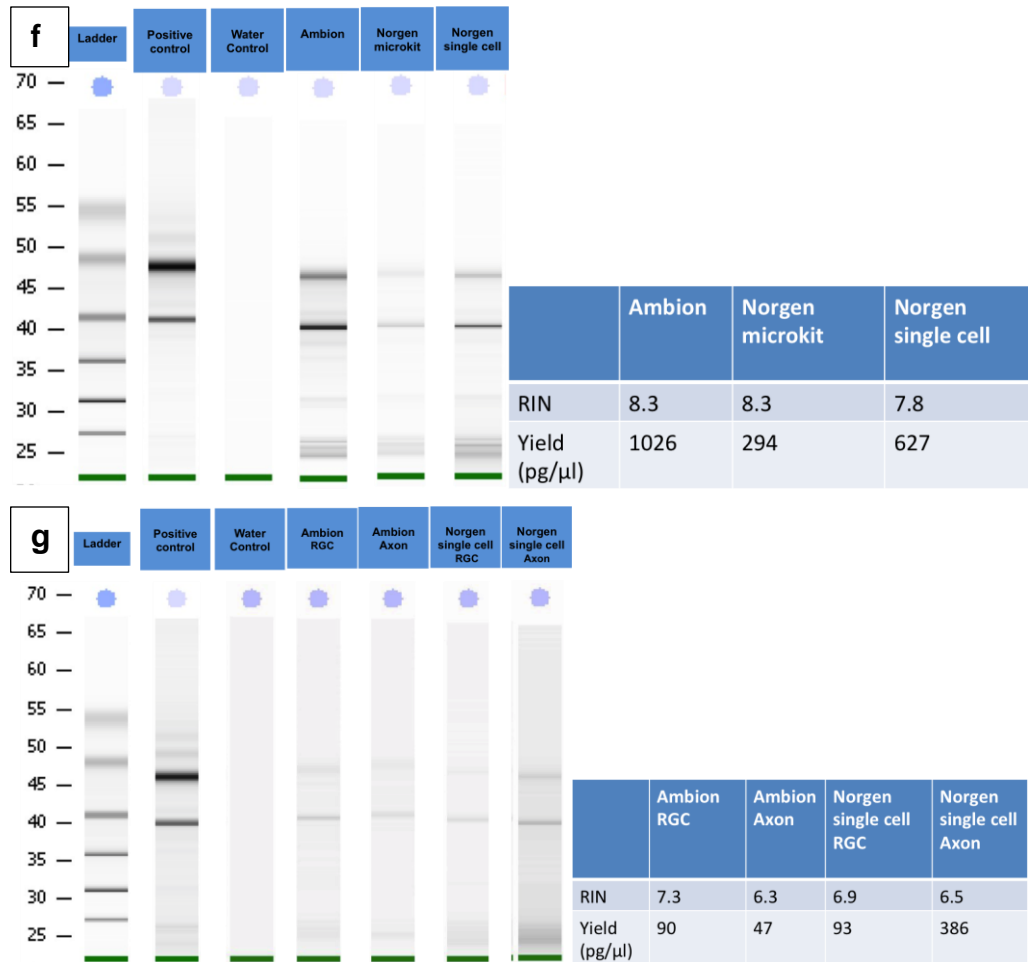


Figure 3-35: Comparison of different RNA extraction kits.

In conclusion, the LCM procedure was optimized with fixation of 15 mins of electroporated embryos. On the day of LCM, embryo sections were dehydrated with ethanol followed by xylene and subsequently the optimised laser settings were used followed by RNA extraction with Norgen Single cell kit.

3.3.1.1.2 Optimisation of library preparation and sequencing:

Library optimization was carried out by Paul Collier and Vladimir Benes at the Genecore Facility, EMBL on samples I collected with LCM. Stephanie Strohbuecker carried out the analysis of the sequencing data. I carried out the biological interpretation of the targets obtained.

Clontech library: Using the RNA extracted from cresyl violet stained RGC layer, the sequencing yielded 169 million and 129 million single-end reads for miR-181-MO and co-MO samples respectively. Of these, 9.12% (miR-181-MO) and 9.54% (co-MO) reads mapped to the *Xenopus laevis* transcriptome using Kallisto (Bray et al. 2016)

However, the RNA did not initially yield successful libraries therefore had to be cleaned up (probably due to residual PFA) and resuspended in water to remove possible PCR contaminants. Re-precipitation resulted in some loss of RNA. Furthermore, the RiboZero rRNA depletion kit, which is a bead-based clean up resulted in further loss of RNA. Importantly this kit (suited for human/mouse/rat) was not specific for *Xenopus* thus rRNA depletion did not work efficiently. 70% of the obtained reads still mapped to rRNA genes.

Nugen library kit: We decided to test another library preparation method wherein the ribosomal RNA could be specifically removed using customized probes for *Xenopus laevis*. In addition, the chosen library preparation protocol removes sequences stemming from rRNAs after cDNA synthesis which should reduce the loss of RNA often observed with other rRNA depletion methods usually performed using RNA as input. The second pilot experiment yielded ~31000 transcripts following rRNA depletion. Using customized probes from Nugen for rRNA depletion, we were able to reduce rRNA contamination by more than 50% from that obtained using Clontech library kit. The total rRNA content was about 25%. See Table 3.3.8.1 for summary.

In addition, with this library preparation method we also obtained a slightly higher number of detectable transcripts compared to previous sequencing results. Therefore, we used the above described optimized RNA extraction method in combination with the Nugen library preparation, to detect miR-181a/b targets following miR-181a/b knockdown with electroporation. Towards this end, samples were obtained as described in materials and methods section 3.2.10). We obtained RNA for 3 independent biological replicates which are currently processed at the EMBL Genomics Core Facility (GeneCore, Heidelberg)

Table 3.3.8.1: Summary of Library preparation and reads obtained

	Clontech	Nugen
Sample used	RGC from co-MO and miR-181-MO	RGC and axons from Wild type
RNA extraction kit	Ambion (eluted in TE buffer)	Norgen Single Cell kit (eluted in nuclease free water)
Library preparation and rRNA depletion kit	SMARTer® stranded total RNA seq kit pico input with Ribo-Zero rRNA removal kit	Ovation® Solo RNA-seq with InDA-C primers against <i>X.laevis</i> rRNA
Percentage rRNA in the libraries	~70%	~24%
Sequencing	Single-end sequencing using HiSeq4000	Paired-end. Illumina Next Seq500
Number of reads obtained	Co-MO: 129 million o-MO: 129 million miR-181-MO: 169 million single-end reads	WT RGC: 13.7 million WT axons: 17.6 million paired-end reads
Percentage mapping to <i>X.laevis</i> transcriptome using Kallisto	co-MO: 10% miR-181-MO: 9%	WT RGCs: 29% WT axons: 42%

3.3.1.1.3 Identification of candidate miR-181a/b targets

Target express predict putative miR-181a/b targets based on transcriptome data

The target prediction was carried out by Stephanie Strohbuecker and I

To gain some early insight into the mRNAs that may be regulated by miR-181, we carried out target prediction using TargetExpress(Ovando-Vázquez et al. 2016). TargetExpress (TE) combines the information of the expression level of a particular

gene in a given cell with its TargetScan(Garcia et al. 2011) Total Context+ score. The latter being a measure for the likelihood of a given transcript to be a miR-181a/b target. From the pilot experiments we obtained preliminary mRNA expression data from 4 samples, namely WT RGCs and axons in addition to co-MO and miR-181-MO. Using TargetExpress with those preliminary expression data, we obtained miR-181a/b candidate targets whose scores ranged from -21 to +16. Negative scores indicate that the putative mRNA is not a likely target in the given cellular context. With increasing positive TE scores which correlate with increasing expression levels the likelihood of the given mRNA to be a miR-181 target increases.

Using TargetScan with *Xenopus laevis* 3'UTRs we obtained 4718 putative miR-181 targets with a Total Context Score+ smaller than zero. These TargetScan results were, together with the expression levels of transcripts with expression levels greater zero, inputted into TargetExpress and provided the following number of targets:

Table 3.3.8.2: Transcriptome data from WT RGC,Axon ,co-MO and miR-181-MO

Sample	Number of mRNAs detected in total	Number of transcripts with a TE score greater than zero
WT RGCs	4129	1461
WT Axons	4505	1581
co-MO	3738	1331
miR-181-MO	4310	1524

We removed those transcripts that were not expressed in any of the four samples and whose annotation did not contain a 'proper' gene name. Genes without a 'proper' gene name, for example with gene names starting with "Xelaev" or "loc" were removed because these gene names often indicate that the annotation is incomplete.

To identify a shortlist of candidate miR-181 targets we ranked the identified predicted miR-181a/b targets according to their TE scores. Thereby we utilized in particular the TE scores obtained for the miR-181 loss-of-function condition reasoning that under the experimental condition with the lowest miR-181 concentration putative miR-181 targets should have a high expression level which in turn should lead to increased TE scores in

comparisons to “normal” conditions (wildtype and co-MO). Among the top ranking putative miR-181 targets seven targets not only had a high TE score in the miR-181-MO condition but also showed high TE scores under “normal” conditions. Three of these top ranking miR-181 candidate targets furthermore showed relevant functional annotation after a survey of the existing literature.

Table 3.3.8.3 Candidate mRNAs identified by their high Target Express scores

Target name	Total context score	miR-181-MO	Target express score			Fold change log2 (miR-181-MO over co-MO) in RGCs
			co-MO	WT RGCs	WT axons	
dpysl2	-0.413	15.91	15.94	15.91	15.99	-0.53
xpr1	-0.534	15.59	15.5	15.8	16.32	-0.09
nav1	-0.599	15.77	15.52	15.77	16.29	0.002
snn	-0.427	15.77	14.63	15.77	15	0.85
khdrbs1	-0.362	15.75	15.82	15.75	15.75	-0.66
tubb3	-0.349	15.7	15.72	15.7	15.77	-0.38
gsk3b	-0.542	15.46	14.62	15.46	14.43	0.38

Of the targets obtained, the topmost target – dpysl2, tubb3 and gsk3b are very interesting candidates due to the following reasons:

dpysl2 (also known as crmp2), a Dihydropyrimidinase–related protein2 that has a GO annotation for axon guidance. It is present within axons of adult mouse cortical and DRG neurons (Balastik et al. 2015). Crmp2 is shown to promote microtubule assembly (Fukata et al. 2002) and is important for Sema3A mediated collapse(Uchida et al. 2005). In presence of Sema3A, Crmp2 is phosphorylated by Gsk3 β also present on the list. It has roles in axonogenesis (Inagaki et al. 2001; Yoshimura et al. 2005) in addition to synaptic plasticity (Zhang et al. 2016).

tubb3 (β -tubulin isotype III): Tubulin is a component of microtubules and its expression is limited to neurons. Its expression coincides with period of axon guidance (Jiang & Oblinger 1992) during development. Required for guidance of commissural and cranial nerves. Mutations in Tubb3 cause ocular motility disorders in humans. (Tischfield et al. 2010). Tubb3 has been localized within Mouse cortical and spinal neurons where netrin-1 increases colocalization of Tubb3 with DSCAM and DCC in axonal branches and this interaction is important for netrin mediated axonal outgrowth and branching (Huang et al. 2015; Qu et al. 2013).

Gsk3 β (Glycogen synthase kinase3 β): Gsk3 β phosphorylates crmp2 within axon upon Sema3A stimulation (Uchida et al. 2005). Gsk3 β is important for neuronal polarity (Yoshimura et al. 2005).

All the above targets have been sorted with respect to their high target score specifically in miR-181 morphants. This suggests that these mRNAs are expressed abundantly and are miR-181 targets. However, with the above filtering criteria, the targets obtained did not show a fold change upon miR-181 loss-of-function.

While these candidates seem promising we also wanted to explore which mRNAs show a high fold change upon miR-181 loss-of-function. Therefore we applied another filtering approach to obtain solely targets that have a high fold change in expression in miR-181-MO conditions.

The second filtering approach entailed sorting mRNAs with high fold change in miR-181-MO over co-MO based on the expression values obtained as total number of reads per million for a given transcript. Shown below are the mRNAs that show high target expression score specifically upon miR-181 loss-of-function.

Table 3.3.8.4 Filtering candidates based on fold change

Target name	Total context score	Target express score in miR-181-MO	Target express score in co-MO	Target express score in WT RGC	Target express score in WT axons	Fold change log2 (miR-181-MO over co-MO)
cox7b	-0.171	10.76	4.85	10.18	9.73	2.58

syndig1	-0.302	13.9	4.65	8.24	12.44	2.10
ppm1e	-0.15	9.39	2.39	6.59	6.52	2.04
scrg1	-0.144	9.41	5.08	3.89	1.82	1.81
rit1	-0.186	10.01	2.42	6.12	4.31	1.70
sub1	-0.237	12.82	9.11	12.86	13.07	1.67
cdk5r2	-0.285	12.15	3.06	14.49	13.9	1.65

As observed by the second filtering approach, we obtained 7 targets that are upregulated in miR-181 morphants. From the targets obtained from the above filtering criteria, syndig1 expression not only changes upon miR-181 loss-of-function but also shows a high target express score within WT axons compared to RGCs. This suggests that this mRNA could be regulated within axons.

Syndig1 is very interesting as a target because it is important for post synapse development and maturation (Kalashnikova et al. 2010). It is possible that syndig1 is one of the transcripts regulated by miR-181 as axons reach the target.

One important consideration is that this fold change information is obtained from RGCs alone. It is possible that miR-181a/b could be regulating transcripts solely in axons and insight into that will be offered by the sequencing approach.

In summary, with target express we were able to get an idea of putative targets for miR-181a/b. Although this data is preliminary, it is interesting to obtain this information and compare this to the results obtained from the sequencing.

3.4 DISCUSSION

During its journey from exiting the eye to reaching the tectum, the GC faces multitude of cues. Appropriate responsiveness and integration of these cues at the GC is important for forming accurate connections. To do this, the GC has a large mRNA repertoire that changes dynamically during development as the GC transitions from one phase of guidance to the next (Zivraj et al. 2010). This pool of mRNA show stage specific expression and their dynamic nature help the GC to face new molecular terrains that enable the GC to adapt their response (Zivraj et al. 2010; Gummy et al. 2011). However, molecular mechanisms underlying regulation of transcript expression during the period of guidance are largely unknown. Specific transcript expression and their translation in response to cues mediate cytoskeletal remodeling to permit GC steering (Jung et al. 2012).

Here I show that miR-181a/b, one of the most abundantly expressed miRNAs within *Xenopus laevis* RGC axons regulate axonal responsiveness and targeting. Loss of miR-181a/b results in mistargeting of axons within the tectum. Moreover, miR-181a/b are required for axons to respond to specific tectal cues- sema3A and netrin-1. This modulation is highly specific, since not all tectal cue responsiveness is altered. Responsiveness to Slit2, another tectal cue is not affected suggesting that this miRNA family selectively regulates the netrin1 and sema3a signaling to enable GCs to mediate precise target recognition. We also determined that miR-181a/b loss-of-function phenotype is specific and can be rescued by use of exogenous mimics specific for miR-181a/b. Thus, miR-181a/b regulate specific mRNA/s that enable GC targeting. We wanted to investigate if the predominant mode of action of miRNA namely, selective mRNA degradation operates within axons. To explore which mRNAs these miRNAs target and if miR-181a/b have a compartmentalized role within GCs we have profiled mRNAs from distinct compartments by high throughput sequencing approach. In addition, target predictions that combine RNA-seq information to generate putative targets has revealed dpysl2, tubb3, gsk3b and syndig1 as interesting candidates that could be important for precise axonal targeting. Our ongoing RNA-seq analysis will enlighten us on the mechanism of action of this miRNA family within RGC compartments towards precise axonal guidance and target recognition.

Here, we explore an interesting family of miRNAs, the miR-181 family. The miR-181 family is a largely conserved family comprising of members miR-181a, b, c and d. miR-181 family originally came into highlight as important for hematopoietic lineage determination in the immune system (Chen et al. 2004). miR-181a have also been reported to be present in axons of mouse cortical and mouse DRG neurons (Sasaki et al. 2013; Wang et al. 2015) highlighting that this miRNA could have a common role in axons. Interestingly, miR-181c and d are not present in *X.laevis* and zebrafish.

It has been shown that miR-124, a cell body enriched miRNA, is important for regulating RGC axonal sensitivity to Sema3A and loss of miR-124 cause RGC axons to misproject ventrally in the tectum (Baudet et al. 2012). Interestingly, we also find here that GC responsiveness to Sema3A is decreased upon miR-181 loss-of-function and that miR-181 affects axonal targeting. However, the phenotype observed upon miR-181a/b loss-of-function is different from that of miR-124. miR-124 loss-of-function leads to RGC axons projecting ventrally within the tectum while miR-181 morphants form aberrant projections in the form of loop like structures. miR-124 is a cell body enriched miRNA and acts as a developmental timer to enable GCs to mediate sensitivity to Sema3A. miR-181a/b on the other hand are abundantly present in both RGC axons and cell bodies and they mediate responsiveness to sema3A and netrin-1 to be able to mediate precise targeting. This suggests that different miRNAs could regulate responsiveness in different aspects of axon guidance. Since both sema3A and netrin-1 responsiveness are altered, it is possible that under normal conditions, upon sema3A/netrin-1 exposure, miR-181 a/b could be targeting an mRNA that codes for repressing a molecule that mediates the collapse response of both cues. Targeting a repressor that inhibits collapse would enable collapse at the right time. Thus upon miRNA loss-of-function, the repressor might be continuing to prevent collapse as it is not targeted by the miRNA and it could prevent the translation of collapse mediator thus preventing axonal collapse.

Axonal pathfinding processes at early stages largely depend on axons moving forward rapidly and choosing the right route. While at later stages axonal GCs need to recognize the target, slow down (Harris et al. 1987) and form synapses with the post synaptic target cells. And indeed to complement these changes, the mRNA profile within the GCs

changes to cater to changing environments (Zivraj et al. 2010). When axons reach the target, transcripts required for initial phases of guidance must be silenced and the GC should be equipped with mRNAs required for targeting and branching initiation. Indeed axonal GCs have a dynamic mRNA repertoire coincidental with different axonal functions within the pathway (Zivraj et al. 2010). Since the phenotype observed is misrouting of axons within the tectum it could mean that the morphant axons still express mRNAs that are needed for pathfinding within the optic tract and hence meander about within the tectum without terminating appropriately suggesting the guidance phase could be still ‘on’ within these axons.

miR-181 could be therefore important in degradation of specific mRNA transcripts upon reaching the tectum that are no longer required for guidance. miR-181a/b could be thus crucial in enabling expression of right mRNAs at stage of axonal targeting while degrading spurious transcripts no longer needed for the next phase of pathfinding and target establishment.

We wanted to explore both scenarios to investigate if miR-181a/b silence mRNA by affecting their translation with or without subsequent mRNA degradation. To first answer if miR-181a/b mediate mRNA destabilization, we used RNA-seq on laser captured tissue to determine exactly which mRNAs are regulated by miR-181a/b. Though currently we do not have information on the transcriptome profile following miR-181a/b loss-of function, we used our preliminary sequencing data to get insight into which possible targets could be regulated. Through this approach of target prediction that combines information of the expression level of a particular gene in a given cell with its TargetScan (Garcia et al. 2011) Total Context+ score we filtered for highest target express scores, Collapsin Response Mediator Protein (Crmp2 (dpysl2)), Glycogen Synthase Kinase (Gsk3 β) and β -III Tubulin (tubb3) present in both RGCs and axons emerge out as possible targets. These targets not only had a high TE score in the miR-181-MO condition but also showed high TE scores under “normal” conditions making them likely candidates for miR-181. Based on what is known in the field, all three targets could be playing interconnected roles.

Crmp2 is known to be a target of miR-181c in embryonic mouse hippocampal neurons(Zhou et al. 2016). miR-181c is absent in *Xenopus laevis* but its seed sequence is

identical to that of miR-181a/b suggesting they could bind to similar targets. Crmp2 is not only in *Xenopus* RGC axons as I show above but also found in distal axons of adult DRG neurons (Balastik et al. 2015). Together, this suggests that miR-181a/b may regulate Crmp2 in RGC GCs. Crmp2 in addition to Cdk5 and Gsk3 β are important in Sema3A signaling (Uchida et al. 2005). Upon exposure to Sema3A, Crmp2 is phosphorylated primarily by Cdk5 and secondarily by Gsk3 β , which leads to GC collapse. Crmp2 is a tubulin heterodimer-binding protein that promotes microtubule assembly (Fukata et al. 2002). Exposure to Sema3A leads to its decreased affinity to tubulin, which leads to microtubule disassembly. Addition /transfection of non-phosphorylated forms of Crmp2 leads to decrease in Sema3A mediated collapse (Uchida et al. 2005). miR-181a/b could be preventing excessive phosphorylation by also targeting Gsk3 β . Maybe, Crmp2 vs phosphorylated CRMP need to be balanced tightly. miR-181a/b loss-of-function leads to increased CRMP2 (which should decrease collapse) however if, at the same time with more GSK3 β there should be more collapse. But if CDK5 is regulated independent from miR181, then it could be the rate-limiting step ensuring that CRMP2 leads to decreased collapse. Thus, basal levels of crmp2 increase and accumulate and therefore upon Sema3A exposure at the tectum, only partial Crmp2 molecules are phosphorylated leading to partial collapse but abundance of non-phosphorylated forms of Crmp2 could lead to decreased collapse as also observed by (Uchida et al. 2005).

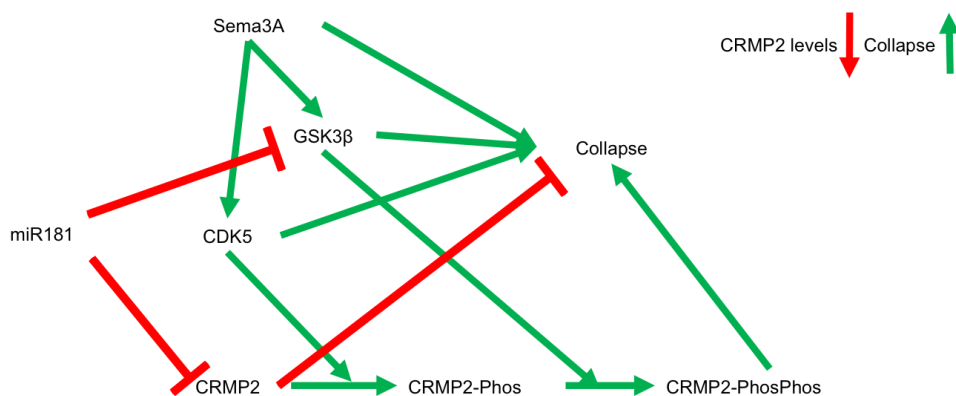


Figure 3-36: Model for miR-181 regulation of Gsk3 β and Crmp2

In addition to Gsk3 β and Crmp2, β -III tubulin is also found to be a target. It has been shown that axons from Superior Cervical Ganglia in newborn rats can synthesize tubulin locally(Eng et al. 1999). Dent et al in 1999(Dent et al. 1999) visualised axonal processes in cortical pyramidal neurons of newborn hamsters upon injection of tubulin (not specified which type). They observed microtubules arranged in the form of loops specifically in paused GCs.

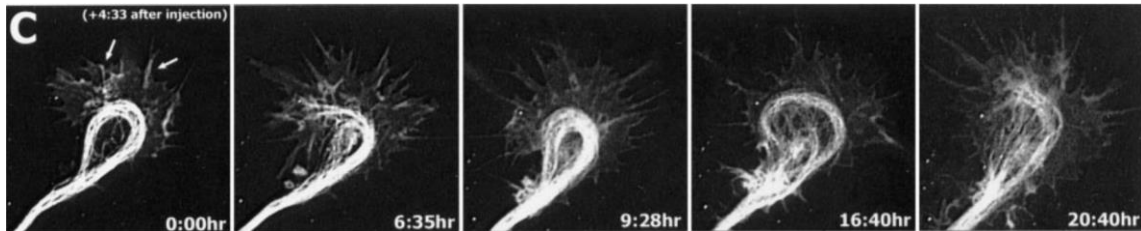


Figure 3-37: Microtubule loop in a paused GC.
From (Dent et al. 1999)

This looping phenomenon was also observed in paused GCs of *Xenopus* spinal neurons by Tanaka et al 1991(Tanaka & Kirschner 1991). Looping of microtubules is thought to be a result of continuous polymerization of tubulin in a paused GC that cause microtubules to bend backwards upon reaching the edge. This is associated with normal GCs that later uncurl to either extend or form branches. It is likely that increase in number of loops in miR-181a/b morphants could be a reflection of increase in tubulin.

As the above data are obtained by predictions in combination with expression data, we will compare these targets with that obtained through RNA-seq. RNA-seq data will enable obtaining information on all transcripts expressed in the GC differentially upon miR-181a/b loss-of-function. In addition, high throughput sequencing will be useful for determining transcript structure. mRNAs that localize to axons and have function in axons are known to have altered 3'UTRs that are selectively present within axons(Andreassi et al. 2010; Taliaferro et al. 2016). Thus, screening axons and RGC compartments can uncover splice variants that are selectively trafficked to axons(Shigeoka et al. 2016).

As specified in the Rationale, we also envision that miRNA may regulate transcripts translation without mRNA decay. Cue-mediated translational repression or de-repression have been reported in various contexts(Huang et al. 2007; Schrott et al. 2006;

Wang et al. 2015). For instance, miR-181c, another member of miR-181a/b family, enriched in mouse Dorsal Root Ganglion (DRG) neurons is involved in cue-induced de-repression of its targets. miR-181c alongwith RNA binding protein FMRP mediate repression of mRNAs –Map1b and Calm1 and regulate axonal elongation. Upon NGF exposure, this repression is relieved and translation of Map1b and Calm1 results in axonal elongation (Wang et al. 2015).

miR-181a/b roles have also been explored by Carrella et al in medaka visual system. In this study, miR-181a/b was found to be involved in retinal axonal specification and growth. miR-181a/b was further shown to target MAPK/ERK pathway(Carrella et al. 2015). MO mediated knock-down from one-cell stage in medaka embryos led to impaired neuritogenesis in amacrine cells and RGCs. In addition, there was impairment in outgrowth in RGC axons. We did not observe any RGC axonal outgrowth defect. This could be largely due to knock down approaches being different. Carrella et al employed broad knock down in all cells beginning from one-cell stage as opposed to temporal and spatially controlled knock down that we carried out specifically in retinal cells. In addition, this target was chosen without bioinformatics analysis or subsequent confirmation with luciferase assays to show it is a direct target of miR-181a/b. Therefore, as opposed to a candidate based approach, high throughput screening approach will give insight into global transcriptome not only within cell bodies but also within axons as miR-181a/b could possibly target multiple mRNAs.

Overall, miR-181a/b are shown to be regulators of axonal targeting and are important for axonal responsiveness to tectal cues in *Xenopus laevis* RGC axons.

Thus, it is likely that miR-181a/b could also be involved in cue-specific mRNA translation repression/de-repression. The section within ‘future perspectives’ will highlight on how this could be studied in our context.

3.5 FUTURE PERSPECTIVES

3.5.1 TRANSLATOME PROFILING

In order to address whether miR-181a/b primarily regulates mRNA translation without mediating mRNA degradation in axons, a translatome analysis needs to be performed and compared to our RNA-seq analysis.

Different techniques can be used to investigate the influence of miRNA on the proteome for instance: Mass spectrometry analysis, Ribosome profiling, Translating Ribosome Affinity purification

Proteomics approach that include Mass spectrometry analysis are possible although extremely technically challenging to use to address our question. Yoon et al., have demonstrated the use 2-dimensional difference gel electrophoresis based separation of proteins extracted from *Xenopus* RGC axons followed by their MALDI-TOF MS. However, this required culturing 1000 explants per condition *in vitro*, manually separating cell bodies prior to cue-stimulation. Addressing miR-181a/b loss-of-function induced changes would entail electroporation mediated MO delivery which would thus be a technical hurdle to obtain enough material.

Ribosome profiling could be used to systematically monitor cellular translation and predict protein abundance (Ingolia 2014; Weiss & Atkins 2011). Samples from RGCs vs axons upon miR-181a/b loss-of-function will indicate which mRNAs are being actively translated, the ribosomal occupancy and speed of translating ribosomes.

However, the downside with respect to our system is that ribosomal profiling requires a large number of cells ($\sim 10^7$) which is very difficult to obtain from axons and RGCs *in vivo*.

Another approach that can be used to overcome this limitation is Translating Ribosome Affinity purification (TRAP)(Heiman et al. 2014). TRAP can be used to isolate mRNA bound to ribosomes from specific cell types by means of an affinity tag expressed by the ribosomal protein 60S *in vivo*. The tissue that expresses this tagged ribosomal protein can be captured and subsequently processed to perform RNA-seq(King & Gerber 2016). Although in *Xenopus laevis*, expression of transgenic tag is difficult, electroporation mediated delivery can be used to introduce the tagged protein.

The experimental paradigm: By electroporating a GFP-tagged ribosomal protein L-10a within retinal cells will later project axons expressing the ribosomal protein with GFP (Yoon et al. 2012). At stage 40 when axons have reached the target, contralateral brain can be collected and affinity purified against GFP. Since, RGC axons are the only projecting neurons from the eye, brain tissue comprising of GFP tag will be solely from axons. This technique will enable isolation of actively translating mRNAs from axons *in vivo*.

3.5.2 ASSESSING LOCAL REGULATION OF miR-181a/b

RNA-seq will provide us with transcripts that are miR-181a/b targets however, we would not be able to answer which one of them could certainly be regulated in a cue-specific manner. Therefore, we could further assess if miR-181a/b regulates mRNA translation in a cue-specific manner locally within axons. Although *in vivo* assessment of presence of transcripts is an ideal approach, further investigation of cue-specific local translation of specific mRNA is difficult to answer *in vivo*. This is because one cannot dissect cue-specific response *in vivo* owing to the presence of various other cues and factors that can be confounding. Secondly, one can also assess the fate of miR-181a/b following cue-exposure. If upon cue stimulation, miR-181a/b lifts off repression from a specific mRNA, does the miRNA get degraded or does it levels within the GC remain unchanged.

Two different methods can be used to specifically isolate axons in order to answer the above 2 questions

a) Cut axons and b) Microfluidic chambers

Morphant or control MO can be transfected within axons, followed by cue-exposure (Sema3A/netrin-1) and RNA extracted from cut axons/ axonal side within chambers can be subjected to RNA seq suitable for low-input samples.

miR-181a/b levels within GCs upon cue-stimulation can be measured by Taqman qPCR.

We were able to transfect eye explants with MOs and as observed with microinjection, collapse responsiveness revealed that miR-181a/b loss-of-function led to decreased collapse in transfected axons. Thus, this system can be used to further ascertain local roles either by cut axons or within axonal side of microfluidic chambers.

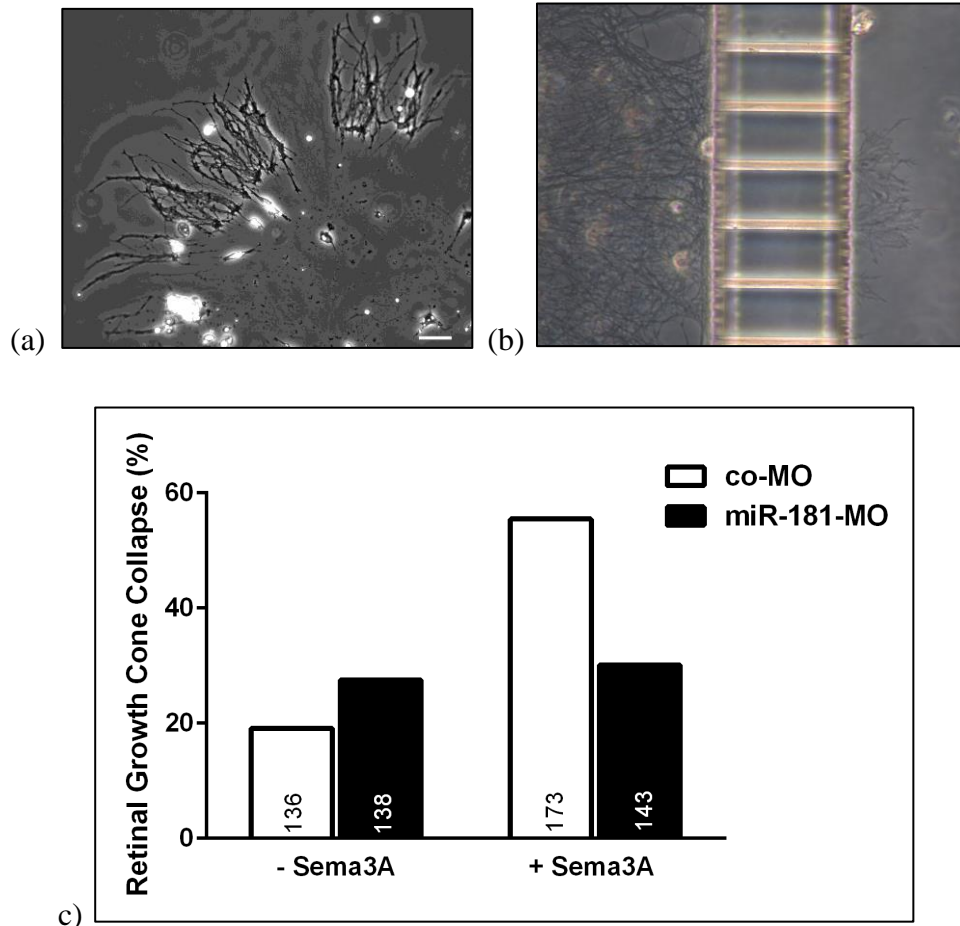


Figure 3-38: Tools to assess local regulation of miRNA in axons

(a) Cut axons separated from cell bodies can be used to determine local roles of miRNAs within axons. (b) Microfluidic chambers can be used to selectively target axons to explore local miRNA roles. Axons can be selectively transfected with MOs followed by cue exposure and transcript analysis. (c) Quantification of GC collapse in response to Sema3A in eye explant cultures transfected with co-MO or miR-181-MO ($n=1$). Numbers in the bar represent number of GCs analysed.

To ascertain if miRNA regulates axonal translation locally, of a specific mRNA *in vivo*, the 3'UTR of the target mRNA can be used to drive the expression of photoconvertible protein Kaede (Leung et al. 2013).

Once Kaede is photoconverted from its native green to red in GCs, newly synthesized protein from the target mRNA can be visualized as green spots. If the miRNA regulates local protein synthesis, upon loss-of-function of the miRNA, we would expect to see an increase in the protein synthesis (increase in green spots). Dissecting out the eye and visualizing the axons expressing the Kaede could, in addition, ascribe the effect to a local role.

Thus, with these future perspectives we will be able to dissect the role of miR-181a/b with respect to modifying the translome locally within GCs.

In conclusion, miRNAs observed in different systems employ different mechanisms to inhibit protein synthesis. By using RNA-seq and ribosomal profiling, we will be able to uncover miR-181a/b roles in the context of axonal responsiveness in *Xenopus laevis*. It is possible that different miRNAs within the same system could be employing mRNA degradation vs translational repression without affecting mRNA levels for varied biological outcomes.

GENERAL DISCUSSION

In this thesis, I have attempted to explore roles of two axonally abundant miRNAs namely miR-182 and miR-181 in *Xenopus laevis* visual circuit formation. I found that both miRNAs play crucial roles in precise targeting within tectum. Interestingly, both miRNAs mediate this role very distinctively. miR-182 mediates precise targeting by restricting axons within a defined tectal area while miR-181 is important to enable axons to project appropriately within the tectum.

Both miRNAs impinge on different signaling pathways. I have uncovered that miR-181a/b regulate growth cone responsiveness to two different chemorepellent cues namely sema3A and netrin-1 while Slit2 response is unaffected. On the contrary, miR-182 regulates Slit2 responsiveness but not Sema3A. netrin-1 was not tested. Specific miRNAs can be important for axonal responsiveness to specific cues. This is in keeping with other findings in the field where *Xenopus* RGC axons exhibit decreased sensitivity to Sema3A upon miR-124 loss-of-function (Baudet, et al. 2012).

The two miRNAs differ remarkably in terms of their expression pattern within the retina suggesting that they may have a different mode of action. miR-182 is expressed mainly by photoreceptors while RGCs express very low levels. On the contrary, miR-181a and b are expressed by RGCs, cells of the inner plexiform layer, but not by photoreceptors. This suggests that although both miRNAs are present abundantly within RGC axons, their presence within RGC cell bodies are different- miR-182 being lowly present while miR-181 being distributed in both cell bodies and axons. This implies that their compartmentalized distribution might be differentially regulated. Mechanisms that regulate miRNA distribution within compartments are slowly emerging. For instance, it is known that pre-miR-134 is localized within hippocampal dendrites and it is mediated through DEAH box helicase DHX 36 (Bicker et al. 2013). Specific terminal loop sequence within the pre-miRNA offers binding sites for RNA binding proteins that can further transport the pre-miRNA within specific locations.

miR-182 being exclusively higher in axons suggests that it could have a local role within axons while miR-181 may act in both compartments. It might be possible that

distributing miRNAs could have different biological roles. miR-182 involved in selecting transcripts for translation similar to miR-134 in dendrites. miR-181a/b present in both cell bodies and axons could be important for regulation of which mRNAs are present in both compartments by mediating degradation of mRNAs that are not relevant for that specific developmental stage.

The miRNAs present within axons have different seed sequences. Using differences within seed sequence between miRNAs, a cell can recruit distinct miRNAs to regulate different mRNAs within the same compartment. Considering the growth cone has a large number of signaling processes ongoing during pathfinding, regulation of each of these pathways by specific miRNAs could enable temporal and spatial precision in guidance.

Although differences in mode of action, commonality exists between the two miRNAs and that is that both miRNAs regulate axonal responsiveness to tectal cues and therefore enable precise targeting. Therefore it is possible to envision that neurons could employ a cohort of miRNAs with different specificity of binding to the mRNA repertoire at the growth cone but with a similar mechanistic role.

CONCLUSIONS AND FUTURE PERSPECTIVES

In conclusion, miR-182 and miR-181 regulate axonal targeting and responsiveness to tectal cues.

In my molecular hypothesis, I had envisioned two possible mode of action of miRNAs at the growth cone (See Molecular hypothesis) 1. Translational regulation and 2. Regulation of mRNA stability.

This issue still remains unresolved. The present data set has conclusively shown that miR-182 silences one mRNA until a cue is encountered and a burst of translation is subsequently induced. We still don't know whether miR-182 selects a pool of mRNAs for translation and whether this miRNA favors translation regulation over degradation induction as a main silencing mechanism. Similarly, we cannot draw conclusions at this stage for miR-181 mode of action in RGCs.

To clearly address this point, one would need to profile the proteome following miRNA perturbation as described in section 3.5.1

Apart from the mode of action that miRNAs undertake, the regulation of miRNAs within GCs could be interesting to explore. The presence of Dicer within RGC GCs (Section 3.3.2) suggests that pre-miRNAs could be trafficked there. Similar strategies as employed by (Bicker et al. 2013) in dendrites could be used to verify if pre-miRNAs can be indeed trafficked within axons and if these occur upon specific cue-exposure.

Overall, these questions will further dissect the molecular mechanisms employed by neurons to achieve high degree of specificity towards extracellular responses.

APPENDIX

Table 3.5.2.1: List of products and catalogue numbers

Acetic Anhydride	Sigma	320102
Anti-DIG AP Fab Fragment	Roche	11093274910
BCIP	Roche	11383221001
Blocking Reagent	Roche	11096176001
CHAPS	Sigma	C9426
CHAPS hydrate	Sigma	C9426
Coverslips, 12mm for culture	Bellco Glass	1943-10012A
Coverslips, 24mm, For open book prep	Marienfeld	0111640
Coverslips, 12mm, for culture	Marienfeld	0111520
Cycloheximide	Sigma	C4859
Denhardt's Solution	Sigma	D2532
Dithiothreitol (DTT)	Sigma	11583786001
DNA low binding tubes	Eppendorf	022431021
Double Open Chamber 150	Xona Microfluidics	DOC150
Ficoll	Carl Roth GmbH	304216763
FM 1-43FX Dye	Thermo Fisher	F35355
Formamide, deionised	Sigma	F9037
Gentamycin solution, 10ml	Sigma	G1397
Glass coverslips, 12mm	Bellco	1943-10012A
Goat Anti mouse IgG Alexa fluor 488	Thermo Scientific	A10684
Goat Anti mouse IgG Alexa fluor 594	Thermo Scientific	A11020

Goat anti rabbit IgG, Alexa fluor 488	Thermo Scientific	A11070
HCl, 6M	Sigma	84429
Immunohistomount	Sigma	I1161
L15, 100%	Gibco	11415-049
Laminin from Engelbroth-Holm Swarm, 1mg/ml	Sigma	L2020
Levamisol (Tetramisole hydrochloride)	Sigma	L9756
LNA probe for miR-181a, <i>Homo sapien</i>	Exiqon	18066-15
LNA probe, miRCURY LNA detection Control probe	Exiqon	99004-15
MS222 (Ethyl 3 aminobenzoate methanesulfonate)	Fluka	A504
NBT (Nitro blue tetrazolium)	Roche	11383213001
Netrin1, Mouse, 25µg	R&D systems	1109-N1-025
Norgen Single Cell RNA extraction Kit	Norgen	51800
O.C.T, Tissue freezing medium	Leica	14020108926
Paraformaldehyde 16%, Methanol free	Thermo Scientific	28908
PBS, 10X, RNase free	Ambion	AM9624
PEN membrane slides, 2µm	Leica	11505189
POL membrane slides, 0.9µm	Leica	11505191
Poly-L-Lysine Hydrobromide, 25mg	Sigma	P-1274
Product	Company	Catalogue no
Prolong Gold	Thermo Scientific	P10144
Proteinase K	Euroclone	5S014631
PSF, Anti anti (antibiotics) ,100X	Gibco	15240-062

Random Hexamer	Thermo Scientific	
Rapamycin	Merck Millipore	553210
RNA Aqueous microkit	Ambion	AM1931
RNase Zap	Invitrogen, ThermoScientific	AM9782
Salmon Sperm DNA	Sigma	D9156
Semaphorin3A, Human, 25µg	R&D systems	1250-S3-025
Sheep serum	Jackson Immunoresearch	013-000-121
Single Cell RNA extraction kit	Norgen	51800
Slit2, Mouse Recombinant, 50µg	R&D systems	5444-SL-050
β mercaptoethanol	Aldrich	M6250
SSC, 20X	Gibco	S6639
Sucrose	Fisher	S/8560/53
Superfrost slides	Thermo Scientific	J1800AMNZ
Total RNA Purification Micro Kit	Norgen	35300
Triethanolamine	Sigma	90279
Tween 20	Sigma	P1379
Water, RNase free	Sigma	W4502
Water, RNase free	Ambion	AM9932
Xylene	Sigma	534056
Yeast RNA	Sigma	R6750

References

- Alajez, N.M. et al., 2011. MiR-218 suppresses nasopharyngeal cancer progression through downregulation of survivin and the SLIT2-ROBO1 pathway. *Cancer research*, 71, pp.2381–2391.
- Ameres, S.L. & Zamore, P.D., 2013. Diversifying microRNA sequence and function. *Nature reviews. Molecular cell biology*, 14(8), pp.475–88. Available at: <http://www.nature.com/nrm/journal/v14/n8/full/nrm3611.html#affil-auth>.
- Andreassi, C. et al., 2010. An NGF-responsive element targets myo-inositol monophosphatase-1 mRNA to sympathetic neuron axons. *Nature Neuroscience*, 13(3), pp.291–301. Available at: <http://www.nature.com/doifinder/10.1038/nn.2486>.
- Aschrafi, A. et al., 2008. MicroRNA-338 regulates local cytochrome c oxidase IV mRNA levels and oxidative phosphorylation in the axons of sympathetic neurons. *The Journal of neuroscience: the official journal of the Society for Neuroscience*, 28(47), pp.12581–90. Available at: <http://www.pubmedcentral.nih.gov/articlerender.fcgi?artid=3496265&tool=pmcentrez&rendertype=abstract> [Accessed October 8, 2013].
- Ashraf, S.I. et al., 2006. Synaptic protein synthesis associated with memory is regulated by the RISC pathway in *Drosophila*. *Cell*, 124, pp.191–205.
- Atkinson-Leadbetter, K. et al., 2010. Dynamic Expression of Axon Guidance Cues Required for Optic Tract Development Is Controlled by Fibroblast Growth Factor Signaling. *Journal of Neuroscience*, 30(2), pp.685–693. Available at: <http://www.jneurosci.org/cgi/doi/10.1523/JNEUROSCI.4165-09.2010>.
- Augsburger, A. et al., 1999. Bmps as mediators of roof plate repulsion of commissural neurons. *Neuron*, 24(1), pp.127–141.
- Auyeung, V.C. et al., 2013. Beyond secondary structure: Primary-sequence determinants license Pri-miRNA hairpins for processing. *Cell*, 152(4), pp.844–858.
- Ayoob, J.C., Terman, J.R. & Kolodkin, A.L., 2006. *Drosophila* Plexin B is a Sema-2a receptor required for axon guidance. *Development (Cambridge, England)*, 133(11), pp.2125–35. Available at: <http://dev.biologists.org/content/133/11/2125>.
- Babiarz, J.E. et al., 2008. Mouse ES cells express endogenous shRNAs, siRNAs, and other microprocessor-independent, dicer-dependent small RNAs. *Genes and Development*, 22(20), pp.2773–2785.

- Baek, D. et al., 2008. The impact of microRNAs on protein output. *Nature*, 455, pp.64–71.
- Bagnard, D., 2007. *Axon Growth and guidance*,
- Bagri, A. et al., 2002. Slit proteins prevent midline crossing and determine the dorsoventral position of major axonal pathways in the mammalian forebrain. *Neuron*, 33(2), pp.233–248.
- Balastik, M. et al., 2015. Prolyl Isomerase Pin1 Regulates Axon Guidance by Stabilizing CRMP2A Selectively in Distal Axons. *Cell Reports*, 13, pp.812–828.
- Banerjee, S., Neveu, P. & Kosik, K.S., 2009. A coordinated local translational control point at the synapse involving relief from silencing and MOV10 degradation. *Neuron*, 64, pp.871–884.
- Bartel, D.P., 2009. MicroRNAs: target recognition and regulatory functions. *Cell*, 136, pp.215–233.
- Bassell, G.J. et al., 1998. Sorting of beta-actin mRNA and protein to neurites and growth cones in culture. *The Journal of neuroscience : the official journal of the Society for Neuroscience*, 18(1), pp.251–65. Available at: <http://www.ncbi.nlm.nih.gov/pubmed/9412505>.
- Baudet, M.-L. et al., 2012. miR-124 acts through CoREST to control onset of Sema3A sensitivity in navigating retinal growth cones. *Nature neuroscience*, 15(1), pp.29–38. Available at: <http://www.ncbi.nlm.nih.gov/pubmed/22138647> [Accessed January 29, 2013].
- Bawankar, P. et al., 2013. NOT10 and C2orf29/NOT11 form a conserved module of the CCR4-NOT complex that docks onto the NOT1 N-terminal domain. *RNA biology*, 10(2), pp.228–44. Available at: <http://www.pubmedcentral.nih.gov/articlerender.fcgi?artid=3594282&tool=pmcentrez&rendertype=abstract>.
- Bazzini, A. a, Lee, M.T. & Giraldez, A.J., 2012. Ribosome profiling shows that miR-430 reduces translation before causing mRNA decay in zebrafish. *Science (New York, N.Y.)*, 336(6078), pp.233–7. Available at: <http://www.pubmedcentral.nih.gov/articlerender.fcgi?artid=3547538&tool=pmcentrez&rendertype=abstract> [Accessed December 15, 2013].
- Behm-Ansmant, I. et al., 2006. mRNA degradation by miRNAs and GW182 requires both CCR4:NOT deadenylase and DCP1:DCP2 decapping complexes. *Genes and Development*, 20(14), pp.1885–1898.
- Bentley, D. & Caudy, M., 1983. Pioneer axons lose directed growth after selective killing of guidepost cells. *Nature*, 304, pp.62–65. Available at: <http://eutils.ncbi.nlm.nih.gov/entrez/eutils/elink.fcgi?dbfrom=pubmed&id=6866090&retm>

ode=ref&cmd=prlinks.

- Berezikov, E. et al., 2007. Mammalian mirtron genes. *Molecular cell*, 28(2), pp.328–36. Available at: <http://www.pubmedcentral.nih.gov/articlerender.fcgi?artid=2763384&tool=pmcentrez&rendertype=abstract> [Accessed December 15, 2013].
- Bernstein, E. et al., 2001. Role for a bidentate ribonuclease in the initiation step of RNA interference. *Nature*, 409, pp.363–366.
- Bevilacqua, C. et al., 2010. Maintaining RNA integrity in a homogeneous population of mammary epithelial cells isolated by Laser Capture Microdissection. *BMC cell biology*, 11(1), p.95. Available at: <http://www.pubmedcentral.nih.gov/articlerender.fcgi?artid=3019183&tool=pmcentrez&rendertype=abstract>.
- Bhattacharyya, S.N. et al., 2006. Relief of microRNA-Mediated Translational Repression in Human Cells Subjected to Stress. *Cell*, 125(6), pp.1111–1124.
- Bicker, S. et al., 2013. The DEAH-box helicase DHX36 mediates dendritic localization of the neuronal precursor-microRNA-134. *Genes & development*, 27(9), pp.991–6. Available at: <http://www.pubmedcentral.nih.gov/articlerender.fcgi?artid=3656329&tool=pmcentrez&rendertype=abstract> [Accessed January 27, 2014].
- Bohnsack, M.T., Czaplinski, K. & Gorlich, D., 2004. Exportin 5 is a RanGTP-dependent dsRNA-binding protein that mediates nuclear export of pre-miRNAs. *RNA (New York, N.Y.)*, 10(2), pp.185–91. Available at: <http://www.ncbi.nlm.nih.gov/pubmed/14730017> <http://www.pubmedcentral.nih.gov/articlerender.fcgi?artid=PMC1370530>.
- Bolger, A.M., Lohse, M. & Usadel, B., 2014. Trimmomatic: A flexible trimmer for Illumina sequence data. *Bioinformatics*, 30(15), pp.2114–2120.
- Braun, J.E. et al., 2012. A direct interaction between DCP1 and XRN1 couples mRNA decapping to 5' exonucleolytic degradation. *Nature structural & molecular biology*, 19(12), pp.1324–31. Available at: <http://www.ncbi.nlm.nih.gov/pubmed/23142987>.
- Braun, J.E. et al., 2011. GW182 proteins directly recruit cytoplasmic deadenylase complexes to miRNA targets. *Molecular Cell*, 44(1), pp.120–133.
- Bray, N.L. et al., 2016. Near-optimal probabilistic RNA-seq quantification. *Nature biotechnology*, 34(5), pp.525–7. Available at: <http://www.ncbi.nlm.nih.gov/pubmed/27043002>.

- Brittis, P.A., Lu, Q. & Flanagan, J.G., 2002. Axonal protein synthesis provides a mechanism for localized regulation at an intermediate target. *Cell*, 110(2), pp.223–235.
- Brose, K. et al., 1999. Slit proteins bind robo receptors and have an evolutionarily conserved role in repulsive axon guidance. *Cell*, 96(6), pp.795–806.
- Campbell, D.S. et al., 2001. Semaphorin 3A elicits stage-dependent collapse, turning, and branching in *Xenopus* retinal growth cones. *The Journal of neuroscience : the official journal of the Society for Neuroscience*, 21(21), pp.8538–8547.
- Campbell, D.S. & Holt, C.E., 2001. Chemotropic responses of retinal growth cones mediated by rapid local protein synthesis and degradation. *Neuron*, 32(6), pp.1013–26. Available at: <http://www.ncbi.nlm.nih.gov/pubmed/11754834>.
- Carrella, S. et al., 2015. TGF- β controls MIR-181/ERK regulatory network during retinal axon specification and growth. *PLoS ONE*, 10, pp.1–22.
- Cazalla, D., Xie, M. & Steitz, J.A., 2011. A Primate Herpesvirus Uses the Integrator Complex to Generate Viral MicroRNAs. *Molecular Cell*, 43(6), pp.982–992.
- Cechmanek, P.B., Hehr, C.L. & McFarlane, S., 2015. Rho kinase is required to prevent retinal axons from entering the contralateral optic nerve. *Molecular and Cellular Neuroscience*, 69, pp.30–40. Available at: <http://dx.doi.org/10.1016/j.mcn.2015.10.001>.
- Chan, S.S.Y. et al., 1996. UNC-40, a *C. elegans* homolog of DCC (Deleted in Colorectal Cancer), is required in motile cells responding to UNC-6 netrin cues. *Cell*, 87(2), pp.187–195.
- Chang, C. et al., 2004. Inhibition of netrin-mediated axon attraction by a receptor protein tyrosine phosphatase. *Science (New York, N.Y.)*, 305, pp.103–106.
- Chang, S. et al., 2004. MicroRNAs act sequentially and asymmetrically to control chemosensory laterality in the nematode. *Nature*, 430, pp.785–789.
- Charron, F. et al., 2003. The morphogen sonic hedgehog is an axonal chemoattractant that collaborates with Netrin-1 in midline axon guidance. *Cell*, 113(1), pp.11–23.
- Chédotal, A., 2007. Slits and their receptors. *Advances in Experimental Medicine and Biology*, 621, pp.65–80.
- Chekulaeva, M. et al., 2011. miRNA repression involves GW182-mediated recruitment of CCR4–NOT through conserved W-containing motifs. *Nature Structural & Molecular Biology*, 18(11), pp.1218–1226. Available at: <http://dx.doi.org/10.1038/nsmb.2166>.

- Cheloufi, S. et al., 2010. A dicer-independent miRNA biogenesis pathway that requires Ago catalysis. *Nature*, 465(7298), pp.584–9. Available at: <http://www.pubmedcentral.nih.gov/articlerender.fcgi?artid=2995450&tool=pmcentrez&rendertype=abstract> [Accessed September 20, 2013].
- Chen, C.-Z. et al., 2004. MicroRNAs modulate hematopoietic lineage differentiation. *Science (New York, N.Y.)*, 303(5654), pp.83–6. Available at: <http://www.ncbi.nlm.nih.gov/pubmed/14657504>.
- Chen, H. et al., 1997. Neuropilin-2, a novel member of the neuropilin family, is a high affinity receptor for the semaphorins Sema E and Sema IV but not Sema III. *Neuron*, 19(3), pp.547–559.
- Chen, J.H. et al., 2000. Embryonic expression and extracellular secretion of Xenopus Slit. *Neuroscience*, 96(1), pp.231–236.
- Chen, J.H. et al., 2001. The N-terminal leucine-rich regions in Slit are sufficient to repel olfactory bulb axons and subventricular zone neurons. *The Journal of neuroscience: the official journal of the Society for Neuroscience*, 21(5), pp.1548–1556.
- Chiu, H., Alqadah, A. & Chang, C., 2014. The role of microRNAs in regulating neuronal connectivity. *Frontiers in cellular neuroscience*, 7(January), p.283. Available at: <http://www.pubmedcentral.nih.gov/articlerender.fcgi?artid=3879460&tool=pmcentrez&rendertype=abstract> [Accessed January 20, 2014].
- Christodoulou, F. et al., 2010. Ancient animal microRNAs and the evolution of tissue identity. *Nature*, 463(7284), pp.1084–8. Available at: <http://www.pubmedcentral.nih.gov/articlerender.fcgi?artid=2981144&tool=pmcentrez&rendertype=abstract> [Accessed February 5, 2013].
- Cifuentes, D. et al., 2010. A novel miRNA processing pathway independent of Dicer requires Argonaute2 catalytic activity. *Science (New York, N.Y.)*, 328(5986), pp.1694–8. Available at: <http://www.pubmedcentral.nih.gov/articlerender.fcgi?artid=3093307&tool=pmcentrez&rendertype=abstract> [Accessed September 19, 2013].
- Cirulli, V. & Yebra, M., 2007. Netrins: beyond the brain. *Nature reviews. Molecular cell biology*, 8(4), pp.296–306. Available at: <http://www.ncbi.nlm.nih.gov/pubmed/17356579>.
- Colamarino, S.A. & Tessier-Lavigne, M., 1995. The axonal chemoattractant netrin-1 is also a chemorepellent for trochlear motor axons. *Cell*, 81(4), pp.621–629.
- Cooke, A., Prigge, A. & Wickens, M., 2010. Translational repression by deadenylases. *Journal of Biological Chemistry*, 285(37), pp.28506–28513.

- Coolen, M. et al., 2012. MiR-9 Controls the Timing of Neurogenesis through the Direct Inhibition of Antagonistic Factors. *Developmental Cell*, 22(5), pp.1052–1064. Available at: <http://dx.doi.org/10.1016/j.devcel.2012.03.003>.
- Cornel, E. & Holt, C., 1992. Precocious pathfinding: Retinal axons can navigate in an axonless brain. *Neuron*, 9(6), pp.1001–1011.
- Cox, M.L. et al., 2006. Assessment of fixatives, fixation, and tissue processing on morphology and RNA integrity. *Experimental and Molecular Pathology*, 80(2), pp.183–191.
- Cui, Y. et al., 2012. MicroRNA-181b and microRNA-9 mediate arsenic-induced angiogenesis via NRP1. *Journal of cellular physiology*, 227, pp.772–83. Available at: <http://www.ncbi.nlm.nih.gov/pubmed/21503876>.
- Dajas-Bailador, F. et al., 2012a. microRNA-9 regulates axon extension and branching by targeting Map1b in mouse cortical neurons. *Nature neuroscience*, (c). Available at: <http://www.ncbi.nlm.nih.gov/pubmed/22484572> [Accessed October 8, 2013].
- Dajas-Bailador, F. et al., 2012b. microRNA-9 regulates axon extension and branching by targeting Map1b in mouse cortical neurons. *Nature neuroscience*, 15(5). Available at: <http://www.ncbi.nlm.nih.gov/pubmed/22484572> [Accessed May 22, 2013].
- Dent, E.W. et al., 1999. Reorganization and movement of microtubules in axonal growth cones and developing interstitial branches. *The Journal of neuroscience : the official journal of the Society for Neuroscience*, 19(20), pp.8894–8908.
- Dent, E.W., Gupton, S.L. & Gertler, F.B., 2011. The growth cone cytoskeleton in axon outgrowth and guidance. *Cold Spring Harbor perspectives in biology*, 3.
- Dingwell KS, Holt CE, H.W., 2000. The multiple decisions made by growth cones of RGCs as they navigate from the retina to the tectum in *Xenopus* embryos. *Journal of Neurobiology*, 44(2), pp.246–259.
- Djuranovic, S., Nahvi, A. & Green, R., 2012. miRNA-Mediated Gene Silencing by Translational Repression Followed by mRNA Deadenylation and Decay. *Science*, 336(6078), pp.237–240. Available at: <http://www.sciencemag.org/content/336/6078/237><http://www.ncbi.nlm.nih.gov/pubmed/22499947><http://www.sciencemag.org/content/336/6078/237.abstract>.
- Drescher, U., Bonhoeffer, F. & Müller, B.K., 1997. The Eph family in retinal axon guidance. *Current Opinion in Neurobiology*, 7(1), pp.75–80.

- Ebert, M.S. & Sharp, P.A., 2012. Roles for MicroRNAs in Conferring Robustness to Biological Processes. *Cell*, 149, pp.515–524.
- Egea, J. & Klein, R., 2007. Bidirectional Eph-ephrin signaling during axon guidance. *Trends in Cell Biology*, 17(5), pp.230–238.
- Eichhorn, S.W. et al., 2014. mRNA Destabilization Is the Dominant Effect of Mammalian MicroRNAs by the Time Substantial Repression Ensues. *Molecular Cell*, 56(1), pp.104–115. Available at: <http://linkinghub.elsevier.com/retrieve/pii/S1097276514007060>.
- Ender, C. et al., 2008. A Human snoRNA with MicroRNA-Like Functions. *Molecular Cell*, 32(4), pp.519–528.
- Eng, H., Lund, K. & Campenot, R.B., 1999. Synthesis of beta-tubulin, actin, and other proteins in axons of sympathetic neurons in compartmented cultures. *The Journal of neuroscience: the official journal of the Society for Neuroscience*, 19(1), pp.1–9. Available at: <http://www.ncbi.nlm.nih.gov/pubmed/9870932>.
- Erskine, L. et al., 2011. VEGF signaling through neuropilin 1 guides commissural axon crossing at the optic chiasm. *Neuron*, 70, pp.951–965.
- Espina, V. et al., 2006. Laser-capture microdissection.
- Eulalio, A., Huntzinger, E. & Izaurralde, E., 2008. GW182 interaction with Argonaute is essential for miRNA-mediated translational repression and mRNA decay. *Nature structural & molecular biology*, 15(4), pp.346–353.
- Fabian, M.R. et al., 2009. Mammalian miRNA RISC Recruits CAF1 and PABP to Affect PABP-Dependent Deadenylation. *Molecular Cell*, 35(6), pp.868–880.
- Fabian, M.R. & Sonenberg, N., 2012. The mechanics of miRNA-mediated gene silencing: a look under the hood of miRISC. *Nature structural & molecular biology*, 19(6), pp.586–93. Available at: <http://www.ncbi.nlm.nih.gov/pubmed/22664986> [Accessed September 17, 2013].
- Falk, J. et al., 2007. Electroporation of cDNA/Morpholinos to targeted areas of embryonic CNS in *Xenopus*. *BMC Developmental Biology*, 7, p.107. Available at: <http://www.ncbi.nlm.nih.gov/pubmed/17900342>.
- Filipowicz, W., Bhattacharyya, S.N. & Sonenberg, N., 2008. Mechanisms of post-transcriptional regulation by microRNAs: are the answers in sight? *Nature reviews. Genetics*, 9(2), pp.102–14. Available at: <http://www.ncbi.nlm.nih.gov/pubmed/18197166> [Accessed May 25, 2013].

- Fiore, R. et al., 2009. Mef2-mediated transcription of the miR379-410 cluster regulates activity-dependent dendritogenesis by fine-tuning Pumilio2 protein levels. *The EMBO journal*, 28(6), pp.697–710. Available at: <http://www.pubmedcentral.nih.gov/articlerender.fcgi?artid=2647767&tool=pmcentrez&rendertype=abstract> [Accessed December 15, 2013].
- Fish, J.E. et al., 2011. A Slit/miR-218/Robo regulatory loop is required during heart tube formation in zebrafish. *Development (Cambridge, England)*, 138(7), pp.1409–19. Available at: <http://www.pubmedcentral.nih.gov/articlerender.fcgi?artid=3050667&tool=pmcentrez&rendertype=abstract> [Accessed December 15, 2013].
- Flynt, A.S. et al., 2010. MicroRNA biogenesis via splicing and exosome-mediated trimming in *Drosophila*. *Molecular cell*, 38(6), pp.900–7. Available at: <http://www.pubmedcentral.nih.gov/articlerender.fcgi?artid=2904328&tool=pmcentrez&rendertype=abstract>.
- Fukata, Y. et al., 2002. CRMP-2 binds to tubulin heterodimers to promote microtubule assembly. *Nature cell biology*, 4(8), pp.583–591.
- Fukaya, T. & Tomari, Y., 2012. MicroRNAs Mediate Gene Silencing via Multiple Different Pathways in *Drosophila*. *Molecular Cell*, 48(6), pp.825–836.
- Fukaya, T. & Tomari, Y., 2011. PABP is not essential for microRNA-mediated translational repression and deadenylation in vitro TL - 30. *The EMBO Journal*, 30 VN-r(24), pp.4998–5009. Available at: [/Users/yurikoharigaya/Documents/ReadCube Media/4998.full.pdf%5Cnhttp://dx.doi.org/10.1038/emboj.2011.426](#).
- Gao, F.-B., 2010. Context-dependent functions of specific microRNAs in neuronal development. *Neural development*, 5, p.25.
- Garcia, D.M. et al., 2011. Weak seed-pairing stability and high target-site abundance decrease the proficiency of lsy-6 and other microRNAs. *Nature Structural & Molecular Biology*, 18(10), pp.1139–1146. Available at: <http://dx.doi.org/10.1038/nsmb.2115%5Cnhttp://www.nature.com/doifinder/10.1038/nsmb.2115>.
- Giraldez, A.J. et al., 2005. MicroRNAs regulate brain morphogenesis in zebrafish. *Science (New York, N.Y.)*, 308(5723), pp.833–8. Available at: <http://www.ncbi.nlm.nih.gov/pubmed/15774722> [Accessed June 9, 2013].
- Giraldez, A.J. et al., 2006. Zebrafish MiR-430 promotes deadenylation and clearance of maternal mRNAs. *Science (New York, N.Y.)*, 312(5770), pp.75–9. Available at:

<http://www.ncbi.nlm.nih.gov/pubmed/16484454> [Accessed May 27, 2013].

- Giuditta, A. et al., 1991. Active polysomes in the axoplasm of the squid giant axon. *Journal of Neuroscience Research*, 28(1), pp.18–28.
- Giuditta, A., Cupello, A. & Lazzarini, G., 1980. Ribosomal RNA in the axoplasm of the squid giant axon. *Journal of Neurochemistry*, 34(6), pp.1757–1760.
- Giuditta, A., Dettbarn, W.D. & Brzin, M., 1968. Protein synthesis in the isolated giant axon of the squid. *Proceedings of the National Academy of Sciences of the United States of America*, 59(4), pp.1284–7. Available at: <http://www.pubmedcentral.nih.gov/articlerender.fcgi?artid=224864&tool=pmcentrez&rendertype=abstract>.
- Giuditta, A., Hunt, T. & Santella, L., 1986. Rapid important paper. Messenger RNA in squid axoplasm. *Neurochemistry International*, 8(3), pp.435–442.
- Gordon Laura, Mansh Matthew, Kinsman Helen, M.R.A., 2010. Xenopus sonic hedgehog guides retinal axons along the optic tract. *Developmental dynamics: an official publication of the American Association of Anatomists*, 239(11), pp.2921–2932.
- Grant, P., Rubin, E. & Cima, C., 1980. Ontogeny of the retina and optic nerve in *Xenopus laevis*. I. Stages in the early development of the retina. *Journal of Comparative Neurology*, 613, pp.593–613. Available at: <http://onlinelibrary.wiley.com/doi/10.1002/cne.901890403/full>.
- Gregory, R.I. et al., 2004. The Microprocessor complex mediates the genesis of microRNAs. *Nature*, 432(7014), pp.235–240.
- Grishok, A. et al., 2001. Genes and mechanisms related to RNA interference regulate expression of the small temporal RNAs that control *C. elegans* developmental timing. *Cell*, 106, pp.23–34.
- Grumet, M., Flaccus, A. & Margolis, R.U., 1993. Functional characterization of chondroitin sulfate proteoglycans of brain: interactions with neurons and neural cell adhesion molecules. *The Journal of cell biology*, 120(3), pp.815–24. Available at: <http://www.ncbi.nlm.nih.gov/pubmed/8425902> <http://www.pubmedcentral.nih.gov/articlerender.fcgi?artid=PMC2119543>.
- Gumy, L.F. et al., 2011. Transcriptome analysis of embryonic and adult sensory axons reveals changes in mRNA repertoire localization. *RNA (New York, N.Y.)*, 17, pp.85–98.
- Guo, H. et al., 2010. Mammalian microRNAs predominantly act to decrease target mRNA levels. *Nature*, 466, pp.835–840.

- Ha, M. & Kim, V.N., 2014. Regulation of microRNA biogenesis. *Nature reviews. Molecular cell biology*, 15(8), pp.509–524. Available at: <http://www.ncbi.nlm.nih.gov/pubmed/25027649>.
- Hammond, S.M. et al., 2001. Argonaute2, a link between genetic and biochemical analyses of RNAi. *Science (New York, N.Y.)*, 293(5532), pp.1146–50. Available at: <http://www.ncbi.nlm.nih.gov/pubmed/11498593>.
- Han, J. et al., 2006. Molecular Basis for the Recognition of Primary microRNAs by the Drosha-DGCR8 Complex. *Cell*, 125(5), pp.887–901.
- Han, L. et al., 2011. Regulation of chemotropic guidance of nerve growth cones by microRNA. *Molecular brain*, 4(1), p.40. Available at: <http://www.pubmedcentral.nih.gov/articlerender.fcgi?artid=3217933&tool=pmcentrez&rendertype=abstract> [Accessed February 5, 2013].
- Hancock, M.L. et al., 2014. MicroRNA-132 Is Enriched in Developing Axons, Locally Regulates Rasal mRNA, and Promotes Axon Extension. *The Journal of neuroscience : the official journal of the Society for Neuroscience*, 34(1), pp.66–78. Available at: <http://www.ncbi.nlm.nih.gov/pubmed/24381269> [Accessed January 30, 2014].
- Hansen, T.B. et al., 2013. Natural RNA circles function as efficient microRNA sponges. *Nature*, 495, pp.384–8. Available at: <http://www.ncbi.nlm.nih.gov/pubmed/23446346>.
- Hao, J.C. et al., 2001. C. elegans slit acts in midline, dorsal-ventral, and anterior-posterior guidance via the SAX-3/Robo receptor. *Neuron*, 32(1), pp.25–38.
- Harrelson, a L. & Goodman, C.S., 1988. Growth cone guidance in insects: fasciclin II is a member of the immunoglobulin superfamily. *Science*, 242(4879), pp.700–708.
- Harris, R., Sabatelli, L.M. & Seeger, M.A., 1996. Guidance cues at the Drosophila CNS midline: Identification and characterization of two Drosophila Netrin/UNC-6 homologs. *Neuron*, 17(2), pp.217–228.
- Harris, W. a, Holt, C.E. & Bonhoeffer, F., 1987. Retinal axons with and without their somata, growing to and arborizing in the tectum of Xenopus embryos: a time-lapse video study of single fibres in vivo. *Development (Cambridge, England)*, 101(1), pp.123–33. Available at: <http://www.ncbi.nlm.nih.gov/pubmed/3449363>.
- He, Z. & Tessier-Lavigne, M., 1997. Neuropilin is a receptor for the axonal chemorepellent semaphorin III. *Cell*, 90(4), pp.739–751.
- Hehr, C.L., Hocking, J.C. & McFarlane, S., 2005. Matrix metalloproteinases are required for retinal

- ganglion cell axon guidance at select decision points. *Development (Cambridge, England)*, 132(15), pp.3371–3379.
- Heidemann, S.R., 1996. Cytoplasmic mechanisms of axonal and dendritic growth in neurons. *International review of cytology*, 165, pp.235–96. Available at: <http://www.ncbi.nlm.nih.gov/pubmed/8900961>.
- Heiman, M. et al., 2014. Cell type-specific mRNA purification by translating ribosome affinity purification (TRAP). *Nature protocols*, 9(6), pp.1282–91. Available at: <http://www.scopus.com/inward/record.url?eid=2-s2.0-84901819558&partnerID=tZOtx3y1>.
- Hendrickson, D.G. et al., 2009. Concordant regulation of translation and mRNA abundance for hundreds of targets of a human microRNA. *PLoS Biology*, 7(11).
- Hengst, U. et al., 2006. Functional and selective RNA interference in developing axons and growth cones. *The Journal of neuroscience : the official journal of the Society for Neuroscience*, 26(21), pp.5727–32. Available at: <http://www.ncbi.nlm.nih.gov/pubmed/16723529> [Accessed July 3, 2013].
- Heo, I. et al., 2012. Mono-uridylation of pre-microRNA as a key step in the biogenesis of group II let-7 microRNAs. *Cell*, 151(3), pp.521–532.
- Hocking, J.C. et al., 2010. Distinct roles for Robo2 in the regulation of axon and dendrite growth by retinal ganglion cells. *Mechanisms of Development*, 127(1–2), pp.36–48. Available at: <http://dx.doi.org/10.1016/j.mod.2009.11.002>.
- Hollyfield, J.G., 1973. Elimination of egg pigment from developing ocular tissues in the frog *Rana pipiens*. *Developmental Biology*, 30, pp.115–128.
- Holt, C., 1980. Cell movements in *Xenopus* eye development. *Nature*, 287, pp.850–2. Available at: <http://www.ncbi.nlm.nih.gov/pubmed/18073535>.
- Holt, C.E., 1989. A single-cell analysis of early retinal ganglion cell differentiation in *Xenopus*: from soma to axon tip. *The Journal of neuroscience : the official journal of the Society for Neuroscience*, 9(9), pp.3123–45. Available at: <http://www.ncbi.nlm.nih.gov/pubmed/2795157>.
- Holt, C.E., 1984. Does timing of axon outgrowth influence initial retinotectal topography in *Xenopus*? *The Journal of Neuroscience*, 4(4), pp.1130–1152. Available at: <http://www.jneurosci.org/content/4/4/1130.long>.
- Holt, C.E. & Harris, W.A., 1998. Target selection: invasion, mapping and cell choice. *Current Opinion in Neurobiology*, 8(1), pp.98–105.

- Holt, E., Bertsch, W. & Harris, A., 1988. Cellular Determination in the Xenopus Retina Is Independent of Lineage and Birth Date division. , 1, pp.15–26.
- Hong, K. et al., 1999. A ligand-gated association between cytoplasmic domains of UNC5 and DCC family receptors converts netrin-induced growth cone attraction to repulsion. *Cell*, 97(7), pp.927–941.
- Höpker, V.H. et al., 1999. Growth-cone attraction to netrin-1 is converted to repulsion by laminin-1. *Nature*, 401(6748), pp.69–73.
- Hörnberg, H. & Holt, C., 2013. RNA-binding proteins and translational regulation in axons and growth cones. *Frontiers in neuroscience*, 7, p.81. Available at: <http://www.pubmedcentral.nih.gov/articlerender.fcgi?artid=3661996&tool=pmcentrez&rendertype=abstract>.
- Hsieh, J., 2012. Orchestrating transcriptional control of adult neurogenesis. *Genes & Development*, 26, pp.1010–1021.
- Huang, H. et al., 2015. Coordinated interaction of Down syndrome cell adhesion molecule and deleted in colorectal cancer with dynamic TUBB3 mediates Netrin-1-induced axon branching. *Neuroscience*, 293, pp.109–122.
- Huang, J. et al., 2007. Derepression of microRNA-mediated protein translation inhibition by apolipoprotein B mRNA-editing enzyme catalytic polypeptide-like 3G (APOBEC3G) and its family members. *Journal of Biological Chemistry*, 282(46), pp.33632–33640.
- Huber, A.B. et al., 2005. Distinct roles for secreted semaphorin signaling in spinal motor axon guidance. *Neuron*, 48(6), pp.949–64. Available at: <http://www.ncbi.nlm.nih.gov/pubmed/16364899> [Accessed November 10, 2013].
- Hughes, A., 1953. The growth of embryonic neurites; a study of cultures of chick neural tissues. *Journal of anatomy*, 87(2), pp.150–62. Available at: <http://www.pubmedcentral.nih.gov/articlerender.fcgi?artid=1244580&tool=pmcentrez&rendertype=abstract>.
- Humphreys, D.T. et al., 2005. MicroRNAs control translation initiation by inhibiting eukaryotic initiation factor 4E/cap and poly(A) tail function. *Proceedings of the National Academy of Sciences of the United States of America*, 102(47), pp.16961–6. Available at: <http://www.pubmedcentral.nih.gov/articlerender.fcgi?artid=1287990&tool=pmcentrez&rendertype=abstract>.
- Huntzinger, E. & Izaurralde, E., 2011. Gene silencing by microRNAs: contributions of translational repression and mRNA decay. *Nature reviews. Genetics*, 12(2), pp.99–110. Available at:

<http://www.nature.com/pros.lib.unimi.it/nrg/journal/v12/n2/full/nrg2936.html>.

- Hur, E.M., Saijilafu & Zhou, F.Q., 2012. Growing the growth cone: Remodeling the cytoskeleton to promote axon regeneration. *Trends in Neurosciences*, 35(3), pp.164–174.
- Hutson, L.D. et al., 2003. Two Divergent slit1 Genes in Zebrafish. *Developmental Dynamics*, 228(3), pp.358–369.
- Inagaki, N. et al., 2001. CRMP-2 induces axons in cultured hippocampal neurons. *Nature neuroscience*, 4(8), pp.781–782.
- Ingolia, N.T., 2014. Ribosome profiling: new views of translation, from single codons to genome scale. *Nature reviews. Genetics*, 15(3), pp.205–13. Available at: <http://www.ncbi.nlm.nih.gov/pubmed/24468696>.
- Ipsaro, J.J. & Joshua-Tor, L., 2015. From guide to target: molecular insights into eukaryotic RNA-interference machinery. *Nature structural & molecular biology*, 22(1), pp.20–8. Available at: <http://www.ncbi.nlm.nih.gov/pubmed/25565029> <http://www.pubmedcentral.nih.gov/articlerender.fcgi?artid=PMC4450863>.
- Irie, A. et al., 2002. Specific heparan sulfate structures involved in retinal axon targeting. *Development*, 129(1), pp.61–70. Available at: <papers://a160a322-7748-499f-b1e5-c793de7b7813/Paper/p229>.
- Ishii, N. et al., 1992. UNC-6, a laminin-related protein, guides cell and pioneer axon migrations in *C. elegans*. *Neuron*, 9(5), pp.873–881.
- Itoh, A. et al., 1998. Cloning and expressions of three mammalian homologues of *Drosophila* slit suggest possible roles for Slit in the formation and maintenance of the nervous system. *Molecular Brain Research*, 62(2), pp.175–186.
- Iwasaki, S., Kawamata, T. & Tomari, Y., 2009. *Drosophila* Argonaute1 and Argonaute2 Employ Distinct Mechanisms for Translational Repression. *Molecular Cell*, 34(1), pp.58–67.
- Iyer, A.N., Bellon, A. & Baudet, M.-L., 2014. microRNAs in axon guidance. *Frontiers in cellular neuroscience*, 8(March), p.78. Available at: <http://www.pubmedcentral.nih.gov/articlerender.fcgi?artid=3953822&tool=pmcentrez&rendertype=abstract>.
- Jd, M., 2016. Guide for Morpholino Users : Toward Therapeutics. , 3(2).
- Jen, J.C. et al., 2004. Mutations in a human ROBO gene disrupt hindbrain axon pathway crossing and morphogenesis. *Science (New York, N.Y.)*, 304(5676), pp.1509–1513. Available at:

papers3://publication/doi/10.1126/science.1096437.

- Jiang, Y.Q. & Oblinger, M.M., 1992. Differential regulation of beta III and other tubulin genes during peripheral and central neuron development. *Journal of cell science*, 103, pp.643–651.
- Johnston, R.J. & Hobert, O., 2003. A microRNA controlling left/right neuronal asymmetry in *Caenorhabditis elegans*. *Nature*, 426, pp.845–849.
- Jonas, S. & Izaurralde, E., 2013. The role of disordered protein regions in the assembly of decapping complexes and RNP granules. *Genes and Development*, 27(24), pp.2628–2641.
- Jonas, S. & Izaurralde, E., 2015. Towards a molecular understanding of microRNA-mediated gene silencing. *Nature reviews. Genetics*, 16(7), pp.421–433. Available at: http://www.nature.com/nrg/journal/v16/n7/full/nrg3965.html?WT.ec_id=NRG-201507.
- Jung, H. & Holt, C.E., 2011. Local translation of mRNAs in neural development. *Wiley interdisciplinary reviews. RNA*, 2, pp.153–65. Available at: <http://www.pubmedcentral.nih.gov/articlerender.fcgi?artid=3683645&tool=pmcentrez&rendertype=abstract>.
- Jung, H., O'Hare, C.M. & Holt, C.E., 2011. Translational regulation in growth cones. *Current opinion in genetics & development*, 21(4), pp.458–64. Available at: <http://www.pubmedcentral.nih.gov/articlerender.fcgi?artid=3683644&tool=pmcentrez&rendertype=abstract> [Accessed October 7, 2013].
- Jung, H., Yoon, B.C. & Holt, C.E., 2012. Axonal mRNA localization and local protein synthesis in nervous system assembly, maintenance and repair. *Nature reviews. Neuroscience*, 13(5), pp.308–24. Available at: <http://www.pubmedcentral.nih.gov/articlerender.fcgi?artid=3682205&tool=pmcentrez&rendertype=abstract> [Accessed September 22, 2013].
- Kalashnikova, E. et al., 2010. SynDIG1: An Activity-Regulated, AMPA- Receptor-Interacting Transmembrane Protein that Regulates Excitatory Synapse Development. *Neuron*, 65(1), pp.80–93.
- Kania, A. & Klein, R., 2016. Mechanisms of ephrin-Eph signalling in development, physiology and disease. *Nature reviews. Molecular cell biology*, 17(4), pp.240–56.
- Kaplan, B.B. et al., 2013. MicroRNAs in the axon and presynaptic nerve terminal. *Frontiers in cellular neuroscience*, 7(August), p.126. Available at: <http://www.pubmedcentral.nih.gov/articlerender.fcgi?artid=3734361&tool=pmcentrez&rendertype=abstract> [Accessed October 8, 2013].

- Kar, A.N. et al., 2013. Intra-axonal synthesis of eukaryotic translation initiation factors regulates local protein synthesis and axon growth in rat sympathetic neurons. *The Journal of neuroscience: the official journal of the Society for Neuroscience*, 33(17), pp.7165–74. Available at: <http://www.pubmedcentral.nih.gov/articlerender.fcgi?artid=3685850&tool=pmcentrez&rendertype=abstract> [Accessed November 26, 2013].
- Keeble, T.R., 2006. The Wnt Receptor Ryk Is Required for Wnt5a-Mediated Axon Guidance on the Contralateral Side of the Corpus Callosum. *Journal of Neuroscience*, 26(21), pp.5840–5848. Available at: <http://www.jneurosci.org/content/26/21/5840.abstract>.
- Keleman, K. & Dickson, B.J., 2001. Short- and long-range repulsion by the Drosophila Unc5 Netrin receptor. *Neuron*, 32(4), pp.605–617.
- Ketting, R.F. et al., 2001. Dicer functions in RNA interference and in synthesis of small RNA involved in developmental timing in *C. elegans*. *Genes & development*, 15, pp.2654–2659.
- Khodosevich, K. et al., 2007. Gene expression analysis of in vivo fluorescent cells. *PLoS ONE*, 2(11).
- Khvorova, A., Reynolds, A. & Jayasena, S.D., 2003. Functional siRNAs and miRNAs exhibit strand bias. *Cell*, 115(2), pp.209–216.
- Kidd, T., Bland, K.S. & Goodman, C.S., 1999. Slit is the midline repellent for the robo receptor in Drosophila. *Cell*, 96(6), pp.785–794.
- Kim, G.J., Shatz, C.J. & McConnell, S.K., 1991. Morphology of pioneer and follower growth cones in the developing cerebral cortex. *Journal of Neurobiology*, 22(0022–3034), pp.629–642.
- King, H.A. & Gerber, A.P., 2016. Translatome profiling: Methods for genome-scale analysis of mRNA translation. *Briefings in Functional Genomics*, 15(1), pp.22–31.
- Kitsukawa, T. et al., 1997. Neuropilin–Semaphorin III/D-Mediated Chemorepulsive Signals Play a Crucial Role in Peripheral Nerve Projection in Mice. *Neuron*, 19(5), pp.995–1005.
- Klein, R., 2004. Eph/ephrin signaling in morphogenesis, neural development and plasticity. *Current Opinion in Cell Biology*, 16(5), pp.580–589.
- Kloosterman, W.P. et al., 2007. Targeted inhibition of miRNA maturation with morpholinos reveals a role for miR-375 in pancreatic islet development. *PLoS Biology*, 5(8), pp.1738–1749.
- Knight, S.W. & Bass, B.L., 2001. A role for the RNase III enzyme DCR-1 in RNA interference and germ line development in *Caenorhabditis elegans*. *Science (New York, N.Y.)*, 293, pp.2269–2271.
- Koenig, E., 1967. Synthetic Mechanisms in the Axon—Iv. in Vitro Incorporation of [3h]precursors into

- Axonal Protein and Rna *. *Journal of Neurochemistry*, 14(4), pp.437–446. Available at: <http://onlinelibrary.wiley.com/doi/10.1111/j.1471-4159.1967.tb09542.x/abstract%5Cnhttp://files/413/abstract.html>.
- Kok, F.O. et al., 2015. Reverse genetic screening reveals poor correlation between morpholino-induced and mutant phenotypes in zebrafish. *Developmental Cell*, 32(1), pp.97–108. Available at: <http://dx.doi.org/10.1016/j.devcel.2014.11.018>.
- Kolodkin, A.L. & Tessier-Lavigne, M., 2011. Mechanisms and molecules of neuronal wiring: A primer. *Cold Spring Harbor Perspectives in Biology*, 3, pp.1–14.
- Kolodkin, A.L. & Tessier-Lavigne, M., 2011a. Mechanisms and molecules of neuronal wiring: a primer. *Cold Spring Harbor perspectives in biology*, 3(6). Available at: <http://www.pubmedcentral.nih.gov/articlerender.fcgi?artid=3098670&tool=pmcentrez&rendertype=abstract> [Accessed January 24, 2014].
- Kolodkin, A.L. & Tessier-Lavigne, M., 2011b. Mechanisms and molecules of neuronal wiring: a primer. *Cold Spring Harbor perspectives in biology*, 3.
- Kolodziej, P.A. et al., 1996. frazzled Encodes a Drosophila member of the DCC immunoglobulin subfamily and is required for CNS and motor axon guidance. *Cell*, 87(2), pp.197–204.
- Kosik, K.S., 2006. The neuronal microRNA system. *Nature reviews. Neuroscience*, 7(12), pp.911–20. Available at: <http://www.ncbi.nlm.nih.gov/pubmed/17115073> [Accessed May 21, 2013].
- Krichevsky, A.M. et al., 2003. A microRNA array reveals extensive regulation of microRNAs during brain development. *RNA (New York, N.Y.)*, 9, pp.1274–1281.
- Krol, J., Loedige, I. & Filipowicz, W., 2010. The widespread regulation of microRNA biogenesis, function and decay. *Nature reviews. Genetics*, 11(9), pp.597–610. Available at: <http://www.ncbi.nlm.nih.gov/pubmed/20661255> [Accessed October 17, 2013].
- Kube, D.M. et al., 2007. Optimization of laser capture microdissection and RNA amplification for gene expression profiling of prostate cancer. *BMC molecular biology*, 8, p.25.
- Kuwajima, T. et al., 2012. Optic Chiasm Presentation of Semaphorin6D in the Context of Plexin-A1 and Nr-CAM Promotes Retinal Axon Midline Crossing. *Neuron*, 74, pp.676–690.
- Kwok, J.C.F. et al., 2012. Chondroitin sulfates in the developing rat hindbrain confine commissural projections of vestibular nuclear neurons. *Neural development*, 7(1), p.6. Available at: <http://www.pubmedcentral.nih.gov/articlerender.fcgi?artid=3295737&tool=pmcentrez&rendertype=abstract> [Accessed December 15, 2013].

- De La Torre, J. et al., 1997. Turning of retinal growth cones in a netrin-1 gradient mediated by the netrin receptor DCC. *Neuron*, 19(6), pp.1211–1224.
- Lai Wing Sun, K., Correia, J.P. & Kennedy, T.E., 2011. Netrins: versatile extracellular cues with diverse functions. *Development (Cambridge, England)*, 138(11), pp.2153–69. Available at: <http://www.ncbi.nlm.nih.gov/pubmed/21558366>.
- Ledizet, B.M. & Piperno, G., 1991. Detection of Acetylated α -Tubulin by Specific Antibodies. *Methods in Enzymology*, 196(1985), pp.264–274.
- Lee, Y. et al., 2004. MicroRNA genes are transcribed by RNA polymerase II. *The European Molecular Biology Organization Journal*, 23(20), pp.4051–4060. Available at: <http://www.pubmedcentral.nih.gov/articlerender.fcgi?artid=524334&tool=pmcentrez&rendertype=abstract>.
- Lee, Y. et al., 2003. The nuclear RNase III Drosha initiates microRNA processing. *Nature*, 425(6956), pp.415–9. Available at: <http://www.ncbi.nlm.nih.gov/pubmed/14508493>.
- Leung, K.-M. et al., 2006. Asymmetrical beta-actin mRNA translation in growth cones mediates attractive turning to netrin-1. *Nature neuroscience*, 9, pp.1247–1256.
- Leung, L.C. et al., 2013. Coupling of NF-protocadherin signaling to axon guidance by cue-induced translation. *Nature neuroscience*, 16(2), pp.166–73. Available at: <http://www.ncbi.nlm.nih.gov/pubmed/23292679> [Accessed June 19, 2013].
- Lilienbaum, A. et al., 1995. Chimeric integrins expressed in retinal ganglion cells impair process outgrowth in vivo. *Molecular and cellular neurosciences*, 6(2), pp.139–152.
- Lin, D.M. & Goodman, C.S., 1994. Ectopic and increased expression of Fasciclin II alters motoneuron growth cone guidance. *Neuron*, 13(3), pp.507–523.
- Lindahl, U., Kusche-Gullberg, M. & Kjellen, L., 1998. Regulated diversity of heparan sulfate. *Journal of Biological Chemistry*, 273(39), pp.24979–24982.
- Liu, H. et al., 2014. Laser capture microdissection for the investigative pathologist. *Veterinary pathology*, 51(1), pp.257–69. Available at: <http://www.ncbi.nlm.nih.gov/pubmed/24227008>.
- Lohof, A.M. et al., 1992. Asymmetric modulation of cytosolic cAMP activity induces growth cone turning. *The Journal of Neuroscience: The Official Journal of the Society for Neuroscience*, 12(4), pp.1253–1261. Available at: <http://www.ncbi.nlm.nih.gov/pubmed/1372932>.
- López-Bendito, G. et al., 2006. Tangential neuronal migration controls axon guidance: a role for

- neuregulin-1 in thalamocortical axon navigation. *Cell*, 125, pp.127–142.
- Lopresti, V., Macagno, E., & Levinthal, C., 1973. Structure and Development of Neuronal Connections in Isogenic Organisms: Cellular interactions in the development of the optic lamina of *Daphnia*. *Proceedings of the National Academy of Sciences of the United States of America*, 70(1), pp.57–61.
- Lowery, L.A. & Van Vactor, D., 2009. The trip of the tip: understanding the growth cone machinery. *Nature reviews. Molecular cell biology*, 10, pp.332–343.
- Lugli, G. et al., 2005. Dicer and eIF2c are enriched at postsynaptic densities in adult mouse brain and are modified by neuronal activity in a calpain-dependent manner. *Journal of neurochemistry*, 94, pp.896–905.
- Lund, E. et al., 2004. Nuclear export of microRNA precursors. *Science*, 303(5654), pp.95–98. Available at: <http://www.ncbi.nlm.nih.gov/pubmed/14631048>.
- Luo, Y., Raible, D. & Raper, J.A., 1993. Collapsin: A protein in brain that induces the collapse and paralysis of neuronal growth cones. *Cell*, 75(2), pp.217–227.
- Luxey, M. et al., 2013. Eph:ephrin-B1 forward signaling controls fasciculation of sensory and motor axons. *Developmental biology*, 383(2), pp.264–74. Available at: <http://www.ncbi.nlm.nih.gov/pubmed/24056079> [Accessed November 11, 2013].
- Lyuksyutova, A.I. et al., 2003. Anterior-posterior guidance of commissural axons by Wnt-frizzled signaling. *Science*, 302(5652), pp.1984–1988.
- Macrae, I.J. et al., 2006. Structural basis for double-stranded RNA processing by Dicer. *Science (New York, N.Y.)*, 311(5758), pp.195–8. Available at: <http://www.ncbi.nlm.nih.gov/pubmed/16410517>.
- Maeda, N., 2015. Proteoglycans and neuronal migration in the cerebral cortex during development and disease. *Frontiers in neuroscience*, 9, p.98. Available at: <http://www.pubmedcentral.nih.gov/articlerender.fcgi?artid=4369650&tool=pmcentrez&rendertype=abstract>.
- Manitt, C. et al., 2009. Netrin participates in the development of retinotectal synaptic connectivity by modulating axon arborization and synapse formation in the developing brain. *The Journal of neuroscience : the official journal of the Society for Neuroscience*, 29(36), pp.11065–77. Available at: <http://www.jneurosci.org/content/29/36/11065.long>
<http://www.pubmedcentral.nih.gov/articlerender.fcgi?artid=2775133&tool=pmcentrez&rendertype=abstract>.
- Mann, F. et al., 2002. Topographic mapping in dorsoventral axis of the *Xenopus* retinotectal system

- depends on signaling through ephrin-B ligands. *Neuron*, 35(3), pp.461–473.
- Mann, F., Harris, W.A. & Holt, C.E., 2004. New views on retinal axon development: A navigation guide. *International Journal of Developmental Biology*, 48(8–9), pp.957–964.
- Marler, K.J. et al., 2014. BDNF promotes axon branching of retinal ganglion cells via miRNA-132 and p250GAP. *The Journal of neuroscience : the official journal of the Society for Neuroscience*, 34(3), pp.969–79. Available at: <http://www.pubmedcentral.nih.gov/articlerender.fcgi?artid=3891972&tool=pmcentrez&rendertype=abstract>.
- Mathonnet, G. et al., 2007. MicroRNA inhibition of translation initiation in vitro by targeting the cap-binding complex eIF4F. *Science (New York, N.Y.)*, 317(5845), pp.1764–1767. Available at: <http://www.ncbi.nlm.nih.gov/pubmed/17656684> http://www.ncbi.nlm.nih.gov/pubmed/17656684?ordinalpos=1&itool=EntrezSystem2.PEntrez.Pubmed.Pubmed_ResultsPanel.Pubmed_DefaultReportPanel.Pubmed_RVDocSum.
- Matsunaga, M. et al., 1988. Guidance of optic nerve fibres by N-cadherin adhesion molecules. *Nature*, 334(6177), pp.62–64. Available at: <http://www.nature.com/doi/10.1038/334062a0>.
- McFarlane, S., McNeill, L. & Holt, C.E., 1995. FGF signaling and target recognition in the developing xenopus visual system. *Neuron*, 15(5), pp.1017–1028.
- McLaughlin, T. et al., 2003. Bifunctional action of ephrin-B1 as a repellent and attractant to control bidirectional branch extension in dorsal-ventral retinotopic mapping. *Development (Cambridge, England)*, 130(11), pp.2407–2418.
- Meister, G., 2013. Argonaute proteins: functional insights and emerging roles. *Nature reviews. Genetics*, 14(7), pp.447–59. Available at: <http://www.ncbi.nlm.nih.gov/pubmed/23732335> [Accessed January 21, 2014].
- Memczak, S. et al., 2013. Circular RNAs are a large class of animal RNAs with regulatory potency. *Nature*, 495, pp.333–8. Available at: <http://www.ncbi.nlm.nih.gov/pubmed/23446348>.
- Ming, G.L. et al., 1997. cAMP-dependent growth cone guidance by netrin-1. *Neuron*, 19(6), pp.1225–1235.
- Mishima, Y. et al., 2012. Translational inhibition by deadenylation-independent mechanisms is central to microRNA-mediated silencing in zebrafish. *Proceedings of the National Academy of Sciences of the United States of America*, 109(4), pp.1104–9. Available at: <http://www.pnas.org/content/109/4/1104.full>.

- Mitchell, K.J. et al., 1996. Genetic analysis of Netrin genes in *Drosophila*: Netrins guide CNS commissural axons and peripheral motor axons. *Neuron*, 17(2), pp.203–215.
- Molnár, Z. et al., 2012. Mechanisms controlling the guidance of thalamocortical axons through the embryonic forebrain. *The European journal of neuroscience*, 35, pp.1573–85. Available at: <http://www.ncbi.nlm.nih.gov/pubmed/22607003>.
- Muddashetty, R.S. et al., 2011. Reversible inhibition of PSD-95 mRNA translation by miR-125a, FMRP phosphorylation, and mGluR signaling. *Molecular cell*, 42, pp.673–688.
- Nagel, A.N. et al., 2015. Netrin-1 directs dendritic growth and connectivity of vertebrate central neurons in vivo. *Neural development*, 10(1), p.14. Available at: <http://www.neuraldevelopment.com/content/10/1/14>.
- Nakagawa, S. et al., 2000. Ephrin-B regulates the Ipsilateral routing of retinal axons at the optic chiasm. *Neuron*, 25, pp.599–610.
- Nakamoto, M. et al., 1996. Topographically specific effects of ELF-1 on retinal axon guidance in vitro and retinal axon mapping in vivo. *Cell*, 86(5), pp.755–766.
- Natera-Naranjo, O. et al., 2010. Identification and quantitative analyses of microRNAs located in the distal axons of sympathetic neurons. *RNA (New York, N.Y.)*, 16(8), pp.1516–29. Available at: <http://www.pubmedcentral.nih.gov/articlerender.fcgi?artid=2905752&tool=pmcentrez&rendertype=abstract> [Accessed May 24, 2013].
- Nedelec, S. et al., 2012. Concentration-Dependent Requirement for Local Protein Synthesis in Motor Neuron Subtype-Specific Response to Axon Guidance Cues. *Journal of Neuroscience*, 32(4), pp.1496–1506. Available at: <http://www.pubmedcentral.nih.gov/articlerender.fcgi?artid=3561907&tool=pmcentrez&rendertype=abstract>.
- Nieuwkoop P., F.J., 1994. *Normal Table of Xenopus Laevis (Daudin): A Systematical & Chronological Survey of the Development from the Fertilized Egg till the End of Metamorphosis*, Available at: <http://www.xenbase.org/anatomy/alldev.do>.
- Nordlander, R.H., 1987. Axonal growth cones in the developing amphibian spinal cord. *Journal of Comparative Neurology*, 263, pp.485–496.
- Obernosterer, G., Martinez, J. & Alenius, M., 2007. Locked nucleic acid-based in situ detection of microRNAs in mouse tissue sections. *Nature protocols*, 2(6), pp.1508–14. Available at: <http://www.ncbi.nlm.nih.gov/pubmed/17571058>.

- Olsen, P.H. & Ambros, V., 1999. The lin-4 regulatory RNA controls developmental timing in *Caenorhabditis elegans* by blocking LIN-14 protein synthesis after the initiation of translation. *Developmental biology*, 216(2), pp.671–80. Available at: <http://www.ncbi.nlm.nih.gov/pubmed/10642801>.
- Oswald Steward, Levy, B.W., 1982. Preferential localization of polyribosomes under the base of dendritic spines in granule cells of the dentate gyrus. *The Journal of Neuroscience*, 2(3), pp.284–291.
- Ovando-Vázquez, C., Lepe-Soltero, D. & Abreu-Goodger, C., 2016. Improving microRNA target prediction with gene expression profiles. *BMC Genomics*, 17(1), p.364. Available at: <http://bmcgenomics.biomedcentral.com/articles/10.1186/s12864-016-2695-1>.
- Palay, S.L. et al., 1968. THE AXON HILLOCK AND THE INITIAL SEGMENT. *Journal of Cell Biology*, 38, p.193.
- Park, J.-E. et al., 2011. Dicer recognizes the 5' end of RNA for efficient and accurate processing. *Nature*, 475(7355), pp.201–205. Available at: <http://dx.doi.org/10.1038/nature10198>.
- Pasterkamp, R.J., 2012. Getting neural circuits into shape with semaphorins. , 13(September), pp.605–618. Available at: <http://dx.doi.org/10.1038/nrn3302>.
- Petersen, C.P. et al., 2006. Short RNAs repress translation after initiation in mammalian cells. *Molecular Cell*, 21(4), pp.533–542.
- Pfaff, J. et al., 2013. Structural features of Argonaute-GW182 protein interactions. *Proceedings of the National Academy of Sciences of the United States of America*, 110, pp.E3770-9. Available at: <http://www.ncbi.nlm.nih.gov/pubmed/24043833>.
- Pillai, R.S. et al., 2005. *Inhibition of translational initiation by Let-7 MicroRNA in human cells*, Available at: http://www.ncbi.nlm.nih.gov/entrez/query.fcgi?db=pubmed&cmd=Retrieve&dopt=AbstractPlus&list_uids=16081698%5Chttp://www.sciencemag.org/content/309/5740/1573.full.pdf.
- Pinter, R. & Hindges, R., 2010. Perturbations of microRNA function in mouse dicer mutants produce retinal defects and lead to aberrant axon pathfinding at the optic chiasm. *PloS one*, 5(4), p.e10021. Available at: <http://www.pubmedcentral.nih.gov/articlerender.fcgi?artid=2850387&tool=pmcentrez&rendertype=abstract> [Accessed July 12, 2013].
- Piper, M. et al., 2008. NF-Protocadherin and TAF1 Regulate Retinal Axon Initiation and Elongation In Vivo. *Journal of Neuroscience*, 28(1), pp.100–105. Available at: <http://www.jneurosci.org/cgi/doi/10.1523/JNEUROSCI.4490-07.2008>.

- Piper, M. et al., 2006. Signaling mechanisms underlying Slit2-induced collapse of *Xenopus* retinal growth cones. *Neuron*, 49, pp.215–228.
- Pittman, A.J., Law, M.-Y. & Chien, C.-B., 2008. Pathfinding in a large vertebrate axon tract: isotypic interactions guide retinotectal axons at multiple choice points. *Development (Cambridge, England)*, 135(17), pp.2865–71. Available at: <http://www.pubmedcentral.nih.gov/articlerender.fcgi?artid=2562560&tool=pmcentrez&rendertype=abstract> [Accessed November 26, 2013].
- Plachez, C. et al., 2008. Robos are required for the correct targeting of retinal ganglion cell axons in the visual pathway of the brain. *Molecular and cellular neurosciences*, 37(4), pp.719–30. Available at: <http://www.ncbi.nlm.nih.gov/pubmed/18272390> [Accessed January 21, 2014].
- Plump, A.S. et al., 2002. Slit1 and Slit2 cooperate to prevent premature midline crossing of retinal axons in the mouse visual system. *Neuron*, 33, pp.219–232.
- Polleux, F., Morrow, T. & Ghosh, A., 2000. Semaphorin 3A is a chemoattractant for cortical apical dendrites. *Nature*, 404(6778), pp.567–573. Available at: <http://www.ncbi.nlm.nih.gov/pubmed/10766232>.
- Portillo, M. et al., 2009. Isolation of RNA from laser-capture-microdissected giant cells at early differentiation stages suitable for differential transcriptome analysis. *Molecular Plant Pathology*, 10(4), pp.523–535.
- Pratt, T. et al., 2006. Heparan sulphation patterns generated by specific heparan sulfotransferase enzymes direct distinct aspects of retinal axon guidance at the optic chiasm. *The Journal of neuroscience : the official journal of the Society for Neuroscience*, 26(26), pp.6911–23. Available at: <http://www.jneurosci.org/content/26/26/6911.abstract>.
- Qu, C. et al., 2013. Direct binding of TUBB3 with DCC couples netrin-1 signaling to intracellular microtubule dynamics in axon outgrowth and guidance. *Journal of cell science*, 126(Pt 14), pp.3070–81. Available at: <http://www.pubmedcentral.nih.gov/articlerender.fcgi?artid=3711200&tool=pmcentrez&rendertype=abstract>.
- Randlett, O. et al., 2011. The Oriented Emergence of Axons from Retinal Ganglion Cells Is Directed by Laminin Contact In Vivo. *Neuron*, 70(2), pp.266–280.
- Raper, J. & Mason, C., 2010. Cellular strategies of axonal pathfinding. *Cold Spring Harbor perspectives in biology*, 2(9), p.a001933. Available at: <http://www.pubmedcentral.nih.gov/articlerender.fcgi?artid=2926747&tool=pmcentrez&rendertype=abstract>.

abstract [Accessed January 23, 2014].

- Ricci, E.P. et al., 2013. MiRNA repression of translation in vitro takes place during 43S ribosomal scanning. *Nucleic Acids Research*, 41(1), pp.586–598.
- Riehl, R. et al., 1996. Cadherin function is required for axon outgrowth in retinal ganglion cells in vivo. *Neuron*, 17(5), pp.837–848.
- Ringstedt, T. et al., 2000. Slit inhibition of retinal axon growth and its role in retinal axon pathfinding and innervation patterns in the diencephalon. *The Journal of neuroscience : the official journal of the Society for Neuroscience*, 20, pp.4983–4991.
- Rossi, A. et al., 2015. Genetic compensation induced by deleterious mutations but not gene knockdowns. *Nature*, Aug 13(524), pp.230–3. Available at: <http://www.ncbi.nlm.nih.gov/pubmed/26168398>.
- Rothberg, J.M. et al., 1988. slit: An EGF-homologous locus of *D. melanogaster* involved in the development of the embryonic central nervous system. *Cell*, 55(6), pp.1047–1059.
- Sabatier, C. et al., 2004. The divergent robo family protein Rig-1/Robo3 is a negative regulator of slit responsiveness required for midline crossing by commissural axons. *Cell*, 117(2), pp.157–169.
- Salmena, L. et al., 2011. A ceRNA Hypothesis: The Rosetta Stone of a Hidden RNA Language? *Cell*, 146, pp.353–358.
- Sasaki, Y. et al., 2013. Identification of axon-enriched MicroRNAs localized to growth cones of cortical neurons. *Developmental neurobiology*. Available at: <http://www.ncbi.nlm.nih.gov/pubmed/23897634> [Accessed November 19, 2013].
- Schmitt, A.M. et al., 2006. Wnt-Ryk signalling mediates medial-lateral retinotectal topographic mapping. *Nature*, 439(7072), pp.31–37.
- Schmitter, D. et al., 2006. Effects of Dicer and Argonaute down-regulation on mRNA levels in human HEK293 cells. *Nucleic Acids Research*, 34(17), pp.4801–4815.
- Schratt, G.M. et al., 2006. A brain-specific microRNA regulates dendritic spine development. *Nature*, 439(7074), pp.283–9. Available at: <http://www.ncbi.nlm.nih.gov/pubmed/16421561> [Accessed February 2, 2013].
- Schwarz, D.S. et al., 2003. Asymmetry in the assembly of the RNAi enzyme complex. *Cell*, 115(2), pp.199–208.
- Seitz, H., 2009. Redefining MicroRNA Targets. *Current Biology*, 19(10), pp.870–873. Available at: <http://dx.doi.org/10.1016/j.cub.2009.03.059>.

- Selbach, M. et al., 2008. Widespread changes in protein synthesis induced by microRNAs. *Nature*, 455, pp.58–63.
- Sempere, L.F. et al., 2004. Expression profiling of mammalian microRNAs uncovers a subset of brain-expressed microRNAs with possible roles in murine and human neuronal differentiation. *Genome biology*, 5, p.R13.
- Serafini, T. et al., 1994. The netrins define a family of axon outgrowth-promoting proteins homologous to *C. elegans* UNC-6. *Cell*, 78(3), pp.409–424.
- Shaw, G. & Bray, D., 1977. MOVEMENT AND EXTENSION OF ISOLATED GROWTH CONES Fifty years ago Levi examined the consequences of cutting nerve fibres in culture [1]. He worked with pieces of the chick nervous system embedded in plasma clots and found that fibres severed from their . *Experimental Cell Research*, 104.
- Shewan, D. et al., 2002. Age-related changes underlie switch in netrin-1 responsiveness as growth cones advance along visual pathway. *Nature neuroscience*, 5(10), pp.955–62. Available at: <http://www.ncbi.nlm.nih.gov/pubmed/12352982> [Accessed July 12, 2013].
- Shibata, M. et al., 2011. MicroRNA-9 regulates neurogenesis in mouse telencephalon by targeting multiple transcription factors. *The Journal of neuroscience : the official journal of the Society for Neuroscience*, 31, pp.3407–3422.
- Shigeoka, T. et al., 2016. Dynamic Axonal Translation in Developing and Mature Visual Circuits. *Cell*, 166(1), pp.181–192.
- Shirkey, N.J. et al., 2012. Dynamic responses of *Xenopus* retinal ganglion cell axon growth cones to netrin-1 as they innervate their in vivo target. *Developmental Neurobiology*, 72(4), pp.628–648.
- Simonneau, L., Broders, F. & Thiery, J.P., 1992. N-cadherin transcripts in *Xenopus laevis* from early tailbud to tadpole. *Developmental dynamics : an official publication of the American Association of Anatomists*, 194(4), pp.247–60. Available at: <http://www.ncbi.nlm.nih.gov/pubmed/1286211>.
- Smirnova, L. et al., 2005. Regulation of miRNA expression during neural cell specification. *The European journal of neuroscience*, 21, pp.1469–1477.
- Song, H., Ming, G. & Poo, M., 1997. cAMP-induced switching in turning direction of nerve growth cones. *Nature*, 388(July), pp.275–279.
- Stein, E. & Tessier-Lavigne, M., 2001. Hierarchical organization of guidance receptors: silencing of netrin attraction by slit through a Robo/DCC receptor complex. *Science (New York, N.Y.)*, 291(5510), pp.1928–1938. Available at: <http://www.ncbi.nlm.nih.gov/pubmed/11239147>.

- Steward, O. & Ribak, C.E., 1986. Polyribosomes Associated with Synaptic Specializations on Axon Initial Segments : Localization of Protein-Synthetic Machinery at Inhibitory Synapses. *J. Neurosci.*, 6(October), pp.3079–3085.
- Su, J.M.F. et al., 2004. Comparison of ethanol versus formalin fixation on preservation of histology and RNA in laser capture microdissected brain tissues. *Brain pathology (Zurich, Switzerland)*, 14(2), pp.175–182.
- Subtelny, A.O. et al., 2014. Poly(A)-tail profiling reveals an embryonic switch in translational control. *Nature*, 508(7494), pp.66–71. Available at: <http://dx.doi.org/10.1038/nature13007>.
- Sun, K. & Lai, E.C., 2013. Adult-specific functions of animal microRNAs. *Nature reviews. Genetics*, 14(8), pp.535–48. Available at: <http://www.nature.com/doi/10.1038/nrg3471><http://www.ncbi.nlm.nih.gov/pubmed/23817310><http://www.pubmedcentral.nih.gov/articlerender.fcgi?artid=PMC4136762>.
- Suter, D.M. & Forscher, P., 2000. Substrate-cytoskeletal coupling as a mechanism for the regulation of growth cone motility and guidance. *Journal of neurobiology*, 44, pp.97–113. Available at: <http://www.ncbi.nlm.nih.gov/pubmed/10934315>http://www.ncbi.nlm.nih.gov/entrez/query.fcgi?cmd=Retrieve&db=PubMed&dopt=Citation&list_uids=10934315.
- Takagi, S. et al., 1987. Specific cell surface labels in the visual centers of *Xenopus laevis* tadpole identified using monoclonal antibodies. *Developmental Biology*, 122(1), pp.90–100.
- Takagi, S. et al., 1991. The A5 antigen, a candidate for the neuronal recognition molecule, has homologies to complement components and coagulation factors. *Neuron*, 7(2), pp.295–307.
- Takahashi, T. et al., 1998. Semaphorins A and E act as antagonists of neuropilin-1 and agonists of neuropilin-2 receptors. *Nature neuroscience*, 1(6), pp.487–493.
- Takimoto, K., Wakiyama, M. & Yokoyama, S., 2009. Mammalian GW182 contains multiple Argonaute-binding sites and functions in microRNA-mediated translational repression. *RNA (New York, N.Y.)*, 15(6), pp.1078–1089.
- Taliaferro, J.M. et al., 2016. Distal Alternative Last Exons Localize mRNAs to Neural Projections. *Molecular Cell*, 61(6), pp.821–833. Available at: <http://dx.doi.org/10.1016/j.molcel.2016.01.020>.
- Tanaka, E.M. & Kirschner, M.W., 1991. Microtubule behavior in the growth cones of living neurons during axon elongation. *Journal of Cell Biology*, 115(2), pp.345–363.
- Taylor, A.M. et al., 2009. Axonal mRNA in uninjured and regenerating cortical mammalian axons. *The Journal of neuroscience : the official journal of the Society for Neuroscience*, 29, pp.4697–4707.

- Tessier-Lavigne, Marc, G.S.C., 1996. The Molecular Biology of Axon Guidance. *Science*, 274(5290), pp.1123–33. Available at: <http://science.sciencemag.org/content/274/5290/1123.full.pdf+html>.
- Tessier-Lavigne, M. & Goodman, C.S., 1996. The Molecular Biology of Axon Guidance. *Science*, 274, pp.1123–1133.
- Tian, Y. et al., 2014. A Phosphate-Binding Pocket within the Platform-PAZ-Connector Helix Cassette of Human Dicer. *Molecular Cell*, 53(4), pp.606–616.
- Till, S. et al., 2007. A conserved motif in Argonaute-interacting proteins mediates functional interactions through the Argonaute PIWI domain. *Nature structural & molecular biology*, 14(10), pp.897–903.
- Tischfield, M.A. et al., 2010. Human TUBB3 Mutations Perturb Microtubule Dynamics, Kinesin Interactions, and Axon Guidance. *Cell*, 140(1), pp.74–87.
- Trousse, F. et al., 2001. Control of retinal ganglion cell axon growth: a new role for Sonic hedgehog. *Development*, 128(20), pp.3927–3936. Available at: <http://dev.biologists.org.proxy1.cl.msu.edu/content/128/20/3927.full>.
- Tsutsumi, A. et al., 2011. Recognition of the pre-miRNA structure by Drosophila Dicer-1. *Nat Struct Mol Biol*, 18(10), pp.1153–1158. Available at: <http://www.ncbi.nlm.nih.gov/pubmed/21926993>.
- Uchida, Y. et al., 2005. Semaphorin3A signalling is mediated via sequential Cdk5 and GSK3?? phosphorylation of CRMP2: Implication of common phosphorylating mechanism underlying axon guidance and Alzheimer's disease. *Genes to Cells*, 10(2), pp.165–179.
- Vitriol, E.A. & Zheng, J.Q., 2012. Growth Cone Travel in Space and Time: the Cellular Ensemble of Cytoskeleton, Adhesion, and Membrane. *Neuron*, 73, pp.1068–1081.
- Wahle, E. & Winkler, G.S., 2013. RNA decay machines: Deadenylation by the Ccr4-Not and Pan2-Pan3 complexes. *Biochimica et Biophysica Acta - Gene Regulatory Mechanisms*, 1829(6–7), pp.561–570.
- Walz, A. et al., 2002. Chondroitin sulfate disrupts axon pathfinding in the optic tract and alters growth cone dynamics. *Journal of Neurobiology*, 53(3), pp.330–342.
- Wang, B. et al., 2015. FMRP-Mediated Axonal Delivery of miR-181d Regulates Axon Elongation by Locally Targeting Map1b and Calm1. *Cell Reports*, 13, pp.2794–2807. Available at: <http://dx.doi.org/10.1016/j.celrep.2015.11.057>.
- Weiss, R.B. & Atkins, J.F., 2011. Molecular biology. Translation goes global. *Science (New York, N.Y.)*, 334(6062), pp.1509–10. Available at: <http://www.scopus.com/inward/record.url?eid=2-s2.0-83755163021&partnerID=tZOtx3y1>.

- Whitford, K.L. et al., 2002. Regulation of cortical dendrite development by Slit-Robo interactions. *Neuron*, 33(1), pp.47–61.
- Williams, S.E. et al., 2003. Ephrin-B2 and EphB1 mediate retinal axon divergence at the optic chiasm. *Neuron*, 39, pp.919–935.
- Willis, D., 2005. Differential Transport and Local Translation of Cytoskeletal, Injury-Response, and Neurodegeneration Protein mRNAs in Axons. *Journal of Neuroscience*, 25(4), pp.778–791. Available at: <http://www.jneurosci.org/cgi/doi/10.1523/JNEUROSCI.4235-04.2005>.
- Willis, D.E. et al., 2007. Extracellular stimuli specifically regulate localized levels of individual neuronal mRNAs. *Journal of Cell Biology*, 178(6), pp.965–980.
- Winberg, M.L. et al., 1998. Plexin A is a neuronal semaphorin receptor that controls axon guidance. *Cell*, 95(7), pp.903–916.
- Winslow, J.W. et al., 1995. Cloning of AL-1, a ligand for an Eph-related tyrosine kinase receptor involved in axon bundle formation. *Neuron*, 14(5), pp.973–981.
- Wolman, M.A. et al., 2004. Repulsion and attraction of axons by semaphorin3D are mediated by different neuropilins in vivo. *The Journal of neuroscience: the official journal of the Society for Neuroscience*, 24, pp.8428–8435.
- Wu, D. & Murashov, A.K., 2013. MicroRNA-431 regulates axon regeneration in mature sensory neurons by targeting the Wnt antagonist Kremen1. *Frontiers in molecular neuroscience*, 6(October), p.35. Available at: <http://www.pubmedcentral.nih.gov/articlerender.fcgi?artid=3807041&tool=pmcentrez&rendertype=abstract> [Accessed February 9, 2014].
- Wu, K.Y. et al., 2005. Local translation of RhoA regulates growth cone collapse. *Nature*, 436(7053), pp.1020–4. Available at: <http://www.pubmedcentral.nih.gov/articlerender.fcgi?artid=1317112&tool=pmcentrez&rendertype=abstract> [Accessed December 11, 2013].
- Wu, L., Fan, J. & Belasco, J.G., 2006. MicroRNAs direct rapid deadenylation of mRNA. *Proceedings of the National Academy of Sciences of the United States of America*, 103(11), pp.4034–4039.
- Xiang, C.C. et al., 2004. Using DSP, a reversible cross-linker, to fix tissue sections for immunostaining, microdissection and expression profiling. *Nucleic acids research*, 32(22), p.e185. Available at: <http://www.pubmedcentral.nih.gov/articlerender.fcgi?artid=545482&tool=pmcentrez&rendertype=abstract>.

- Xie, M. & Steitz, J.A., 2014. Versatile microRNA biogenesis in animals and their viruses. *RNA biology*, 11(6), pp.673–81. Available at: <http://www.pubmedcentral.nih.gov/articlerender.fcgi?artid=4156499&tool=pmcentrez&rendertype=abstract>.
- Yam, P.T. & Charron, F., 2013. Signaling mechanisms of non-conventional axon guidance cues: The Shh, BMP and Wnt morphogens. *Current Opinion in Neurobiology*, 23(6), pp.965–973.
- Yamaguchi, Y., Mann, D.M. & Ruoslahti, E., 1990. Negative regulation of transforming growth factor-beta by the proteoglycan decorin. *Nature*, 346(6281), pp.281–4. Available at: <http://www.nature.com/nature/journal/v346/n6281/abs/346281a0.html%5Cnhttp://www.ncbi.nlm.nih.gov/pubmed/2374594>.
- Yamauchi, K., Phan, K.D. & Butler, S.J., 2008. BMP type I receptor complexes have distinct activities mediating cell fate and axon guidance decisions. *Development (Cambridge, England)*, 135(6), pp.1119–1128.
- Yang, J.-S. et al., 2010. Conserved vertebrate mir-451 provides a platform for Dicer-independent, Ago2-mediated microRNA biogenesis. *Proceedings of the National Academy of Sciences of the United States of America*, 107, pp.15163–15168.
- Yang, J.S. & Lai, E.C., 2011. Alternative miRNA Biogenesis Pathways and the Interpretation of Core miRNA Pathway Mutants. *Molecular Cell*, 43(6), pp.892–903.
- Yang, L. et al., 2012. Silencing of miRNA-218 promotes migration and invasion of breast cancer via Slit2-Robo1 pathway. *Biomedicine & pharmacotherapy = Biomédecine & pharmacothérapie*, 66(7), pp.535–40. Available at: <http://www.ncbi.nlm.nih.gov/pubmed/22898079> [Accessed December 15, 2013].
- Yao, B. et al., 2011. Mapping of Ago2-GW182 functional interactions. *Methods in Molecular Biology*, 725(3), pp.45–62. Available at: <http://www.springerlink.com/index/10.1007/978-1-61779-046-1%5Cnhttp://www.ncbi.nlm.nih.gov/pubmed/21528446>.
- Yao, J. et al., 2006. An essential role for beta-actin mRNA localization and translation in Ca²⁺-dependent growth cone guidance. *Nature neuroscience*, 9(10), pp.1265–1273.
- Yates, P. a et al., 2001. Topographic-specific axon branching controlled by ephrin-As is the critical event in retinotectal map development. *The Journal of neuroscience : the official journal of the Society for Neuroscience*, 21(21), pp.8548–8563.
- Yi, R. et al., 2003. Exportin-5 mediates the nuclear export of pre-microRNAs and short hairpin RNAs. *Genes and Development*, 17(24), pp.3011–3016.

- Yoon, B.C. et al., 2012. Local translation of extranuclear lamin B promotes axon maintenance. *Cell*, 148(4), pp.752–764. Available at: <http://dx.doi.org/10.1016/j.cell.2011.11.064>.
- Yoshimura, T. et al., 2005. GSK-3 β regulates phosphorylation of CRMP-2 and neuronal polarity. *Cell*, 120(1), pp.137–149.
- Zekri, L., Kuzuoğlu-Öztürk, D. & Izaurralde, E., 2013. GW182 proteins cause PABP dissociation from silenced miRNA targets in the absence of deadenylation. *The EMBO journal*, 32(7), pp.1052–65. Available at: <http://www.pubmedcentral.nih.gov/articlerender.fcgi?artid=3616289&tool=pmcentrez&rendertype=abstract>.
- Zhang, H. et al., 2016. Brain-specific Crmp2 deletion leads to neuronal development deficits and behavioural impairments in mice. *Nature Communications*, 7, p.0. Available at: <http://www.nature.com/ncomms/2016/160601/ncomms11773/full/ncomms11773.html>.
- Zhang, H. et al., 2004. Single processing center models for human Dicer and bacterial RNase III. *Cell*, 118(1), pp.57–68.
- Zhang, Y. et al., 2012. microRNA-320a inhibits tumor invasion by targeting neuropilin 1 and is associated with liver metastasis in colorectal cancer. *Oncology reports*, 27, pp.685–94. Available at: <http://www.ncbi.nlm.nih.gov/pubmed/22134529>.
- Zhang, Y. et al., 2013. The MicroRNA-17-92 cluster enhances axonal outgrowth in embryonic cortical neurons. *The Journal of neuroscience : the official journal of the Society for Neuroscience*, 33(16), pp.6885–94. Available at: <http://www.ncbi.nlm.nih.gov/pubmed/23595747> [Accessed October 8, 2013].
- Zhou, H. et al., 2016. Deregulation of miRNA-181c potentially contributes to the pathogenesis of AD by targeting collapsin response mediator protein 2 in mice. *Journal of the Neurological Sciences*, 367, pp.3–10.
- Zivraj, K.H. et al., 2010. Subcellular profiling reveals distinct and developmentally regulated repertoire of growth cone mRNAs. *The Journal of neuroscience : the official journal of the Society for Neuroscience*, 30(46), pp.15464–78. Available at: <http://www.pubmedcentral.nih.gov/articlerender.fcgi?artid=3683943&tool=pmcentrez&rendertype=abstract> [Accessed October 7, 2013].
- Zou, Y. et al., 2013. Developmental decline in neuronal regeneration by the progressive change of two intrinsic timers. *Science (New York, N.Y.)*, 340, pp.372–6. Available at: <http://www.ncbi.nlm.nih.gov/pubmed/23599497>.

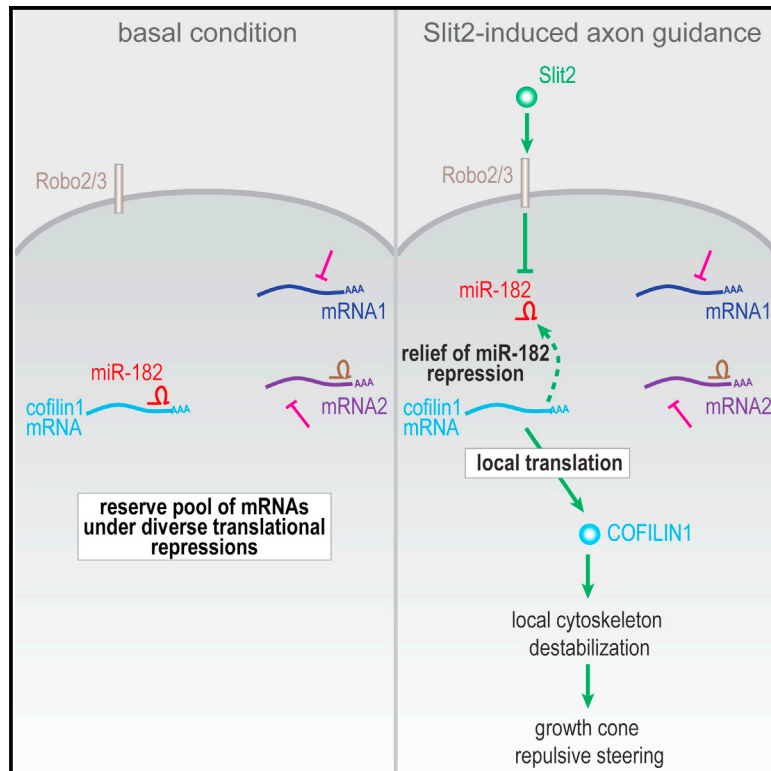
Zou, Y. et al., 2012. The lin-4 microRNA targets the LIN-14 transcription factor to inhibit netrin-mediated axon attraction. *Science signaling*, 5(228), p.ra43. Available at: <http://www.pubmedcentral.nih.gov/articlerender.fcgi?artid=3670680&tool=pmcentrez&rendertype=abstract> [Accessed October 8, 2013].

Annexure

- 1) Article - Bellon A, **Iyer A**, Bridi S, Lee FC, Ovando-Vázquez C, Corradi E, Longhi S, Rocuzzo M, Strohbuecker S, Naik S, Sarkies P, Miska E, Abreu-Goodger C, Holt CE, Baudet ML. miR-182 regulates Slit2-mediated axon guidance by modulating the local translation of a specific mRNA (2017) Cell Reports - Jan 31;18(5):1171-1186. doi: 10.1016/j.celrep.2016.12.093.
- 2) Review- **Iyer, A.N.**, Bellon, A., & Baudet, M.-L. microRNAs in axon guidance. Front Cell Neurosci. 2014 Mar 14;8:78. doi: 10.3389/fncel.2014.00078.

miR-182 Regulates Slit2-Mediated Axon Guidance by Modulating the Local Translation of a Specific mRNA

Graphical Abstract



Authors

Anaïs Bellon, Archana Iyer, Simone Bridi, ..., Ceil Abreu-Goodger, Christine E. Holt, Marie-Laure Baudet

Correspondence

ceh33@cam.ac.uk (C.E.H.), marielaure.baudet@unitn.it (M.-L.B.)

In Brief

Bellon et al. examine how specific mRNAs are selected for cue-induced local protein synthesis during axon guidance and find that miR-182 reversibly regulates the selective translation of a specific transcript to facilitate fast growth cone steering and axon guidance.

Highlights

- Small RNA-seq analysis reveals that miR-182 is the most abundant miRNA in RGC axons
- miR-182 regulates Slit2-mediated axon guidance of RGCs in vitro and in vivo
- miR-182 silences cofilin-1 local protein synthesis in growth cones
- Slit2 rapidly lifts miR-182-mediated repression of cofilin-1 without degrading it

Accession Numbers

GSE86883



miR-182 Regulates Slit2-Mediated Axon Guidance by Modulating the Local Translation of a Specific mRNA

Anaïs Bellon,^{1,5} Archana Iyer,² Simone Bridi,² Flora C.Y. Lee,¹ Cesaré Ovando-Vázquez,³ Eloina Corradi,² Sara Longhi,² Michela Rocuzzo,² Stephanie Strohbuecker,² Sindhu Naik,² Peter Sarkies,^{4,6} Eric Miska,⁴ Cei Abreu-Goodger,³ Christine E. Holt,^{1,*} and Marie-Laure Baudet^{2,7,*}

¹PDN Department, University of Cambridge, Cambridge CB23DY, UK

²CIBIO, University of Trento, Trento 38123, Italy

³Unidad de Genómica Avanzada (Langebio), Cinvestav, Irapuato 36821, Mexico

⁴Gurdon Institute, University of Cambridge, Cambridge CB21QN, UK

⁵Present address: Aix-Marseille Université, CNRS, IBDM UMR 7288, 13288 Marseille, France

⁶Present address: MRC London Institute for Medical Research, Imperial College London, London W120NN, UK

⁷Lead Contact

*Correspondence: ceh33@cam.ac.uk (C.E.H.), marielaure.baudet@unitn.it (M.-L.B.)

<http://dx.doi.org/10.1016/j.celrep.2016.12.093>

SUMMARY

During brain wiring, cue-induced axon behaviors such as directional steering and branching are aided by localized mRNA translation. Different guidance cues elicit translation of subsets of mRNAs that differentially regulate the cytoskeleton, yet little is understood about how specific mRNAs are selected for translation. MicroRNAs (miRNAs) are critical translational regulators that act through a sequence-specific mechanism. Here, we investigate the local role of miRNAs in mRNA-specific translation during pathfinding of *Xenopus laevis* retinal ganglion cell (RGC) axons. Among a rich repertoire of axonal miRNAs, miR-182 is identified as the most abundant. Loss of miR-182 causes RGC axon targeting defects in vivo and impairs Slit2-induced growth cone (GC) repulsion. We find that miR-182 targets cofilin-1 mRNA, silencing its translation, and Slit2 rapidly relieves the repression without causing miR-182 degradation. Our data support a model whereby miR-182 reversibly gates the selection of transcripts for fast translation depending on the extrinsic cue.

INTRODUCTION

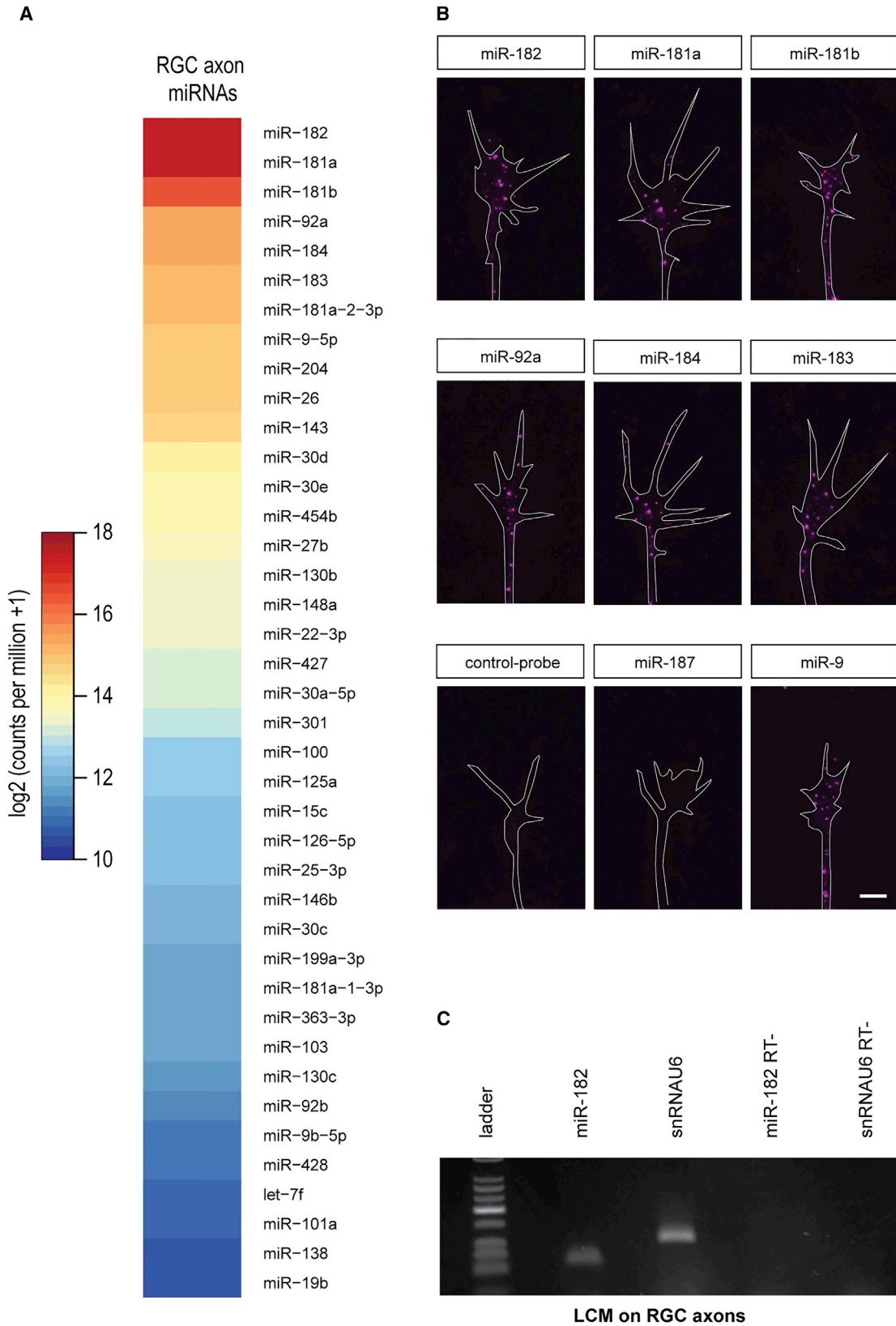
The accurate wiring of the nervous system depends on the ability of axons to extend from neuronal somata to reach their specific synaptic targets during development. Growth cones (GCs) lead growing axons to their correct destinations by responding directionally to attractive and repulsive cues encountered along the pathway (Bouquet and Nothias, 2007). Given the extreme distance that can separate pre- and post-synaptic populations of neurons, axon pathfinding presents a unique challenge for neurons in ensuring that GCs respond properly and rapidly to guidance stimuli. During recent years, it has become clear that axons

and GCs possess a high degree of functional autonomy and that this is aided by local protein synthesis (LPS) (Holt and Schuman, 2013). A complex and changing repertoire of mRNAs is trafficked into growing axons and GCs (Zivraj et al., 2010; Gumy et al., 2011, 2014), where some are locally translated in response to guidance cues independent of cell bodies (Campbell and Holt, 2001; Brittis et al., 2002; Yao et al., 2006; Lin and Holt, 2007). Studies investigating LPS regulation in axons have linked guidance signaling with the regulation of global translational activity in the GC, such as the activation of the initiation factor eIF-4E (eukaryotic initiation factor 4E) (Campbell and Holt, 2001; Piper et al., 2006), or the sequestration of ribosomal components (Tcherkezian et al., 2010). However, evidence points to a selective model of translation whereby specific subsets of mRNAs from a complex mRNA pool (Lin and Holt, 2007; Deglincerti and Jaffrey, 2012) are differentially translated in response to different extrinsic cues while others remain translationally silent. For example, Slit2 and Semaphorin3A (Sema3A) mediate GC repulsion via the translation of cofilin-1 (Cfl1) and RhoA (Piper et al., 2006; Wu et al., 2005), respectively, whereas Netrin-1 and brain-derived neurotrophic factor (BDNF) promote attraction by the local synthesis of β -actin (Leung et al., 2006; Yao et al., 2006). A major unresolved question is how a given transcript is specifically selected for translation in GCs in response to a given guidance cue.

Although extrinsic cues facilitate mRNA-specific translation in GCs through the regulation of RNA-binding protein (RBP)-mediated axonal transport (Vuppalachchi et al., 2009), no mechanisms directly regulating the translation of specific mRNAs in the GC have been identified so far for directional steering. Moreover, given the complex nature of mRNA translation in developing axons (Shigeoka et al., 2013), RBPs alone are unlikely to account fully for the complex regulation of mRNA-specific translation in GCs during guidance, and additional layers of regulation are probably involved.

MicroRNAs (miRNAs) have emerged as key translational regulators possessing mRNA target specificity. miRNAs are first transcribed as long primary molecules, pri-miRNAs, and then processed by Drosha and Dicer to generate mature miRNA





(legend on next page)

molecules (Kim et al., 2009). These non-coding ~21 nt long molecules bind to complementary sequences on mRNAs (Bartel, 2009) and modulate their stability and/or translation (Bazzini et al., 2012; Djuranovic et al., 2012; Eichhorn et al., 2014). Due to the sequence-specific regulation of mRNA translation by miRNAs, one way to control mRNA-specific translation during axon guidance could be regulation by miRNAs. Several lines of evidence suggest that miRNAs are involved in axon guidance and GC steering, but their mechanism of action remains poorly understood (Iyer et al., 2014). First, in mouse, the absence of Dicer induces severe axon pathfinding defects in the visual pathway in vivo (Pinter and Hindges, 2010). Second, in *Xenopus* retinal axons, miR-124 regulates the onset of expression of neuropilin1 (Sema3A receptor) and controls a Sema3A-mediated guidance decision in vivo (Baudet et al., 2011). Finally, miR-134 is required in *Xenopus* spinal neurons for BDNF-induced GC steering in vitro (Han et al., 2011). miRNAs (Hancock et al., 2014; Natera-Naranjo et al., 2010; Sasaki et al., 2014) and the functional RNA-induced silencing complex (RISC) (Hengst et al., 2006) have been shown to reside in developing axons, suggesting that miRNAs may act locally within this neuronal compartment.

Here we have investigated whether miR-182, identified from an axonal profiling screen, can regulate the guidance of *Xenopus* retinal ganglion cell (RGC) axons in the visual pathway by modulating the axonal translation of specific mRNAs. We show that miR-182 depletion causes RGC axon targeting defects in vivo that phenocopy Slit2 knockdown in the brain. In the absence of miR-182, protein synthesis-dependent GC repulsive steering in response to Slit2 is abolished. Furthermore, we demonstrate that miR-182 directly targets Cfl1 mRNA, a key cytoskeleton regulator, and is required for Slit2-induced axonal Cfl1 synthesis. Finally, we show that Slit2 inhibits the activity of miR-182 in GCs, without degrading it. We propose that under basal conditions, axonal miR-182 represses the de novo synthesis of Cfl1 in the GC. Upon Slit2 stimulation, miR-182 is inactivated, temporarily relieving Cfl1 mRNA from its repression and allowing its local translation, which facilitates the cytoskeletal changes that underlie directional steering.

RESULTS

Growing RGC Axons Contain a Rich Repertoire of miRNAs

To characterize the full repertoire of miRNAs in developing RGC axons, we performed an unbiased analysis of miRNAs residing in the axonal compartment using Illumina Next-Generation Sequencing technology. To obtain sufficient axonal material, 1,000 eyes from stage 37/38 (according to Nieuwkoop and Faber, 1994) *Xenopus* larvae were cultured for 48 hr for each experiment. Intact eyes were explanted with the optic nerve exit point (back of

eye) positioned in contact with the culture substrate to facilitate the outgrowth, exclusively, of RGC axons. RGC axons were subsequently harvested from the culture substrate by manual removal of the explanted eyes (Figures S1A and S1B). This approach has been used previously to successfully obtain pure axon material (Yoon et al., 2012). The purity of the axonal material was validated by RT-PCR, which showed the presence of β -actin mRNA, known to be expressed in developing axons (Leung et al., 2006), and the absence of microtubule-associated protein 2 (MAP2) transcript, whose expression is known to be restricted to cell bodies and dendrites (Figure S1C) (Kleiman et al., 1990). Libraries from two biological replicates of 22–30 nt gel-excised small RNAs were sequenced. The two libraries yielded 7.8 and 10.8 million reads and revealed the presence of 148 miRNAs in growing RGC axons, with at least 1 read in both replicates (Figure 1A; Table S1). The two replicates were highly correlated, as judged by the expression level of all miRNAs (Pearson's correlation coefficient = 0.93) (Figure S1D). The most abundant miRNAs detected were miR-182, miR-181a, miR-181b, miR-92a, miR-184, and miR-183, representing 25%, 17.8%, 7.9%, 4.6%, 3.9%, and 3.8%, respectively, of the total miRNAs in developing RGC axons (Figure 1A). In situ hybridization (ISH) experiments were performed to validate the sequencing results. We successfully detected the presence of an ISH signal in cultured RGC axons and GCs for the 15 most abundant sequenced axonal miRNAs, as well as for the brain-specific miRNA miR-9 (Figure 1B) (data not shown). In contrast, no signal was detected when using a control probe or a probe against miR-187, a miRNA not detected in RGC axons by sequencing (Figure 1B).

Analysis of the RNA sequencing (RNA-seq) results identified miR-182 as the most abundant axonal miRNA. Its presence in axons was validated using ISH (as described earlier) (Figure 1B) and qPCR from axons collected by laser capture microdissection (LCM) (Figure 1C). Although miR-182 presence was undetectable in RGC soma through ISH in vivo (Figure S2B), the presence of miR-182 in axons suggests that it is, at least transiently, expressed in the RGC cell body. TaqMan qPCR, a more sensitive detection method, detected miR-182 in RGC soma in vivo, collected by LCM (average Ct: 27.65 ± 1.52 ; positive control U6 small nuclear RNA [snRNA], average Ct: 23.26 ± 0.61) (Figure S1E). In comparison with whole eye, miR-182 showed an average 8.0 ± 2.31 -fold depletion in RGC soma using the $\Delta\Delta$ Ct method, with U6 snRNA as a normalizer. Because eye cells also comprise many non-miR-182-expressing or poorly miR-182-expressing cells, this is a likely underestimation of the extent of miR-182 depletion in RGC soma compared to miR-182-expressing photoreceptor cells.

We next addressed whether miR-182 activity reflects its compartmentalized distribution using a reporter sensor of miRNA activity, similar in design to a previously used construct (De Pietri

Figure 1. miR-182 Is Localized in RGC Axons

(A) Heatmap representing the average expression of mature miRNAs from two axonal small RNA-sequencing (sRNA-seq) libraries prepared from stage 37/38 retinal cultures. The figure is sorted by decreasing axonal average values.

(B) Fluorescent ISH on stage 35/36 RGC GCs cultured in vitro for 24 hr.

(C) TaqMan qPCR performed on RNA extracted from laser-captured stage 37/38 RGC axons. U6 snRNA was used as positive control, because it is found in developing axons (Natera-Naranjo et al., 2010; Zhang et al., 2013; Hancock et al., 2014).

RT–, no template negative control; snRNAU6, U6 snRNA. Scale bar, 5 μ m (B). See also Figure S1 and Table S1.

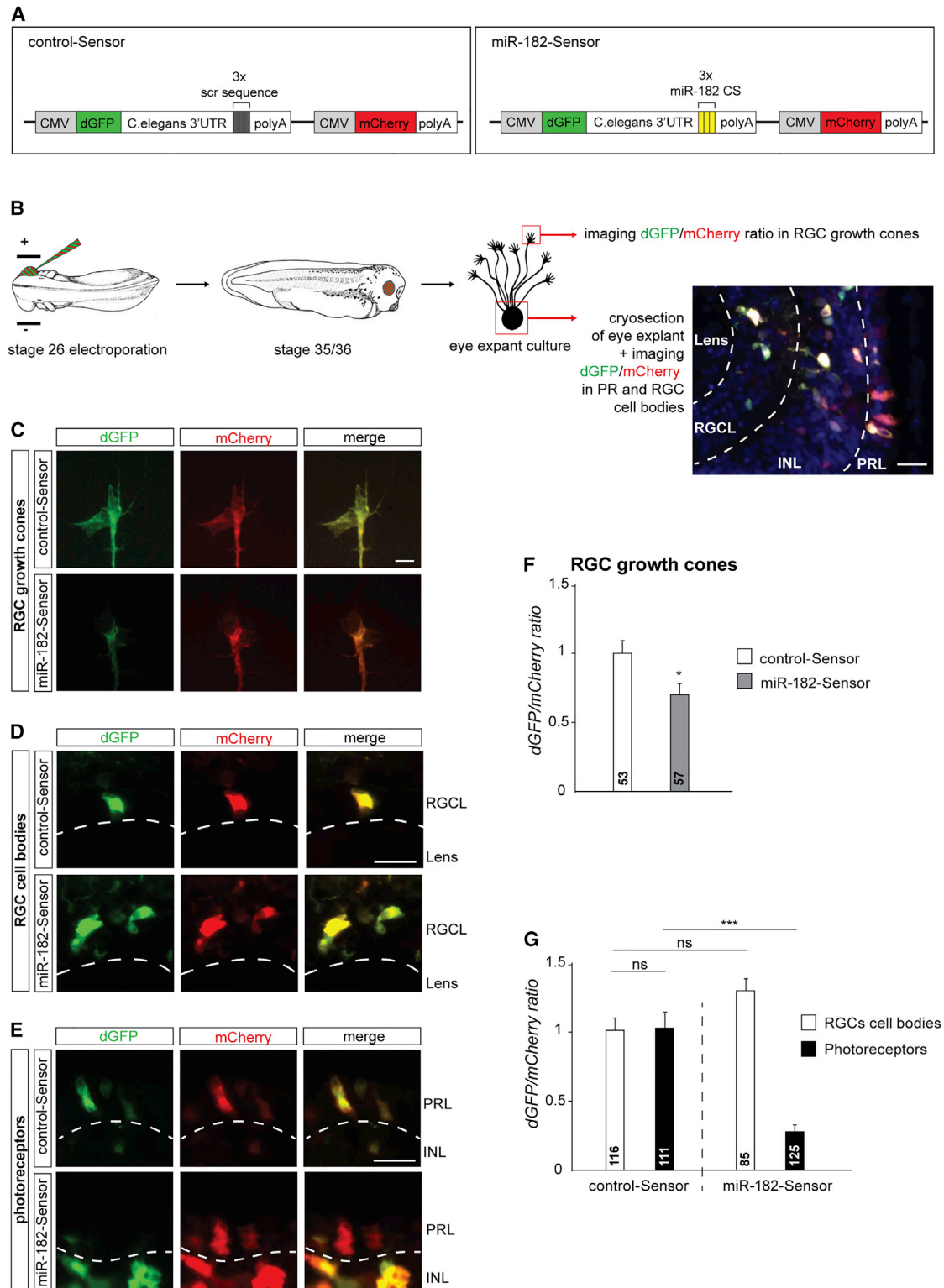


Figure 2. miR-182 Is Active and Enriched in RGC Axons

(A) Sensor construct design.

(B) Schematic representation of the experimental protocol.

(C–E) Illustrative images of RGC GCs (C), RGC soma (D), or PRs (E) following retinal electroporation of control-Sensor or miR-182-Sensor. Clear examples of dGFP/mCherry ratio decrease are shown in (C) and (E).

(legend continued on next page)

Tonelli et al., 2006). miR-182-Sensor expresses destabilized GFP (dGFP) under the regulation of a 3' untranslated region (3' UTR) containing three sequences complementary to miR-182, with mCherry as an internal control (Figure 2A). Any increase in miR-182 activity should lead to the decrease of dGFP while leaving mCherry expression levels unaltered. In control-Sensor, the three sequences complementary to miR-182 are replaced by scrambled sequences. It should thus be inert to change in miR-182 activity.

Sensor sensitivity was first validated in vivo in photoreceptors (PRs), where miR-182 is abundantly expressed (Figure S2B). Electroporation of sensors into stage 26 eyes and comparison of the dGFP/mCherry ratio in stage 41 retinas shows that the dGFP/mCherry ratio from miR-182-Sensor, but not from control-Sensor, is significantly decreased in PRs ($-61\% \pm 0.02\%$) but not in amacrine-like cells ($+1\% \pm 0.07\%$) (Figures S2A and S2C–S2E). This suggests that miR-182-Sensor specifically detects endogenous miR-182 activity in PRs in vivo but not in cells with no or low miR-182 expression.

To explore the compartmentalized action of miR-182 activity, we measured miR-182 activity in retinal explant-derived RGC soma and axons. The evaluation of local regulation of dGFP and mCherry transcripts in axons was possible, because dGFP and mCherry mRNAs are detected in this compartment (Figure S2F). Sensor-electroporated retinas were thus cultured at stage 35/36, and the fluorescence levels of dGFP and mCherry were measured directly in RGC GCs or in RGC soma and PRs of cryosectioned explants (Figure 2B). Quantification reveals that while the dGFP/mCherry ratio of control-Sensor remains unchanged between both cell types and compartments, the ratio of miR-182-Sensor is significantly decreased in RGC axons ($-31\% \pm 8.1\%$) and PRs ($-73.3\% \pm 0.04\%$) but not in RGC soma ($+33.4\% \pm 0.11\%$) (Figures 2C–2G). This indicates that miR-182 is specifically active in the axonal compartment of RGCs but not in the soma.

Altogether, these results confirm the enrichment and activity of miR-182 in RGC axons and GCs and the reliability of our sequencing results.

miR-182 Regulates Axon Targeting in the Optic Tectum In Vivo

To assess whether miR-182 plays a role in RGC axon guidance in vivo, we used a loss-of-function approach in the *Xenopus* visual system using miRNA antisense morpholino oligomers (MOs) and axon tracing. A miR-182 MO blocking the function of endogenous mature *Xenopus laevis* (xla) xla-miR-182 was injected into the dorsal blastomeres of eight-cell-stage embryos (Figure S3A). These two dorsal blastomeres are fated to give rise to the entire CNS; therefore, targeting them for MO delivery induces specific knockdown in the CNS, including the neural retina, at later stages (Leung and Holt, 2008). At stage 37/38, miR-182 morphants show almost no expression of miR-182 in the CNS by ISH. In contrast, control embryos show expression

of miR-182 in the outer retina and different regions of the brain, such as the pineal gland, the otic vesicle, or the olfactory pit areas (Figure S3B), consistent with previously reported expression of miR-182 (Wei et al., 2015). This result indicates that injection of miR-182 MO at the eight-cell stage efficiently knocks down endogenous miR-182 until later developmental stages. No gross morphological defects were observed in miR-182 morphants (Figure S3A). The eye size and the number of RGCs, counted as Islet-1 positive/Sox2 negative cells on cryosections at stage 40 (Baudet et al., 2011), were similar to controls (Figures S3C–S3E). Altogether, these results indicate that the knockdown of miR-182 in the CNS does not affect the gross development of the eye or the maturation of RGCs.

Next, we investigated whether miR-182 is involved in the pathfinding of RGC axons in vivo. During development, pioneering RGC axons exit the eye at stage 28, cross the optic chiasm at stage 32, and grow dorsally to project to their midbrain target, the optic tectum, at stage 37/38. By stage 40, most axons from the central retina have reached their final destination (Holt, 1989). miR-182 morphants and control embryos were raised to stage 40, and RGC axons were anterogradely labeled by lipophilic Dil filling of the eye (Figure 3A). In miR-182 morphant embryos, RGC axons project appropriately through the optic pathway on the contralateral side of the brain (Figure 3A), and no difference in RGC axon length is observed between control and miR-182 MO-injected embryos (Figures 3B, S3F, and S3G). This suggests that miR-182 is not essential for growth and long-range pathfinding of RGC axons to the tectal area. However, immediately after entering the tectum, the trajectories of the RGC axon terminals appear to disperse more widely in miR-182 morphants (Figure 3A, insets) with axons often straying aberrantly toward the dorsal midline. The width of the Dil-labeled RGC axon pathway was measured at regular intervals from the optic chiasm to the tectal posterior boundary. Those intervals were defined by tracing ten concentric circles from the optic chiasm to the posterior boundary of the tectum, and tract widths were measured as the distance between the two outermost axons intersecting each circle. The width was normalized to the size of the brain measured from the optic chiasm to the posterior boundary of the tectum (Figure 3B). Quantification shows that the RGC axon pathway width of morphant embryos is similar to controls in the optic tract but is increased (by up to 35%, $\sim 40 \mu\text{m}$) in the tectal region. This indicates that RGC axons of miR-182 morphants are appropriately bundled along the optic tract but that they project more expansively across the tectum compared to controls (Figure 3B), suggesting that miR-182 is involved in restricting the targeting area of RGC axons within the tectum. Though the described axon defect appears modest in terms of size, in comparison to the size, approximately $150 \mu\text{m}$, of the tectal neuropil at this age, this $40 \mu\text{m}$ expansion of the projection in the target represents a significant change in retinotectal connectivity.

Because the blastomere microinjection approach targets the entire CNS, the axonal phenotype could be attributed to a loss

(F and G) Quantification of the dGFP/mCherry ratio at the RGC GCs, soma, or PRs.

Values are mean \pm SEM. Mann-Whitney test (F) and two-way ANOVA followed by Tukey post hoc test (G), * $p < 0.05$, **** $p < 0.0001$. ns, nonsignificant; CMV, cytomegalovirus promoter; CS, complementary sequence; dGFP, destabilized GFP; INL, inner nuclear layer; PRL, photoreceptor layer; RGCL, retinal ganglion cell layer. Scale bars, $20 \mu\text{m}$ (B, D, and E) and $5 \mu\text{m}$ (C). See also Figure S2.

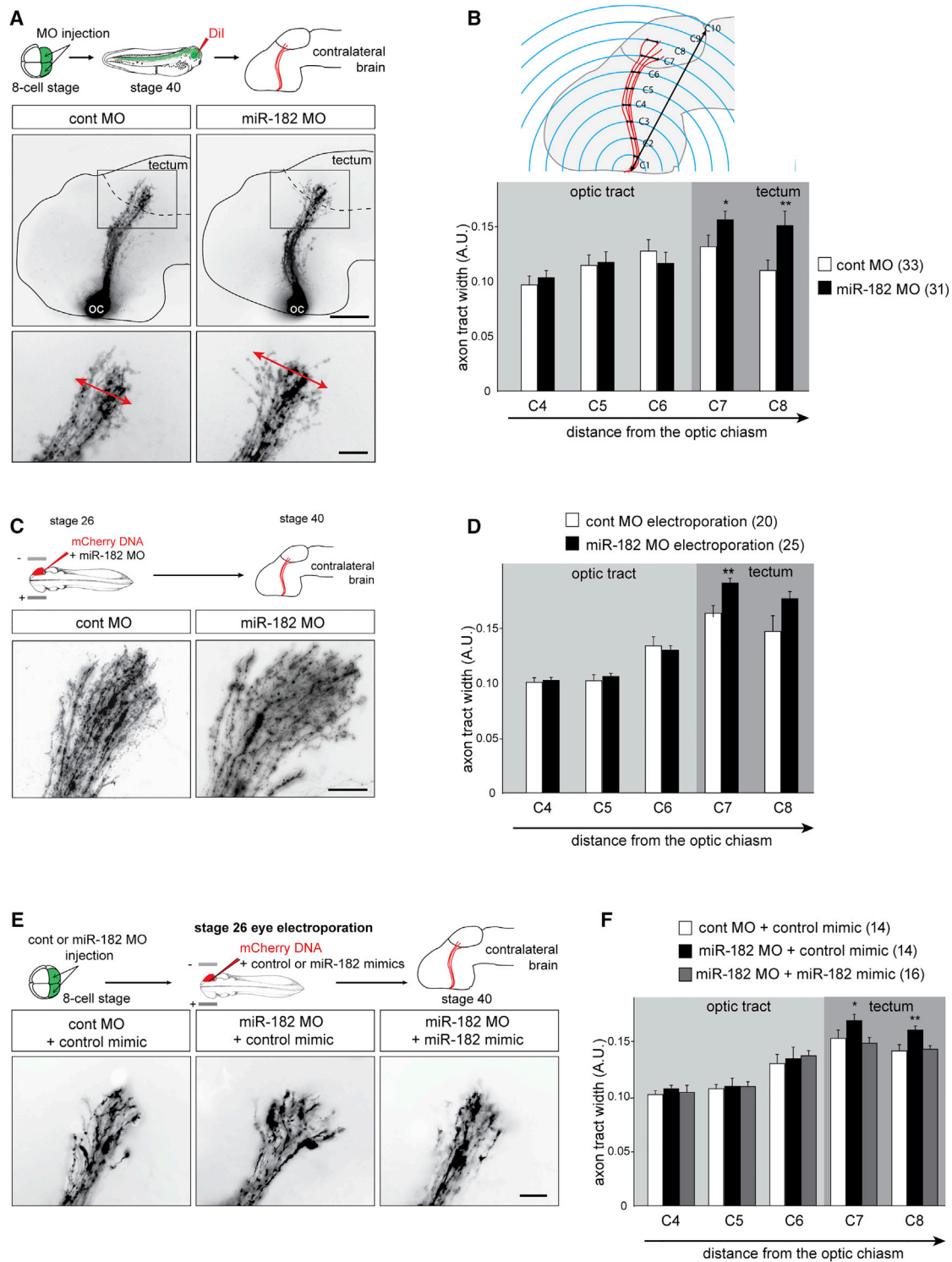


Figure 3. In Vivo, miR-182 Is Involved in RGC Axon Targeting but Not Long-Range Pathfinding

(A, C, and E) Schematic representation of the experimental protocols and representative images of brains, where RGC axons are stained with Dil or expressing mCherry. Arrows delineate the width of the pathway (A).

(B, D, and F) Quantification of pathway width. (B) Schematic representation of the methodology applied for pathway width measurements.

Values are mean \pm SEM. Numbers of brains analyzed are between brackets. Two-way ANOVA followed by Bonferroni post-test, * $p < 0.05$, ** $p < 0.01$. Cont, control; MO, morpholino oligomer; RGC, retinal ganglion cell. Scale bars, 150 μ m (A, top panels) and 50 μ m (A, bottom panel; C; and E). See also Figure S3.

of function of miR-182 in the RGCs (i.e., autonomous) or in the cells forming the pathway substrate in the brain (i.e., non-autonomous), although the latter possibility is rather unlikely due to the absence of miR-182 expression in the midbrain. To formally distinguish between these possibilities, we abolished miR-182 function specifically in retinal cells by electroporating miR-182 MO, plus a mCherry reporter, into stage 26 eye primordia when RGC axonogenesis is just beginning. The phenotype of miR-182 MO eye-electroporated embryos was similar to that of blastomere-injected miR-182 morphants, with both exhibiting an expanded RGC axon targeting area in the tectum (Figures 3C, 3D, and S3H). Finally, to validate the specificity of the miR-182 MO, we performed rescue experiments by electroporating retinal cells of stage 26 morphant embryos with miR-182 mimic or control mimic. The electroporation of miR-182 mimic, but not control mimic, induced a re-expression of miR-182 in retinal cells (Figure S3I) and rescued the guidance phenotype of miR-182-depleted RGC axons in the tectum (Figures 3E and 3F). This confirms that the phenotype observed in miR-182 morphants is due to the specific knockdown of this miRNA in retinal cells. Altogether, these data show that, in vivo, miR-182 acts cell autonomously in RGCs to delimit axons to a restricted area within the tectum.

miR-182 Modulates RGC GC Responsiveness to Slit2

The aberrant expansion of the projection observed in the miR-182 morphant tecta suggests that miR-182 may regulate the responsiveness of RGC axons to tectal repulsive cues that restrict the targeting area. Among multiple cues expressed within the tectum, the repulsive cue Slit2 is known to play a role in confining the growth of axons to specific areas (Erskine et al., 2000; Piper et al., 2006). Therefore, we hypothesized that Slit2 is involved in delimiting the RGC axon-recipient area of the tectum. To test this, we first asked whether loss of Slit2 in the brain causes a phenotype similar to that seen with miR-182 depletion. MO successfully blocked Slit2 translation (Figure S4). To achieve Slit2 knockdown in the brain, but not in the eye, control wild-type eyes were transplanted into Slit2 morphant host embryos at stage 24 and the RGC axon projections were subsequently assessed at stage 40 by Dil anterograde labeling (Figure 4A). In these embryos, RGC axons grow appropriately through the optic tract but project over a larger area in the tectum (Figures 4A and 4B), confirming the function of Slit2 as a target-restricting cue for RGC axons in vivo. This phenotype is similar to miR-182 morphant eye projections (Figure 3), consistent with the possibility that miR-182 interacts with Slit2 signaling in RGC axons. Moreover, covisualization of Slit2 (ISH) and RGC axons (horseradish peroxidase [HRP] anterograde labeling) at stage 40 shows that RGC axons grow closer to the Slit2-expressing tectal territory in miR-182 morphants than in control embryos, with some axons even invading Slit2 domains (Figures 4C and 4D). These results indicate that miR-182-depleted RGC axons fail to respond appropriately to Slit2 in vivo, resulting in targeting defects.

To test whether miR-182 alters axonal Slit2 sensitivity, we used the GC turning assay (Lohof et al., 1992). Stage 35/36 eye explants were cultured for 24 hr, a period that corresponds to the time when the RGC axons are beginning to enter the optic

tectum in vivo (Piper et al., 2006). Turning assays were performed on axons severed from their cell bodies to exclude soma-derived effects. Control RGC axons showed robust repulsive turning from the Slit2 gradient (average turning angle of $-18.7 \pm 5.28^\circ$) (Figures 4E–4G) (Piper et al., 2006). By contrast, miR-182 morphant axons failed to exhibit a turning response to a Slit2 gradient (average turning angle of $+1.91 \pm 3.58^\circ$). These results show that Slit2-induced repulsive turning requires miR-182 activity and that this requirement is local. However, miR-182 morphant axons are still repelled by Sema3A, another guidance cue involved in target restriction in the tectum (Figures S5A–S5C). Thus, axonally localized miR-182 appears to regulate the responsiveness of GCs specifically to Slit2.

miR-182 Regulates Slit2-Induced Cfl1 mRNA Translation

We next examined the mechanisms of action of miR-182 as a modulator of Slit2-induced axon guidance and targeting. Slit2-induced repulsive turning of RGC GCs is reported to be dependent upon LPS (Piper et al., 2006). Given the preceding findings, we reasoned that axonal miR-182 may mediate Slit2 signaling by targeting mRNAs that are locally translated in RGC GCs in response to Slit2.

To gain insight about miR-182 putative targets in axons, we use our recently developed algorithm, TargetExpress (Ovando-Vázquez et al., 2016). We identified 1,064 potential miR-182 targets expressed in *Xenopus* RGC growth cones (Zivraj et al., 2010) (see Supplemental Experimental Procedures for details). Pyruvate dehydrogenase kinase 4, a metabolic enzyme with no known activity in axons and no known link to Slit2, has the highest probability and Cfl1 has the second-highest probability of miR-182 targeting (Figure 5A; Table S2). The 3' UTR of Cfl1 mRNA is predicted to contain one highly conserved miR-182 8-mer binding site (Figure 5B). Slit2 induces the local synthesis of Cfl1, a regulator of actin cytoskeleton dynamics, in GCs, and this is known to mediate RGC GCs' repulsive responses to Slit2 (Piper et al., 2006). We thus hypothesized that miR-182 modulates GC responsiveness to Slit2 by locally silencing Cfl1 mRNA translation.

To assess this, we first validated that *Xenopus laevis* Cfl1-3' UTR is a bona fide target of miR-182 through a dual Renilla: Firefly luciferase reporter assay in HEK293T cells. Cfl1-3' UTR was subcloned downstream of Renilla luciferase (Figure 5C). With this dual luciferase construct, the expression and activity of the Renilla luciferase depends on Cfl1-3' UTR regulation, whereas the Firefly luciferase activity is independent. The dual luciferase reporter was transfected into HEK293T cells, along with miR-182 or control mimic, and the activity of both luciferases was measured. The expression of miR-182, but not the control mimic, induced a significant decrease in the Renilla/Firefly activity ratio ($-28.8\% \pm 2.7\%$) (Figure 5D). However, the control miR-182 mimic had no significant effect on the Renilla/Firefly activity ratio when the predicted miR-182 site of Cfl1-3' UTR was mutated (Figures 5B–5D). This assay showed that *Xenopus laevis* Cfl1 mRNA is directly targeted and silenced by miR-182 through its predicted binding site.

We next determined whether miR-182 directly regulates Cfl1 expression levels in RGC GCs. As a first approach, we measured

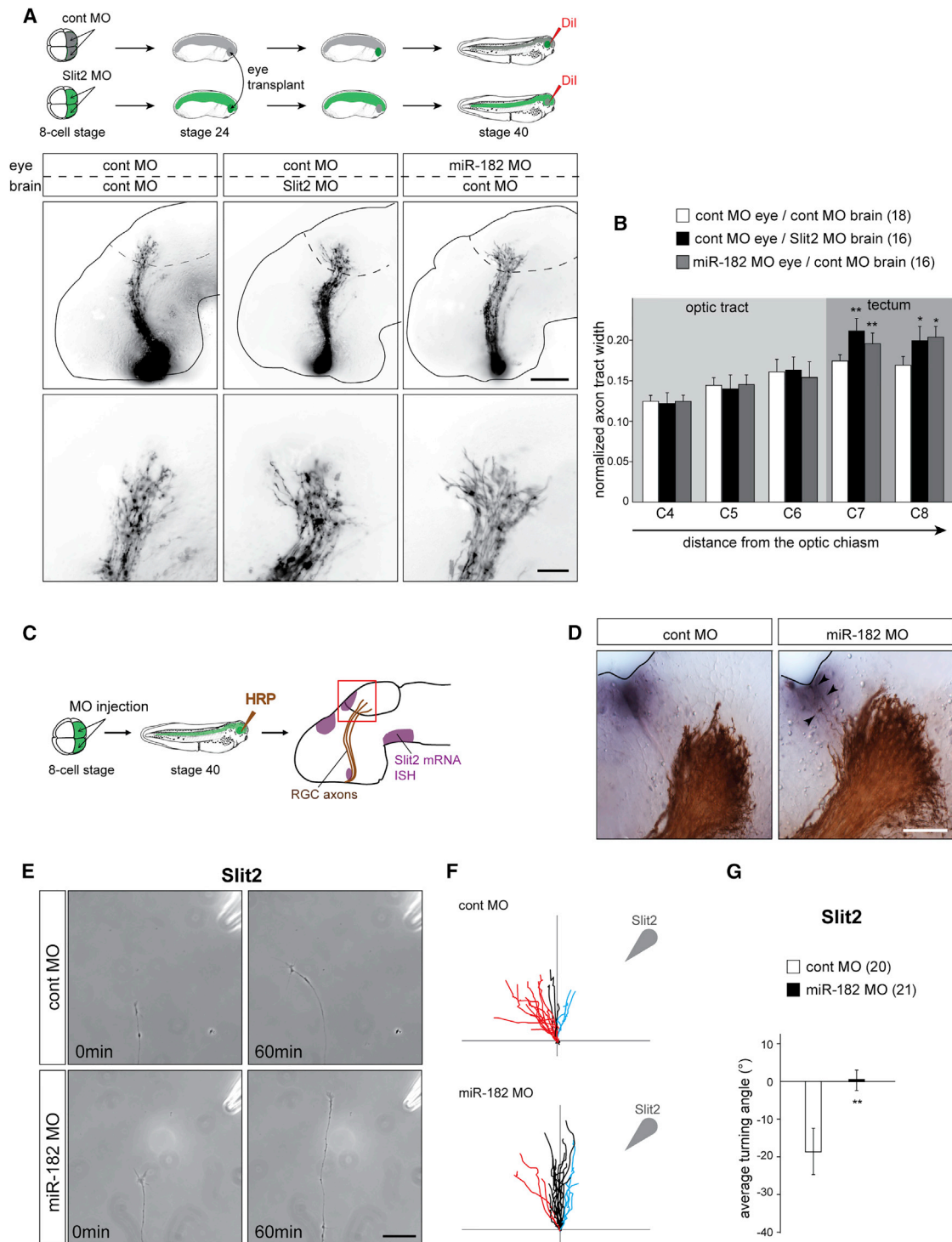


Figure 4. miR-182 Is Involved in Slit2-Driven RGC Axon Guidance and Targeting In Vivo and In Vitro

(A) Schematic representation of the experimental protocol and representative images of brains, where RGC axons are stained with Dil.

(B) Quantification of pathway width. Numbers of brains analyzed are between brackets.

(C and D) Schematic representation of the experimental protocols (C) and representative images (D) of brains, where RGC axons are stained with HRP and Slit2 mRNAs are revealed by ISH.

(E–G) In vitro turning assay on stage 35/36 RGC axons cultured for 24 hr and isolated from their cell bodies. (E) Representative images of control of miR-182 morphant RGC GC before and 60 min after being exposed to a gradient of Slit2 established from a pipette (top right corner) set at 45° angle from the initial (legend continued on next page)

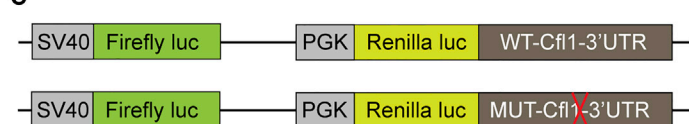
A

Symbol	Description	XenbaseID	Function	Average Axonal Expression	TargetScan ContextScore	TargetExpress Score
pdk4	pyruvate dehydrogenase kinase 4	XB-GENE-866081	dehydrogenase kinase	5,34	-0,687	16,48
cfl1	cofilin 1 (non-muscle)	XB-GENE-1016488	actin depolymerizing factor	5,19	-0,577	16,24
actr2	ARP2 actin-related protein 2 homolog	XB-GENE-17346170	cytoskeletal protein binding	5,49	-0,452	16,17
rgs19	regulator of G-protein signaling 19	XB-GENE-5736067	NA	5,07	-0,633	16,15

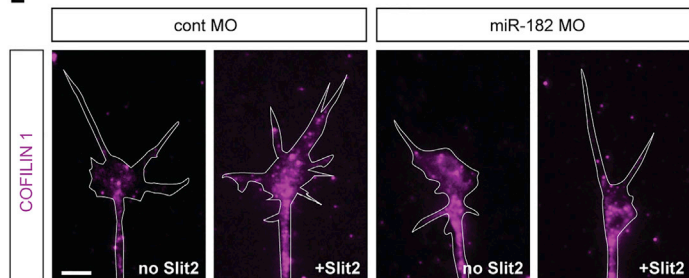
B

3' UCACACUCAAGAUGGUACGGUUU 5' Xla-miR-182
X laevis 5' - CUCAGAUUUGAGUUAUUUUGCCAAAUAUCUUCUGGC -3'
Human GCAAUCCCUUCACCCCAGUUGCCAAAACAGACCCCCCA
M musculus GCUAUCCCUUCACCCCAGUUGCCAAAACAUCUUCUCCCA
X laevis MUT CUCAGAUUUGAGUUAUUUUCGGAUUUAUCUUCUGGC

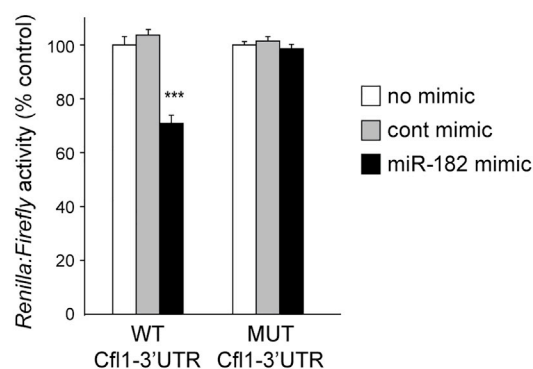
C



E



D



F

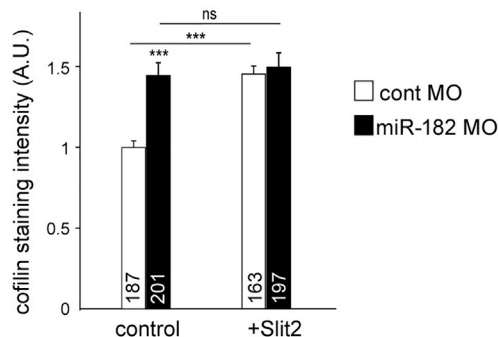


Figure 5. miR-182 Targets Cfl1 mRNA and Regulates Its Expression in RGC Axons

(A) Top predicted miR-182 targets expressed in *Xenopus laevis* growth cones.

(B) Sequence alignment of the 3' UTR of Cfl1. The predicted miR-182 binding site is highlighted in red.

(C) Schematic representation of *Xenopus* Cfl1-3' UTR, subcloned downstream of a dual Renilla:Firefly luciferase reporter.

(D) Quantification of reporter activity in HEK293T cells.

(E and F) Representative images (E) and quantification (F) of Cfl1 immunostaining. White lines delineate RGC growth cones. Bath application of Slit2 was used at a suboptimal concentration to avoid collapse.

Values are mean \pm SEM (D and F). Numbers of GCs analyzed are indicated in bars (F). ANOVA followed by Bonferroni post-test, *** $p < 0.001$. ns, nonsignificant; cfl1, Cfl1; cont, control; MO, morpholino oligomer; MUT, mutated; WT, wild-type. Scale bar, 5 μ m (E). See also Table S2.

by quantitative immunostaining the expression level of Cfl1 protein in RGC GCs of control or miR-182 morphants (Figures 5E and 5F). Under basal conditions, Cfl1 expression is significantly increased in miR-182 morphant GCs (+45% \pm 7%), indicating

that miR-182 represses Cfl1 mRNA in the absence of a stimulus, maintaining a dormant state. After stimulation by Slit2, Cfl1 levels significantly increase (+45.7% \pm 5%) in control RGC GCs, as previously reported (Piper et al., 2006). In contrast, in the

direction of growth. (F) Tracings of RGC axons are analyzed. The source of the guidance cue is indicated by the arrowhead. Red, black, and blue traces represent, respectively, repulsive behaviors (angle $< -5^\circ$), nonsignificant changes in the direction of growth ($-5^\circ < \text{angle} < 5^\circ$), and attractive turning (angle $> 5^\circ$). (G) Quantification of the average turning angle. Numbers of GCs analyzed are between brackets.

Values are mean \pm SEM (B and G). Two-way ANOVA followed by Bonferroni post-test (B) or Mann-Whitney test (G), * $p < 0.05$, ** $p < 0.01$. Cont, control; HRP, horseradish peroxidase; ISH, in situ hybridization; MO, morpholino oligomer; RGC, retinal ganglion cell. Scale bars, 150 μ m (A, top panels), 50 μ m (A, bottom panel, and D), and 30 μ m (E). See also Figures S4 and S5.

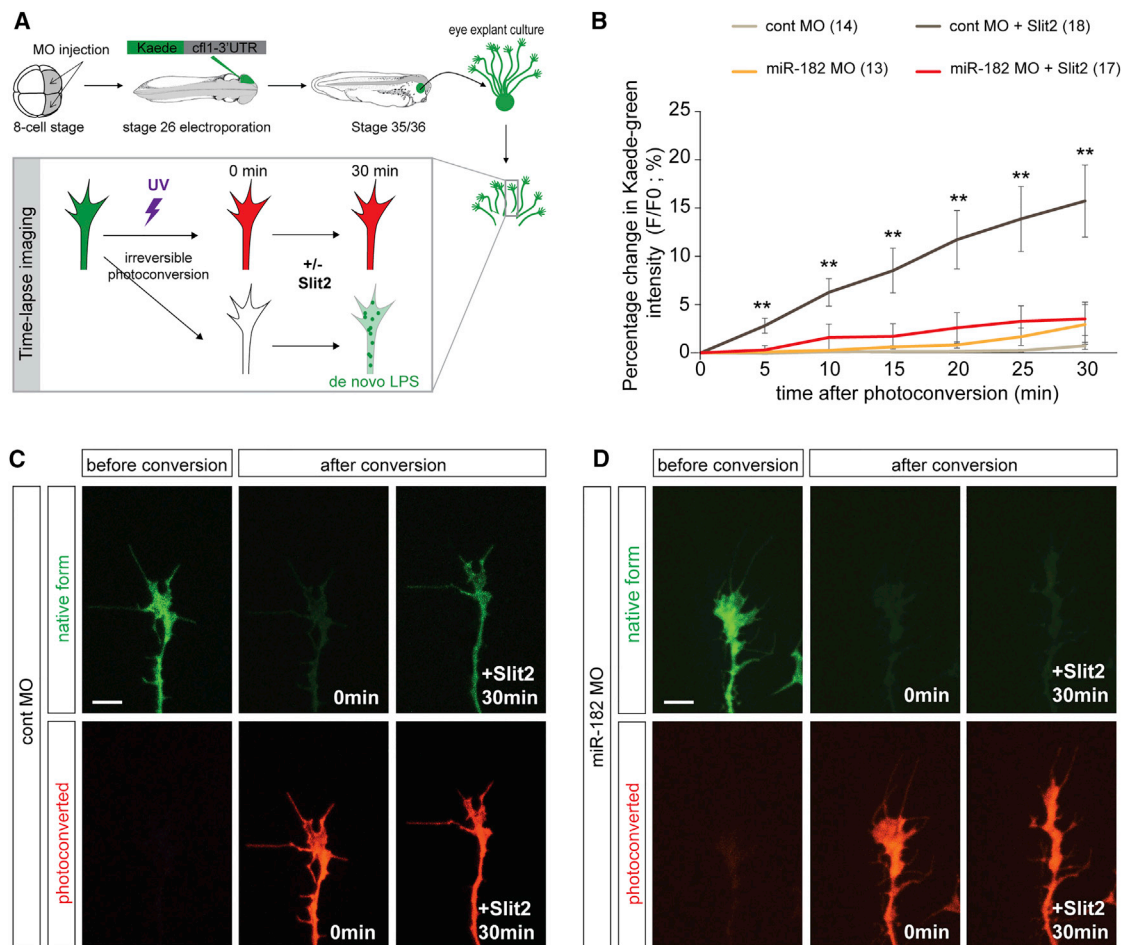


Figure 6. miR-182 Is Required for Slit2-Induced Local Translation of Cfl1 in RGCs

(A) Schematic representation of the experimental protocol. After 24 hr, RGC axons were isolated from their cell bodies. Bath application of Slit2 at a suboptimal concentration was used to avoid collapse. Vehicle was used as control. Recovery of the newly synthesized Kaede green protein was monitored over time.

(B) Quantification of the recovery of Kaede green signal. Data are presented as the percentage change of the fluorescence intensity (F) over time. Numbers of GCs analyzed are indicated in the legend of the graph.

(C and D) Representative pre- and post-photoconversion images of severed control (C) or miR-182 morphant (D) axons.

Values are mean \pm SEM (B). Kruskal-Wallis test, * $p < 0.05$, ** $p < 0.01$. Scale bars, 10 μ m (C and D). Cont, control; LPS, local protein synthesis; MO, morpholino oligomer. See also Figure S6.

absence of miR-182, Slit2 stimulation does not induce any further increase of Cfl1 protein level in RGC GCs (Figures 5E and 5F). Our results thus further indicate that miR-182 is required to mediate a Slit2-induced increase of Cfl1 expression in the GC.

The increase of Cfl1 protein in the GC after Slit2 stimulation is consistent with de novo protein synthesis of Cfl1 in GCs. Alternatively, it may be due to increased transport of preexisting proteins from the axonal shaft. To distinguish between these possibilities, we tested directly whether miR-182 modulates Slit2-induced local de novo protein synthesis of Cfl1. To do so, a Kaede protein-based translation reporter (Leung and Holt, 2008) was generated to visualize live Cfl1 de novo protein synthesis in isolated GCs after Slit2 stimulation in vitro. The green fluorescence of native Kaede can be proteolytically and irreversibly photoconverted to red by UV illumination, and subsequent recovery of a green signal enables the detection of newly synthe-

sized protein versus pre-existing protein. Because the miR-182 binding site is located in the Cfl1-3' UTR, we made a reporter construct with the Kaede sequence linked to the 3' UTR of Cfl1 mRNA (Kaede-Cfl1-3' UTR). The Kaede-Cfl1-3' UTR reporter construct was electroporated into the eye primordia of control or miR-182 morphant embryos at stage 26, and 12 hr later, eyes were explanted and grown for 24 hr in culture. To verify that the reappearance of the green signal was due to LPS specifically within the GC and not to transport from the cell body, axons were isolated from their cell bodies (Figure 6A). Under basal conditions, miR-182 morphant GCs exhibited a significantly higher basal level of Kaede fluorescence (+29% \pm 9%) (Figure S6), consistent with our finding that miR-182 silences Cfl1 mRNA (Figure 5). For the green/red ratio comparative analysis, the intensity of the Kaede green signal was normalized to its intensity before photoconversion. In control GCs, the Kaede green signal

reappears progressively after Slit2 stimulation ($15.7\% \pm 3.7\%$, at 30 min), while no significant recovery is seen without stimulation ($0.7\% \pm 0.3\%$, at 30 min). This confirms that Slit2 induces Cfl1 local translation directly in RGC GCs. In contrast, in the absence of axonal miR-182, no significant reappearance of the Kaede green signal is observed during the 30 min of imaging with or without stimulation by Slit2 (Figures 6B–6D), indicating that miR-182 is required to mediate Slit2-induced LPS of Cfl1 in RGC GCs in vitro.

Collectively, these results show that miR-182 modulates Cfl1 translation in RGC axons by both silencing Cfl1 mRNA under basal conditions and enabling its translation upon Slit2 stimulation.

Slit2 Modulates miR-182 Activity in RGC GCs

The finding that miR-182 is a critical factor in Slit2 signaling pathway in the GC points to the possibility that Slit2 modulates miR-182 function in this neuronal compartment. To test whether Slit2 stimulation alters miR-182 activity directly in GCs, we electroporated the miR-182-Sensor or control-Sensor into eyes and made eye explant cultures (Figure 7A). Slit2 was bath applied to these cultures at a concentration determined to induce a protein synthesis-dependent response (Figure S7A). The fluorescence levels of dGFP and mCherry in RGC GCs were then measured. As expected, no change was detected in the dGFP/mCherry fluorescence ratio upon Slit2 stimulation in control-Sensor-expressing axons ($+15\% \pm 10.5\%$) (Figures S7C and S7D). By contrast, a significant increase in the dGFP/mCherry ratio ($+37.4\% \pm 10.8\%$) occurred upon Slit2 stimulation in the miR-182-Sensor-expressing axons (Figures 7B and 7C). Expression of the miR-182-Sensor or the control-Sensor did not affect Slit2-induced GC collapse, because the presence of either sensor does not alter GC responsiveness to Slit2 (Figure S7B). We further investigated whether and which Slit2 receptor variants, Robos, are putatively involved in Slit2-mediated miR-182 regulation. Robo2 and Robo3, but not Robo1, are expressed in *Xenopus* RGCs (Hocking et al., 2010; Piper et al., 2006). *Xenopus* Robo2 and Robo3 are, respectively, highly and poorly conserved with their rodent counterparts. While mammalian Robo3 silences Slit repulsion, non-mammalian Robo3 mediates it (Zelina et al., 2014). Using an experimental paradigm similar to that used earlier, we coelectroporated miR-182-Sensor with dominant-negative rat Robo2 (dnRobo2) and dominant-negative *Xenopus* Robo3 (dnRobo3) expression plasmids (Figure 7D). Dominant negatives have been previously used to assess the role of Robo signaling in axon guidance, including in *Xenopus* (Hocking et al., 2010). Fluorescence analysis shows that the dGFP/mCherry ratio is decreased in growth cones stimulated with Slit2 when dnRobo2/3 was electroporated compared to control (Figure 7E). Altogether, these data reveal that miR-182 is active and represses Cfl1 translation in the axonal compartment under basal conditions and that Slit2, via Robo2 and Robo3, inhibits its repressive activity in RGC GCs.

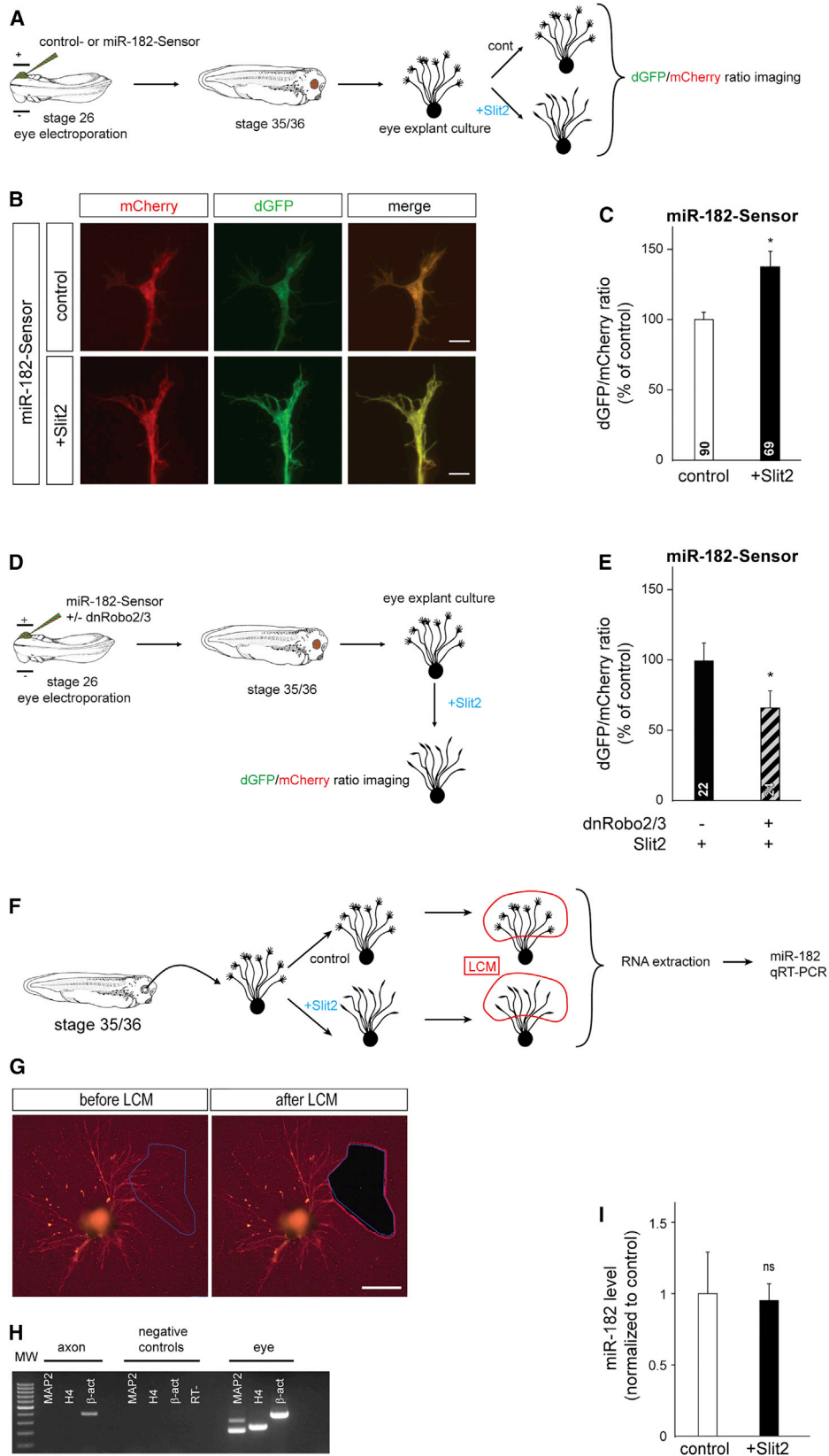
A common mechanism to modulate the activity of miRNAs is the regulation of their turnover or decay (Rüegger and Großhans, 2012). The Slit2-induced decrease in miR-182 activity in RGC GCs could thus arise due to the degradation of miR-182; alternatively, miR-182 could remain intact but be sequestered from its

targets. To examine this, we asked whether miRNA levels changed in GCs following Slit2 stimulation by performing qRT-PCR for miR-182 on RGC axons. RGC axons were collected by LCM to avoid cell body contamination (Figures 7F and 7G), and the purity of the axonal material was confirmed by the presence of β -actin and the absence of dendritic marker MAP2 and nuclear marker histone H4 mRNA (Figure 7H). miR-182 levels were unaltered in Slit2-treated axons compared to controls, indicating that miR-182 is not degraded upon Slit2 signaling ($-4.7\% \pm 10.9\%$) (Figure 7I). These results indicate that Slit2 triggers miR-182 inactivation in RGC GCs without causing its degradation and point toward the possibility of a reversible inactivation and activation mechanism.

DISCUSSION

During development, navigating GCs contain a rich transcriptome. Some of these transcripts are selected for translation to mediate cue-induced GC steering. However, the regulatory mechanisms conferring specificity of translation have remained largely elusive. We have addressed here whether miRNAs could contribute to the selection of specific transcripts for LPS in axon guidance. We show that elongating *Xenopus* RGC axons have a specific population of miRNAs and that miR-182 is enriched in this neuronal compartment. Our data show that miR-182 acts to modulate GC responsiveness to Slit2 in vitro and in vivo specifically within the tectum, where it plays a role in restricting axons to the appropriate target area. miR-182 does so, at least partly, by repressing the axonal translation of Cfl1, a key mediator of Slit2-induced GC repulsion. Slit2, in turn, triggers both a loss of activity of this miRNA, without leading to its degradation, and a concomitant rise in Cfl1 LPS. Collectively, these results indicate that the axon-enriched miR-182 is a key modulator of Slit2-mediated LPS during guidance.

To understand whether miRNAs could act as specific regulators of the axonal transcriptome, Next-Generation Sequencing-based profiling was first performed. Such a high-throughput unbiased approach has not been previously reported for axons. This revealed a complex repertoire of miRNAs within axons and GCs. Previous studies have documented not only the presence but also the enrichment and depletion of miRNAs in this neuronal compartment during development in various systems and organisms (Hancock et al., 2014; Natera-Naranjo et al., 2010; Sasaki et al., 2014), but the nature and abundance of miRNAs vary broadly among these studies, including ours. The differences could be attributed to variations in the types of cultures or methodologies or to bona fide biological differences. In support of this latter possibility, neurons of distinct types and stages express varied pools of axonal transcripts (Gumy et al., 2011; Zivraj et al., 2010). Some commonalities also appear. Rat superior cervical ganglia (Natera-Naranjo et al., 2010) and mouse cortical neurons (Sasaki et al., 2014) contain similar numbers of axonal miRNAs. In addition, miR-182 is enriched in mouse dorsal root ganglia distal axons (Hancock et al., 2014), and these cells respond to Slit2 (Nguyen-Ba-Charvet et al., 2001). This suggests that this miRNA might affect the axonal development in projection neurons regardless of cell type and species. It further indicates that miR-182 might have a conserved role in modulating



(legend on next page)

cue-mediated axon guidance. Overall, it is tempting to speculate that each axon expresses a unique transcriptome and matching miRNome, depending on the cellular requirements at a given time of development, and that a limited set of conserved mRNA-miRNA pairs regulates key GC behaviors.

A key question is whether miR-182 acts locally to regulate protein synthesis. Evidence presented here indicates that miR-182 represses Slit2-induced Cfl1 protein synthesis specifically at the GC. First, miR-182 is present, abundant, and active in RGC axons and GCs, as shown by small RNA sequencing analysis, TaqMan PCR, in situ hybridization, and miRNA-Sensor-based detection approaches in unstimulated cultures. Its absence in RGC bodies by in situ analysis, together with its depletion in RGC bodies compared to other retinal cells revealed by TaqMan qPCR and the lack of miR-182-Sensor activity in RGC soma, further suggests that this miRNA is enriched in axons and GCs. miR-182 is thus likely to exclusively act in this compartment. Second, translational repression of Cfl1 by miR-182 appears to occur within GCs. In miR-182 morphants, Cfl1 protein immunoreactivity is increased specifically in this compartment, as detected by quantitative immunofluorescence. In addition, Cfl1-3' UTR-driven expression of Kaede protein is higher in morphant GCs. The possibility that miRNAs regulate local translation was shown previously but not in the context of axon guidance. Several reports have documented that axonal miRNAs control levels of axonal protein (Aschrafi et al., 2008; Dajas-Bailador et al., 2012; Hancock et al., 2014; Kar et al., 2013; Wang et al., 2015; Zhang et al., 2013), including by modulating LPS of axonal transcript (Hancock et al., 2014; Wang et al., 2015). These previous reports were conducted in neuronal culture to investigate miRNA-regulated axon outgrowth. This study reveals that a miRNA modulates cue-induced LPS to promote GC steering during axon guidance. Along with the present dataset, these findings highlight the importance of miRNAs, as a class of molecule, in local regulation of translation within developing axons. What might be the added value for the GC of this miRNA-mediated LPS regulation? miRNAs could uniquely control the specificity of mRNA translation and contribute to selecting only a limited set of axonal targets for translation from the numerous pool of mRNAs present at the GC. In addition, miRNAs could limit, or avoid, unwanted expression of their mRNA targets outside the subregion of the GC close to cue exposure, thus enhancing precise spatial control of LPS. Finally, because miRNA action can be modulated, miRNAs may constitute an additional layer of regulation that could help set the specific time of LPS, avoiding spurious translation.

One finding is that Cfl1 LPS is not triggered by Slit2 exposure in miR-182 morphant axons, as shown by immunofluorescence and Kaede reporter construct. If miR-182 silences Cfl1 expression in the GC until a cue is encountered, Slit2-induced Cfl1 translation should occur even in the absence of miRNA. Several explanations can be provided for these results. First, the elevated levels of Cfl1 detected in miR-182 morphant axons may negatively feed back on Cfl1 LPS and prevent a further increase in Cfl1 levels. In the absence of miR-182, Cfl1 LPS would thus be uncoupled from Slit2 stimulation and Slit2 would be unable to affect the translational status of Cfl1 mRNA. Second, miR-182 loss of function may deregulate additional direct targets, other than Cfl1, implicated in the Slit2 signaling cascade or regulating LPS per se. In support of this, miR-182 is predicted to silence cofactors of mTOR, as well as mitogen-activated protein kinases (MAPKs) and associated or interacting proteins, all known to be important for Slit2-induced Cfl1 LPS (Piper et al., 2006). Furthermore, miR-182 is predicted to target a few transcripts involved in translation and known to be present in RGCs (Zivraj et al., 2010). Accordingly, miR-182 inactivation by Slit2 would impinge on multiple pathways that would converge to modulate Cfl1 LPS.

Although miRNAs were initially thought to be stable, the active degradation of mature miRNAs was recognized as a key process to modulate miRNA homeostasis (Rüegger and Großhans, 2012). This prompted us to investigate whether mature miR-182 levels decrease upon Slit2 exposure. However, we do not detect any change in miR-182 levels by qPCR. These results contrast with a report documenting that miR-182 decays in neurons within 90 min of stimulation (Krol et al., 2010a). Because this fast degradation was observed in mature neurons, but not in immature neurons (Krol et al., 2010a), this discrepancy may be explained by developing, and not fully differentiated, RGCs being used in the present work and/or by the varying type and length of stimulus exposure employed. However, our finding is in agreement with another study, which showed in dendritic spines that BDNF lifts the repression that miR-134 exerts on *limk1* without altering the miRNA level (Schratt et al., 2006). From this emerges a putative common regulatory mechanism of miRNA inactivation in subregions of neurons not relying on degradation. The loss of activity of miR-182 without its associated decay might be induced by RBPs. RBPs are reported to compete with miRNAs for 3' UTR binding regions or to bind directly to miRNAs, counteracting miRNA-mediated target repression. RBPs also cooperate with miRNAs to regulate mRNA silencing through shared mRNA *cis*-acting elements

Figure 7. Slit2 Inhibits miR-182 Activity in RGC Axons without Decay

(A, D, and F) Schematic representation of the experimental paradigm. Stage 35/36 retinal explants were cultured for 24 hr, and then Slit2 or vehicle were bath applied for 10 min.

(B) Illustrative images of GCs from miR-182-Sensor-electroporated RGCs grown in culture. A clear example of dGFP/mCherry ratio increase is shown in (B).

(C and E) Quantification of the dGFP/mCherry fluorescent ratio at the GC.

(G) Illustrative images of explants and axons before and after LCM.

(H) Illustrative gel of RT-PCR reaction for β -actin (β -act), MAP2, and histone H4 (H4) mRNA from cultured axons collected from stage 37/38 by LCM. In MAP2, H4, and β -act negative controls, PCR template was omitted.

(I) Quantification of miR-182 by the $\Delta\Delta C_t$ method in LCM axons.

Values are mean \pm SEM (C, E, and I). Mann-Whitney test, * $p < 0.05$. ns, nonsignificant; LCM, laser capture microdissection; RT-, RT no template negative control. Scale bars, 5 μ m (B) and 200 μ m (G). See also Figure S7.

and/or through promoting and modulating RISC-mediated repression (Gardiner et al., 2015; Krol et al., 2010b). It is thus conceivable that Slit2 activates a competing RBP or inactivates a cooperating RBP, and this in turn terminates miR-182-mediated Cfl1 repression. One possible advantage of reducing miRNA activity without clearing it from neuronal compartments is that miRNAs can be readily available for future function without the costly need to transcribe and ship new molecules to regions far from the cell body. This type of reversible and bidirectional mechanism would be particularly well suited to these compartments, which are constantly exposed and respond rapidly to various stimuli.

In conclusion, we provide evidence demonstrating that a miRNA, miR-182, acts locally at the GC to confer selectivity of Slit2-induced Cfl1 translation, pointing to the following model. Under basal conditions, miR-182 keeps Cfl1 mRNA silent in RGC axons. Upon Slit2 stimulation, miR-182 activity is abolished in RGC GCs. This leads to the local de-repression of Cfl1 mRNA and its concomitant translation in the GC, while other mRNAs are kept silent by their own repressors. This localized burst of Cfl1 de novo synthesis, in turn, locally affects the cytoskeletal dynamics, subsequently inducing GC repulsive turning. Conceptually, different axonal miRNAs might silence different sets of mRNAs in the GC, preventing their LPS and constituting a reserve pool of mRNAs ready to be translated on demand. Inhibition of specific miRNA activity in the GC, in response to acute stimulation by guidance cues, will therefore act as a switch to relieve specific mRNAs from repression on site in the GC. Such a mechanism could represent an efficient way to ensure rapid selective translation, aiding the immediate response of the GC.

EXPERIMENTAL PROCEDURES

Embryos

Xenopus laevis embryos were obtained by in vitro fertilization as previously described (Cornel and Holt, 1992), raised in 0.1× modified Barth's saline at 14°C–22°C, and staged according to Nieuwkoop and Faber (1994). All animal experiments were approved by the University of Cambridge and University of Trento Ethical Review Committees.

DNA plasmids, antisense oligonucleotides, and mimics used are described in Supplemental Experimental Procedures.

Blastomere Microinjection

A total of 5 ng of morpholinos were injected into both dorsal animal blastomeres of eight-cell-stage embryos as described previously (Piper et al., 2008).

Electroporation

DNA constructs, morpholinos, or miR-182 mimics were electroporated in one eye of stage 26 embryos, with conditions similar to those previously described (Falk et al., 2007).

Optic Pathway Analysis

Stage 40 embryos were anesthetized and fixed in 4% paraformaldehyde (PFA) for 2 hr to overnight. RGC axons were labeled by anterograde Dil filling of the eye or directly visualized by mCherry fluorescence when electroporated. Brains were dissected and mounted to visualize the optic tract on the contralateral side of the brain. The z stacks of serial images comprising the entire contralateral optic pathway were captured. Analysis on the width and the length of the pathway were performed as previously described (Walz et al., 2002), except that all measurements were normalized to brain size.

Retinal Explant Culture

Whole retinas of anesthetized stage 35/36 or 37/38 embryos were dissected and cultured at 20°C for 24 hr, unless otherwise stated, in 60% L15 minimal medium (Invitrogen) and 1× penicillin, streptomycin, and fungizone on glass coverslips (Bellco) or glass-bottom dishes (MatTek) coated with poly-L-lysine (10 µg/mL, Sigma) and laminin (10 µg/mL, Sigma).

Axonal Small RNA Sequencing

For 48 hr, 1,000 whole eye explants from stage 37/38 were cultured. Eye explants and contaminating cells were manually removed to isolate distal axons only. Total RNA was extracted from both the axonal and the explant fractions by phenol-chloroform extraction. The quality, quantity, and purity of the axonal material were tested as described in Supplemental Experimental Procedures. Small RNA libraries were prepared without pre-amplification, using the TruSeq Small RNA Library Preparation Kit (Illumina) and sequenced on a MiSeq sequencer (Illumina). Sequencing data analysis was performed as described in Supplemental Experimental Procedures.

Laser Capture Microdissection

LCM of axons and RGC soma were performed on LMD6500 (Leica). The quality, quantity, and purity of the collected RNA were assessed as described in Supplemental Experimental Procedures.

Axons

Stage 35/36 whole eye explants were cultured on RNase-DNase free polyester (POL) membranes (Leica) for 24 hr and then processed for LCM as previously described (Zivraj et al., 2010), except that 1% PFA was used instead. Distal axons and explants from the same culture were collected in separate tubes. RNA was extracted using the RNAqueous-Micro kit (Ambion). In vivo, laser capture of axons was performed from stage 40 sections, and RNA was extracted using the Single Cell kit (Norgen).

RGC Soma

LCM of the RGC layer was performed on sectioned stage 40 embryos, and stage 37/38 whole eyes were used as control. RNA was extracted using the Total RNA Purification Kit (Norgen).

TaqMan qPCR for miR-182

Total RNA collected following LCM (described earlier) was retro-transcribed using the TaqMan MiRNA Reverse Transcription Kit. The cDNA obtained was used for the TaqMan Micro RNA assay using xtr-miR-182-5p and U6 snRNA-specific primers and probes and the TaqMan Universal Master Mix II (MMIX II) no AmpErase Uracil N-Glycosylase (UNG) (all Thermo Fisher). Reactions were run on a Bio-Rad CFX96 Real-Time System. For quantitative analysis, cycle threshold (Ct) mean values were measured in biological triplicates or more, and the $\Delta\Delta Ct$ method (Schmittgen and Livak, 2008) was applied as follows: fold change is $-1/(2^{[(Ct_{miR-182} - Ct_{U6})_{RGC} - (Ct_{miR-182} - Ct_{U6})_{eye}]})$.

Quantitative Fluorescence Analysis

Quantitative Fluorescence of RGC GCs

Isolated GCs were selected at random with phase optics. To avoid subjective bias, analyses were performed blind to the experimental condition. For each experiment, all acquisitions were performed during the same day with the same settings. The outline of each unsaturated GC was traced to define a region of interest (ROI), and the mean intensity of each channel was measured using ImageJ or Leica Application SuiteX software. The background fluorescence was measured in a ROI as close as possible to the GC selected and subtracted to the GC mean fluorescence value.

Quantitative Fluorescence of Retinal Cells

Quantitation on cryosectioned retina pictures was performed as described earlier, except that retinal cells in the photoreceptor (PR) layer and the innermost part of the inner nuclear layer were defined as the ROI.

GC Turning Assay

Turning assays were performed as described in Campbell and Holt (2001). Further details are provided in Supplemental Experimental Procedures.

miRNA In Situ Hybridization

miRNA ISH protocols for (1) whole-mount, (2) cultured GCs, and (3) for retinal sections were adapted from (1) Wienholds et al. (2005), (2) Han et al., 2011, and from (3) Baudet et al. (2011) and Obernosterer et al. (2007). More details are provided in [Supplemental Experimental Procedures](#).

HRP Axon Tracing

HRP axon tracing and Slit2 ISH were performed as in [Piper et al. \(2006\)](#) on stage 40 embryos. An overview of the HRP labeling protocol is available in [Supplemental Experimental Procedures](#).

Dual Luciferase Reporter Assay

Using Jet prime reagent (Polyplus Transfection), 250 ng of psiCHECK2-Cfl1-WT-3' UTR or psiCHECK2-Cfl1-MUT-3' UTR were transfected with or without 12 pmol of control mimic or miR-182 mimic into HEK293T cells plated 12 hr earlier on 48-well plates. The activity of both Renilla and Firefly luciferase was measured 36 hr after transfection using the Dual Luciferase Reporter Kit (Promega) and a DLReady TD-20/20 single-tube luminometer (Turner Biosystems).

Live Imaging of the Kaede-Cfl1-3' UTR Translation Reporter in Cultured Axons

After injection of control MO or miR-182 MO at the eight-cell stage, one eye of the embryo was electroporated at stage 26 with pCS2+Kaede or pCS2+Kaede-Cfl1-3' UTR reporter constructs. Electroporated eyes were dissected at stage 36 and cultured for 24 hr to allow axonal growth. Before cue stimulation, RGC axons were isolated from their cell bodies by manual removal of the explant. Analysis of local translation of the Kaede reporter was performed as previously described for the β -actin-3' UTR ([Piper et al., 2006, 2008](#)). A brief description is available in [Supplemental Experimental Procedures](#).

Statistical Analysis

Each experiment was conducted at least three times unless otherwise stated. For all tests, the significance level was $\alpha = 0.05$. Data were analyzed with Prism 5 (GraphPad). The normal distribution of datasets was tested by the D'Agostino and Pearson omnibus normality test. Statistical tests used are mentioned in figure legends.

ACCESSION NUMBERS

The accession number for all the RNA-seq data reported in this paper is GEO: GSE86883.

SUPPLEMENTAL INFORMATION

Supplemental Information includes Supplemental Experimental Procedures, seven figures, and two tables and can be found with this article online at <http://dx.doi.org/10.1016/j.celrep.2016.12.093>.

AUTHOR CONTRIBUTIONS

Conceptualization and Writing—Original Draft, A.B., C.E.H., and M.-L.B.; Investigation and Validation, A.B., A.I., S.B., F.L., C.O.-V., E.C., S.L., M.R., S.St., S.N., P.S., C.A.-G., and M.-L.B.; Software, C.O.-V., S.St., and C.A.-G.; Resources, E.M.; Supervision, A.B., E.M., C.A.-G., C.E.H., and M.-L.B.

ACKNOWLEDGMENTS

We thank F. Lamprea, H. Lynn, S. Mansy, D. Cecchi, D. De Pietri Tonelli, P. Macchi, P. Sgadò, Y. Bozzi, S. Casarosa, A. Messina, and CIBIO MOF and Imaging facilities for technical help and S. McFarlane for pCS2-dnRobo2 and pCS2-dnRobo3 constructs. We also thank members of the M.-L.B., Harris, and C.E.H. laboratories for assistance and discussions on the manuscript. This study was supported by EMBO (ALTF992-2011) and HFSP fellowships (LT000136/2012) (to A.B.), University of Trento PhD studentship (to A.I.), Well-

come Trust Programme (085314/Z/08/Z) (to C.E.H.), and Marie Curie Career Integration (618969 GUIDANCE-miR), G. Armenise-Harvard Foundation Career, and MIUR SIR (RBSI144NZ4) grants (to M.-L.B.).

Received: February 13, 2016

Revised: December 7, 2016

Accepted: December 27, 2016

Published: January 31, 2017

REFERENCES

- Aschrafi, A., Schwechter, A.D., Mameza, M.G., Natera-Naranjo, O., Gioio, A.E., and Kaplan, B.B. (2008). MicroRNA-338 regulates local cytochrome c oxidase IV mRNA levels and oxidative phosphorylation in the axons of sympathetic neurons. *J. Neurosci.* *28*, 12581–12590.
- Bartel, D.P. (2009). MicroRNAs: target recognition and regulatory functions. *Cell* *136*, 215–233.
- Baudet, M.L., Zivraj, K.H., Abreu-Goodger, C., Muldal, A., Armisen, J., Blenkiron, C., Goldstein, L.D., Miska, E.A., and Holt, C.E. (2011). miR-124 acts through CoREST to control onset of Sema3A sensitivity in navigating retinal growth cones. *Nat. Neurosci.* *15*, 29–38.
- Bazzini, A.A., Lee, M.T., and Giraldez, A.J. (2012). Ribosome profiling shows that miR-430 reduces translation before causing mRNA decay in zebrafish. *Science* *336*, 233–237.
- Bouquet, C., and Nothias, F. (2007). Molecular mechanisms of axonal growth. *Adv. Exp. Med. Biol.* *621*, 1–16.
- Brittis, P.A., Lu, Q., and Flanagan, J.G. (2002). Axonal protein synthesis provides a mechanism for localized regulation at an intermediate target. *Cell* *110*, 223–235.
- Campbell, D.S., and Holt, C.E. (2001). Chemotropic responses of retinal growth cones mediated by rapid local protein synthesis and degradation. *Neuron* *32*, 1013–1026.
- Cornel, E., and Holt, C. (1992). Precocious pathfinding: retinal axons can navigate in an axonless brain. *Neuron* *9*, 1001–1011.
- Dajas-Bailador, F., Bonev, B., Garcez, P., Stanley, P., Guillemot, F., and Papalopulu, N. (2012). MicroRNA-9 regulates axon extension and branching by targeting Map1b in mouse cortical neurons. *Nat. Neurosci.* *15*, 697–699.
- De Pietri Tonelli, D., Calegari, F., Fei, J.F., Nomura, T., Osumi, N., Heisenberg, C.P., and Huttner, W.B. (2006). Single-cell detection of microRNAs in developing vertebrate embryos after acute administration of a dual-fluorescence reporter/sensor plasmid. *Biotechniques* *41*, 727–732.
- Deglinerti, A., and Jaffrey, S.R. (2012). Insights into the roles of local translation from the axonal transcriptome. *Open Biol.* *2*, 120079.
- Djuranovic, S., Nahvi, A., and Green, R. (2012). miRNA-mediated gene silencing by translational repression followed by mRNA deadenylation and decay. *Science* *336*, 237–240.
- Eichhorn, S.W., Guo, H., McGeary, S.E., Rodriguez-Mias, R.A., Shin, C., Baek, D., Hsu, S.H., Ghoshal, K., Villén, J., and Bartel, D.P. (2014). mRNA destabilization is the dominant effect of mammalian microRNAs by the time substantial repression ensues. *Mol. Cell* *56*, 104–115.
- Erskine, L., Williams, S.E., Brose, K., Kidd, T., Rachel, R.A., Goodman, C.S., Tessier-Lavigne, M., and Mason, C.A. (2000). Retinal ganglion cell axon guidance in the mouse optic chiasm: expression and function of robo and slits. *J. Neurosci.* *20*, 4975–4982.
- Falk, J., Drinjakovic, J., Leung, K.M., Dwivedy, A., Regan, A.G., Piper, M., and Holt, C.E. (2007). Electroporation of cDNA/morpholinos to targeted areas of embryonic CNS in *Xenopus*. *BMC Dev. Biol.* *7*, 107.
- Gardiner, A.S., Twiss, J.L., and Perrone-Bizzozero, N.I. (2015). Competing interactions of RNA-binding proteins, microRNAs, and their targets control neuronal development and function. *Biomolecules* *5*, 2903–2918.
- Gumy, L.F., Yeo, G.S., Tung, Y.C., Zivraj, K.H., Willis, D., Coppola, G., Lam, B.Y., Twiss, J.L., Holt, C.E., and Fawcett, J.W. (2011). Transcriptome analysis

- of embryonic and adult sensory axons reveals changes in mRNA repertoire localization. *RNA* 17, 85–98.
- Gumy, L.F., Katrukha, E.A., Kapitein, L.C., and Hoogenraad, C.C. (2014). New insights into mRNA trafficking in axons. *Dev. Neurobiol.* 74, 233–244.
- Han, L., Wen, Z., Lynn, R.C., Baudet, M.L., Holt, C.E., Sasaki, Y., Bassell, G.J., and Zheng, J.Q. (2011). Regulation of chemotropic guidance of nerve growth cones by microRNA. *Mol. Brain* 4, 40.
- Hancock, M.L., Preitner, N., Quan, J., and Flanagan, J.G. (2014). MicroRNA-132 is enriched in developing axons, locally regulates *Rasa1* mRNA, and promotes axon extension. *J. Neurosci.* 34, 66–78.
- Hengst, U., Cox, L.J., Macosko, E.Z., and Jaffrey, S.R. (2006). Functional and selective RNA interference in developing axons and growth cones. *J. Neurosci.* 26, 5727–5732.
- Hocking, J.C., Hehr, C.L., Bertolesi, G.E., Wu, J.Y., and McFarlane, S. (2010). Distinct roles for *Robo2* in the regulation of axon and dendrite growth by retinal ganglion cells. *Mech. Dev.* 127, 36–48.
- Holt, C.E. (1989). A single-cell analysis of early retinal ganglion cell differentiation in *Xenopus*: from soma to axon tip. *J. Neurosci.* 9, 3123–3145.
- Holt, C.E., and Schuman, E.M. (2013). The central dogma decentralized: new perspectives on RNA function and local translation in neurons. *Neuron* 80, 648–657.
- Iyer, A.N., Bellon, A., and Baudet, M.L. (2014). MicroRNAs in axon guidance. *Front. Cell. Neurosci.* 8, 78.
- Kar, A.N., MacGibeny, M.A., Gervasi, N.M., Gioio, A.E., and Kaplan, B.B. (2013). Intra-axonal synthesis of eukaryotic translation initiation factors regulates local protein synthesis and axon growth in rat sympathetic neurons. *J. Neurosci.* 33, 7165–7174.
- Kim, V.N., Han, J., and Siomi, M.C. (2009). Biogenesis of small RNAs in animals. *Nat. Rev. Mol. Cell Biol.* 10, 126–139.
- Kleiman, R., Banker, G., and Steward, O. (1990). Differential subcellular localization of particular mRNAs in hippocampal neurons in culture. *Neuron* 5, 821–830.
- Krol, J., Busskamp, V., Markiewicz, I., Stadler, M.B., Ribi, S., Richter, J., Duebel, J., Bicker, S., Fehling, H.J., Schübeler, D., et al. (2010a). Characterizing light-regulated retinal microRNAs reveals rapid turnover as a common property of neuronal microRNAs. *Cell* 141, 618–631.
- Krol, J., Loedige, I., and Filipowicz, W. (2010b). The widespread regulation of microRNA biogenesis, function and decay. *Nat. Rev. Genet.* 11, 597–610.
- Leung, K.M., and Holt, C.E. (2008). Live visualization of protein synthesis in axonal growth cones by microinjection of photoconvertible Kaede into *Xenopus* embryos. *Nat. Protoc.* 3, 1318–1327.
- Leung, K.M., van Horck, F.P., Lin, A.C., Allison, R., Standart, N., and Holt, C.E. (2006). Asymmetrical beta-actin mRNA translation in growth cones mediates attractive turning to netrin-1. *Nat. Neurosci.* 9, 1247–1256.
- Lin, A.C., and Holt, C.E. (2007). Local translation and directional steering in axons. *EMBO J.* 26, 3729–3736.
- Lohof, A.M., Quillan, M., Dan, Y., and Poo, M.M. (1992). Asymmetric modulation of cytosolic cAMP activity induces growth cone turning. *J. Neurosci.* 12, 1253–1261.
- Natera-Naranjo, O., Aschrafi, A., Gioio, A.E., and Kaplan, B.B. (2010). Identification and quantitative analyses of microRNAs located in the distal axons of sympathetic neurons. *RNA* 16, 1516–1529.
- Nguyen-Ba-Charvet, K.T., Brose, K., Marillat, V., Sotelo, C., Tessier-Lavigne, M., and Chédotal, A. (2001). Sensory axon response to substrate-bound *Slit2* is modulated by laminin and cyclic GMP. *Mol. Cell. Neurosci.* 17, 1048–1058.
- Nieuwkoop, P.D., and Faber, J. (1994). Normal table of *xenopus laevis* (daudin) (Garland Publishing Inc.).
- Obernosterer, G., Martinez, J., and Alenius, M. (2007). Locked nucleic acid-based in situ detection of microRNAs in mouse tissue sections. *Nat. Protoc.* 2, 1508–1514.
- Ovando-Vázquez, C., Lepe-Soltero, D., and Abreu-Goodger, C. (2016). Improving microRNA target prediction with gene expression profiles. *BMC Genomics* 17, 364.
- Pinter, R., and Hindges, R. (2010). Perturbations of microRNA function in mouse *dicer* mutants produce retinal defects and lead to aberrant axon pathfinding at the optic chiasm. *PLoS ONE* 5, e10021.
- Piper, M., Anderson, R., Dwivedy, A., Weinl, C., van Horck, F., Leung, K.M., Cogill, E., and Holt, C. (2006). Signaling mechanisms underlying *Slit2*-induced collapse of *Xenopus* retinal growth cones. *Neuron* 49, 215–228.
- Piper, M., Dwivedy, A., Leung, L., Bradley, R.S., and Holt, C.E. (2008). NF-protocadherin and TAF1 regulate retinal axon initiation and elongation in vivo. *J. Neurosci.* 28, 100–105.
- Rüegger, S., and Großhans, H. (2012). MicroRNA turnover: when, how, and why. *Trends Biochem. Sci.* 37, 436–446.
- Sasaki, Y., Gross, C., Xing, L., Goshima, Y., and Bassell, G.J. (2014). Identification of axon-enriched microRNAs localized to growth cones of cortical neurons. *Dev. Neurobiol.* 74, 397–406.
- Schmittgen, T.D., and Livak, K.J. (2008). Analyzing real-time PCR data by the comparative C(T) method. *Nat. Protoc.* 3, 1101–1108.
- Schratt, G.M., Tuebing, F., Nigh, E.A., Kane, C.G., Sabatini, M.E., Kiebler, M., and Greenberg, M.E. (2006). A brain-specific microRNA regulates dendritic spine development. *Nature* 439, 283–289.
- Shigeoka, T., Lu, B., and Holt, C.E. (2013). Cell biology in neuroscience: RNA-based mechanisms underlying axon guidance. *J. Cell Biol.* 202, 991–999.
- Tcherkezian, J., Brittis, P.A., Thomas, F., Roux, P.P., and Flanagan, J.G. (2010). Transmembrane receptor DCC associates with protein synthesis machinery and regulates translation. *Cell* 141, 632–644.
- Vuppalachchi, D., Willis, D.E., and Twiss, J.L. (2009). Regulation of mRNA transport and translation in axons. *Results Probl. Cell Differ.* 48, 193–224.
- Walz, A., Anderson, R.B., Irie, A., Chien, C.B., and Holt, C.E. (2002). Chondroitin sulfate disrupts axon pathfinding in the optic tract and alters growth cone dynamics. *J. Neurobiol.* 53, 330–342.
- Wang, B., Pan, L., Wei, M., Wang, Q., Liu, W.W., Wang, N., Jiang, X.Y., Zhang, X., and Bao, L. (2015). FMRP-mediated axonal delivery of miR-181d regulates axon elongation by locally targeting *Map1b* and *Calm1*. *Cell Rep.* 13, 2794–2807.
- Wei, Q., Lei, R., and Hu, G. (2015). Roles of miR-182 in sensory organ development and cancer. *Thorac. Cancer* 6, 2–9.
- Wienholds, E., Kloosterman, W.P., Miska, E., Alvarez-Saavedra, E., Berezikov, E., de Bruijn, E., Horvitz, H.R., Kauppinen, S., and Plasterk, R.H. (2005). MicroRNA expression in zebrafish embryonic development. *Science* 309, 310–311.
- Wu, K.Y., Hengst, U., Cox, L.J., Macosko, E.Z., Jeromin, A., Urquhart, E.R., and Jaffrey, S.R. (2005). Local translation of *RhoA* regulates growth cone collapse. *Nature* 436, 1020–1024.
- Yao, J., Sasaki, Y., Wen, Z., Bassell, G.J., and Zheng, J.Q. (2006). An essential role for beta-actin mRNA localization and translation in Ca^{2+} -dependent growth cone guidance. *Nat. Neurosci.* 9, 1265–1273.
- Yoon, B.C., Jung, H., Dwivedy, A., O'Hare, C.M., Zivraj, K.H., and Holt, C.E. (2012). Local translation of extranuclear lamin B promotes axon maintenance. *Cell* 148, 752–764.
- Zelina, P., Blockus, H., Zagar, Y., Péres, A., Friocourt, F., Wu, Z., Rama, N., Fouquet, C., Hohenester, E., Tessier-Lavigne, M., et al. (2014). Signaling switch of the axon guidance receptor *Robo3* during vertebrate evolution. *Neuron* 84, 1258–1272.
- Zhang, Y., Ueno, Y., Liu, X.S., Buller, B., Wang, X., Chopp, M., and Zhang, Z.G. (2013). The microRNA-17-92 cluster enhances axonal outgrowth in embryonic cortical neurons. *J. Neurosci.* 33, 6885–6894.
- Zivraj, K.H., Tung, Y.C., Piper, M., Gumy, L., Fawcett, J.W., Yeo, G.S., and Holt, C.E. (2010). Subcellular profiling reveals distinct and developmentally regulated repertoire of growth cone mRNAs. *J. Neurosci.* 30, 15464–15478.



microRNAs in axon guidance

Archana N. Iyer¹, Anaïs Bellon² and Marie-Laure Baudet^{1*}

¹ Center for Integrative Biology, University of Trento, Trento, Italy

² Department of Physiology, Development and Neuroscience, University of Cambridge, Cambridge, UK

Edited by:

Tommaso Pizzorusso, *UniFI*
- Università degli Studi di Firenze,
Italy

Reviewed by:

Jeroen Pasterkamp, *UMC Utrecht*,
Netherlands
Harold Cremer, *Centre National de
la Recherche Scientifique, France*
Chieh Chang, *Cincinnati Children's
Hospital Research Foundation, USA*
Jessica Kwok, *University of
Cambridge, UK*

*Correspondence:

Marie-Laure Baudet, *Center for
Integrative Biology, University of
Trento, Via delle Regole, 101,
Trento 38123, Italy*
e-mail: marielaure.baudet@unitn.it

Brain wiring is a highly intricate process in which trillions of neuronal connections are established. Its initial phase is particularly crucial in establishing the general framework of neuronal circuits. During this early step, differentiating neurons extend axons, which reach their target by navigating through a complex environment with extreme precision. Research in the past 20 years has unraveled a vast and complex array of chemotropic cues that guide the leading tip of axons, the growth cone, throughout its journey. Tight regulation of these cues, and of their receptors and signaling pathways, is necessary for the high degree of accuracy required during circuit formation. However, little is known about the nature of regulatory molecules or mechanisms fine-tuning axonal cue response. Here we review recent, and somewhat fragmented, research on the possibility that microRNAs (miRNAs) could be key fine-tuning regulatory molecules in axon guidance. miRNAs appear to shape long-range axon guidance, fasciculation and targeting. We also present several lines of evidence suggesting that miRNAs could have a compartmentalized and differential action at the cell soma, and within axons and growth cones.

Keywords: miRNAs, axon guidance, axon, growth cone, neuron, development

INTRODUCTION

Brain wiring occurs during the development of the nervous system and ensures the formation of a highly complex network of inter-communicating neurons. For these circuits to be established, neurons form remarkably accurate connections with their target cells. Initially, neurons send out cell protrusions called axons, which navigate a complex environment to reach their exact targets: a process known as axon guidance (or “pathfinding”). How do axons know where to go? Specific molecules present along the pathway act as signposts to guide axons to their final destination by either repelling or attracting the leading tip of the axon—the growth cone. These guidance cues are also capable of promoting axon fasciculation, i.e., the bundling of axons together, and interactions between axons and their substrate (Tessier-Lavigne and Goodman, 1996). Over the past two decades, genetic, biochemical and cell culture analysis have unraveled four major families of guidance molecules, which can be classified into four families: Ephrins, Semaphorins, Slits, and Netrins (Dickson, 2002). More recent works demonstrated that some morphogens, growth factors, and cell-adhesion molecules also have guidance function (Kolodkin and Tessier-Lavigne, 2011). Cue-mediated signaling leads to complex remodeling of the cytoskeleton in growth cones, which in turn regulates its directional steering and interactions with other axons, cells, and the environment (Dent et al., 2011).

The nervous system contains up to a few billions of neurons depending on the species, and each neuron is at the core of a highly complex connectome, which can receive and project to up to hundreds of thousands of synaptic partners. The startling complexity of this system has long confronted neuroscientists with the incongruity of the seemingly inadequate size of the genome of roughly 20,000 defined genes. Alternative splicing is thought

to partly account for such complexity, since it can generate hundreds of isoforms from a single coding gene (Schmucker et al., 2000; Li et al., 2007). In addition to this, the non-coding regulatory regions of the transcriptome, or “dark matter” (Johnson et al., 2005), is increasingly thought to account for the complexity of the neuronal connectome at the molecular level. This includes a growing number of families of small RNAs, primarily the microRNAs (miRNAs).

miRNAs are a class of small ~22 nt non-coding RNAs that have emerged, in recent years, as key post-transcriptional regulators in most eukaryotic cells. They do so by specifically binding to mRNA through partial complementarity, thereby inhibiting transcript translation, and/or stability (Bartel, 2009). Since the discovery of the first miRNA, *lin-4*, more than 20 years ago in *C. elegans* (Lee et al., 1993; Wightman et al., 1993), hundreds of new miRNAs have been identified (Griffiths-Jones, 2004; Griffiths-Jones et al., 2008; Kozomara and Griffiths-Jones, 2011, 2013) (www.miRbase.org). Importantly, the nervous system is the site of an intricate “miRNnome,” as numerous miRNAs are enriched or specifically expressed there in time and place (Johnston and Hobert, 2003; Krichevsky et al., 2003; Chang et al., 2004b; Hsieh, 2012; Zou et al., 2013). Recent large-scale studies have further revealed that individual miRNAs fine-tune the expression of hundreds of transcripts (Baek et al., 2008; Selbach et al., 2008; Guo et al., 2010). The regulatory potential of miRNAs in developing organisms, and particularly in the nervous system, thus appears infinite. The roles of miRNAs in promoting the complexity and accuracy required for circuit formation, and axon guidance in particular, has however just started to emerge.

Here, we review a small, but compelling body of research suggesting that miRNAs are important players in axon guidance. We first examine the roles of miRNAs in key steps of axon

pathfinding, namely long-range guidance, fasciculation, and targeting. We then expose some evidence which points toward the possibility that miRNAs might have a compartmentalized action in projecting neurons, in the soma, axon, or growth cone.

ROLES OF miRNAs IN AXON GUIDANCE

LONG-RANGE GUIDANCE

In the initial phase of axon navigation, axons must first polarize, and subsequently navigate through a complex cellular terrain containing guidance cue-expressing “guidepost” cells. Neuronal or glial cells can take on the role of guidepost cells and act as substrates or intermediary targets for the growing axon. This enables axons to extend in a directed manner rather than by passive adhesion in a step-wise manner, using mechanisms that are highly conserved in both vertebrates and invertebrates (Raper and Mason, 2010). miRNAs could impact the transcriptome of projection neurons, regulating the expression of molecules that transduce cue signaling. Alternatively, they could affect guidepost cells to regulate directly or indirectly cue expression. In this section, we review a few recent findings on different model systems suggesting multiple roles and sites for miRNA action, which regulates both the navigating neuron and its environment.

Pinter and Hindges (2010) were the first to report that miRNAs, as a class of molecules, are important for long-range axon navigation using mice retinal ganglion cells (RGCs) as a model. RGCs are the only projection neurons of the retina and convey visual information to higher brain centers. In wild type monocular species, almost all RGC axons decussate at the optic chiasm, a midline structure. Whereas in binocular species, such as mice, some axons do not cross at the chiasm, but remain ipsilateral. The midline is thus an important choice point. The authors observed that, in absence of most miRNAs, many contralateral-projecting RGC axons failed to cross at the chiasm, and instead, aberrantly navigated ipsilaterally or overshot the midline. The molecular mechanisms leading to this phenotype is unknown to date. To abolish miRNAs function, Pinter and Hindges used mutants mice where Dicer, a key enzyme responsible for the maturation of most miRNAs (Bernstein et al., 2001; Grishok et al., 2001; Ketting et al., 2001; Knight and Bass, 2001), was conditionally ablated in Rx-expressing cells including RGCs and cells forming the optic chiasm. Depletion of miRNAs in these mutants could, therefore, either lead to impaired cue expression by guidepost cells at the midline, or to altered sensitivity of RGC growth cones to midline cues following misexpression of their cognate receptors or associated signaling molecules. Several ligand-receptor pairs are known to mediate midline crossing in mice: ephrin-B2/EphB1 (Nakagawa et al., 2000; Williams et al., 2003) Slit 1/2/Robo 1/2 (Plump et al., 2002; Plachez et al., 2008) VEGF164/Neuropilin-1 (Erskine et al., 2011), Sema 6D/Nr-CAM, and Plexin A1 (Kuwajima et al., 2012). Their direct or indirect regulation by miRNAs is however unknown to date except for Neuropilin-1 (Baudet et al., 2012; Cui et al., 2012; Zhang et al., 2012) and Robo 1 and 2 (Alajez et al., 2011; Fish et al., 2011; Yang et al., 2012). Of interest, miR-218 was documented to target Slit receptors Robo 1 and 2 in non-neural cells such as cancer cells (Alajez et al., 2011; Fish et al., 2011; Yang et al., 2012) suggesting it might also play a role in neurons including axons where

it is also expressed (Sasaki et al., 2013). Overall, this study is the first *in vivo* evidence to show that miRNAs may impact projecting neurons, guidepost cells, or both.

miR-9 was also recently documented to regulate the long-range guidance of thalamocortical (TCAs) and corticofugal axons (CFAs) tracts (Shibata et al., 2011). Both tracts cross the telencephalon and navigate through the internal capsule, a telencephalic structure, before reaching their final destination (Molnár et al., 2012). Migration of guidepost cells called “corridor cells” to the internal capsule is a crucial event in TCA and CFA pathfinding. These cells create a permissive corridor within the medial ganglionic eminence (MGE), a telencephalic region, normally non-permissive to the growth of TCAs, and thus enable these axons to cross the telencephalon prior to reaching their final destination (López-Bendito et al., 2006). To address the roles of miR-9 specifically in telencephalic development, Shibata, and colleagues generated miR-9-2/3 double mutant mice lacking two of the three miR-9 pre-cursors, namely miR-9-2, and miR-9-3 (Shibata et al., 2011). In miR-9-2/3 double mutants, CFAs and TCAs were severely misrouted. CFAs poorly innervated the internal capsule. Similarly, TCAs failed to reach this region, and instead aberrantly projected into the hypothalamus, an area that they normally avoid. The deregulated molecular mechanisms leading to this phenotype are unclear, and likely to be complex. Evidence suggests that the TCA and CFA aberrant projections might be attributed to impaired patterning of corridor cells, although the possibility that miR-9 acts cell-autonomously in these projecting tracts cannot be excluded. Indeed, the topographical distribution of corridor cells within the telencephalon was affected; corridor neurons were expanded or dispersed in mutant animals. In addition, corridor cell markers *islet-1* and *Meis2* (predicted targets of miR-9) expression appeared to be qualitatively up-regulated in miR-9-2/3 double mutant mice. The mechanistic implication of this dysregulation on the pathfinding defects observed is, however, unclear. Thus, these data suggest that miR-9 may ensure the proper development of corridor cells and in turn the accurate projection of TCA and CFA to this intermediate target. Together, this study points to the interesting possibility that long-range axon guidance defects might indirectly rise from miRNA-induced impaired patterning of guidepost cells.

Finally, *lin-4* was recently reported to also regulate long-range guidance of the axonal projection of anterior ventral microtubule (AVM) neurons in *C. elegans* larvae (Zou et al., 2012). In wild type animals, AVM axons project to the nerve ring, a neuropil considered as the *C. elegans*' brain. Before projecting anteriorly toward their target, AVM neurons are guided by two chemotropic cues that, together, orient the axons ventrally toward the midline. SLT-1 (Slit) repels AVM axons, preventing them from projecting dorsally, and UNC-6 (Netrin) attracts AVM axons ventrally (Chang et al., 2004a). The authors examined whether *lin-4*, a miRNA expressed in AVM during axon pathfinding, is important for UNC-6-mediated axon guidance. *lin-4* was found to inhibit UNC-6 signaling during AVM axon guidance (Zou et al., 2012). Importantly, *lin-4* acted cell-autonomously, at least in part, and specifically in post-migrating neurons. LIN-14, a transcription factor and well-described target of *lin-4*, is also expressed in AVM neurons. LIN-14 was found to mediate *lin-4* action on AVM

guidance and to potentiate UNC-6 mediated attraction of AVM axons by acting on UNC-40 (DCC) receptors. Surprisingly, *lin-14* did not alter *unc-40* promoter activity. Instead, it enhanced UNC-40 protein expression via an unknown mechanism, shifting its distribution from the confined perinuclear region to the whole cell. Intriguingly, *lin-4* and *lin-14* are broadly expressed in *C. elegans*, and both are found in several UNC-40 guided neurons. This suggests that a *lin-4/lin-14* based conserved regulatory pathway might modulate UNC-6-mediated axon attraction of other tracts. In addition, miR-125, a *lin-4* ortholog, is also present in neurons of vertebrates (Sempere et al., 2004; Smirnova et al., 2005), indicating that this ancient microRNA may have conserved its guidance function. Overall, this study revealed that *lin-4* regulates cue-mediated attraction by modulating the signaling pathway of a receptor to guidance cue. Importantly, it also provided evidence that miRNAs can act cell-autonomously to modulate axon guidance to the midline. In summary, a few studies have revealed that miRNAs regulate long-range axon navigation, acting cell autonomously on projecting neurons, and possibly on guidepost cells.

FASCICULATION

Pioneer axons begin their pathfinding journey in an environment devoid of axons and are the first to establish connection with the target. Follower axons arise at a later time point in development and can progress along the pathway through axon-axon contact, thereby using topographical information provided by pioneers (Pittman et al., 2008). The process by which those co-extending axons form tight bundles is called fasciculation and is thought to be mediated by various classes of molecules including neural cell adhesion molecules (NCAM) but also guidance cues (Huber et al., 2005; Luxey et al., 2013). As reviewed below, some evidence suggests that miRNAs could play a role in the formation of these fasciculated bundles.

Giraldez et al. (2005) reported that Maternal Zygotic (MZ) Dicer zebrafish mutants, devoid of maternal and embryonic sources of Dicer, exhibit several defasciculated axon tracts. Specifically, fasciculation of the post-optic commissure and hindbrain axonal scaffold, formed by longitudinal and commissural tracts, were severely disrupted in the absence of most miRNAs. Although defasciculation can lead to aberrant axonal trajectory (Huber et al., 2005), projections were correctly established at least for longitudinal hindbrain axons. In addition, early patterning and fate specification was preserved in these animals. This suggests that these defects may be linked to altered molecular programs specifically in these projecting neurons, although impaired cue expression within the axonal environment cannot be formally ruled-out. Interestingly, exogenous miR-430 family members partly rescued this phenotype. This suggests that members of this family, or other uncharacterized miRNAs, may alter the expression or signaling of molecules mediating bundling of these tracts. Such molecules may include *Sema3D* and its cognate receptor *Neuropilin-1A*, which is known to promote fasciculation of hindbrain longitudinal axons in zebrafish (Wolman et al., 2004; Kwok et al., 2012). A defasciculation phenotype of RGC axons was also observed in Rx-conditional Dicer knockout mice (Pinter and Hindges, 2010). In these animals, RGC axons failed to

form a tight bundle within the retina. In addition at the midline, axons that aberrantly projected ipsilaterally were defasciculated, while axons overshooting the chiasm formed a secondary defasciculated tract. Interestingly, *Sema 3D*, *Plexin A-1*, *Nr-CAM*, *Slit1*, and *2* are implicated in the fasciculation of RGC axons (Ringstedt et al., 2000; Plump et al., 2002; Kuwajima et al., 2012) suggesting that their signaling might be derailed in Dicer mutants. Overall, miRNAs appear to regulate fasciculation, although the molecular mechanisms and the nature of the miRNAs involved are still largely elusive.

AXON TARGETING

After their long journey, axons reach their final destinations. Targeting of axons to their exact partner is absolutely essential, as it ensures proper circuit formation. This process is highly complex and requires several classes of molecules that promote defasciculation and specific entry within the target region, restricts any further elongation but also prevent axons from exiting the target-area. Cue-mediated restriction of the target-area is a highly regulated process in which miRNAs have been recently shown to play a role (Baudet et al., 2012).

Using *Xenopus laevis*, Baudet et al. (2012) uncovered a miRNA based signaling pathway that regulates axon targeting of RGCs to the optic tectum. Knockdown of miR-124 neither altered the birth of RGCs nor the general progression of their differentiation. However, it appeared to affect post-mitotic RGCs axon projection. While long-range guidance was unaffected, a subset of axons failed to appropriately stall within the optic tectum. Instead, they invaded *Sema3A* expressing territories in the ventral border, normally repellent to these axons at this stage. The effect of miR-124 is likely to be cell-autonomous, as straying axons were observed both when miR-124 was knocked down in cells of the central nervous system (which include RGCs and tectal cells), and also when knocked down at a later developmental stage in retinal cells. In addition, growth cone responsiveness to *Sema3A* was impaired in miR-124 morphants. The authors also elucidated the molecular pathway mediating miR-124-regulated *Sema3A* repulsion. miR-124 indirectly promoted the expression of *Neuropilin-1*, a *Sema3A* receptor, at the growth cone, since its depletion decreased *Neuropilin-1* levels within growth cones *in vitro* and axons *in vivo*. miR124 regulated *Neuropilin-1* via the silencing of its conserved target *coREST*, a cofactor of the global neuronal repressor *REST* (*RE1-silencing transcription factor*). Indeed, knockdown of *coREST* rescued *Neuropilin-1* levels at the growth cone, and also growth cone responsiveness to *Sema3A*, in miR-124 morphants *in vitro*. Overall, this study uncovered a complex mechanism whereby miR-124 ensures RGC axonal response to *Sema3A*, at the right time and place, by dynamically inhibiting *coREST* repression of *Neuropilin-1* within maturing RGCs. It also revealed for the first time that a miRNA regulates axon guidance (targeting) *in vivo*.

CONCLUSION

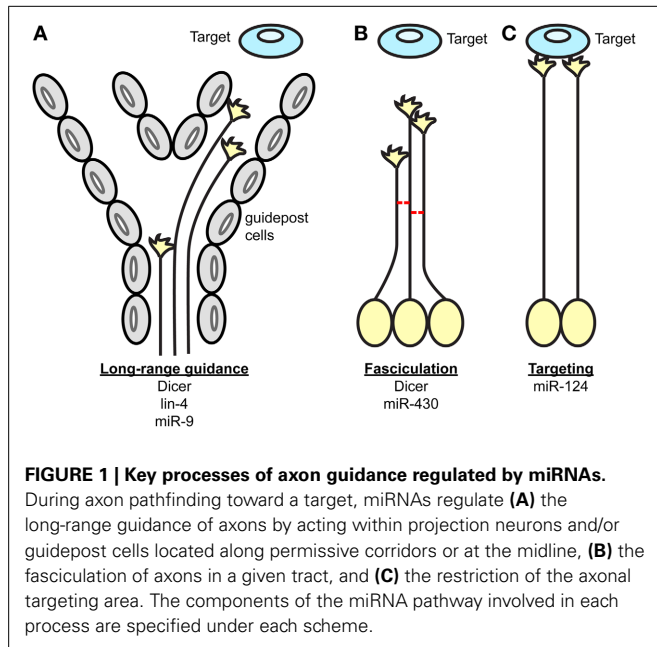
In summary, several studies have together revealed the function of miRNAs in axonal navigation to their final destinations using central nervous system projections as model (Table 1, Figure 1) (Giraldez et al., 2005; Pinter and Hindges, 2010; Shibata et al.,

Table 1 | List miRNAs and their target involved in guidance.

miRNA	mRNA	Age	Species	Neuron type	Phenotype*	References
<i>lin-4</i>	LIN-14	L1 and L2 stage	<i>C. elegans</i>	AVM	Impaired long-range guidance	Zou et al., 2012
miR-124	CoREST	St 24,32,40	<i>X. laevis</i>	RGC	Impaired targeting	Baudet et al., 2012
miR-134	Xlimk1	St 22	<i>X. laevis</i>	Spinal	Loss of BDNF-induced growth cone turning	Han et al., 2011

*upon loss of function.

Abbreviations: AVM, Anterior Ventral Microtubule; RGC, Retinal Ganglion Cells; st, stage; X, *Xenopus*.



2011; Baudet et al., 2012; Zhang et al., 2013; Chiu et al., 2014). Earlier work took a broad approach, and knocked down the entire pool of miRNAs using a Dicer loss-of-function strategy (Giraldez et al., 2005; Pinter and Hindges, 2010). This was particularly important at that time to determine whether miRNAs, as a class of molecules, are involved in axon guidance. Although striking phenotypes were observed suggesting the importance of miRNAs in this process, the full extent of miRNAs' implication in guidance maybe somewhat underestimated for several reasons. miRNA turn-over varies, and some can be particularly stable for a long time following ablation of Dicer (Schaefer et al., 2007). In addition, recent studies have shown that miRNAs can be synthesized via a Dicer-independent mechanism (Cheloufi et al., 2010; Cifuentes et al., 2010; Yang et al., 2010)—although, only one miRNA, miR-451, is documented to employ this non-canonical pathway (Yang et al., 2010). Of interest, Dicer is also involved in small interfering (si) RNA processing from various sources such as small nuclear (sn) RNA and viral double stranded (ds) RNA (Bernstein et al., 2001; Grishok et al., 2001; Ketting et al., 2001; Knight and Bass, 2001; Li et al., 2002). Dicer loss-of-function in these initial analyses (Giraldez et al., 2005; Pinter and Hindges, 2010) could thus impair this processing also. The importance of these additional roles has yet to be demonstrated in neurons however. Later studies went on to unravel the roles of individual

miRNAs in axon guidance. New insight has come from those that have explored the cell-autonomous roles of miRNAs *in vivo*; for instance directly in projecting neurons (Baudet et al., 2012; Zou et al., 2012). Future research *in vivo* should however reveal additional functions of miRNAs, and their associated mechanisms of action. In particular, it is unknown whether miRNAs modulate cue expression in the pathway, either by acting directly on post-transcriptional regulation of transcripts expressed in guidepost cells, or on their patterning. However, gaining future insight will be complicated by the fact that this field has several pitfalls. High level of redundancy of miRNA function exists, especially for those miRNAs derived from the same family (Choi et al., 2008) or the same polycistron (Ventura et al., 2008) making the identification of individual guidance miRNAs particularly difficult. Deciphering the molecular mechanisms at play represents also a hurdle, since miRNAs are often part of complex molecular networks. Overcoming these challenges will thus be crucial in the future elucidation of miRNA function in guidance.

COMPARTMENTALIZED ACTION OF miRNAs

Numerous miRNAs appear to be differentially distributed within organisms, tissues, and cells. This is particularly true for the nervous system where miRNAs are enriched and specifically located in different regions and cell types (Krichevsky et al., 2003; Landgraf et al., 2007; Pichardo-Casas et al., 2012). Intriguingly, differential distribution is also observed at the subcellular level. Specific miRNAs are found to be enriched at synapses and dendrites compared to the cell soma (Siegel et al., 2009). This is perhaps not surprising considering that neurons are highly polarized cells with compartmentalized mRNA repertoires (Taylor et al., 2009; Zivraj et al., 2010; Gumy et al., 2011; Kaplan et al., 2013) implying that different compartments may have different regulatory requirements. Recent data have emerged suggesting that miRNAs are localized and might function within different subcellular location of projection neurons. For instance, some miRNAs may act within soma, affecting targets that have a global range of action; whilst others may have a more restricted, compartmentalized action within axons, and possibly, restricted to growth cones. The following section presents data summarizing these two possibilities.

SOMATIC ROLES OF miRNAs

Aforementioned studies have provided evidence that at least two specific miRNAs are likely to act primarily within the neuronal cell body during axon guidance. miR-124 in *Xenopus* (Baudet et al., 2012) and *lin-4* in *C.elegans* (Zou et al., 2013) have somatic distribution within RGCs and AVM, respectively. *lin-4* ortholog

miR-125b is enriched in axons of the superior cervical ganglion (SCG) in mice (Natera-Naranjo et al., 2010) however, suggesting that the subcellular distribution might be cell or species specific. In contrast, miR-124 is enriched in the perinuclear cell soma of various neurons, compared to axons, synapses, or dendrites (Kye et al., 2007; Siegel et al., 2009; Natera-Naranjo et al., 2010), suggesting that this miRNA might have a conserved site of action. In addition, the molecular nature of the miR-124 and *lin-4* targets strongly suggest restricted action within cell bodies, as both targets are transcription factors: coREST (Baudet et al., 2012) and *lin-14* (Zou et al., 2012). Taken together, this suggests that miR-124 and *lin-4* acts within neuronal cell soma of projecting neurons to regulate axonal pathfinding.

miRNAs were first described as heterochronic genes regulating the developmental timing of many *C.elegans* cell lineages (Lee et al., 1993; Wightman et al., 1993; Reinhart et al., 2000). Their roles as timers also occur in vertebrates including in neuronal lineages (Decembrini et al., 2009; Cremisi, 2013; La Torre et al., 2013). Intriguingly, miRNAs might also function as timers in in post-mitotic neurons during later developmental events (Olsson-Carter and Slack, 2010; Baudet et al., 2012; Zou et al., 2012) but also following terminal differentiation (Chiu and Chang, 2013; Zou et al., 2013). In particular, *lin-4* and miR-124 were reported to affect the developmental aging of post-mitotic differentiating neurons during the period of axon elongation and guidance. As mentioned above, miR-124 regulates Sema3A-mediated RGC axon targeting within the tectum through transcriptional depression of Neuropilin-1 by coREST silencing (Baudet et al., 2012). Importantly, RGC axons gain responsiveness to Sema3A over time, as they navigate along the pathway, and this onset of responsiveness is due to the increase in Neuropilin-1 expression at the growth cone (Campbell et al., 2001). Remarkably, miR-124 may act as a timer, regulating the timetable of neuropilin-1 expression. Indeed, Baudet et al. (2012) showed series of evidence suggesting that a temporal increase of miR-124 in differentiating RGCs, during the period of guidance, accelerates the clearance of coREST transcripts, which progressively releases the transcriptional repression on Neuropilin-1. In turn, Neuropilin-1 protein levels increase at the growth cone over time. All-in-all, miR-124 indirectly determines the time at which Neuropilin-1 is expressed above a level that is necessary for growth cones to gain sensitivity to Sema3A. This mechanism enables growth cones to respond appropriately to this repellent at the right time and place.

Similarly to RGC growth cones, AVM axons progressively switch and lose responsiveness to UNC-6 toward the end of the axon guidance period (Zou et al., 2013). This loss-of-sensitivity is thought to enable axons to subsequently proceed with synaptogenesis (Zou et al., 2013). *C. elegans lin-4* is a well acknowledged regulator of developmental timing, affecting numerous cell types (Chalfie et al., 1981; Lee et al., 1993; Wightman et al., 1993). In AVM neurons, *lin-4*, like miR-124, displays a clear dynamic temporal regulation suggesting it might also regulate developmental timing in these cells. Importantly, it starts being expressed in AVM neurons only after cell fate determination and cell migration has occurred. Moreover, the 3'UTR activity of its target, *lin-14*, is also down-regulated overtime in these cells (Zou et al., 2013).

This indicates that it could act as a timer to promote neuronal differentiation and axon guidance.

Two different molecular pathways have thus been uncovered, where miRNAs appear to endorse a timer function by regulating a switch in growth cone responsiveness over time. The regulatory mechanisms leading to the dynamic expression of these two miRNAs is however unknown. It would be interesting to investigate whether a master clock, regulating this common timetable of growth cone sensitivity, exists upstream that regulate the temporal expression of these miRNAs.

LOCAL ROLES OF miRNAs AT THE GROWTH CONE

The growth cone is a subcellular compartment that can function with a great deal of independence from the cell body, since severed growth cones can navigate on their own along the pathway for a few hours (Harris et al., 1987) and possess all the machinery necessary to respond to cues (Vitriol and Zheng, 2012). Remarkably, growth cones and axons are packed with complex and dynamically changing mRNA repertoires (Taylor et al., 2009; Zivraj et al., 2010). mRNA translation is also shown to mediate growth cone turning in response to several cues (Jung and Holt, 2011). Interestingly, mRNA regulation has emerged as an important mechanism to promote crisp growth cone steering (Jung et al., 2011). However, the identity of key molecular players, their modes of action, and the mechanisms employed by extracellular signals to modulate mRNA translation, are largely unknown. miRNAs may thus be important post-transcriptional regulators for growth cone behavior (Jung et al., 2011), since they ensure that proteins are expressed at precise levels, at the right time and place (Bartel, 2009; Ebert and Sharp, 2012). Although this has yet to be demonstrated, a few lines of evidence support this possibility.

miRNA profiling within axons

Recent studies have profiled miRNAs directly within developing distal axons (also comprising growth cones) using different technical approaches and biological systems (Natera-Naranjo et al., 2010; Sasaki et al., 2013; Hancock et al., 2014). These have revealed that a complex miRNome exists in distal axons and that several miRNAs are enriched (or depleted) in this compartment (Table 2). As suggested (Hancock et al., 2014), this would be consistent with the differential expression of axonal mRNA repertoires at different developmental stages or in different species (Zivraj et al., 2010; Gumy et al., 2011). High throughput profiling of miRNAs have yet to be documented. However, in these studies, several miRNAs were also detected in growth cones by fluorescent *in situ* hybridization: miR-16 and miR-221 in SCG neurons (Natera-Naranjo et al., 2010), miR-532 and miR-181a-1* in E16 cortical neurons and in dissociated hippocampal neurons (Sasaki et al., 2013) and miR-132 in E13.5 DRG explants culture (Hancock et al., 2014). Importantly the list and number of enriched axonal miRNAs, in all three studies, is strikingly different. Several reasons might explain these results. First, miRNAs might be differentially distributed in axons depending on the species (rat vs. mouse), cell type (SCG, cortical, and DRG neurons) and developmental stage (P3, E16, E13.5). Second, these differences may be due to different axonal culture (compartmentalized chamber vs. neuronal ball) and profiling methodologies

Table 2 | List of miRNAs enriched or depleted in axons, or present in growth cones during axon development.

miRNAs	Age	Species	Neuron type	Enriched/Depleted in axons ^a	Method used	References
let-7c	P3 ^c	Rat	SCG	Enriched	Microarray and qRT-PCR	Natera-Naranjo et al., 2010
let-7-e	E13.5 ^d	Mouse	DRG	Enriched	qRT-PCR	Hancock et al., 2014
let-7-i	E13.5 ^d	Mouse	DRG	Depleted	qRT-PCR	Hancock et al., 2014
miR-9	E16 ^d	Mouse	Cortical	Depleted	Multiplex qRT-PCR	Sasaki et al., 2013
miR-9 ^a	E17 ^d	Mouse	Cortical	Present	qRT-PCR	Dajas-Bailador et al., 2012
miR-15b	P3 ^c	Rat	SCG	Enriched	Microarray and qRT-PCR	Natera-Naranjo et al., 2010
miR-16 ^b	P3 ^c	Rat	SCG	Enriched	Microarray and qRT-PCR	Natera-Naranjo et al., 2010
miR-16	E13.5 ^d	Mouse	DRG	Depleted	qRT-PCR	Hancock et al., 2014
miR-17	E13.5 ^d	Mouse	DRG	Enriched	qRT-PCR	Hancock et al., 2014
miR-18a	E18	Rat	Cortical	Enriched	RT-PCR	Zhang et al., 2013
miR-19a	E18	Rat	Cortical	Enriched	RT-PCR	Zhang et al., 2013
miR-19b	E13.5 ^d	Mouse	DRG	Enriched	qRT-PCR	Hancock et al., 2014
miR-23a	P3 ^c	Rat	SCG	Enriched	Microarray and qRT-PCR	Natera-Naranjo et al., 2010
miR-23b	P3 ^c	Rat	SCG	Enriched	Microarray and qRT-PCR	Natera-Naranjo et al., 2010
miR-24	P3 ^c	Rat	SCG	Enriched	Microarray and qRT-PCR	Natera-Naranjo et al., 2010
miR-24	E13.5 ^d	Mouse	DRG	Enriched	qRT-PCR	Hancock et al., 2014
miR-26a	P3 ^c	Rat	SCG	Enriched	Microarray and qRT-PCR	Natera-Naranjo et al., 2010
miR-29a	E13.5 ^d	Mouse	DRG	Enriched	qRT-PCR	Hancock et al., 2014
miR-30b	E13.5 ^d	Mouse	DRG	Enriched	qRT-PCR	Hancock et al., 2014
miR-30c	E13.5 ^d	Mouse	DRG	Enriched	qRT-PCR	Hancock et al., 2014
miR-34b-3p	E13.5 ^d	Mouse	DRG	Depleted	qRT-PCR	Hancock et al., 2014
miR-92	E18	Rat	Cortical	Enriched	RT-PCR	Zhang et al., 2013
miR-103	P3 ^c	Rat	SCG	Enriched	Microarray and qRT-PCR	Natera-Naranjo et al., 2010
miR-106a	E13.5 ^d	Mouse	DRG	Enriched	qRT-PCR	Hancock et al., 2014
miR-124	P3 ^c	Rat	SCG	Depleted	Microarray and qRT-PCR	Natera-Naranjo et al., 2010
miR-125a-5p	E13.5 ^d	Mouse	DRG	Enriched	qRT-PCR	Hancock et al., 2014
miR-125b	P3 ^c	Rat	SCG	Enriched	Microarray and qRT-PCR	Natera-Naranjo et al., 2010
miR-127	P3 ^c	Rat	SCG	Enriched	Microarray and qRT-PCR	Natera-Naranjo et al., 2010
miR-132 ^b	E13.5 ^d	Mouse	DRG	Enriched	qRT-PCR	Hancock et al., 2014
miR-134 ^a	St22	<i>Xen.</i>	Spinal	Present	qRT-PCR, FISH	Han et al., 2011
miR-135a	E16 ^d	Mouse	Cortical	Depleted	Multiplex qRT-PCR	Sasaki et al., 2013
miR-137	E16 ^d	Mouse	Cortical	Depleted	Multiplex qRT-PCR	Sasaki et al., 2013
miR-138	E13.5 ^d	Mouse	DRG	Enriched	qRT-PCR	Hancock et al., 2014
miR-181a-1 ^b	E16 ^d	Mouse	Cortical	Enriched	Multiplex qRT-PCR	Sasaki et al., 2013
miR-182	E13.5 ^d	Mouse	DRG	Enriched	qRT-PCR	Hancock et al., 2014
miR-185	P3 ^c	Rat	SCG	Enriched	Microarray and qRT-PCR	Natera-Naranjo et al., 2010
miR-191	E13.5 ^d	Mouse	DRG	Enriched	qRT-PCR	Hancock et al., 2014
miR-195	E16 ^d	Mouse	Cortical	Depleted	Multiplex qRT-PCR	Sasaki et al., 2013
miR-196c	E13.5 ^d	Mouse	DRG	Depleted	qRT-PCR	Hancock et al., 2014
miR-204	P3 ^c	Rat	SCG	Enriched	Microarray and qRT-PCR	Natera-Naranjo et al., 2010
miR-206	P3 ^c	Rat	SCG	Depleted	Microarray and qRT-PCR	Natera-Naranjo et al., 2010
miR-218	E16 ^d	Mouse	Cortical	Depleted	Multiplex qRT-PCR	Sasaki et al., 2013
miR-221 ^b	P3 ^c	Rat	SCG	Enriched	Microarray and qRT-PCR	Natera-Naranjo et al., 2010
miR-296	E16 ^d	Mouse	Cortical	Depleted	Multiplex qRT-PCR	Sasaki et al., 2013
miR-297	P3 ^c	Rat	SCG	Depleted	Microarray and qRT-PCR	Natera-Naranjo et al., 2010
miR-320	P3 ^c	Rat	SCG	Enriched	Microarray and qRT-PCR	Natera-Naranjo et al., 2010
miR-328	E16 ^d	Mouse	Cortical	Depleted	Multiplex qRT-PCR	Sasaki et al., 2013
miR-328	E13.5 ^d	Mouse	DRG	Enriched	qRT-PCR	Hancock et al., 2014
miR-329	P3 ^c	Rat	SCG	Enriched	Microarray and qRT-PCR	Natera-Naranjo et al., 2010
miR-342-3p	E13.5 ^d	Mouse	DRG	Enriched	qRT-PCR	Hancock et al., 2014
miR-361	E16 ^d	Mouse	Cortical	Enriched	Multiplex qRT-PCR	Sasaki et al., 2013

(Continued)

Table 2 | Continued

miRNAs	Age	Species	Neuron type	Enriched/Depleted in axons ^a	Method used	References
miR-379	E16 ^d	Mouse	Cortical	Depleted	Multiplex qRT-PCR	Sasaki et al., 2013
miR-382	P3 ^c	Rat	SCG	Enriched	Microarray and qRT-PCR	Natera-Naranjo et al., 2010
miR-384-5p	E13.5 ^d	Mouse	DRG	Enriched	qRT-PCR	Hancock et al., 2014
miR-423	E16 ^d	Mouse	Cortical	Depleted	Multiplex qRT-PCR	Sasaki et al., 2013
miR-434-3p	E16 ^d	Mouse	Cortical	Depleted	Multiplex qRT-PCR	Sasaki et al., 2013
miR-434-3p	E13.5 ^d	Mouse	DRG	Enriched	qRT-PCR	Hancock et al., 2014
miR-484	E13.5 ^d	Mouse	DRG	Enriched	qRT-PCR	Hancock et al., 2014
miR-495	E13.5 ^d	Mouse	DRG	Enriched	qRT-PCR	Hancock et al., 2014
miR-532 ^b	E16 ^d	Mouse	Cortical	Enriched	Multiplex qRT-PCR	Sasaki et al., 2013
miR-541	P3 ^c	Rat	SCG	Enriched	Microarray and qRT-PCR	Natera-Naranjo et al., 2010
miR-680	E13.5 ^d	Mouse	DRG	Enriched	qRT-PCR	Hancock et al., 2014
miR-685	E16 ^d	Mouse	Cortical	Enriched	Multiplex qRT-PCR	Sasaki et al., 2013
miR-709	E16 ^d	Mouse	Cortical	Enriched	Multiplex qRT-PCR	Sasaki et al., 2013
miR-720	E16 ^d	Mouse	Cortical	Enriched	Multiplex qRT-PCR	Sasaki et al., 2013

^a miRNA detected ("present") in axons and growth cones.

^b miRNAs enriched in axons and detected in growth cones by fluorescent *in situ* hybridization.

^c neuron cultured for 3–10 days *in vitro*.

^d neurons cultured for 4 days *in vitro*.

Abbreviations: E, embryonic day; DRG, Dorsal Root Ganglion; SCG, Superior Cervical Ganglion; st, stage; P, postnatal day; Xen., Xenopus.

(microarray/qRT-PCR vs. multiplex qRT-PCR). Third, they may be due to limited coverage of the known mature miRNAs to date (miRbase release 19), and the different cut-off values used for analyses. In addition in the first two studies, the majority of miRNAs appear to be distributed in both cell body and axonal compartments, suggesting that most miRNAs might not have a preferred site of action (Natera-Naranjo et al., 2010; Sasaki et al., 2013). Intriguingly, the presence of miRNAs in axons and growth cones, and to some extent differentially expressed miRNAs derived from the same polycistron (Natera-Naranjo et al., 2010; Kaplan et al., 2013; Zhang et al., 2013), suggest that a mechanism of transport similar to that speculated for dendrites exists (Kosik, 2006). Mature miRNAs could thus be translocated along axons to growth cones either as individual molecules, as precursors, or within ribonucleoparticle bound to their targets and components of the silencing machinery. For instance, pre-miR-134 was recently documented to localize to dendrites through DEAH-box helicase DHX36-mediated transport (Bicker et al., 2013). Overall, these findings point to the possibility that miRNAs might be transported to and function within growth cones to modulate steering.

miRNA RISC machinery is present in growth cones

Several studies have demonstrated the silencing machinery RISC (RNA-induced silencing complex) is present and functional in growth cone, further supporting a potential role of miRNA in growth cones. Argonautes (ago) are the catalytic components of RISC. Four Ago proteins are reported in vertebrates (mammals), each binding a similar repertoire of miRNA and mRNA targets (Meister, 2013). While ago 2 was reported to induce mRNA target cleavage with perfect complementarity with a given miRNA, the roles of ago1, 3, and 4 are still elusive. Another RISC component,

Table 3 | Reports of miRNA processing machinery in neurons.

RISC component	Species	Neuron type	Age	References
Dicer	Rat	DRG	E15 ^a	Hengst et al., 2006
	Rat	Cortical	E18	Zhang et al., 2013
	Rat	SCG	P3 ^b	Aschrafi et al., 2008
	Mouse	DRG	E13.5 ^b	Hancock et al., 2014
ago2	Rat	Cortical	E18	Zhang et al., 2013
	Mouse	DRG	E13.5 ^b	Hancock et al., 2014
ago3	Rat	DRG	E15 ^b	Hengst et al., 2006
ago4	Rat	DRG	E15 ^b	Hengst et al., 2006
GW182	Mouse	Cortical	E17 ^b	Dajas-Bailador et al., 2012

^a neurons cultured for 3–7 days *in vitro*; ^b neurons cultured for 3 days *in vitro*.
Abbreviations: DIV, Days *in vitro*; DRG, Dorsal Root Ganglion; SCG, Superior Cervical Ganglion.

GW182 protein family (TNRC6 in mammals), coordinates all downstream steps in gene silencing (Pfaff et al., 2013). Key molecules for small RNA-mediated silencing such as ago2 (Zhang et al., 2013; Hancock et al., 2014), ago 3 and 4 (Hengst et al., 2006), eIF2c (Eukaryotic Initiation Factor 2C) (Aschrafi et al., 2008) and GW182 (Dajas-Bailador et al., 2012) were detected in the embryonic and perinatal distal axons, and/or growth cones of various cell types (Table 3). In addition, one study also revealed that RISC is functional in distal axons (Hengst et al., 2006). Exogenous siRNA directed against RhoA, a small GTPase protein led to the decrease in RhoA transcript and RhoA immunoreactivity in distal axons. Importantly, FITC-labeled siRNA was not detected in proximal axons, and no RhoA mRNA knockdown was

detected in the somatodendritic compartment. Taken together, these data revealed that exogenous siRNA-induced silencing exists in distal axons (Hengst et al., 2006). It would be interesting to explore whether RISC can also mediate endogenous miRNA action in this compartment, and most specifically in growth cones. Intriguingly, the RISC component Dicer is also detected in distal axons, including growth cones (Hengst et al., 2006; Zhang et al., 2013; Hancock et al., 2014). This suggests that, as in dendrites (Bicker et al., 2013), pre-miRNAs could be transported and processed into mature miRNAs, in this compartment. Axonal transfection of pre-miR-338 and pre-miR-16 indeed result in a substantial increase in their concomitant mature form in axons, suggesting that miRNA processing does occur in distal axons (Aschrafi et al., 2008; Kar et al., 2013). Several key components are thus present in growth cones and/or distal axons, and RNA interference occurs in this compartment, suggesting that miRNAs are likely to be functional there. The documented presence of RISC components Armitage, MOV10 and Dicer (Lugli et al., 2005; Ashraf et al., 2006; Banerjee et al., 2009) in pre- and post-synaptic compartments underscore that miRNAs may have broader subcellular sites of action in polarized cells like neurons.

Do miRNAs play a local role in growth cone turning?

The presence of RISC within growth cones suggests that miRNAs could act locally within this compartment and shape the local transcriptome during axon guidance. In particular, miRNAs could regulate local translation, known to play a role in growth cone steering in response to some cues (Jung et al., 2011). Although this has yet to be clearly demonstrated, recent studies suggest that it might be the case.

miRNAs are known to regulate outgrowth in development and following injury (Wu and Murashov, 2013; Chiu et al., 2014). miRNA-mediated silencing of mRNA was recently reported to occur locally within axons to modulate outgrowth. Axonal miRNAs were initially documented to inhibit the translation of cytoskeletal regulatory molecules locally (Dajas-Bailador et al., 2012; Hancock et al., 2014). Using mice cortical neurons, Dajas-Bailador et al. (2012) first revealed that a miRNA, miR-9, modulates the translational repression of exogenous Map1b (microtubule-associated protein 1b) 3'UTR, which has a key role in the regulation of dynamic microtubules. Short BDNF stimulation modulated miR-9 expression, while inhibition of miR-9 affected axonal growth only when applied locally in axons, suggesting that BDNF affects this developmental process via local, miRNA-mediated translational control of a cytoskeletal regulator. Further support for such local mechanisms came in a recent study from Flanagan's group (Hancock et al., 2014). Hancock and colleagues reported that axon-enriched miR-132 promotes embryonic DRG axon outgrowth by targeting endogenous p120RasGAP (Rasa1), a protein involved in cytoskeletal regulation (Hancock et al., 2014). Interestingly, miR-132-induced increase in axonal Rasa1 protein level was dependent on local protein synthesis, as it was abolished in the presence of translation inhibitor applied to severed axons (Hancock et al., 2014). This demonstrated that miR-132 acts indeed within this cell compartment to regulate target translation, removing the possibility of cross-talk with the cell body. Of note, Rasa 1 was previously reported to mediate

responsiveness to chemotropic cues but here, miR-132 activity did not change upon stimulation by a few guidance molecules suggesting that these findings may not be strictly transposed to the guidance field (Hancock et al., 2014). In addition, axonal miRNAs were also recently documented to promote outgrowth by silencing axonal transcripts other than cytoskeletal regulators. Using 3d rat SCG neurons, Kar and colleagues reported that axon abundant miR-16 reduces the levels of the eukaryotic translation initiation factors eIF2B2 and eIF4G2 mRNAs, specifically within axons without affecting the levels of these transcripts in the soma (Kar et al., 2013). Interestingly, axonal miR-16 reduced outgrowth, and siRNA-mediated decrease in eIF2B2 and eIF4G2 levels in axons lead to inhibition of local protein synthesis and reduced axon extension. Together, this suggests that miR-16 might regulate elongation by modulating the axonal protein synthetic system. Finally using rat E18 cortical neurons, Zhang et al. (2013) documented that axonal miR-19a, a member of the miR-17-92 cluster, regulates axon outgrowth via PTEN (phosphatase and tensin homolog), a negative regulator of the PI3K/mTOR signaling pathway. Importantly, axonal miR-19a regulates PTEN protein levels specifically within axons and not at the cell soma suggesting compartmentalized action for this miRNA. Local regulation of mRNA by miRNA has thus been reported in axons in a biological context of elongation.

The possibility that miRNA-mediated regulation of growth cone turning via local regulation of mRNA is further supported by a recent study. Several years ago, miR-134 was shown to locally modulate the size of dendritic spines of rat hippocampal cells (Schratt et al., 2006). This miRNA keeps Limk1, a kinase regulating actin polymerization, in a dormant untranslated state, and releases its repression in response to extracellular BDNF stimulation. Limk1 is thus translated, resulting in spine size increase (Schratt et al., 2006). Zheng's group recently investigated whether this mechanism is conserved in growth cones of *X. laevis* spinal neurons, where they detected this miRNA (Han et al., 2011). Similar to dendritic spines, miR-134 was found to be important for BDNF-induced growth cone attraction. In addition, miR-134 appeared to regulate protein synthesis in response to this cue, as loss- and gain-of-function of miR-134 in the whole embryo blocked protein synthesis dependent turning response of growth cones. The effect of this miRNAs on spinal neuron cell bodies cannot be formally excluded, since miR-134 was knocked down or overexpressed in whole embryos, and not exclusively in axons. Limk1, also detected in spinal growth cones, was confirmed as a *bona fide* target of miR-134 in *Xenopus* by *in vivo* luciferase assay. This suggests that Limk1 may mediate miR-134 regulation of BDNF-induced growth cone attraction. All-in-all, this study provided the first evidence, that growth cone turning can be modulated by miRNAs. It also indicated that conserved miRNA-based local control may exist in neuronal compartments, enabling the acute regulation of cytoskeletal dynamics in response to external stimuli.

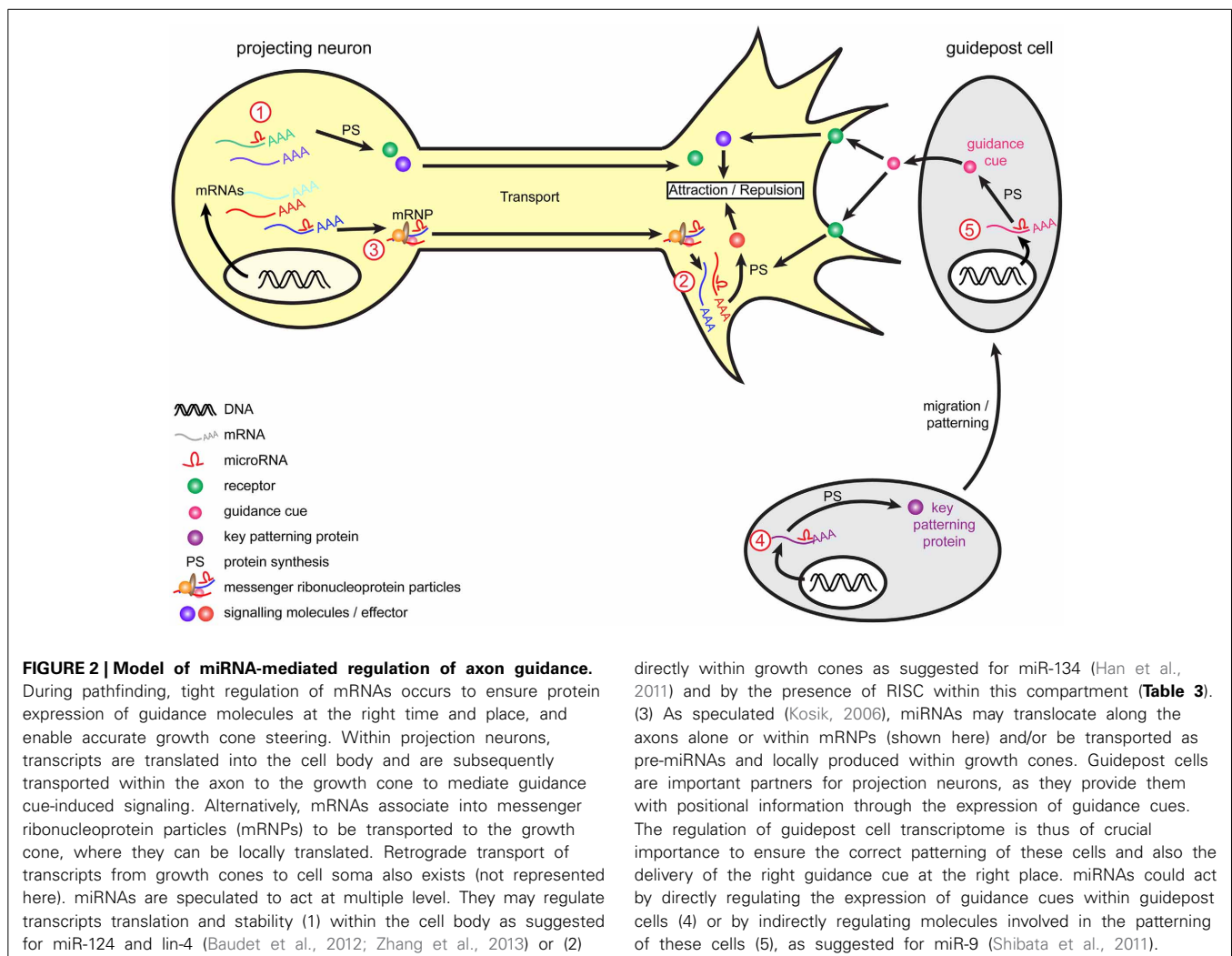
Based on these recent findings, one could speculate that several possible mechanisms of mRNA regulation in growth cones exist during steering. On the one hand miRNAs could silence translation, keeping the transcript dormant until a cue is encountered, and a newly synthesized protein is asymmetrically required.

Similar mechanisms of action are also reported in dendrites (Schratt et al., 2006; Siegel et al., 2009) suggesting they could be conserved across neuronal compartments. On the other end, cue-induced activation of miRNAs could lead to the inhibition of transcript translation and/or stability, when newly synthesized protein(s) are no longer required for guidance. In particular, such silencing could arrest cue-induced translation of mRNA, thereby terminating growth cone response to a given chemotropic cue. Furthermore, an asymmetric rise in local mRNA translation of a cytoskeletal protein was reported to occur at the growth cone on the side of cue exposure (Leung et al., 2006). From this, one could finally conceive that miRNAs may have an asymmetric function in this compartment, allowing silencing to occur on one side of the growth cone, and translation on the other. This putative mechanism might be unique to growth cones, as opposed to dendrites or synapses, to support directional steering.

CONCLUSIVE REMARKS AND PERSPECTIVES

In conclusion, recent studies have uncovered that miRNAs are hitherto unsuspected, important regulatory molecules in axon guidance (Figure 1) (Giraldez et al., 2005; Pinter and Hindges,

2010; Han et al., 2011; Shibata et al., 2011; Baudet et al., 2012; Zou et al., 2012). These have revealed that miRNAs are likely to have widespread and important roles, affecting different species and several projections, and when knocked out, result in varying degrees of severity in guidance errors. The studies have also shown that miRNAs are likely to regulate both guidance response to cues or cue expression. In particular, miRNAs can specifically modulate growth cone steering (Han et al., 2011; Baudet et al., 2012). To do so, they can act cell-autonomously to fine-tune the molecular make-up of projection neurons, thereby affecting their responsiveness to cues. This regulation may take place at the soma, via transcription factor regulation, which in turn, modulates expression levels of receptors to cues (Baudet et al., 2012; Zou et al., 2012). miRNAs are also suspected to act locally, and affect downstream signaling molecules of various nature including axon cytoskeleton (Han et al., 2011; Dajas-Bailador et al., 2012; Kar et al., 2013; Hancock et al., 2014). Although the evidence is more elusive, miRNAs could also modulate brain patterning, and thereby control either the presence of guidepost cells or the expression of guidance cues at key topographical locations (Pinter and Hindges, 2010; Shibata et al., 2011) (Figures 1, 2).



Guidance molecules appear to have pleiotropic roles and as such, are involved in several processes outside of the nervous system development. In particular, they are now acknowledged regulators of the immune and cardiovascular systems, including of vascular development, and angiogenesis (Adams and Eichmann, 2010; Kumanogoh and Kikutani, 2013). Guidance cues are also involved in pathological processes such as cancer and tumor progression (Chédotal, 2007; Mehlen et al., 2011). miRNAs, as key post-transcriptional regulator in most eukaryotic cells, are also implicated in these physiological and pathophysiological processes (Croce, 2009; Xiao and Rajewsky, 2009; Small and Olson, 2011) suggesting a possible mechanistic link between the two class of molecules outside of the nervous system. Importantly, several miRNAs modulate guidance cues and their receptors in cells other than neurons, including cancer cell lines but also in endothelial cells (Table 4) (Baudet et al., 2013). This raises the intriguing possibility that a given miRNA may regulate the same guidance molecules in different cellular contexts.

miRNAs may have conserved important developmental roles, including axon guidance, throughout evolution. Indeed, miRNAs appear to regulate pathfinding in several species, ranging from *Drosophila* and *C. elegans* to mice and guidance miRNAs affect the same pathway in different species (e.g., the visual pathway of lower vertebrate Baudet et al., 2012 vs. higher vertebrates Pinter and Hindges, 2010). Moreover, a specific miRNA, miR-9, regulates guidance of different tracts (Shibata et al., 2011). Interestingly, two of the four miRNAs involved in guidance, miR-124, lin-4/miR-125, are highly conserved, and considered as ancient miRNAs with neural-like function (Christodoulou et al., 2010). Unsurprisingly, these miRNAs appear to have

multifactorial neural action, and besides regulating guidance, also modulate earlier developmental events such as neurogenesis, cell fate determination, lineage progression, and later events such as synaptogenesis (Gao, 2010).

Guidance miRNAs appear to have a delicate regulatory action on guidance signaling pathways. The three miRNAs, for which signaling mechanisms have been uncovered, fine-tune the levels of their endogenous (Baudet et al., 2012; Zou et al., 2012) or exogenous targets (Han et al., 2011). This is very much in agreement with recent evidence that miRNAs do not act as off-switches, as originally thought from earlier studies in *C. elegans*, but rather as a rheostat, which fine-tunes protein output to functional levels (Baek et al., 2008; Selbach et al., 2008; Bartel, 2009; Guo et al., 2010). It is thus particularly interesting that mRNAs translated in the growth cone give rise to only small increases in protein levels (Jung et al., 2011), consistent with the hypothesis that miRNAs might be responsible for this. miRNAs may thus provide an additional layer of gene regulation in projection neurons, to ensure that guidance molecules are expressed at the right time and place, supporting the high level of precision critical for axon guidance.

Navigating growth cones are exposed to a myriad of cues along their pathway, and it appears that cross-talk exists between these cues and miRNAs. miRNAs can intrinsically alter the way growth cones respond to a cue, modulating the levels of their cognate receptor (Baudet et al., 2012; Zou et al., 2012). Conversely, cues also modulate miRNA's silencing potential at the growth cone. For instance, they are suspected to repress miRNA-mediated silencing, leading to local protein translation and growth cone steering (Han et al., 2011). Cues can induce a rise in miRNA levels in axons, which in turn leads to increased post-transcriptional gene silencing (Dajas-Bailador et al., 2012). The exact signaling mechanisms mediating cue-regulated miRNA action are unknown. One possibility, as has been previously shown in dendrites (Schratt et al., 2006), includes phosphorylation and activation of mTOR pathway, which is a suspected global regulator of translational activity in growth cones (Jung et al., 2012). Furthermore, cues or any external stimulus affecting the neuronal projection could also shape the miRNA repertoire of the whole neuron or specifically that of the growth cone. External stimuli were reported to either activate Dicer (Lugli et al., 2005) or degrade the RISC component (MOV10) (Banerjee et al., 2009) at the synapse- another neuronal compartment. In addition, neuronal activity was also shown to regulate miRNA turnover rate, by modulating their transcription or promoting their decay (Krol et al., 2010a), which in turn can affect dendritic remodeling (Fiore et al., 2009). A similar cue-mediated regulation of miRNA levels is conceivable in axons of projecting neurons.

Recent evidence has revealed that miRNA function could be modulated by different means. For instance, RNA-binding proteins (RNA-BP) were shown to either act in concert with miRNAs to promote silencing or, on the contrary, to compete for binding sites (Krol et al., 2010b). For instance miR-125a and Fragile X mental retardation protein (FMRP) were revealed to act cooperatively at the 3'UTR of PSD-95 mRNA to inhibit translation of this transcript within synapses (Muddashetty et al., 2011). miRNAs can also actively regulate RNA-BP in neurons (Fiore et al.,

Table 4 | List of miRNAs regulating guidance molecules in non-neuronal cells.

miRNA	Target	Cell type	References
miR-9	Neuropilin-1	Endothelial cells	Cui et al., 2012
miR 27a/b	Sema 6a	Endothelial cells	Urbich et al., 2012
miR-34	Sema 4b	Cardiomyoblast H9c2 cells	Bernardo et al., 2012
miR-181b	Neuropilin-1	Endothelial cells	Cui et al., 2012
miR-210	EphrinA3	U2OS osteosarcoma cell line	Fasanaro et al., 2008
miR-210	EphrinA3	293T cells	Pulkkinen et al., 2008
miR-214	Plexin -B1	HeLa cells	Qiang et al., 2011
miR-218	Robo1	Human breast cancer cells	Yang et al., 2012
miR-218	Robo1	Nasopharyngeal carcinoma	Alajez et al., 2011
miR-218	Robo1 and 2	HeLa cells	Fish et al., 2011
miR-218	Robo1 and 2	COS cells	Small et al., 2010
miR-218	Robo1	Human gastric cell lines	Tie et al., 2010
miR-320	Neuropilin-1	Colorectal cancer cells	Zhang et al., 2012
miR-331-3p	Neuropilin-2	Glioblastoma multiforme	Epis et al., 2009

2009). RNA-BPs play important roles in developing projection neurons, ensuring mRNA transport and translational repression (Hörnberg and Holt, 2013). It is therefore conceivable that these two classes of molecules act in a coordinated manner to modulate transcript levels during axon guidance. In addition, other classes of non-coding RNAs, such as endogenous circular miRNA (Hansen et al., 2013; Memczak et al., 2013) and long-non-coding RNAs, have emerged as important regulators of miRNA action, acting as decoy or sponges that sequester, and thus buffer miRNAs in the cell (Salmena et al., 2011). Such endogenous competing RNAs (ceRNAs) might also include transcripts of protein-coding genes, whose miRNA-mediated silencing does not affect their function (Seitz, 2009; Salmena et al., 2011). In projection neurons, these ceRNAs could modulate miRNA access to their target transcript, providing an additional layer of regulation, and enabling fine-tuning of their translation. However, their existence and function in cells during axon guidance is yet to be demonstrated.

In conclusion, while the body of work reviewed here has just started to reveal the role of miRNAs in axon guidance, future research promises to unravel how these key regulatory molecules are embedded in the molecular network that enables axons to navigate to their targets with extreme precision.

ACKNOWLEDGMENTS

The authors thank Giovanni Stefani (University of Trento, Italy), Hosung Jung (Yonsei University College of Medicine, Korea) and ASK Scientific (askscientific.com) for their valuable comments on the manuscript. Archana N. Iyer is a recipient of a University of Trento PhD studentship, Anaïs Bellon of EMBO and Human Frontier Fellowships, Marie-Laure Baudet of a G. Armenise-Harvard Foundation Career Development grant, and of a University of Trento start-up grant.

REFERENCES

- Adams, R. H., and Eichmann, A. (2010). Axon guidance molecules in vascular patterning. *Cold Spring Harb. Perspect. Biol.* 2:a001875. doi: 10.1101/cshperspect.a001875
- Alajez, N. M., Lenarduzzi, M., Ito, E., Hui, A. B., Shi, W., Bruce, J., et al. (2011). MiR-218 suppresses nasopharyngeal cancer progression through downregulation of survivin and the SLIT2-ROBO1 pathway. *Cancer Res.* 71, 2381–2391. doi: 10.1158/0008-5472.CAN-10-2754
- Aschrafi, A., Schwechter, A. D., Mameza, M. G., Natera-Naranjo, O., Gioio, A. E., and Kaplan, B. B. (2008). MicroRNA-338 regulates local cytochrome c oxidase IV mRNA levels and oxidative phosphorylation in the axons of sympathetic neurons. *J. Neurosci.* 28, 12581–12590. doi: 10.1523/JNEUROSCI.3338-08.2008
- Ashraf, S. I., McLoon, A. L., Sclarsic, S. M., and Kunes, S. (2006). Synaptic protein synthesis associated with memory is regulated by the RISC pathway in *Drosophila*. *Cell* 124, 191–205. doi: 10.1016/j.cell.2005.12.017
- Baek, D., Villén, J., Shin, C., Camargo, F. D., Gygi, S. P., and Bartel, D. P. (2008). The impact of microRNAs on protein output. *Nature* 455, 64–71. doi: 10.1038/nature07242
- Banerjee, S., Neveu, P., and Kosik, K. S. (2009). A coordinated local translational control point at the synapse involving relief from silencing and MOV10 degradation. *Neuron* 64, 871–884. doi: 10.1016/j.neuron.2009.11.023
- Bartel, D. P. (2009). MicroRNAs: target recognition and regulatory functions. *Cell* 136, 215–233. doi: 10.1016/j.cell.2009.01.002
- Baudet, M.-L., Bellon, A., and Holt, C. E. (2013). Role of microRNAs in Semaphorin function and neural circuit formation. *Semin. Cell Dev. Biol.* 24, 146–155. doi: 10.1016/j.semcdb.2012.11.004
- Baudet, M.-L., Zivraj, K. H., Abreu-Goodger, C., Muldal, A., Armisen, J., Blenkinsop, C., et al. (2012). miR-124 acts through CoREST to control onset of Sema3A sensitivity in navigating retinal growth cones. *Nat. Neurosci.* 15, 29–38. doi: 10.1038/nn.2979
- Bernardo, B. C., Gao, X.-M., Winbanks, C. E., Boey, E. J. H., Tham, Y. K., Kiriazis, H., et al. (2012). Therapeutic inhibition of the miR-34 family attenuates pathological cardiac remodeling and improves heart function. *Proc. Natl. Acad. Sci.* 109, 17615–17620. doi: 10.1073/pnas.1206432109
- Bernstein, E., Caudy, A. A., Hammond, S. M., and Hannon, G. J. (2001). Role for a bidentate ribonuclease in the initiation step of RNA interference. *Nature* 409, 363–366. doi: 10.1038/35053110
- Bicker, S., Khudayberdiev, S., Weiß, K., Zocher, K., Baumeister, S., and Schrat, G. (2013). The DEAH-box helicase DHX36 mediates dendritic localization of the neuronal precursor-microRNA-134. *Genes Dev.* 27, 991–996. doi: 10.1101/gad.211243.112
- Campbell, D. S., Regan, A. G., Lopez, J. S., Tannahill, D., Harris, W. A., and Holt, C. E. (2001). Semaphorin 3A elicits stage-dependent collapse, turning, and branching in *Xenopus* retinal growth cones. *J. Neurosci.* 21, 8538–8547.
- Chalfie, M., Horvitz, H. R., and Sulston, J. E. (1981). Mutations that lead to reiterations in the cell lineages of *C. elegans*. *Cell* 24, 59–69. doi: 10.1016/0092-8674(81)90501-8
- Chang, C., Yu, T. W., Bargmann, C. I., and Tessier-Lavigne, M. (2004a). Inhibition of netrin-mediated axon attraction by a receptor protein tyrosine phosphatase. *Science* 305, 103–106. doi: 10.1126/science.1096983
- Chang, S., Johnston, R. J., Frøkjær-Jensen, C., Lockery, S., and Hobert, O. (2004b). MicroRNAs act sequentially and asymmetrically to control chemosensory laterality in the nematode. *Nature* 430, 785–789. doi: 10.1038/nature02752
- Chédotal, A. (2007). Chemotropic axon guidance molecules in tumorigenesis. *Prog. Exp. Tumor Res.* 39, 78–90. doi: 10.1159/000100048
- Cheloufi, S., Dos Santos, C. O., Chong, M. M. W., and Hannon, G. J. (2010). A Dicer-independent miRNA biogenesis pathway that requires Ago catalysis. *Nature* 465, 584–589. doi: 10.1038/nature09092
- Chiu, H., Alqadah, A., and Chang, C. (2014). The role of microRNAs in regulating neuronal connectivity. *Front. Cell. Neurosci.* 7:283. doi: 10.3389/fncel.2013.00283
- Chiu, H., and Chang, C. (2013). Rejuvenating nerve cells in adults. *Aging (Albany, NY)* 5, 485–486.
- Choi, P. S., Zakhary, L., Choi, W.-Y., Caron, S., Alvarez-Saavedra, E., Miska, E. A., et al. (2008). Members of the miRNA-200 family regulate olfactory neurogenesis. *Neuron* 57, 41–55. doi: 10.1016/j.neuron.2007.11.018
- Christodoulou, F., Raible, F., Tomer, R., Simakov, O., Trachana, K., Klaus, S., et al. (2010). Ancient animal microRNAs and the evolution of tissue identity. *Nature* 463, 1084–1088. doi: 10.1038/nature08744
- Cifuentes, D., Xue, H., Taylor, D. W., Patnode, H., Mishima, Y., Cheloufi, S., et al. (2010). A novel miRNA processing pathway independent of Dicer requires Argonaute2 catalytic activity. *Science* 328, 1694–1698. doi: 10.1126/science.1190809
- Cremisi, F. (2013). MicroRNAs and cell fate in cortical and retinal development. *Front. Cell. Neurosci.* 7:141. doi: 10.3389/fncel.2013.00141
- Croce, C. M. (2009). Causes and consequences of microRNA dysregulation in cancer. *Nat. Rev. Genet.* 10, 704–714. doi: 10.1038/nrg2634
- Cui, Y., Han, Z., Hu, Y., Song, G., Hao, C., Xia, H., et al. (2012). MicroRNA-181b and microRNA-9 mediate arsenic-induced angiogenesis via NRP1. *J. Cell. Physiol.* 227, 772–783. doi: 10.1002/jcp.22789
- Dajas-Bailador, F., Bonev, B., Garcez, P., Stanley, P., Guillemot, E., and Papalopulu, N. (2012). microRNA-9 regulates axon extension and branching by targeting Map1b in mouse cortical neurons. *Nat. Neurosci.* 15, 697–699. doi: 10.1038/nn.3082
- Decembrini, S., Bressan, D., Vignali, R., Pitto, L., Mariotti, S., Rainaldi, G., et al. (2009). MicroRNAs couple cell fate and developmental timing in retina. *Proc. Natl. Acad. Sci. U.S.A.* 106, 21179–21184. doi: 10.1073/pnas.0909167106
- Dent, E. W., Gupton, S. L., and Gertler, F. B. (2011). The growth cone cytoskeleton in axon outgrowth and guidance. *Cold Spring Harb. Perspect. Biol.* 3:a001800. doi: 10.1101/cshperspect.a001800
- Dickson, B. J. (2002). Molecular mechanisms of axon guidance. *Science* 298, 1959–1964. doi: 10.1126/science.1072165
- Ebert, M. S., and Sharp, P. A. (2012). Roles for MicroRNAs in conferring robustness to biological processes. *Cell* 149, 515–524. doi: 10.1016/j.cell.2012.04.005
- Epis, M. R., Giles, K. M., Barker, A., Kendrick, T. S., and Leedman, P. J. (2009). miR-331-3p regulates ERBB-2 expression and androgen receptor signaling in prostate cancer. *J. Biol. Chem.* 284, 24696–24704. doi: 10.1074/jbc.M109.030098

- Erskine, L., Reijntjes, S., Pratt, T., Denti, L., Schwarz, Q., Vieira, J. M., et al. (2011). VEGF signaling through neuropilin 1 guides commissural axon crossing at the optic chiasm. *Neuron* 70, 951–965. doi: 10.1016/j.neuron.2011.02.052
- Fasanaro, P., D'Alessandra, Y., Di Stefano, V., Melchionna, R., Romani, S., Pompilio, G., et al. (2008). MicroRNA-210 modulates endothelial cell response to hypoxia and inhibits the receptor tyrosine kinase ligand Ephrin-A3. *J. Biol. Chem.* 283, 15878–15883. doi: 10.1074/jbc.M800731200
- Fiore, R., Khudayberdiev, S., Christensen, M., Siegel, G., Flavell, S. W., Kim, T.-K., et al. (2009). Mef2-mediated transcription of the miR379–410 cluster regulates activity-dependent dendritogenesis by fine-tuning Pumilio2 protein levels. *EMBO J.* 28, 697–710. doi: 10.1038/emboj.2009.10
- Fish, J. E., Wythe, J. D., Xiao, T., Bruneau, B. G., Stainier, D. Y. R., Srivastava, D., et al. (2011). A Slit/miR-218/Robo regulatory loop is required during heart tube formation in zebrafish. *Development* 138, 1409–1419. doi: 10.1242/dev.060046
- Gao, F.-B. (2010). Context-dependent functions of specific microRNAs in neuronal development. *Neural Dev.* 5, 25. doi: 10.1186/1749-8104-5-25
- Giraldez, A. J., Cinalli, R. M., Glasner, M. E., Enright, A. J., Thomson, J. M., Baskerville, S., et al. (2005). MicroRNAs regulate brain morphogenesis in zebrafish. *Science* 308, 833–838. doi: 10.1126/science.1109020
- Griffiths-Jones, S. (2004). The microRNA Registry. *Nucleic Acids Res.* 32, D109–D111. doi: 10.1093/nar/gkh023
- Griffiths-Jones, S., Saini, H. K., van Dongen, S., and Enright, A. J. (2008). miR-Base: tools for microRNA genomics. *Nucleic Acids Res.* 36, D154–D158. doi: 10.1093/nar/gkm952
- Grishok, A., Pasquinelli, A. E., Conte, D., Li, N., Parrish, S., Ha, I., et al. (2001). Genes and mechanisms related to RNA interference regulate expression of the small temporal RNAs that control *C. elegans* developmental timing. *Cell* 106, 23–34. doi: 10.1016/S0092-8674(01)00431-7
- Gumy, L. F., Yeo, G. S. H., Tung, Y.-C. L., Zivraj, K. H., Willis, D., Coppola, G., et al. (2011). Transcriptome analysis of embryonic and adult sensory axons reveals changes in mRNA repertoire localization. *RNA* 17, 85–98. doi: 10.1261/rna.2386111
- Guo, H., Ingolia, N. T., Weissman, J. S., and Bartel, D. P. (2010). Mammalian microRNAs predominantly act to decrease target mRNA levels. *Nature* 466, 835–840. doi: 10.1038/nature09267
- Han, L., Wen, Z., Lynn, R. C., Baudet, M.-L., Holt, C. E., Sasaki, Y., et al. (2011). Regulation of chemotropic guidance of nerve growth cones by microRNA. *Mol. Brain* 4, 40. doi: 10.1186/1756-6606-4-40
- Hancock, M. L., Preitner, N., Quan, J., and Flanagan, J. G. (2014). MicroRNA-132 Is Enriched in Developing Axons, Locally Regulates Rasa1 mRNA, and Promotes Axon Extension. *J. Neurosci.* 34, 66–78. doi: 10.1523/JNEUROSCI.3371-13.2014
- Hansen, T. B., Jensen, T. I., Clausen, B. H., Bramsen, J. B., Finsen, B., Damgaard, C. K., et al. (2013). Natural RNA circles function as efficient microRNA sponges. *Nature* 495, 384–388. doi: 10.1038/nature11993
- Harris, W. A., Holt, C. E., and Bonhoeffer, F. (1987). Retinal axons with and without their somata, growing to and arborizing in the tectum of *Xenopus* embryos: a time-lapse video study of single fibres *in vivo*. *Development* 101, 123–133.
- Hengst, U., Cox, L. J., Macosko, E. Z., and Jaffrey, S. R. (2006). Functional and selective RNA interference in developing axons and growth cones. *J. Neurosci.* 26, 5727–5732. doi: 10.1523/JNEUROSCI.5229-05.2006
- Hörnberg, H., and Holt, C. (2013). RNA-binding proteins and translational regulation in axons and growth cones. *Front. Neurosci.* 7:81. doi: 10.3389/fnins.2013.00081
- Hsieh, J. (2012). Orchestrating transcriptional control of adult neurogenesis. *Genes Dev.* 26, 1010–1021. doi: 10.1101/gad.187336.112
- Huber, A. B., Kania, A., Tran, T. S., Gu, C., De Marco Garcia, N., Lieberam, I., et al. (2005). Distinct roles for secreted semaphorin signaling in spinal motor axon guidance. *Neuron* 48, 949–964. doi: 10.1016/j.neuron.2005.12.003
- Johnson, J. M., Edwards, S., Shoemaker, D., and Schadt, E. E. (2005). Dark matter in the genome: evidence of widespread transcription detected by microarray tiling experiments. *Trends Genet.* 21, 93–102. doi: 10.1016/j.tig.2004.12.009
- Johnston, R. J., and Hobert, O. (2003). A microRNA controlling left/right neuronal asymmetry in *Caenorhabditis elegans*. *Nature* 426, 845–849. doi: 10.1038/nature02255
- Jung, H., and Holt, C. E. (2011). Local translation of mRNAs in neural development. *Wiley Interdiscip. Rev. RNA* 2, 153–165. doi: 10.1002/wrna.53
- Jung, H., O'Hare, C. M., and Holt, C. E. (2011). Translational regulation in growth cones. *Curr. Opin. Genet. Dev.* 21, 458–464. doi: 10.1016/j.gde.2011.04.004
- Jung, H., Yoon, B. C., and Holt, C. E. (2012). Axonal mRNA localization and local protein synthesis in nervous system assembly, maintenance and repair. *Nat. Rev. Neurosci.* 13, 308–324. doi: 10.1038/nrn3274
- Kaplan, B. B., Kar, A. N., Gioio, A. E., and Aschrafi, A. (2013). MicroRNAs in the axon and presynaptic nerve terminal. *Front. Cell. Neurosci.* 7:126. doi: 10.3389/fncel.2013.00126
- Kar, A. N., MacGibeny, M. A., Gervasi, N. M., Gioio, A. E., and Kaplan, B. B. (2013). Intra-axonal synthesis of eukaryotic translation initiation factors regulates local protein synthesis and axon growth in rat sympathetic neurons. *J. Neurosci.* 33, 7165–7174. doi: 10.1523/JNEUROSCI.2040-12.2013
- Ketting, R. F., Fischer, S. E., Bernstein, E., Sijen, T., Hannon, G. J., and Plasterk, R. H. (2001). Dicer functions in RNA interference and in synthesis of small RNA involved in developmental timing in *C. elegans*. *Genes Dev.* 15, 2654–2659. doi: 10.1101/gad.927801
- Knight, S. W., and Bass, B. L. (2001). A role for the RNase III enzyme DCR-1 in RNA interference and germ line development in *Caenorhabditis elegans*. *Science* 293, 2269–2271. doi: 10.1126/science.1062039
- Kolodkin, A. L., and Tessier-Lavigne, M. (2011). Mechanisms and molecules of neuronal wiring: a primer. *Cold Spring Harb. Perspect. Biol.* 3:a001727. doi: 10.1101/cshperspect.a001727
- Kosik, K. S. (2006). The neuronal microRNA system. *Nat. Rev. Neurosci.* 7, 911–920. doi: 10.1038/nrn2037
- Kozomara, A., and Griffiths-Jones, S. (2011). miRBase: integrating microRNA annotation and deep-sequencing data. *Nucleic Acids Res.* 39, D152–D157. doi: 10.1093/nar/gkq1027
- Kozomara, A., and Griffiths-Jones, S. (2013). miRBase: annotating high confidence microRNAs using deep sequencing data. *Nucleic Acids Res.* 42, D68–D73. doi: 10.1093/nar/gkt1181
- Krichevsky, A. M., King, K. S., Donahue, C. P., Khrapko, K., and Kosik, K. S. (2003). A microRNA array reveals extensive regulation of microRNAs during brain development. *RNA* 9, 1274–1281. doi: 10.1261/rna.5980303
- Krol, J., Busskamp, V., Markiewicz, I., Stadler, M. B., Ribi, S., Richter, J., et al. (2010a). Characterizing light-regulated retinal microRNAs reveals rapid turnover as a common property of neuronal microRNAs. *Cell* 141, 618–631. doi: 10.1016/j.cell.2010.03.039
- Krol, J., Loedige, I., and Filipowicz, W. (2010b). The widespread regulation of microRNA biogenesis, function and decay. *Nat. Rev. Genet.* 11, 597–610. doi: 10.1038/nrg2843
- Kumanogoh, A., and Kikutani, H. (2013). Immunological functions of the neuropilins and plexins as receptors for semaphorins. *Nat. Rev. Immunol.* 13, 802–814. doi: 10.1038/nri3545
- Kuwajima, T., Yoshida, Y., Takegahara, N., Petros, T. J., Kumanogoh, A., Jessell, T. M., et al. (2012). Optic chiasm presentation of Semaphorin6D in the context of Plexin-A1 and Nr-CAM promotes retinal axon midline crossing. *Neuron* 74, 676–690. doi: 10.1016/j.neuron.2012.03.025
- Kwok, J. C. F., Yuen, Y.-L., Lau, W.-K., Zhang, F.-X., Fawcett, J. W., Chan, Y.-S., et al. (2012). Chondroitin sulfates in the developing rat hindbrain confine commissural projections of vestibular nuclear neurons. *Neural Dev.* 7, 6. doi: 10.1186/1749-8104-7-6
- Kye, M.-J., Liu, T., Levy, S. F., Xu, N. L., Groves, B. B., Bonneau, R., et al. (2007). Somatodendritic microRNAs identified by laser capture and multiplex RT-PCR. *RNA* 13, 1224–1234. doi: 10.1261/rna.480407
- Landgraf, P., Rusu, M., Sheridan, R., Sewer, A., Iovino, N., Aravin, A., et al. (2007). A mammalian microRNA expression atlas based on small RNA library sequencing. *Cell* 129, 1401–1414. doi: 10.1016/j.cell.2007.04.040
- La Torre, A., Georgi, S., and Reh, T. A. (2013). Conserved microRNA pathway regulates developmental timing of retinal neurogenesis. *Proc. Natl. Acad. Sci. U.S.A.* 110, E2362–E2370. doi: 10.1073/pnas.1301837110
- Lee, R. C., Feinbaum, R. L., and Ambros, V. (1993). The *C. elegans* heterochronic gene lin-4 encodes small RNAs with antisense complementarity to lin-14. *Cell* 75, 843–854. doi: 10.1016/0092-8674(93)90529-Y
- Leung, K.-M., van Horck, F. P. G., Lin, A. C., Allison, R., Standart, N., and Holt, C. E. (2006). Asymmetrical beta-actin mRNA translation in growth cones mediates attractive turning to netrin-1. *Nat. Neurosci.* 9, 1247–1256. doi: 10.1038/nn1775
- Li, H., Li, W. X., and Ding, S. W. (2002). Induction and suppression of RNA silencing by an animal virus. *Science* 296, 1319–1321. doi: 10.1126/science.1070948
- Li, Q., Lee, J.-A., and Black, D. L. (2007). Neuronal regulation of alternative pre-mRNA splicing. *Nat. Rev. Neurosci.* 8, 819–831. doi: 10.1038/nrn2237

- López-Bendito, G., Cautinat, A., Sánchez, J. A., Bielle, F., Flames, N., Garratt, A. N., et al. (2006). Tangential neuronal migration controls axon guidance: a role for neuregulin-1 in thalamocortical axon navigation. *Cell* 125, 127–142. doi: 10.1016/j.cell.2006.01.042
- Lugli, G., Larson, J., Martone, M. E., Jones, Y., and Smalheiser, N. R. (2005). Dicer and eIF2c are enriched at post-synaptic densities in adult mouse brain and are modified by neuronal activity in a calpain-dependent manner. *J. Neurochem.* 94, 896–905. doi: 10.1111/j.1471-4159.2005.03224.x
- Luxe, M., Jungas, T., Laussy, J., Audouard, C., Garces, A., and Davy, A. (2013). Eph:ephrin-B1 forward signaling controls fasciculation of sensory and motor axons. *Dev. Biol.* 383, 264–274. doi: 10.1016/j.ydbio.2013.09.010
- Mehlen, P., Delloye-Bourgeois, C., and Chédotal, A. (2011). Novel roles for Slits and netrins: axon guidance cues as anticancer targets? *Nat. Rev. Cancer* 11, 188–197. doi: 10.1038/nrc3005
- Meister, G. (2013). Argonaute proteins: functional insights and emerging roles. *Nat. Rev. Genet.* 14, 447–459. doi: 10.1038/nrg3462
- Memczak, S., Jens, M., Elefsinioti, A., Torti, F., Krueger, J., Rybak, A., et al. (2013). Circular RNAs are a large class of animal RNAs with regulatory potency. *Nature* 495, 333–338. doi: 10.1038/nature11928
- Molnár, Z., Garek, S., López-Bendito, G., Maness, P., and Price, D. J. (2012). Mechanisms controlling the guidance of thalamocortical axons through the embryonic forebrain. *Eur. J. Neurosci.* 35, 1573–1585. doi: 10.1111/j.1460-9568.2012.08119.x
- Muddashetty, R. S., Nalavadi, V. C., Gross, C., Yao, X., Xing, L., Laur, O., et al. (2011). Reversible inhibition of PSD-95 mRNA translation by miR-125a, FMRP phosphorylation, and mGluR signaling. *Mol. Cell* 42, 673–688. doi: 10.1016/j.molcel.2011.05.006
- Nakagawa, S., Brennan, C., Johnson, K. G., Shewan, D., Harris, W. A., and Holt, C. E. (2000). Ephrin-B regulates the Ipsilateral routing of retinal axons at the optic chiasm. *Neuron* 25, 599–610. doi: 10.1016/S0896-6273(00)81063-6
- Natera-Naranjo, O., Aschrafi, A., Gioio, A. E., and Kaplan, B. B. (2010). Identification and quantitative analyses of microRNAs located in the distal axons of sympathetic neurons. *RNA* 16, 1516–1529. doi: 10.1261/rna.1833310
- Olsson-Carter, K., and Slack, F. J. (2010). A developmental timing switch promotes axon outgrowth independent of known guidance receptors. *PLoS Genet.* 6: e1001054. doi: 10.1371/journal.pgen.1001054
- Pfaff, J., Hennig, J., Herzog, F., Aebersold, R., Sattler, M., Niessing, D., et al. (2013). Structural features of Argonaute-GW182 protein interactions. *Proc. Natl. Acad. Sci. U.S.A.* 110, E3770–E3779. doi: 10.1073/pnas.1308510110
- Pichardo-Casas, I., Goff, L. A., Swedel, M. R., Athie, A., Davila, J., Ramos-Brossier, M., et al. (2012). Expression profiling of synaptic microRNAs from the adult rat brain identifies regional differences and seizure-induced dynamic modulation. *Brain Res.* 1436, 20–33. doi: 10.1016/j.brainres.2011.12.001
- Pinter, R., and Hindges, R. (2010). Perturbations of microRNA function in mouse dicer mutants produce retinal defects and lead to aberrant axon pathfinding at the optic chiasm. *PLoS ONE* 5: e10021. doi: 10.1371/journal.pone.0010021
- Pittman, A. J., Law, M.-Y., and Chien, C.-B. (2008). Pathfinding in a large vertebrate axon tract: isotopic interactions guide retinotectal axons at multiple choice points. *Development* 135, 2865–2871. doi: 10.1242/dev.025049
- Plachez, C., Andrews, W., Liapi, A., Knoell, B., Drescher, U., Mankoo, B., et al. (2008). Robos are required for the correct targeting of retinal ganglion cell axons in the visual pathway of the brain. *Mol. Cell. Neurosci.* 37, 719–730. doi: 10.1016/j.mcn.2007.12.017
- Plump, A. S., Erskine, L., Sabatier, C., Brose, K., Epstein, C. J., Goodman, C. S., et al. (2002). Slit1 and Slit2 cooperate to prevent premature midline crossing of retinal axons in the mouse visual system. *Neuron* 33, 219–232. doi: 10.1016/S0896-6273(01)00586-4
- Pulkkinen, K., Malm, T., Turunen, M., Koistinaho, J., and Ylä-Herttua, S. (2008). Hypoxia induces microRNA miR-210 *in vitro* and *in vivo* ephrin-A3 and neuronal pentraxin 1 are potentially regulated by miR-210. *FEBS Lett.* 582, 2397–2401. doi: 10.1016/j.febslet.2008.05.048
- Qiang, R., Wang, F., Shi, L.-Y., Liu, M., Chen, S., Wan, H.-Y., et al. (2011). Plexin-B1 is a target of miR-214 in cervical cancer and promotes the growth and invasion of HeLa cells. *Int. J. Biochem. Cell Biol.* 43, 632–641. doi: 10.1016/j.biocel.2011.01.002
- Raper, J., and Mason, C. (2010). Cellular strategies of axonal pathfinding. *Cold Spring Harb. Perspect. Biol.* 2: a001933. doi: 10.1101/cshperspect.a001933
- Reinhart, B. J., Slack, F. J., Basson, M., Pasquinelli, A. E., Bettinger, J. C., Rougvie, A. E., et al. (2000). The 21-nucleotide let-7 RNA regulates developmental timing in *Caenorhabditis elegans*. *Nature* 403, 901–906. doi: 10.1038/35002607
- Ringstedt, T., Braisted, J. E., Brose, K., Kidd, T., Goodman, C., Tessier-Lavigne, M., et al. (2000). Slit inhibition of retinal axon growth and its role in retinal axon pathfinding and innervation patterns in the diencephalon. *J. Neurosci.* 20, 4983–4991.
- Salmena, L., Poliseno, L., Tay, Y., Kats, L., and Pandolfi, P. P. (2011). A ceRNA hypothesis: the Rosetta Stone of a hidden RNA language? *Cell* 146, 353–358. doi: 10.1016/j.cell.2011.07.014
- Sasaki, Y., Gross, C., Xing, L., Goshima, Y., and Bassell, G. J. (2013). Identification of axon-enriched MicroRNAs localized to growth cones of cortical neurons. *Dev. Neurobiol.* 74, 397–406. doi: 10.1002/dneu.22113
- Schaefer, A., O'Carroll, D., Tan, C. L., Hillman, D., Sugimori, M., Llinas, R., et al. (2007). Cerebellar neurodegeneration in the absence of microRNAs. *J. Exp. Med.* 204, 1553–1558. doi: 10.1084/jem.20070823
- Schmucker, D., Clemens, J. C., Shu, H., Wörby, C. A., Xiao, J., Muda, M., et al. (2000). Drosophila Dscam is an axon guidance receptor exhibiting extraordinary molecular diversity. *Cell* 101, 671–684. doi: 10.1016/S0092-8674(00)80878-8
- Schratt, G. M., Tuebing, F., Nigh, E. A., Kane, C. G., Sabatini, M. E., Kiebler, M., et al. (2006). A brain-specific microRNA regulates dendritic spine development. *Nature* 439, 283–289. doi: 10.1038/nature04367
- Seitz, H. (2009). Redefining microRNA targets. *Curr. Biol.* 19, 870–873. doi: 10.1016/j.cub.2009.03.059
- Selbach, M., Schwanhäusser, B., Thierfelder, N., Fang, Z., Khanin, R., and Rajewsky, N. (2008). Widespread changes in protein synthesis induced by microRNAs. *Nature* 455, 58–63. doi: 10.1038/nature07228
- Sempere, L. F., Freemantle, S., Pitha-Rowe, I., Moss, E., Dmitrovsky, E., and Ambros, V. (2004). Expression profiling of mammalian microRNAs uncovers a subset of brain-expressed microRNAs with possible roles in murine and human neuronal differentiation. *Genome Biol.* 5: R13. doi: 10.1186/gb-2004-5-3-r13
- Shibata, M., Nakao, H., Kiyonari, H., Abe, T., and Aizawa, S. (2011). MicroRNA-9 regulates neurogenesis in mouse telencephalon by targeting multiple transcription factors. *J. Neurosci.* 31, 3407–3422. doi: 10.1523/JNEUROSCI.5085-10.2011
- Siegel, G., Obernosterer, G., Fiore, R., Oehmen, M., Bicker, S., Christensen, M., et al. (2009). A functional screen implicates microRNA-138-dependent regulation of the depalmitoylation enzyme APT1 in dendritic spine morphogenesis. *Nat. Cell Biol.* 11, 705–716. doi: 10.1038/ncb1876
- Small, E. M., and Olson, E. N. (2011). Pervasive roles of microRNAs in cardiovascular biology. *Nature* 469, 336–342. doi: 10.1038/nature09783
- Small, E. M., Sutherland, L. B., Rajagopalan, K. N., Wang, S., and Olson, E. N. (2010). MicroRNA-218 regulates vascular patterning by modulation of Slit-Robo signaling. *Circ. Res.* 107, 1336–1344. doi: 10.1161/CIRCRESAHA.110.227926
- Smirnova, L., Gräfe, A., Seiler, A., Schumacher, S., Nitsch, R., and Wulczyn, F. G. (2005). Regulation of miRNA expression during neural cell specification. *Eur. J. Neurosci.* 21, 1469–1477. doi: 10.1111/j.1460-9568.2005.03978.x
- Taylor, A. M., Berchtold, N. C., Perreau, V. M., Tu, C. H., Li Jeon, N., and Cotman, C. W. (2009). Axonal mRNA in uninjured and regenerating cortical mammalian axons. *J. Neurosci.* 29, 4697–4707. doi: 10.1523/JNEUROSCI.6130-08.2009
- Tessier-Lavigne, M., and Goodman, C. S. (1996). The molecular biology of Axon guidance. *Science* 274, 1123–1133. doi: 10.1126/science.274.5290.1123
- Tie, J., Pan, Y., Zhao, L., Wu, K., Liu, J., Sun, S., et al. (2010). MiR-218 inhibits invasion and metastasis of gastric cancer by targeting the Robo1 receptor. *PLoS Genet.* 6: e1000879. doi: 10.1371/journal.pgen.1000879
- Urbich, C., Kaluza, D., Frömel, T., Knau, A., Bennewitz, K., Boon, R. A., et al. (2012). MicroRNA-27a/b controls endothelial cell repulsion and angiogenesis by targeting semaphorin 6A. *Blood* 119, 1607–1616. doi: 10.1182/blood-2011-08-373886
- Ventura, A., Young, A. G., Winslow, M. M., Lintault, L., Meissner, A., Erkeland, S. J., et al. (2008). Targeted deletion reveals essential and overlapping functions of the miR-17 through 92 family of miRNA clusters. *Cell* 132, 875–886. doi: 10.1016/j.cell.2008.02.019
- Vitriol, E. A., and Zheng, J. Q. (2012). Growth cone travel in space and time: the cellular ensemble of cytoskeleton, adhesion, and membrane. *Neuron* 73, 1068–1081. doi: 10.1016/j.neuron.2012.03.005
- Wightman, B., Ha, I., and Ruvkun, G. (1993). Posttranscriptional regulation of the heterochronic gene lin-14 by lin-4 mediates temporal pattern formation in *C. elegans*. *Cell* 75, 855–862. doi: 10.1016/0092-8674(93)90530-4
- Williams, S. E., Mann, F., Erskine, L., Sakurai, T., Wei, S., Rossi, D. J., et al. (2003). Ephrin-B2 and EphB1 mediate retinal axon divergence at the optic chiasm. *Neuron* 39, 919–935. doi: 10.1016/j.neuron.2003.08.017

- Wolman, M. A., Liu, Y., Tawarayama, H., Shoji, W., and Halloran, M. C. (2004). Repulsion and attraction of axons by semaphorin3D are mediated by different neuropilins *in vivo*. *J. Neurosci.* 24, 8428–8435. doi: 10.1523/JNEUROSCI.2349-04.2004
- Wu, D., and Murashov, A. K. (2013). MicroRNA-431 regulates axon regeneration in mature sensory neurons by targeting the Wnt antagonist Kremen1. *Front. Mol. Neurosci.* 6:35. doi: 10.3389/fnmol.2013.00035
- Xiao, C., and Rajewsky, K. (2009). MicroRNA control in the immune system: basic principles. *Cell* 136, 26–36. doi: 10.1016/j.cell.2008.12.027
- Yang, J.-S., Maurin, T., Robine, N., Rasmussen, K. D., Jeffrey, K. L., Chandwani, R., et al. (2010). Conserved vertebrate mir-451 provides a platform for Dicer-independent, Ago2-mediated microRNA biogenesis. *Proc. Natl. Acad. Sci. U.S.A.* 107, 15163–15168. doi: 10.1073/pnas.1006432107
- Yang, L., Li, Q., Wang, Q., Jiang, Z., and Zhang, L. (2012). Silencing of miRNA-218 promotes migration and invasion of breast cancer via Slit2-Robo1 pathway. *Biomed. Pharmacother.* 66, 535–540. doi: 10.1016/j.biopha.2012.04.006
- Zhang, Y., He, X., Liu, Y., Ye, Y., Zhang, H., He, P., et al. (2012). microRNA-320a inhibits tumor invasion by targeting neuropilin 1 and is associated with liver metastasis in colorectal cancer. *Oncol. Rep.* 27, 685–694. doi: 10.3892/or.2011.1561
- Zhang, Y., Ueno, Y., Liu, X. S., Buller, B., Wang, X., Chopp, M., et al. (2013). The MicroRNA-17-92 cluster enhances axonal outgrowth in embryonic cortical neurons. *J. Neurosci.* 33, 6885–6894. doi: 10.1523/JNEUROSCI.5180-12.2013
- Zivraj, K. H., Tung, Y. C. L., Piper, M., Gumy, L., Fawcett, J. W., Yeo, G. S. H., et al. (2010). Subcellular profiling reveals distinct and developmentally regulated repertoire of growth cone mRNAs. *J. Neurosci.* 30, 15464–15478. doi: 10.1523/JNEUROSCI.1800-10.2010
- Zou, Y., Chiu, H., Domenger, D., Chuang, C.-F., and Chang, C. (2012). The lin-4 microRNA targets the LIN-14 transcription factor to inhibit netrin-mediated axon attraction. *Sci. Signal.* 5, ra43. doi: 10.1126/scisignal.2002437
- Zou, Y., Chiu, H., Zinovyeva, A., Ambros, V., Chuang, C.-F., and Chang, C. (2013). Developmental decline in neuronal regeneration by the progressive change of two intrinsic timers. *Science* 340, 372–376. doi: 10.1126/science.1231321

Conflict of Interest Statement: The authors declare that the research was conducted in the absence of any commercial or financial relationships that could be construed as a potential conflict of interest.

Received: 15 December 2013; accepted: 23 February 2014; published online: 14 March 2014.

Citation: Iyer AN, Bellon A and Baudet M-L (2014) microRNAs in axon guidance. *Front. Cell. Neurosci.* 8:78. doi: 10.3389/fncel.2014.00078

This article was submitted to the journal *Frontiers in Cellular Neuroscience*.

Copyright © 2014 Iyer, Bellon and Baudet. This is an open-access article distributed under the terms of the Creative Commons Attribution License (CC BY). The use, distribution or reproduction in other forums is permitted, provided the original author(s) or licensor are credited and that the original publication in this journal is cited, in accordance with accepted academic practice. No use, distribution or reproduction is permitted which does not comply with these terms.